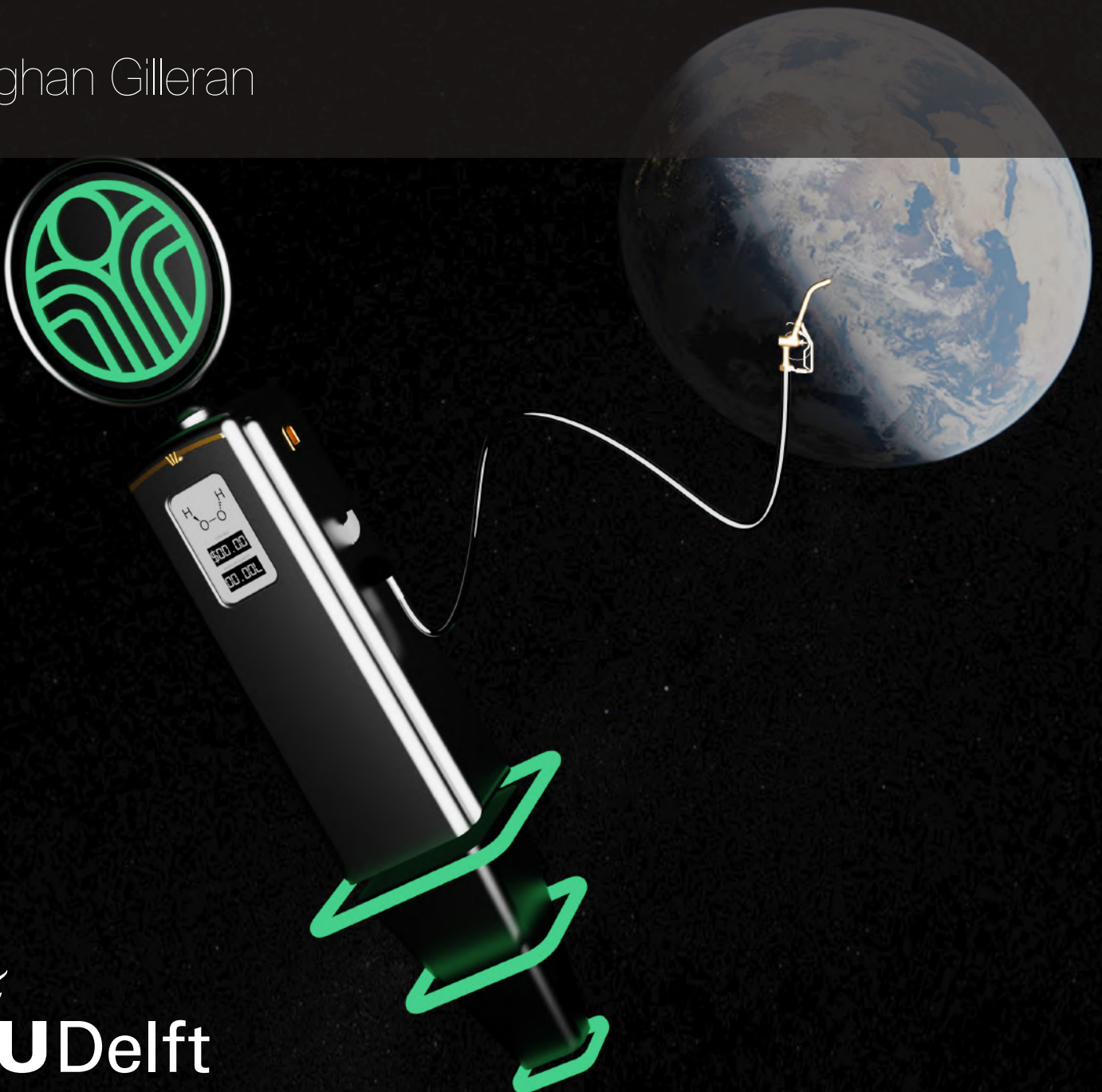


In-orbit Refuelling with Hydrogen Peroxide: An Architecture and Transfer Mechanism

Masters Thesis

Eoghan Gilleran

Delft University of Technology



In-orbit Refuelling with Hydrogen Peroxide: An Architecture and Transfer Mechanism

Masters Thesis

by

Eoghan Gilleran

Master Thesis Aerospace Engineering

Student Number 4443101

Supervisor: Dr. B.V.S. Jyoti
Institution: Delft University of Technology
Faculty of Aerospace Engineering, Delft
Project Duration: 10 January 2022 - 29 September 2022

Cover Image Source: Eoghan Gilleran

Preface

Returning from my internship at Rocket Factory Augsburg in search of a thesis topic I was increasingly aware of how the focus in the space industry was shifting from how we get things into space cheaply, to what we do now that access to space is relatively cheap. This has given birth to a wide range of opportunities, from space mining, manufacturing of satellites in-orbit, zero-G production of medicines and other compounds, and more. With this surge of in-space activities, combined with a more reusable approach to launching items into orbit, solutions are needed for how in-orbit activities may also be conducted sustainably, and this comes in the form of in-orbit servicing and refuelling.

When I reached out to Dr. Jyoti regarding potential in-orbit refuelling topics it was a perfect match, as SolvGE had already spotted this emerging opportunity. As well as a growing need for so called orbiting fuel stations, the go-to propellant of recent years, hydrazine, is in the process of being outlawed due to its toxic and carcinogenic qualities. SolvGE has knowledge of how to produce and concentrate hydrogen peroxide, a green propellant that poses a good alternative to hydrazine, and may be produced anywhere in the solar system that water is present. In order to facilitate space activities pushing out into the solar system in a sustainable manner, it is proposed to produce hydrogen peroxide off-Earth, and supply it to customers in the locality. Thus my thesis would focus on the final piece of this refuelling architecture, the delivery, and study the viability of this refuelling architecture and how exactly the hydrogen peroxide could be transferred from a refuelling craft to a customer in zero gravity.

My thesis project went on for a little longer than what might be considered nominal. This can mainly be attributed to my last hurrah in the Delft Aerospace Rocket Engineering student team, where I decided we must be represented at the second edition of the European Rocketry Challenge. Along with a small team we designed, tested, and built, in absolute record time, a rocket capable of flying to 3 km with dual solid motors, releasing a payload, and returning intact to the ground. While the flight itself may not have been 100% nominal I am immensely proud of what we achieved as a team, including in my opinion the best looking rocket in DARE history.

I was hugely lucky to be able to conduct this thesis research as a part of SolvGE. Having an enthusiastic team of people to bounce ideas off of and interact with daily, as well as lend a helping hand during testing, has been of huge assistance. My sincere thanks to Jaime, Nico, Pranav, Larissa, and Deniz, as well as the other thesis and internship students including Emre, Pieter, and Pepijn. Additional thanks to all of the member of Delft Aerospace Rocket Engineering that I have bounced ideas and problems off of, especially members of Dodo/Delta V of Nathaniel and Jonathan, as well as Jeije and Sari. I benefited from the expert oversight of the most excellent Dr B.V.S. Jyoti and Dr Dinesh Mengu. Your detailed feedback and well directed questions provided great guidance and I could not have been luckier in terms of supervisors, I hope we have the chance to work together again some day. I want to thank my family for always supporting me in whatever I choose to pursue, I would never have made it this far down this exhilarating path without your unending encouragement and support for which I am so grateful. Lastly I would like to thank my girlfriend who has kept me motivated over the course of my thesis work, especially during the final months. Thanks for being the ever willing proof reader, practise presentation audience and all round general supporter.

*Eoghan Gilleran
Delft, September 2022*

Summary

With the ever-growing number of spacecraft launching into orbit, alongside the growing desire for propulsion systems on many of these craft, an emerging opportunity is present in the potential servicing and refuelling of these spacecraft. Proposals for propellant resupply services are growing in abundance, primarily with architectures involving craft launching from the Earth's surface to transfer their cargo of propellant to in-orbit customers. Current state of the art solutions utilise hydrazine, however its popularity is dwindling with the European Chemicals Agency considering outlawing it due to its toxic and carcinogenic nature. For this reason, SolvGE, a start-up based at TU Delft, has proposed a sustainable architecture involving the production of high concentration hydrogen peroxide (H_2O_2) from water-ice present at off-Earth locations. While H_2O_2 does possess a lower specific impulse than hydrazine, it has several other attractive characteristics such as its high density, storability, and non-toxicity, as well as applicability in both propulsion and power systems.

To investigate the viability of such an architecture, a Single Stage to Orbit refuelling craft is sized using the Tsiolkovsky equation, as well as ΔV values between the lunar surface and Earth-Moon Lagrange points 1 and 2, and low lunar orbit, and between the Martian surface, Phobos and Deimos and Low Martian orbit. I_{sp} values of 330 s - 340 s, spanning a combinations of H_2O_2 and a range of fuels, are used, as well as a payload mass of 290 kg (200 L) of H_2O_2 to be supplied to a customer. The output of this sizing has shown that with a minimum structural coefficient of 0.3 a refuelling craft could launch from the Moon to low lunar orbit, and from Deimos and Phobos to low Martian orbit.

A trade-off of potential refuelling mechanisms shows that a piston-based system, used in conjunction with pressurant gas, a gas generator, or a pump, is a good candidate for high cycle usage. A first order mass sizing based off of a variety of methods from literature is conducted to study the total transfer system mass for different combinations of a piston and actuation system. This shows low variation in total transfer system mass (< 2%) over different transfer volumes (200 L and 1000 L) and transfer rates (0.1 kg/s and 1.0 kg/s). A prototype test set up of the transfer mechanism using solely pressurant gas is created to investigate the functioning of the piston system and the relevant pressurant parameters. This test set up consists of a high pressure tank, with a pressure regulator used to set the pressure in the system, as well as a piston tank. Transfer tests are conducted at a range of storage pressures (5, 10, 20, 40 bar) and regulated pressures (1.5, 2.0, 2.5 bar), both with and without the piston head in the cylinder. These tests are conducted using 1 L of deionised water. The pressure in the storage tank is used to gauge the pressurant gas mass used during each transfer using the ideal gas law, and it is found that transfers with the piston head show a 17%-25% increase in pressurant mass required compared to without. Testing with the system inverted shows 9% more pressurant is required due to the adverse gravity gradient, thus providing an estimate of how the system may behave in microgravity. Lastly transfer tests were conducted using 30% H_2O_2 and due to minor amounts of decomposition occurring it was found that 2.38% less pressurant gas was required. With more than 60 transfer tests conducted the piston was never found to jam or become stuck, and it is likely that minor leakage issues around the piston head may be remedied with improved fabrication methods.

A model of the transfer system is created in the Matlab Simscape in order to be used in estimating the mass of a scaled up version of the system. Issues are encountered in replicating the dynamic behaviour of the pressure regulator present in the test set up in the model. Despite attempts to replace the regulator block with a custom mass-spring-damper model and tune it to recorded test data, no useful results are obtained. Thus extrapolation of the test results instead are used to estimate the mass of a scaled up system. It is found that for a system transferring 200 L, with 200 bar storage pressure and 3 bar regulated pressure, 2.224 kg of pressurant gas are required, with a total propellant transfer system mass of 343.01 kg, and a transfer rate of 0.157 kg/s.

In conclusion, an reusable refuelling craft capable of supplying 200 L of H_2O_2 weighs approximately the same as the wet mass of the Apollo lunar lander (16000 kg) and is able to serve customers in low lunar and Martian orbits in a sustainable manner. Further research on high cycles of the piston as well as possible mass savings, and actuation using H_2O_2 gas generators will further assess the applicability of piston transfer systems for in-orbit refuelling.

Nomenclature

Abbreviations

Abbreviation	Definition
ATO	Assisted Take Off
COG	Centre of Gravity
DLR	German Aerospace Centre
EE	Expulsion Efficiency
EM	Electromagnetic
ESA	European Space Agency
FKM	Fluro-Elastomer
GLOW	Gross Lift Off Weight
H ₂ O ₂	Hydrogen Peroxide
HTP	High Test Peroxide
ISS	International Space Station
LAD	Liquid Acquisition Device
LH ₂	Liquid Helium
LIDAR	Light Detection and Ranging
LLO	Low Lunar Orbit
LMO	Low Martian Orbit
LOX	Liquid Oxygen
MAPO	Magnetically Actuated Propellant Orientation Experiment
MTI	Main Tank Injection
N ₂	Nitrogen
NASA	National Aeronautics and Space Administration
NLR	Royal Netherlands Aerospace Centre
NTUA	National Technical University of Athens
P(&)ID	Piping and Instrumentation Diagram
PMD	Propellant Management Device
PTFE	Polytetrafluoroethylene
PVT	Pressure, Volume, Temperature
RCS	Reaction Control System
RMS	Root Mean Square
SSTO	Single Stage to Orbit
TAS	Thales Alenia Space
TRL	Technology Readiness Level

Symbols

Symbol	Definition	Unit
Bo	Bond Number	[-]
D	Diameter	[m]
E	Energy	[J]
f	Frictional Coefficient	[-]
g	Gravitational Acceleration	[m/s ²]
H	Head	[m]
I_{sp}	Specific Impulse	[s]
I_{tot}	Total Impulse	[Ns]
L_c	Characteristic Length	[m]
M	Mass	[kg]
\dot{m}	Mass Flow	[kg/s]
N_s	Specific Velocity	[m ² /s]
P	Power	[W]
P	Pressure	[Pa]
Q	Volumetric Flow Rate	[m ³ /s]
R	Gas Constant	[J mol ⁻¹ K ⁻¹]
Re	Reynolds Number	[-]
T	Temperature	[K]
T	Thrust	[N]
t_b	Burn Time	[s]
u	Velocity	[m/s]
v	Flow Velocity	[m/s]
V	Volume	[m ³]
γ	specific Heat Ratio	[-]
γ_{LV}	Surface Tension at Liquid Vapour Interface	[N/m]
δ	Power Density	[W/kg]
ΔP	Pressure Change	[Pa]
ΔV	Velocity Increment	[m/s]
η	Efficiency	[-]
κ	Structural Margin	[-]
λ	Structural Coefficient	[-]
μ	Dynamic Viscosity	[kg/ms]
ρ	Density	[kg/m ³]
ω	Rotational Speed	[RPM]

List of Figures

1.1	Research question planned approach flow diagram	2
2.1	RCS system and storage method of H ₂ O ₂ in the X-1B aircraft [36]	5
2.2	X-15 Reaction Control Propellant Supply System [9]	6
2.3	H ₂ O ₂ control systems of early satellites	7
2.4	H ₂ O ₂ control systems of the Centaur rocket [24]	7
2.5	Schematic Drawing of H ₂ O ₂ system used for lift rockets and attitude control in the LLRV [3]	8
2.6	Orbit Fab Geostationary Depot [56]	15
2.7	Overview of Orbital Express Spacecraft ASTRO and NEXTSat [15]	18
2.8	Fluid Transfer and Propulsion System Schematic for the Orbital Express Mission [15]	18
2.9	Different fluid transfer paths of the Orbital Express Mission [15]	20
2.10	Design options of feed systems for liquid propellant rocket engines. The more common types are designated with a double line at the bottom of the box [61]	22
2.11	Three concepts of propellant tanks with positive expulsion: (a) inflatable dual bladder; (b) rolling, peeling diaphragm; (c) sliding piston. As the propellant volume expands or contracts with changes in ambient temperature, the piston or diaphragm will also move slightly and the ullage volume will change during storage [61]	23
2.12	Linear acceleration propellant transfer [7]	24
2.13	Main Tank Injection System Schematic [21]	25
2.14	Magnetic Propellant Positioning Options for Paramagnetic Propellants (LO ₂) and Diamagnetic Propellants (LH ₂) [25]	26
2.15	Magnetic Susceptibility of H ₂ O ₂ - Water Solutions[57]	26
2.16	Trap types as well as various trap shapes [34]	28
2.17	Trap types as well as various trap shapes [34]	28
2.18	Types of ring baffles used for circular cylindrical tanks [31]	29
2.19	A variety of vane configurations [35]	30
2.20	A Conventional Sponge with Liquid Attached [33]	31
2.21	A variety of sponge PMD configurations [33]	31
2.22	Illustrations of a Gallery PMD [32]	33
2.23	Thermal balance of a spacecraft in a planetary orbit	35
2.24	Service/Fuelling spacecraft end effector developed by the ASSIST initiative [47]	37
2.25	Service/Fuelling spacecraft end effector developed by the ASSIST initiative[56]	37
2.26	The fluid transfer interface developed for and used by the Orbital Express mission	38
3.1	Context diagrams of the refuelling system and the propellant transfer subsystem, illustrating the interaction between the systems and their environments.	40
4.1	Segment location example showing options one and six from Table 4.1	48
4.2	Naming of segments with chosen locations	49
4.3	Refuelling Craft Flight Profile	50
4.4	Delta-V Map of the Earth, Moon, and Mars System. chart by R. Penn ¹	51
4.5	Satellite propellant mass versus year of launch. Reproduced from Zandbergen[78]	52
4.6	LOW vs λ for a variety of Lunar based production destinations and I_{sp} values of 300s, 320s, and 340s	53
4.7	GLOW vs λ for a variety of Martian system based production destinations and I_{sp} values of 300s, 320s, and 340s	54
4.8	Possible placement of the transfer mechanism	55
4.9	Schematic of the system layouts used for comparative mass sizing	56

4.10	Symbol legend for Piping and Instrumentation Diagrams	59
4.11	Mass sizing of three different piston based transfer methods at varying propellant volume and transfer rates	61
5.1	Symbol legend for Piping and Instrumentation Diagrams	63
5.2	Concept Architecture of Propellant Transfer System with Transfer Mechanism Inside of Refuelling Craft	65
5.3	Concept Architecture of Propellant Transfer System with Transfer Mechanism Outside of Refuelling Craft	66
5.4	Piston sealing element details taken from SKF hydraulic seals catalogue [58]	67
5.5	PID of piston test set up	68
5.6	Labelled section view of piston assembly	68
5.7	Paintball tank used as high pressure tank	69
5.8	Adjustable regulator	69
5.9	Various valves used in the set up	70
5.10	Exploded and isometric view of servo-valve CAD assembly. The left hand image shows the servo valve, the servo horn, the adaptor to the valve, and the ball valve, as well as the housing of the assembly in an exploded view. The right hand figure shows the assembly.	70
5.11	Various pressure sensors used in the set up	71
5.12	Various lines and fittings	71
5.13	Section view of piston showing seals on endcap and piston head	72
5.14	Sealing elements of the piston head	72
5.15	Fabrication of the piston assembly	74
5.16	Front panel of LabVIEW interface	75
5.17	Block diagram of LabVIEW programme	76
5.18	Multiple views of the assembled test set up	77
5.19	Side by side comparison of transfer test set up picture and PID. The components are labelled as follows; 1 - high pressure tank, 2 - high pressure pressure sensor, 3- high pressure relief valve, 4 - pressure regulator, 5 - pressure sensor, 6 - manual ball valve, 7 - solenoid gas valve, 8 - solenoid bleed valve (obscured by test frame in picture), 9 - pressure sensor, 10 - pressure relief valve, 11 - piston assembly, 12 - manual fill ball valve, 13 - liquid servo valve, 14 - pressure sensor, 15 - outlet.	78
6.1	Procedure followed to assemble piston head	81
6.2	Damage to the piston seal and leak location visible	82
6.3	Leak rates with piston head at bottom and centre of cylinder. The bottom two lines are from the piston head being held in the centre of the cylinder and the upper two are with the piston head directly above the endcap.	82
6.4	Endcap o-ring damage and remedy	83
6.5	Leak locations and leak remedies	84
6.6	Calibration of pressure sensors	85
6.7	Compatibility testing of test set up components with 30% H ₂ O ₂	86
6.8	Timed runs of the piston head at three different pressure settings of 1.3 bar, 1.4 bar, and 1.5 bar, with two runs at each pressure setting	87
6.9	Piston head visible at top endcap after water filling	88
6.10	Assistant holding test set up inverted	88
6.11	Test set up in large fume hood of chemistry lab for 30 % H ₂ O ₂ testing	89
7.1	Various blocks used in Matlab-Simscape model	92
7.2	Details of Matlab-Simulink friction block	93
7.3	Model used for tuning of piston head friction	94
7.4	Model of system using standard regulator block	96
7.5	Regulator modelled in Simulink as a mass-spring-damper system	97
7.6	Test	98
7.7	Model of system using custom Simulink regulator model	99
8.1	Example of previewed test data	102

8.2	Fourier plot of typical test data	103
8.3	Pressure data from test - No Piston Head - 40bar_1.5bar-1 including data labels and axis indicators	104
8.4	Scatter plots of pressurant mass used for tests with and without piston head	106
8.5	Plot of percentage pressurant mass increase due to piston head	107
8.6	Scatter plots of transfer duration excluding two outlier points with two forms of best fit surfaces	108
8.7	Plots of model and test data superimposed	110
9.1	Research question implemented approach flow diagram	113
D.1	Piston endcap technical drawing	131
D.2	Piston head technical drawing	132
D.3	Piston cylinder technical drawing	133
D.4	Piston production process technical drawing	134
F.1	Pressure data from test - No Piston Head - 10bar_1.5bar-1	139
F.2	Pressure data from test - No Piston Head - 10bar_1.5bar-2	140
F.3	Pressure data from test - No Piston Head - 10bar_2.0bar-1	140
F.4	Pressure data from test - No Piston Head - 10bar_2.0bar-2	141
F.5	Pressure data from test - No Piston Head - 10bar_2.5bar-1	141
F.6	Pressure data from test - No Piston Head - 10bar_2.5bar-2	142
F.7	Pressure data from test - No Piston Head - 20bar_1.5bar-1	142
F.8	Pressure data from test - No Piston Head - 20bar_1.5bar-2	143
F.9	Pressure data from test - No Piston Head - 20bar_2.0bar-1	143
F.10	Pressure data from test - No Piston Head - 20bar_2.0bar-2	144
F.11	Pressure data from test - No Piston Head - 20bar_2.5bar-1	144
F.12	Pressure data from test - No Piston Head - 20bar_2.5bar-2	145
F.13	Pressure data from test - No Piston Head - 40bar_1.5bar-1	145
F.14	Pressure data from test - No Piston Head - 40bar_1.5bar-2	146
F.15	Pressure data from test - No Piston Head - 40bar_2.0bar-1	146
F.16	Pressure data from test - No Piston Head - 40bar_2.0bar-2	147
F.17	Pressure data from test - No Piston Head - 40bar_2.5bar-1	147
F.18	Pressure data from test - No Piston Head - 40bar_2.5bar-2	148
F.19	Pressure data from test - With Piston Head - 10bar_1.5bar-1	148
F.20	Pressure data from test - With Piston Head - 10bar_1.5bar-2	149
F.21	Pressure data from test - With Piston Head - 10bar_2.0bar-1	149
F.22	Pressure data from test - With Piston Head - 10bar_2.0bar-2	150
F.23	Pressure data from test - With Piston Head - 10bar_2.5bar-1	150
F.24	Pressure data from test - With Piston Head - 10bar_2.5bar-2	151
F.25	Pressure data from test - With Piston Head - 20bar_1.5bar-1	151
F.26	Pressure data from test - With Piston Head - 20bar_1.5bar-2	152
F.27	Pressure data from test - With Piston Head - 20bar_2.0bar-1	152
F.28	Pressure data from test - With Piston Head - 20bar_2.0bar-2	153
F.29	Pressure data from test - With Piston Head - 20bar_2.5bar-1	153
F.30	Pressure data from test - With Piston Head - 20bar_2.5bar-2	154
F.31	Pressure data from test - With Piston Head - 40bar_1.5bar-1	154
F.32	Pressure data from test - With Piston Head - 40bar_1.5bar-2	155
F.33	Pressure data from test - With Piston Head - 40bar_2.0bar-1	155
F.34	Pressure data from test - With Piston Head - 40bar_2.0bar-2	156
F.35	Pressure data from test - With Piston Head - 40bar_2.5bar-1	156
F.36	Pressure data from test - With Piston Head - 40bar_2.5bar-2	157
F.37	Pressure data from test - With Piston Head - 20bar_2.5bar-Upside Down-1	157
F.38	Pressure data from test - With Piston Head - 20bar_2.5bar-Upside Down-2	158
F.39	Pressure data from test - With Piston Head - 10bar_2.0-H2O2-1	158
F.40	Pressure data from test - With Piston Head - 10bar_2.0-H2O2-2	159

List of Tables

2.1	Tabulated properties of commercial and historical H ₂ O ₂ uses with inferred H ₂ O ₂ masses and volumes used. Published properties are in bold while the remainder are calculated	11
2.2	Compatibility of Elastomers and Sealing Materials with H ₂ O ₂ at 21 °C[17][51]	13
2.3	Compatibility of Aluminium Alloys with H ₂ O ₂ at 21 °C[17][51]	13
2.4	Compatibility of Stainless Steel Alloys with H ₂ O ₂ at 21°C[17][51]	13
2.5	Compatibility of Inconel Alloys with H ₂ O ₂ at 21°C[17][51]	13
2.6	Survey of historic and current in-orbit transfer/servicing	16
2.7	Comparison of Propellant Expulsion Methods for Spacecraft. Reproduced from [61]	23
2.8	Propellant Transfer Methods [7]	27
2.9	Propellant Handling and Settling Methods [25]	34
3.1	Stakeholder desires	41
3.2	Preliminary System Requirements for the H ₂ O ₂ Depot and Transfer System	41
3.3	An illustration displaying which of the transfer, PMD and settling systems can fulfil the functions of transfer, management, handling and mass gauging. Green (2) indicates a possibility to fulfil this function, orange (1) indicates potential to fulfil the function indirectly or with modification, and red (0) indicates a lack of ability to fulfil a function. Numbering is provided purely for black/white compatibility and colour blindness.	42
3.4	Trade-off of in-space propellant transfer methods	46
4.1	Segment location possibilities	48
4.2	Tabulated delta-V data for likely refuelling routes and additional routes of interest	51
4.3	GLOW and structural fraction calculation for the Moon surface to EML-1 route with an I_{sp} of 300 s and a payload of 290 kg	53
4.4	Calculated structural coefficient for a variety of vehicles, primarily Lunar ferry vehicles	54
4.5	Mass of sub-components of transfer systems using pressurant gas, gas generator, and pumped, for 200L transferred at .1 kg/s	59
5.1	Fluid transfer method applicability, reproduced from [16]	64
5.2	Calculations of failure modes for PVC and aluminium piston cylinder	73
6.1	Requirements on testing of the H ₂ O ₂ transfer system	79
6.2	Systematic Testing Plan	80
6.3	Compliance with requirements on testing of the H ₂ O ₂ transfer system	90
8.1	Example comparison of ideal gas law mass change and measured mass change	103
8.2	Pressurant mass expelled for the different tests completed	105
C.1	Mass of sub-components of transfer systems using pressurant gas, gas generator, and pumped, for 200L transferred at 0.1 kg/s	127
C.2	Mass of sub-components of transfer systems using pressurant gas, gas generator, and pumped, for 200L transferred at 1.0 kg/s	128
C.3	Mass of sub-components of transfer systems using pressurant gas, gas generator, and pumped, for 1000L transferred at 0.1 kg/s	128
C.4	Mass of sub-components of transfer systems using pressurant gas, gas generator, and pumped, for 1000L transferred at 1.0 kg/s	129
E.1	Test log of tests without piston head	136
E.2	Test log of tests with piston head	137
E.3	Test log of inverted tests and tests using H ₂ O ₂	138

Contents

Preface	i
Summary	ii
Nomenclature	iii
List of Figures	v
List of Tables	viii
1 Introduction	1
1.1 Research Question	2
2 Literature Study	3
2.1 Hydrogen Peroxide: Historic and Current Usage for Propulsion and Power	3
2.1.1 Historic Development.	3
2.1.2 Modern Thruster Applications	9
2.1.3 Fuel Cell Applications	11
2.2 Hydrogen Peroxide: Chemistry and Considerations	11
2.2.1 H ₂ O ₂ Material Compatibility	12
2.2.2 H ₂ O ₂ Design Guidelines and System Handling	14
2.3 Refuelling System: Relevant Work and Current Developments	15
2.4 Refuelling System: Transfer, Management and Handling Methods.	20
2.4.1 Propellant Transfer Methods.	21
2.4.2 Propellant Management Devices & Liquid Acquisition Devices	27
2.4.3 Propellant Handling & Settling Methods.	33
2.4.4 Propellant Thermal Control Methods	34
2.4.5 Propellant Mass Gauging Methods	35
2.5 Refuelling System: Peripheral Systems to the Transfer System	36
2.5.1 Tanks	36
2.5.2 Refuelling Interface.	36
2.5.3 Propulsion System	38
2.6 Conclusion	38
3 Refuelling System Concept	39
3.1 Requirements.	39
3.2 Design Trade Off	41
3.3 Conclusion	45
4 Refuelling Architecture	47
4.1 Segment Location	47
4.2 Resupply Craft Sizing	49
4.3 Mass Sizing of Transfer Mechanism Variations	55
4.4 Conclusion	62
5 Piston Design and Experimental Test Set Up	63
5.1 Piston Transfer System Design	63
5.2 Piston Test Set Up	68
5.2.1 High Pressure Tank	69
5.2.2 Regulator	69
5.2.3 Valves	69
5.2.4 Sensors	70
5.2.5 Lines and Fittings.	71

5.2.6	Piston	71
5.2.7	Other Hardware.	74
5.2.8	Data Acquisition and Control.	74
5.3	Conclusion	77
6	Testing	79
6.1	Test Plan	79
6.2	Challenges Encountered	80
6.3	Initial and Unit Testing	83
6.3.1	Leak Testing	83
6.3.2	Sensor Calibration	84
6.3.3	Compatibility Testing	85
6.3.4	Friction Testing	86
6.4	Systematic Testing	86
6.4.1	Without Piston Head	86
6.4.2	With Piston Head	87
6.4.3	Inverted	88
6.4.4	H ₂ O ₂ Testing	89
6.5	Conclusion	89
7	Model	91
7.1	Foundation of Model	91
7.2	Tuning of Piston Friction Model	92
7.3	Model with Standard Regulator Block	95
7.4	Model with Custom Regulator	97
7.5	Conclusion	100
8	Results and Implications for Large Scale System	101
8.1	Post Processing and Plotting Test Data	101
8.2	Ideal Gas Mass Assumption	103
8.3	Results	104
8.4	Comparison to Model.	109
8.5	Sizing of Full Scale System	111
8.6	Conclusion	111
9	Conclusion	113
9.1	Recommendations	115
	References	119
A	H₂O₂ Material Compatibility	120
B	Peripheral Systems	124
C	Refuelling Architecture	127
D	Engineering Drawings	130
E	Transfer Test Test Logs	135
F	Transfer Test Plotted Results	139
G	Post-processing Python Code	160

1

Introduction

The number of spacecraft being placed into orbit is growing on a yearly basis. These spacecraft are also shrinking in size as electronics are miniaturised. Increasingly propulsion systems are being flown on both the larger and smaller spacecraft as propulsion systems are also miniaturised. This addition increases the flexibility of satellites as well as their service life. A popular propellant for use on spacecraft as either a fuel or monopropellant is hydrazine due to the high specific impulse it can yield. However given hydrazine's toxic and carcinogenic qualities there is a growing move to stop its usage and the European Chemicals Agency is considering placing a ban on it. Instead attention is turning to high concentration hydrogen peroxide as a replacement. Hydrogen peroxide is a relatively high density liquid oxidiser with the advantageous capability of decomposing exothermically into water steam and oxygen and being non-toxic. SolvGE has developed technology capable of producing H_2O_2 from water and concentrating it to high concentrations (90-95%) appropriate for in-space power and propulsion applications. The use of such a technology in space would allow for H_2O_2 to be supplied to customer spacecraft with only water as an input, doing away with the necessity to refuel spacecraft by launching the propellant from the Earth's surface and creating a truly sustainable refueling architecture.

Such a hydrogen peroxide refuelling infrastructure would require the capability to transfer the propellant internally from one vessel to another as well as externally from the depot or refuelling craft to the customer spacecraft. This function may be trivial on the Earth's surface however this is not so under in-space conditions. In microgravity liquids are dominated by surface tension forces rather than gravitational forces and thus cling to the walls of a tank or form bubbles stuck in the tank interior. A dedicated system must be developed capable of transferring propellant under these conditions. Additionally this refuelling architecture will start at the location of water ice somewhere in the solar system, and end at a customer spacecraft. A first order analysis of the optimal layout of this refuelling system will provide the context needed for assessing the transfer mechanism itself. The goal of this thesis will be to design, develop and test a prototype of this system, within the context of the refuelling system design.

The structure of this thesis is as follows; firstly a comprehensive literature study on the topics of hydrogen peroxide's space related usage, and refuelling systems is presented in Chapter 2. Chapter 3 compares the optimal propellant transfer methods and selects one for development. Chapter 4 examines the full refueling architecture, how it may be laid out and the best configuration of the propellant transfer mechanism for this layout. Chapter 5 presents the design of the prototype piston transfer system and the supporting set up for testing purposes. Chapter 6 covers the approach and challenges encountered during testing of the transfer mechanism. Chapter 7 describes the model created to parallel the test set up. Chapter 8 presents the results of the testing and how they may be used to investigate the use of this transfer mechanism on a full scale system. Finally Chapter 9 concludes the research question of this thesis and provides some recommendations for future work.

Please note that all pressures mentioned in this report are absolute and not gauge, therefore an unpressurised test set up is at approximately 1.01 bar or 101325 Pa.

1.1. Research Question

In order to direct the focus of this thesis a research gap shall be used to define a research objective, from which a specific research question may be distilled.

Among the state of the art of current in-orbit refuelling initiatives, the focus lies on refuelling satellites with primarily hydrazine, using refuelling missions launched from the Earth's surface or as secondary objectives of launcher kick-stages. This approach not only supplies spacecraft with a toxic and unsustainable propellant, but in utilising a launch from the Earth's gravity well, refuels in an unsustainable manner. A gap is present that may be filled by a system supplying a green propellant in a long term viable manner. This research gap yields the following research objective;

To investigate the feasibility of an in-situ H_2O_2 refuelling architecture and reusable refuelling craft, with the inclusion of a novel H_2O_2 propellant transfer mechanism, through top level sizing and prototype testing

Based on this research objective, a number of research questions may be defined;

1. What refuelling craft mass is viable and for what routes in the solar system?
2. What is the optimal transfer mechanism for a sustainable propellant resupply system?
 - (a) What systems must the transfer mechanism be used in conjunction with, and how sensitive are these configurations to changes in system requirements?
 - (b) What challenges face the transfer mechanism and can they be overcome?
 - (c) Can the transfer system function in a representative environment?

These questions will be approached by sizing of the refuelling architecture, as well as testing of the prototype transfer mechanism, the results of which will be used to model the system and flesh out the parameters for a larger scale system. This approach is illustrated in Figure 1.1.

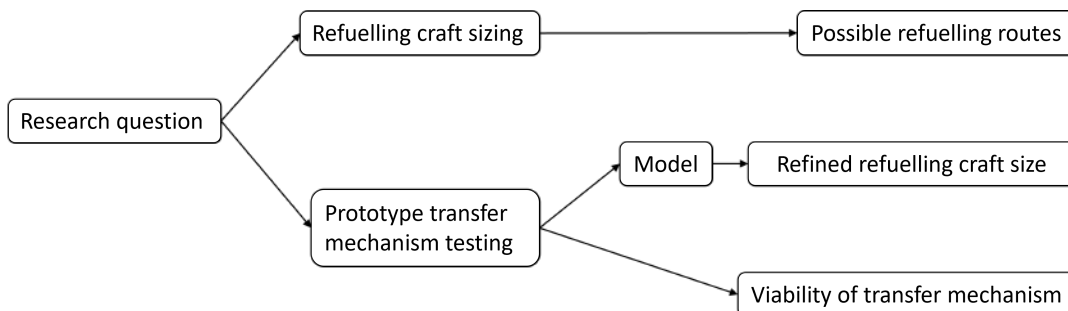


Figure 1.1: Research question planned approach flow diagram

2

Literature Study

This chapter provides the necessary background information on the topics of hydrogen peroxide, its historic applications for power and propulsion provision in space systems as well as the current trends in its usage, before delving into the state of the art in current space depots and refuelling, the methods of transferring, managing and handling fluids in space, and finally the peripheral systems to a propellant transfer system.

2.1. Hydrogen Peroxide: Historic and Current Usage for Propulsion and Power

In July of 1818 the Paris Academy of Sciences was notified of the discovery of "oxidised water", later to be called hydrogen peroxide, by Louis-Jacques Thenard [70]. After its discovery Thenard conducted an extensive study of the chemical, observing reactions with some 130 elements and remarking that in many of these reactions "chemical action" was missing and instead attributed these reactions to electricity. This mechanism was later recognised by Berzelius as that of catalysts and catalytic activity [70]. The only two uses Thenard was initially able to find for hydrogen peroxide were removing sulphide from oil paintings and as a skin irritant for healthcare applications, however in the intervening two centuries a myriad of additional uses have been found, specifically in the areas of propulsion and power provision.

Hydrogen peroxide is a relatively high density liquid oxidiser with the advantageous capability of decomposing exothermically (with the release of heat) into water steam and oxygen. H_2O_2 also possesses the advantage of being relatively easy to handle as it is non-toxic, a property that is also desirable from an environmental impact standpoint [67]. Further attributes of the chemical will be discussed in Section 2.2 however these three qualities of density, exothermic decomposition, and handling ease make H_2O_2 rather attractive for propulsion and power applications, which is what the following section will explore. As this review is being conducted in the context of a propellant depot and propellant transfer, the method of transfer and storage in these historic and current applications is covered where information is provided. And as the application under development lies in the space domain primary focus is given to past applications in this or somewhat relevant domains.

This section is structured as follows, Section 2.1.1 first treats the historical uses of H_2O_2 in a variety of applications and mentions details of the H_2O_2 storage and transfer methods used, Section 2.1.2 lists a number of propulsion systems currently on the market using H_2O_2 and some relevant details such as their I_{sp} , burn time and the concentration of H_2O_2 used, lastly Section 2.1.3 summarises H_2O_2 uses in fuel cell technology and how this may pose constraints on the system to be designed.

2.1.1. Historic Development

One of the first proposed applications for H_2O_2 was that of propellant for submarines [43]. In the run up to the Second World War the German Navy sought a number of improvements to their submarine technologies, solutions to which Hellmuth Walter developed the so called "triple feed pump" submarine engine, where H_2O_2 was decomposed on a catalyst bed of porcelain stones coated in calcium,

potassium, or sodium permanganate, before the resulting steam and oxygen were combusted with diesel and sea water was used to cool the combustion chamber, after which the combustion gasses drove a steam turbine and the submarine propeller. This means of propelling submarines saw little implementation during the war, however H_2O_2 was also applied to torpedo propulsion.

For this application a combined liquid catalyst and fuel was first brought into contact with the H_2O_2 and after two to three seconds this first fuel mix was cut off and a pure fuel flow was introduced and the chamber heat was used to sustain the combustion. The timing of this fluid interaction was critical to preventing explosions. One uniquely remarkable aspect of the submarine propulsion system employed by the Germans was that the H_2O_2 was stored in collapsible Polyvinyl-Chloride bags, exterior to the pressurised hull of the submarine and the pressure of the surrounding seawater provided positive pressure for the pump system [43]. Such a storage method may be interesting to investigate for the application at hand.

Walter continued the development of H_2O_2 systems in other domains, namely Assisted Take Off (ATO) devices as well as primary propulsion units for fighter planes. Here both monopropellant units and bipropellant units were developed, with the bipropellant systems functioning in the same manner as the aforementioned torpedo systems, except the propulsion gases were used directly as a jet rather than driving a steam turbine [43]. Both the United Kingdom and the United States continued investigation of the torpedo propulsion, as well as ATO devices after the war.

In the domain of rocketry H_2O_2 saw applications in Reaction Control Systems (RCS), Gas Generator Systems for Turbopumps, and as an oxidiser in bipropellant rocket engines. H_2O_2 occupied a position as essentially the first monopropellant, and was extensively used in many early high altitude research vehicles and spacecraft. The following is a list of applications employing H_2O_2 RCS reproduced from [67]:

- X-1
- Centaur RCS
- Centaur propellant settling
- X-15
- Mercury
- Scout Roll Control
- Little Joe II
- Burner II
- SATAR
- 122Y
- Astronaut Manoeuvring Unit
- SYNCOM
- COMSAT
- HS 303A
- ATS

The RCS for the X-1B aircraft is interesting to briefly assess. It employed a H_2O_2 RCS, shown in Figure 2.1a, to provide control in each axis. The H_2O_2 was stored in a piston type expulsion system. This vessel, shown in Figure 2.1b, has a capacity of 2.4 gallons (c. 9.1 L) and was fabricated from 321 stainless steel. H_2O_2 was expelled under both positive, zero and negative vertical accelerations by means of applying N_2 pressure on one side of the piston. A central tube is used to align the piston, which is seated on a Teflon bushing, and two Viton O-rings on the inner and outer surfaces for sealing. The tank is nominally pressurised to 451 psi (28.6 bar) with a three way solenoid valve connecting the N_2 tank to the H_2O_2 tank, and a frangible disk (burst disk) is present in the system as a pressure safety valve. All piping in the RCS uses 300 series stainless steel and fibreglass blankets are used where insulation is needed. The thrusters themselves employed a silver screen catalyst. Difficulties encountered during development centred on material compatibility, with a number of aluminium alloy solenoid valves deteriorating quickly. A final configuration using 300 series steels and Teflon chevron O-rings was chosen.

The X-15 aircraft also used H_2O_2 for its RCS and auxiliary power system, however in this system, shown in Figure 2.2, the H_2O_2 was stored in a Vicone or Teflon bladder inside of an ellipsoidal pressure vessel. Pressurised helium is used to exert a pressure on bladder, forcing H_2O_2 out of the tank through the standpipe, providing propellant flow regardless of acceleration direction. After 80 percent of the H_2O_2 has been consumed from the tank the bladder collapses in around the stand pipe and the pressure exerted by the helium is supported by the stand pipe and not the remaining H_2O_2 . When a certain pressure differential between the helium and H_2O_2 was reached a valve opened admitting helium to the top of the stand pipe and expelling the remaining H_2O_2 from the system. In this regime the craft had to maintain a positive normal acceleration to ensure H_2O_2 flow. This was acceptable for the flight

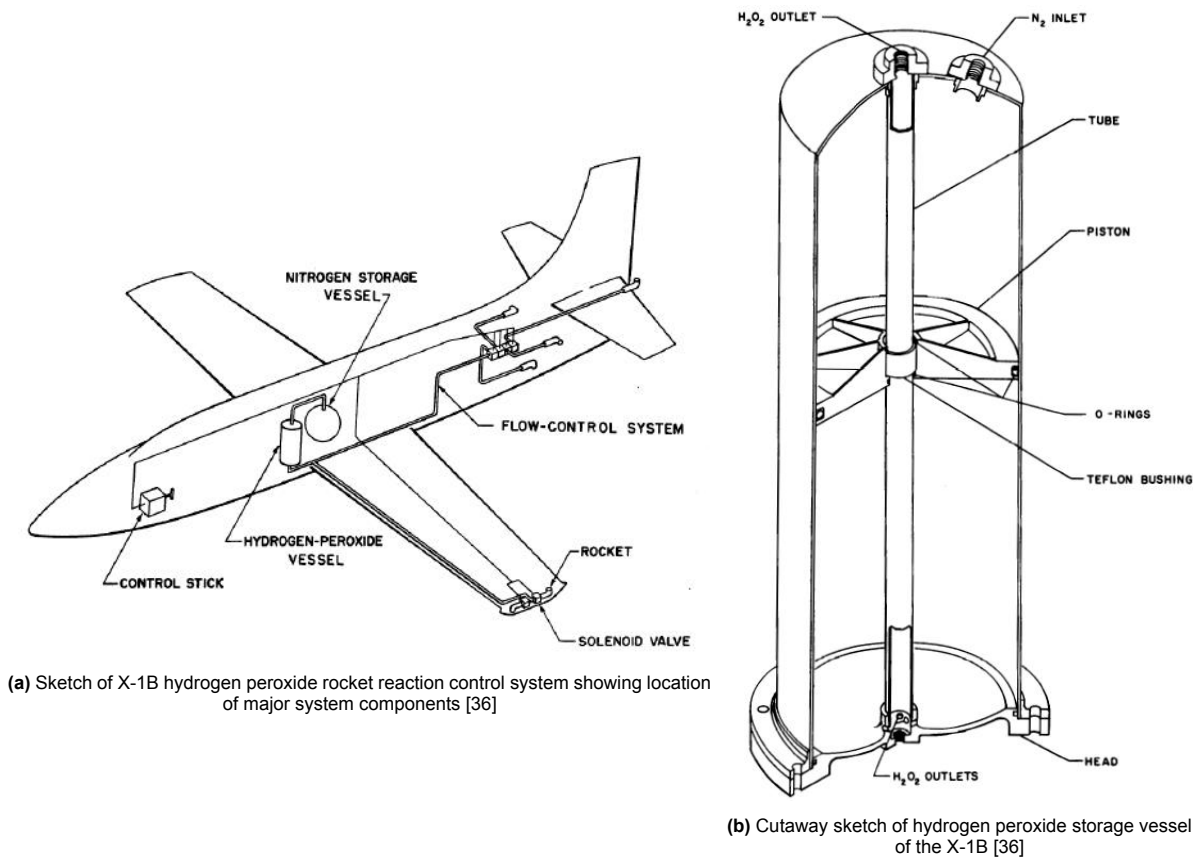


Figure 2.1: RCS system and storage method of H_2O_2 in the X-1B aircraft [36]

profile of the X-15. From a tank of 155 pounds (70.3 kg) of H_2O_2 12 pounds (5.4 kg) remained unusable in the system, giving a 92% expulsion efficiency [9].

Similar material compatibility challenges as encountered by the X-1 aircraft were also encountered during the X-15 development. The 90% concentrated H_2O_2 made it difficult to source a material for the bladder due to the long term exposure, repeated flexing cycles and low temperature environment. Teflon and Vitone were found as suitable candidates however both suffer from rupturing along crease lines when the propellant is expelled. Issues were also encountered when using aluminium alloys where hydroxide deposits caused issues, or a combination of aluminium alloy and steel alloy components when electrolytic action occurred at contact areas. All valves and tubing were eventually fabricated from stainless steel. The heat produced from decomposition made sealing difficult to achieve with welding being the solution, however this prevented catalyst inspection.

Syncom II was the first geosynchronous satellite entering orbit on the 26th of July 1963 and Syncom III was the first geostationary satellite entering orbit on 16th August 1964. Both satellites used a SR-12-1 H_2O_2 thruster for attitude control with remarkable success for the non-existent flight heritage. These two craft relied upon spin stabilisation as "The spin acceleration eliminates the zero "g" problem with fluids." [5]. As can be seen in Figure 2.3a the outlets of the tank are at its furthest point from the centre of rotation, where the centrifugal force will draw the propellant towards. Similarly the "Early Bird" or Intelsat I satellite employed H_2O_2 thruster for attitude control in combination with roll control for propellant control [26].

Figure 2.4a shows the layout of the Centaur rocket RCS, where each vehicle quadrant has a pair of lateral thrusters, and two opposing quadrants (II and IV) have two axial thrusters too. These axial thrusters are used for propellant management in the main LOX and LH_2 tanks as well as retro manoeuvres. These lateral thrusters are fired continually during coasting. The Centaur also utilises H_2O_2 to power the boost pumps providing the net positive suction heads to the main engine turbines. Each H_2O_2 bottle holds a positive expulsion bladder holding 108 kg of usable propellant each and is pressurised for expulsion by helium. One continuous manifold lines connects each RCS cluster to the bottle,

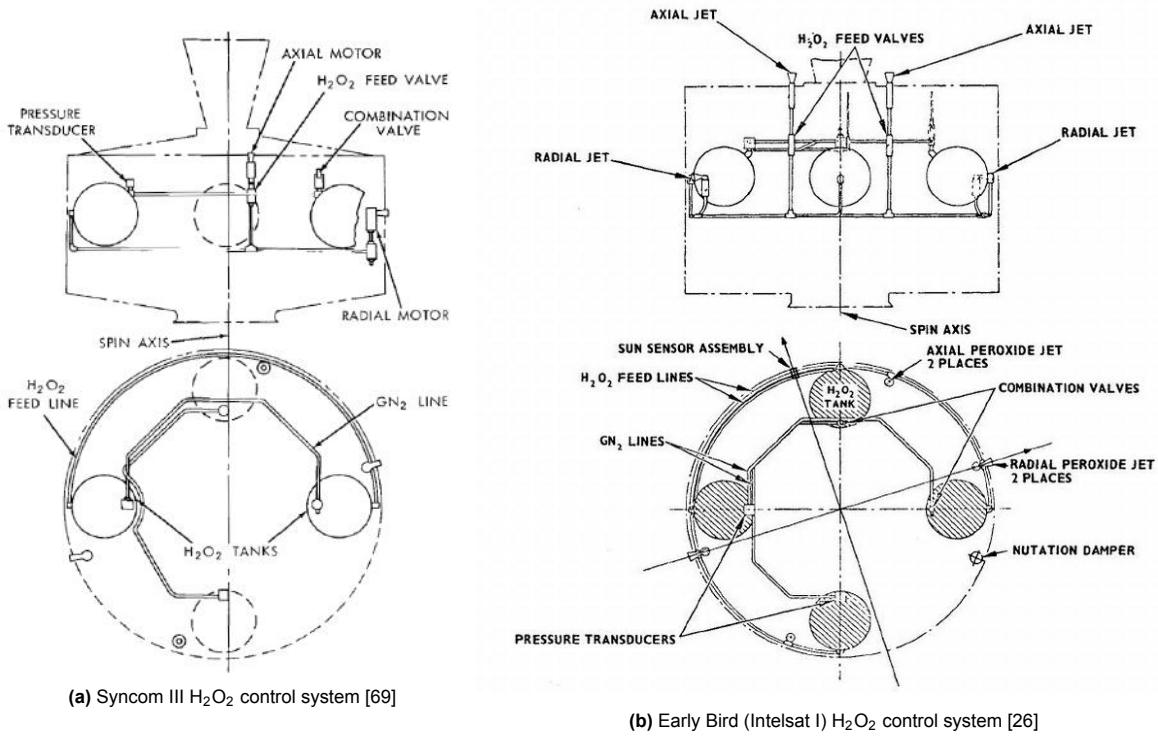


Figure 2.3: H₂O₂ control systems of early satellites

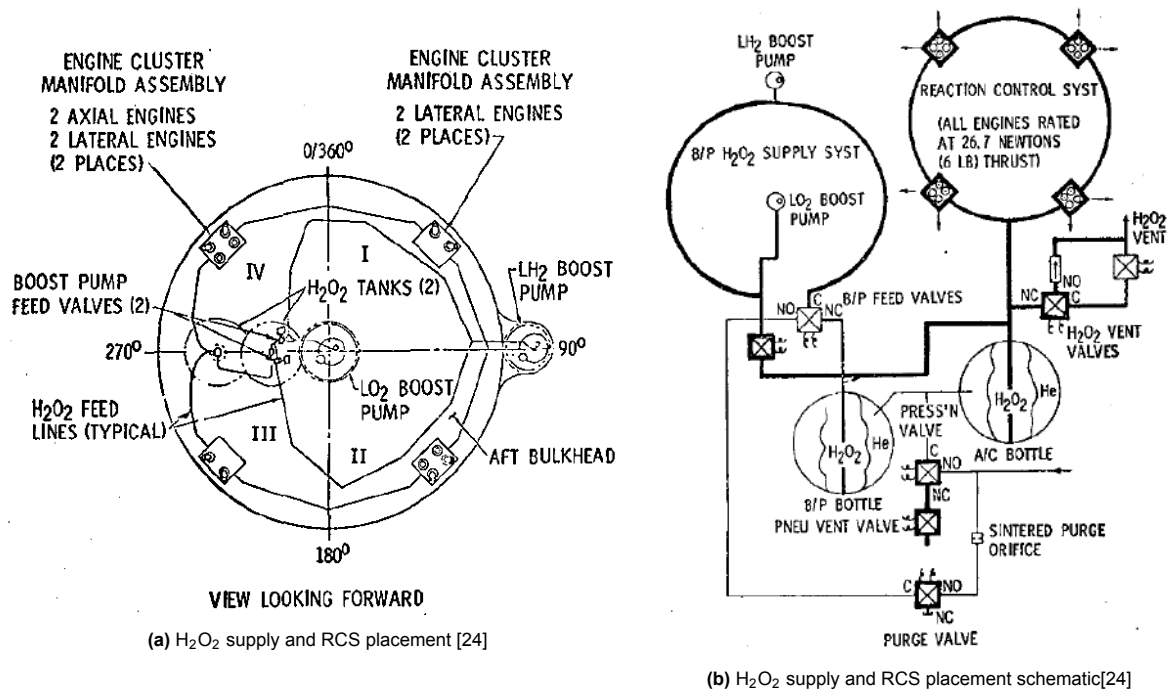


Figure 2.4: H₂O₂ control systems of the Centaur rocket [24]

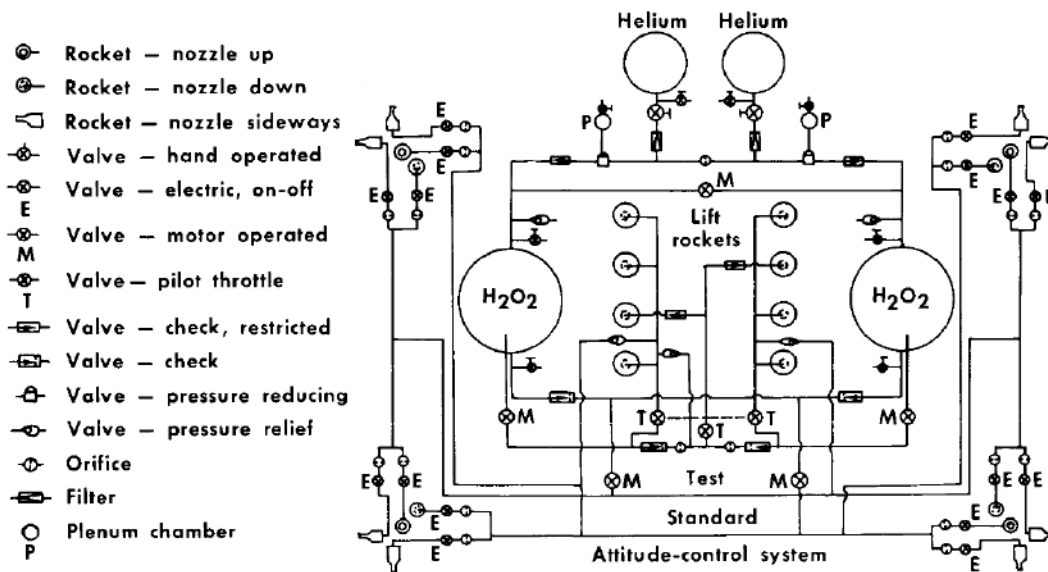


Figure 2.5: Schematic Drawing of H₂O₂ system used for lift rockets and attitude control in the LLRV [3]

Prior to the advent of liquid oxygen and nitrogen tetroxide as the bipropellant oxidisers of choice, H₂O₂ was used in several successful rocket engines, a variety of which are presented below, reproduced from [67].

- Me 163 Komet Rocket Plane
- Gamma 201 Rocket Engine
- Gamma 301 Rocket Engine
- AR Family of Rocket Engines
- LR 40 Rocket Engine
- PR 37 Rocket Engine
- BS 605

The aforementioned ATO engines developed by Walter were developed further with a hypergolic fuel comprised of hydrazine hydrate, methyl alcohol and copper salt (C-stoff) for use in the Me 163B rocket plane. Little documentation is available on the fuel transfer methodology of the Komet, aside from the tank placement behind and next to the pilot, and one reference to an incident when testing the top speed where "negative g load caused the fuel flow into the engine to be interrupted; this was followed by sudden engine shutdown" [52]. From this it may be presumed that supply of H₂O₂ to the engine was reliant on the direction of acceleration and not additional devices. This aircraft was studied by the UK after the second world war and much of the technology transferred to the Gamma rocket engine series, which powered the Black Knight sounding rocket and Black Arrow orbital launcher. Little literature could be sourced on the propellant management within these two vehicles, and it is presumed that as they were conventional launcher and the H₂O₂ was employed on the first two stages, that little additional devices were employed for propellant management.

In the U.S. the AR family of rockets were developed by Rocketdyne for the US Airforce, using HTP and kerosene, and was installed on both the North American F-86F(R) and the Lockheed NF-104A, the latter of which was a modified supersonic astronaut training vehicle. This aircraft employed a similar RCS to the X-15, and while little material could be sourced on the storage of H₂O₂, literature does mention similar material compatibility issues and leaks being encountered. Material compatibility issues were solved through electro-polishing of the stainless steel in contact with the oxidiser [71]. Reaction motors similarly developed the LR-40 running on 90% H₂O₂ and kerosene for the U.S. Navy. This engine was renowned for its compactness and ability to operate in all orientations, as well as its manned rating, though little literature is available on how these qualifications were achieved [68].

The use of H₂O₂ in these space applications began to taper off when the issues encountered with Hydrazine usage were overcome with the advent of ultra-high purity hydrazine and Shell 405, a hydrazine catalyst. Hydrazine possesses a vacuum specific impulse in the range of 220-240 s where as 90% H₂O₂ achieves in the range of 160-180 s, therefore when assessed purely on a performance metric hydrazine is the better propellant. However H₂O₂'s other properties, such as its high density,

storability, non-toxicity, lack of reactivity with the atmosphere, low vapour pressure, high specific heat, high O/F ratio, and compatibility with many pressurant gasses (all elaborated on in Section 2.2) have caused a resurgence of interest. On top of this the toxic and carcinogenic nature of hydrazine has led the European Chemicals Agency to consider outlawing its use, further spurring the development of alternate propellants [72].

While the exact areas of development occurring in the space industry are obscured by the secrecy surrounding commercial work some insight is provided by the scientific publications associated with this work, which will be reviewed in the Section 2.1.2 and Section 2.1.3. An indication of the renewed direction of research, at least in the U.S is provided by Anderson et al., particularly in the continued development of the AR2-3 engine and the USFE 10k engine [2]. The AR2-3 has since been used in orbit by the X-37 experimental spaceplane.

2.1.2. Modern Thruster Applications

Monopropellant

Company/Institution: Nammo Space (Nammo Raufoss AS)

Thrust_{vac}: Nominal 220 N (100 N - 250 N)

Isp_{vac}: 160 s for steady state firing, 130 s for pulsed firing

Concentration: 87.5%

Application: Roll and Attitude Control system, primarily for Vega-C Upper Stage

System Details: Total impulse 200'000 Ns, maximum single firing duration 120 s, propellant inlet temperature 15°C-80°C, silver catalyst [49]

Company/Institution: T4I - Technology for Propulsion and Innovation S.P.A.

Thrust_{vac}: 1-500 N

Isp_{vac}: 150s

System Details: Thrust time of >500 s [64]

Company/Institution: ALTAS.p.A., DELTACAT Ltd, University of Southampton, ESA-ESTEC

Thrust_{vac}: 5 N and 25 N variants

Isp_{vac}:

Concentration: 87.5%

Application: Catalytic bed research

System Details:

Bipropellant

Company/Institution: Nammo Raufoss AS

Thrust_{sea}: 30 kN

Isp_{vac}: 270 s

Concentration: 87.5%

Application: Nucleus sounding rocket

System Details: 40 s firing, total impulse 1'000 kNs [50]

Company/Institution: Laboratory of Advanced Jet Propulsion (LAJP)

Thrust_{vac}: 410 N nominal (370-450 N)

Isp_{vac}: 295 s - 327 s

Application: Orbit insertion for communication satellites, trajectory correction

System Details: Fuel - Ethanol, Inlet pressure 50-150 bar, max duration single fire 42000 s, cumulative duration fire - 30 000s, throughput 4000 kg [40]

Company/Institution: Benchmark Space Systems - Peregrine Thruster

Thrust_{vac}: 100 mN - 22 N

Isp_{vac}: 270 s

Application: Up to 6U cubesat, Orbit insertion, collision avoidance, station keeping, orbit transfer, life extension, RPO & Services

System Details: NHMF fuel, "patent pending micromixing technique eliminates the need for catalyst

beds”, configuration options 1750 Ns, 3500 Ns, 10000 Ns, up to 200 kNs [4]

Company/Institution: T4I - Technology for Propulsion and Innovation S.P.A.

Thrust_{vac}: 100-10'000 N

Isp_{vac}: 285 s smaller scale - 300 s larger scale

Concentration: 90%-95%

System Details: Fuel - paraffin wax[63]

Company/Institution: T4I - Technology for Propulsion and Innovation S.P.A.

Thrust_{vac}: 1-50 N

Isp_{vac}: 270 s smaller scale - 300 s larger scale

Concentration: 90%-95%

System Details: Fuel - Kerosene or other hydrocarbons[62]

Dual Mode

Company/Institution: Benchmark Space Systems - Halycon Thruster

Thrust_{vac}: 100mN - 22 N

Isp_{vac}: 140s -320 s

Application: Up to 6U cubesat, Orbit insertion, collision avoidance, station keeping, orbit transfer, life extension, RPO & Services

System Details: Butane optional as a fuel for dual mode, also sold as monopropellant. [4]

This section focuses on commercial thrusters as they are what is on the market and may end up as potential clients for the refuelling system being developed. Research grade thrusters studied appear to generally not operate at ideal design points such as concentration or thrust, or represent what customer desire, as their goal is instead to study design or performance behaviour, and thus are not elaborated on here.

Trends in H₂O₂ masses and volumes

Sufficient data is available from a number of these applications for the mass and volume of H₂O₂ stored in the system may be ascertained. For the thrusters typically a combination of the values for the thrust, specific impulse, burn time and total impulse are known, and using the equations set forth in Equation 2.1 the mass flow, total mass and H₂O₂ volume may be obtained. The density of H₂O₂ is taken as 1450 kg/m³. Table 2.1 shows these tabulated results, please note that the Orbit Fab system will be discussed in Section 2.3.

$$\begin{aligned}
 I_{tot} &= t_b \cdot T \\
 \dot{m} &= \frac{T}{I_{sp} \cdot g_0} \\
 M &= \dot{m} \cdot t_b \\
 V &= \frac{M}{\rho}
 \end{aligned}
 \tag{2.1}$$

Table 2.1: Tabulated properties of commercial and historical H₂O₂ uses with inferred H₂O₂ masses and volumes used. Published properties are in bold while the remainder are calculated

		T [N]	isp [s]	t_b [s]	Total Imp [Ns]	m_dot [kg/s]	m [kg]	V [m ³]	V [L]	V [mL]
T4i	Mono	1	150	500	500	0.001	0.340	0.000	0.234	23.434
		500	150	500	250000	0.340	169.895	0.117	117.169	11716.873
	Bi	1	300	100	100	0.000	0.034	0.000	0.023	2.343
		500	300	100	50000	0.170	16.989	0.012	11.717	1171.687
Benchmark	Bi - Peregrine	-	270	-	1750	-	0.661	0.000	0.456	45.566
		-	270	-	3500	-	1.321	0.001	0.911	91.131
		-	270	-	10000	-	3.775	0.003	2.604	260.375
X-15		-	-	-	-	70.360	0.049	48.524	4852.414	
Orbit Fab (100lbs)		-	-	-	-	45.359	0.031	31.282	3128.221	
Orbit Fab (200lbs)		-	-	-	-	90.719	0.063	62.564	6256.448	

2.1.3. Fuel Cell Applications

While the previous section covering modern thruster applications focused on thrusters readily available on the market the technology surrounding H₂O₂ fuel cells possesses a lower TRL and thus the information presented here is purely from academic sources. Due to this only a brief summary of H₂O₂ fuel cell technology is presented as it is a less concrete foundation on which to base the design of a H₂O₂ transfer system as it is further away from implementation. Fuel cells utilise a fuel, often hydrogen, and an oxidant, typically oxygen, to produce electricity through an electrochemical reaction. The hydrogen and oxygen are normally present in gaseous form, and for applications without the presence of ambient air, such as in space, the oxygen must be carried in a compressed tank. This hindrance has been overcome by the development of fuel cells employing H₂O₂ as an oxidant, with the advantage of being in liquid form and thus denser to store. H₂O₂ fuel cells have recently been developed using borohydride[77][10], metals[28][75], methanol[6][54], hydrazine[41] and biofuels[65] as reductants. H₂O₂ may also be used as a reductant as well as an oxidant, producing a fuel cell with only H₂O₂ as the working liquid, and a number of these direct H₂O₂ fuel cells have been recently researched [38] [74] [73] [55]. Research surrounding fuel cells for use in space have focused on energy-density as a criterion of primary interest and sodium borohydride (NaBH₄) has emerged as a favourable reductant [48][44]. These sources have utilised H₂O₂ with a wide range of concentrations. The performance of the fuel cell is directly related to the concentration of the H₂O₂ with higher concentrations resulting in higher output power. Typically above 65% concentration is required for the fuel cell to equal the energy density of fuel cells with more common oxidants and reductants, and thus this value will be taken as the guiding value for the design of the H₂O₂ system in question. These publications also highlight the great advantage that lies in the H₂O₂/NaBH₄ fuel cells ability to regenerate power due to the dual liquid combination.

2.2. Hydrogen Peroxide: Chemistry and Considerations

While H₂O₂ is considered a safer, non-toxic alternative to other rocketry propellants it is still an energetic material and requires a number of considerations to be taken to mitigate hazards that may otherwise be presented. H₂O₂ may present a detonation, explosion, fire, and spillage hazard, and its susceptibility to these phenomena varies considerably under different concentrations and pressures [14]. Contaminants may also drastically alter the behaviour of H₂O₂ making it much more susceptible to explosion, detonation and fire. The decomposition of H₂O₂ which may be initiated by the presence of contaminants, particularly organic contaminants, is highly exothermic and produces a large amount of heated oxygen and steam according to $\text{H}_2\text{O}_{2(l)} \rightarrow \text{H}_2\text{O}_{(l)} + 1/2\text{O}_{2(g)}$ $\Delta H = 97.4$ kJ/mole. Inherently H₂O₂ is thermodynamically unstable and will slowly decompose. This rate of decomposition is accelerated by the presence of heat, be it from an external source or the decomposition itself. Venting is recommended on vessels storing H₂O₂ in order to prevent over pressurisation by exhausting ullage gasses, prevent the accumulation of oxygen, and to remove heat from the vessel. It is found that H₂O₂ in the vapour phase is more susceptible than in the liquid phase to fire, detonation and explosion. Liquid H₂O₂ shows no sensitivity to impacts, it is sensitive to shocks produced by explosions, and as already mentioned shows significant thermal sensitivity. Regarding thermal sensitivity, it is found that

H₂O₂ in general is thermally unstable if heated above 100°C and above 95% concentration, though the threshold is lowered on either of these values if the other is increased [14].

This section is structured as follows Section 2.2.1 covers the material compatibility of a variety of metal alloys as well as some popular sealing materials with H₂O₂, and Section 2.2.2 covers a number of design guidelines and system handling approaches when working with H₂O₂.

2.2.1. H₂O₂ Material Compatibility

The interaction between H₂O₂ and materials that it is in contact with can potentially be unfavourable for a number of reasons (reproduced from Davis et. al [14]):

- The majority of materials induce or catalyse the decomposition of H₂O₂ and lower its concentration.
- H₂O₂ can change the nature of the materials it contacts through corrosion, absorption and other chemical processes which may both degrade the performance of this material and hinder the function of a catalyst on the H₂O₂.
- Products formed through the reaction of H₂O₂ and materials may be hazardous or detrimental to the system (eg. insoluble products blocking filters)
- H₂O₂ has the potential to react violently, either slowly or suddenly with some materials and contaminants which may result in the destruction of a system.

When assessing material compatibility it is important to consider the quantity, phase, temperature, concentration, and presence of stabilisers and contaminants in H₂O₂. For the material in contact it is important to assess the bulk chemical composition, the surface chemical composition, the surface characteristics, passivation, cleanliness and surface area in contact with liquid and vapour. Beyond these factors elements such as exposure time, temperature, and acceptable levels of degradation of H₂O₂ or the material should be considered. It is also highlighted by Davis et. al. that much of the existing compatibility data for H₂O₂ does not cover newly developed materials, and that extrapolating short term compatibility data over long time scales can often be inaccurate[14].

The classification system used to assess material compatibility with H₂O₂ is outlined below. This classification is based off of the decomposition rate when in contact with a given material and the classification varies depending on the concentration of the H₂O₂.

- **Class 1:** Materials Satisfactory for Unrestricted use with H₂O₂. Typically used for storage containers.
- **Class 2:** Materials Satisfactory for Repeated Short-Time Contact with H₂O₂. Maximum of 4 hours at 72°C or 1 week at 22°C. Typically used for valves and pumps in transfer lines or tanks.
- **Class 3:** Materials Satisfactory for Short-Term Contact Only, Less than 1 minute at 72°C and 1 hour at 22°C for unpressurised systems. Single use only.
- **Class 4:** Not recommended for use with H₂O₂. These materials can cause significant decomposition of H₂O₂ over short contact times.

Section 2.2.1 and Section 2.2.1 outline which classification a number of commonly used elastomers and seals, and metal alloys fall in to, for 90% H₂O₂ and 98% H₂O₂ at 21 °C as presented in the Hydrogen Peroxide Handbook [17] and re-tabulated by [51]. Section 2.2.1 details materials to be avoided when working with H₂O₂. As previously stated these classifications are purely for relative assessment of material compatibility, which remains subject to concentration, temperature, pressure, surface finish and a number of other factors. Appendix A provides a slightly more extensive list with some additional details provided for specific temperature ranges and applications of materials.

Elastomers and Seals

Table 2.2: Compatibility of Elastomers and Sealing Materials with H₂O₂ at 21 °C[17][51]

Material	90% H ₂ O ₂	98% H ₂ O ₂
Buna N	Class 4	Class 4
Butyl Rubber	Class 4	Class 4
Delrin	Class 4	Class 4
Kel-F	Class 1 to 3	Class 1 to 3
Polyethylene	Class 2 to 4	Class 2 to 4
Silicon	Class 2 to 4	Class 2 to 4
Teflon (Virgin)	Class 1	Class 1
Viton A	Class 2 to 4	Class 2 to 4
Viton B (805)	Class 1	Unknown

Metals

Table 2.3: Compatibility of Aluminium Alloys with H₂O₂ at 21 °C[17][51]

Material	90% H ₂ O ₂	98% H ₂ O ₂
355	Class 2	Class 3
B356	Class 1	Class 1
1060	Class 1	Class 1
1160	Class 1	Class 1
1260	Class 1	Class 1
2014	Class 4	Class 4
2017	Class 4	Class 4
2024	Class 3	Class 4
5254	Class 1	Class 1
5652	Class 1	Class 1
6061	Class 2	Class 2
7072	Class 1	Class 1
7075	Class 4	Class 4

Table 2.4: Compatibility of Stainless Steel Alloys with H₂O₂ at 21 °C[17][51]

Material	90% H ₂ O ₂	98% H ₂ O ₂
301	Class 2 / 3	Class 2 / 3
302	Class 2 / 3	Class 2 / 3
304	Class 2	Class 2
316	Class 2	Class 2
329	Class 3 / 4	Class 3 / 4
347	Class 2	Class 2
443	Class 4	Class 4
446	Class 4	Class 4

Table 2.5: Compatibility of Inconel Alloys with H₂O₂ at 21 °C[17][51]

Material	90% H ₂ O ₂	98% H ₂ O ₂	Temp.
718	Class 2	Class 2	70 F
718	Class 4	Class 4	151 F

Materials To Avoid

- Beryllium
- Cadmium
- Chromium
- Cobalt
- Columbium
- Copper
- Gold
- Iron
- Lead
- Magnesium
- Manganese
- Mercury
- Molybdenum
- Nickel
- Platinum
- Silver
- Sodium
- Titanium
- Tungsten
- Zinc

2.2.2. H₂O₂ Design Guidelines and System Handling

A number of considerations must be taken into account when handling H₂O₂ both by personnel and by a system. For the protection of personnel appropriate PPE and facilities are required, in the case of 90% H₂O₂ these take the form of polyester or acrylic full cover clothing, with rubber or nitrile shoes and gloves, as well as appropriate respirators and monitoring equipment depending on the circumstances. As the propellant depot in question will be automated and function remotely it is more pertinent in this subsection however to discuss the engineering considerations required for handling H₂O₂.

Systems that handle H₂O₂ must account for its corrosive and oxidising properties, as well as its propensity to decompose and release both heat energy and gas. As the decomposition of H₂O₂ occurs on material surfaces, parts of a system where the surface-to-volume ratio is high are likely to encounter this issue more often, such as pumps and valves compared to tanks. This issue is further exacerbated by components with rough surface finishes. As feedsystem components rarely are designed to allow for an ullage volume very little gas production is needed within these lines to produce a large rise in pressure. Trapped volumes between valves or within valve components themselves may also result in gas formation and over pressurisation. Thus pressure relief systems, and operational considerations that ensure no trapped or sealed compartments are crucial for a safe and long lived system. Expected decomposition rates and knowledge of a systems geometry and finishes can assist the designer in sizing pressure relief systems, however in the event that H₂O₂ undergoes rapid decomposition due to contact with contaminants or a heat source then the large production of heat and steam will likely be catastrophic for a system. In order to avoid this all materials must be carefully chosen and passivated before use [14].

In order to prevent leaks it is encouraged to minimise the number of sealed connections in a system. Thus, for example, elbow joints should be replaced with bent piping. Threaded connections are also discouraged as threads present a significant surface area for H₂O₂ to come into contact with, decompose and generate gas. Therefore welding is the preferred method of joining, however care must be taken to avoid weld spatter on the interior and weld locations should be smoothed if possible. Lastly, in the presence of H₂O₂, dissimilar metals in contact may undergo electrolytic corrosion. If contact of dissimilar metals is unavoidable then they may be insulated from one another with plastic, or the metal that corrodes (the anodic metal) should have a larger surface area than the other (the cathodic metal)[14].

During the final assembly of systems that utilise H₂O₂ a number of steps should be followed. Clean, degreased tools should be used, by operators with clean, lint-free gloves and outer garments. Components should be assembled in a clean, dust free environment and assemblies should be protected with polyethylene film or caps. Before assembly components should be cleaned and passivated. Cleaning involves the removal of contaminants from a material surface while passivation involves the formation of an oxide layer on the material surface through chemical treatment. The general process for the passivation of metal surfaces consists of [59];

- Grinding to remove weld spatter and smooth out scratches.
- Degreasing with a trisodium phosphate/sodium metasilicate solution to remove oil and grease films.
- Pickling with a sodium hydroxide solution to chemically clean the surface.

- Passivating with a nitric acid solution to form an oxide film.
- Testing with dilute HP solution to ensure successful treatment.

Further details as well as further sources for passivation of specific alloys and components/systems for various applications are provided by Davis et. al. [14].

2.3. Refuelling System: Relevant Work and Current Developments

This section will briefly present an overview of the relevant missions and research to depot and in-orbit propellant transfer technology carried out by space agencies and commercial entities both historically and currently. Table 2.6 displays a summary of relevant missions, projects and companies who have historically or are currently investigating in-orbit propellant transfer.

Orbit Fab based in San Francisco is the best example of a contemporary propellant depot project. Orbit Fab has filed three patents focused on their general storage and transfer architecture[20], their concept for expandable tanks[19] and the third on their refuelling interface[18]. While the patents are rather vague it is implied that a bladder method is employed to transfer the propellant where a stored gas or gas generator is used to pressurise the bladder system. Details are also provided regarding expandable tank systems and the possibility is explored to use the pressurising gas to provide structural rigidity to the walls of these expanding tanks. It is also mentioned that there is potential to produce the propellant on the depot and the propellant may be used in a gas generator. While the use of the bladder system in tandem with the expandable tank architecture is logical as folding or stowing other transfer methods inside of an expanding tank would be near impossible, it is unclear how these tanks are refilled, presumably by separate resupply launches. The interface system developed by Orbit Fab is detailed in Section 2.5. While expandable pressure vessels in space are being intensively researched, exhibited by the BEAM module demonstrated on the International Space Station by Bigelow Aerospace, inflatable space structures still possess a relatively low TRL compared to other conventional structure designs [66]. Given that depot technology itself is of a low TRL, combining two very novel systems may prove to be a great technical risk for Orbit Fab.



Figure 2.6: Orbit Fab Geostationary Depot [56]

The Orbital Express mission conducted in 2006 aimed to demonstrate a number of technologies deemed necessary for routine servicing such as autonomous rendezvous, docking, propellant transfer and replacement of hardware. The mission consisted of two spacecraft as depicted in Figure 2.7 with the service spacecraft ASTRO and the client spacecraft NEXTSat. The design of the propulsion system on NEXTSat allowed for a variety of client types to be simulated from diaphragm of PMD tank blow-down systems with only re-compression ullage to pressure regulated systems with venting required. The client spacecraft systems are mostly passive with the active elements being present on the servicing craft for weight saving purposes.

Table 2.6: Survey of historic and current in-orbit transfer/servicing

Company	Nation	Craft	Purpose	Status
Orbit Fab	USA	Tanker 001 Tenzing	Orbital fuel depot. Currently has carried out testing on the ISS. Aiming to launch their Tenzing prototype in 2021 carrying HTP. Have developed their own fluid transfer interface system (RAFTI) compatible with MMH, UDMH, Water, H2O2, Methanol, Kerosene, Green Monoprops, Isopropyl Alcohol, HFE, N2O4.	In-space testing complete, launched 2021
Benchmark Space Systems	USA	Sherpa tug	Has developed a number of propulsive systems including the Halcyon thruster system using HTP, partnered with OrbitFab to make the Tenzing depot. Offers Halcyon thrusters to customer who can then refuel with Orbitfab. Unsure if the Sherpa tug also uses H2O2. Working with Starfish systems developing precision in orbit rendezvous for servicing.	In development, offering products
MDA	Canadian/USA	Space Infrastructure Servicing	Depot for servicing and refuelling communication satellites in GEO. Working with SES, previously Intelsat and DARPA. System capable of servicing and refuelling spacecraft that are not equipped for it.	In development
Roscosmos	Russia	Progress	Transfers UDMH and NTO from refuelling module to space station using bladder system.	In service
ESA	EU	Automated Transfer Vehicle	Uses the same system as Progress	Successful but discontinued
Vivisat / Orbital ATK	USA	Mission Extension Vehicle	Essentially a tug vehicle capable of docking near the motor of a unfuelled or malfunctioning satellite and repositioning it	Successful and in service
DARPA	USA	ASTRO (Orbital Express programme)	Autonomous satellite docking, refuelling (hydrazine) and component replacement	Completed Successfully
NASA	USA	Robotic Refuelling Mission	ISS based series of experiments conducted to test in space refuelling technologies, primarily using representative hardware of satellites not designed for this function. Used a borescope inspection tool for internal satellite repair work. Mainly seems to have tested NTO and cryogenics.	Numerous experiments conducted successfully
United States Naval Academy	USA	Repair Satellite Prototype	Minor in orbit repair operations conducted by 3U CubeSat	In orbit, undefined of progress
ULA	USA	Advanced Cryogenic Evolved Stage (Vulcan / Centaur V)	Extended life upper stage investigated for use as in orbit propellant depot. Discontinued however ULA has continued research in depot architecture as seen in numerous academic papers.	Discontinued
SpaceX	USA	Starship	Developing propellant transfer technology for refuelling of Starship in LEO. Granted funding by NASA under the tipping point programme to investigate this and demonstrate the transfer of 10 metric tons of LOX between tanks	In development
Eta Space, Lockheed Martin, ULA	USA		Both companies received funding from NASA under the tipping point programme to investigate different methods of cryogenic management systems	In development

Maxar	USA	OSAM-1 Restore-L	Service, assembly, manufacture test mission, focusing on robotics and automation aspects.	In development
Astroscale	USA/UK	Lex	Developing a range of vehicles for orbital inspection, servicing, debris detection & removal	In development
ULA/NASA	USA	CRYOTE	Testbed for cryogenic handling that sits as a secondary payload on an Atlas V.	In development
Cislunar Development Company	USA		Developing a full system architecture for space tugs, shuttles and depots, seems to be very vague and still on paper.	In development
DLR/OHB/Astrium	German	DEOS	Technology demonstration mission from DLR with numerous subcontractors, OHB primary contractor. Two craft will be put into orbit after which they will rendezvous, demonstrate technologies and deorbit together. Unsure if refuelling is included.	Cancelled?
CNSA	China		Has apparently completed in orbit refuelling tests, very minimal information available	?

The ASTRO fluid transfer and propulsion system is made up of the following elements and a schematic is shown in Figure 2.8:

- A regulated pressure source to supply the fluid transfer system on both spacecraft as well as the ASTRO propulsion system itself
- A surface tension PMD fluid transfer tank
- A fluid transfer pump providing flows from 0.03 to 0.21 lbm/sec (0.014 - 0.095 kg/s)
- Propellant gauging hardware
- A vent system
- A propellant tank for thruster use (hydrazine can be transferred from the fluid transfer system to the propulsion system)
- Sixteen 4-N hydrazine thrusters for DOF control
- A servicing interface electronics unit for control of the coupling, pump, and a large number of valves as well as for telemetry conditioning for transmission across the spacecraft bus.

The pump is a derivative of the Space Shuttle auxiliary power unit which was turbine driven whereas this one is driven by a DC motor. The fluid transfer tank uses a standard shell with a customised PMD allowing for positive ullage bubble position during high fill-fraction-venting activities. The flow sensor is mechanically passive and is adapted from one used on the F-18 aircraft. The Orbital Express mission successfully demonstrated a number of activities being:

- Transfer of monopropellant hydrazine to and from ASTRO and NEXTSat, simulating a variety of potential operational client refueling scenarios:
 - Closed-loop transfers (propellant in, pressurant back) (from ASTRO to NEXTSat shown in Figure 2.9a, from NEXTSat to ASTRO shown in Figure 2.9b)
 - Ullage recompression (no pressurant exchange) (shown in Figure 2.9c)
- Transfer to surface tension element (PMD) tankage as well as non-PMD tankage
- Mated system leakage integrity
- Pump and pressure-fed transfers
- Propellant gauging – integrating (flow rate sensor, pump speed) and static (delta PVT, thermal capacitance)
- Liquid leak-free demate, including pre-demate venting.

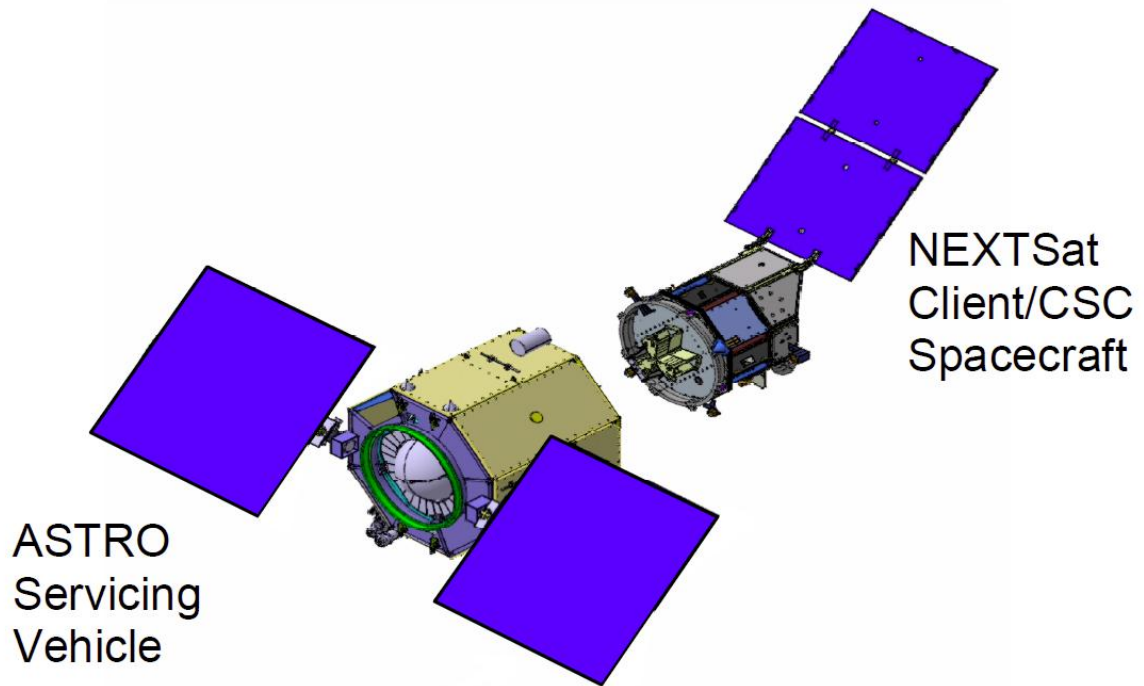


Figure 2.7: Overview of Orbital Express Spacecraft ASTRO and NEXTSat [15]

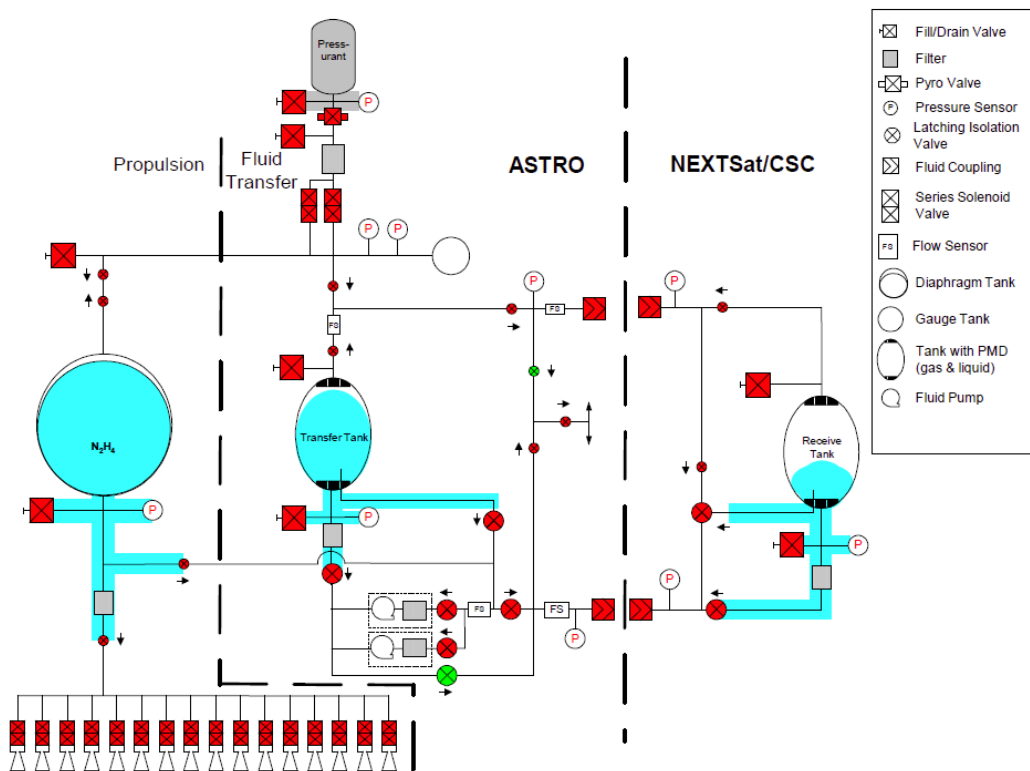
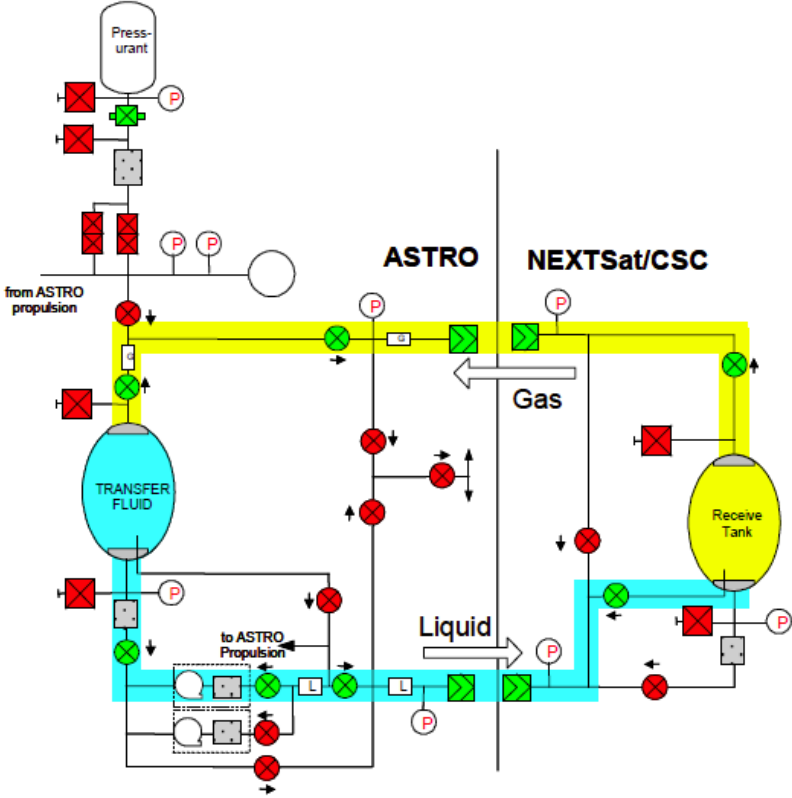
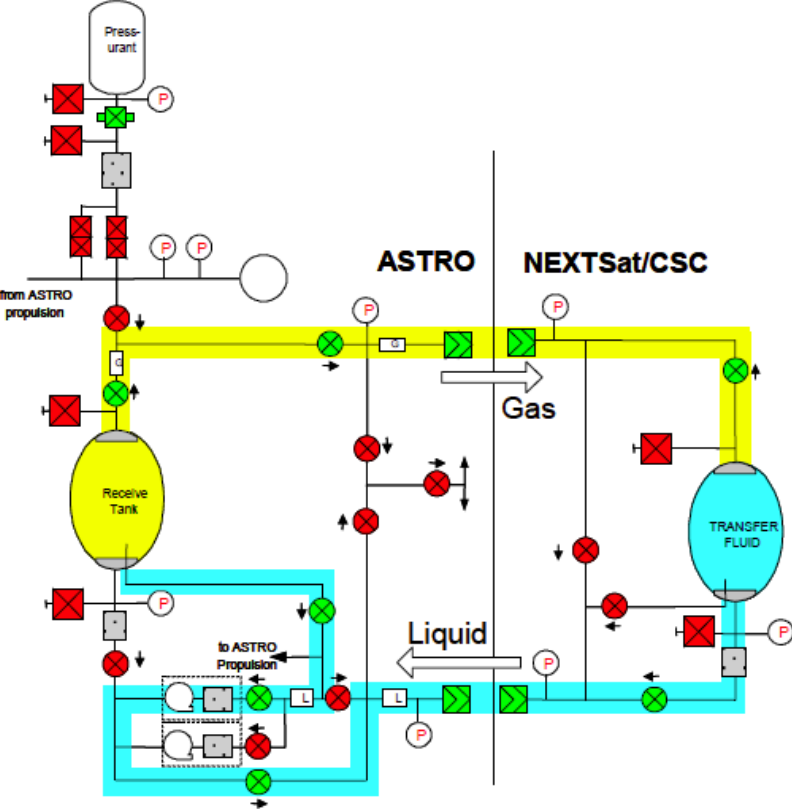


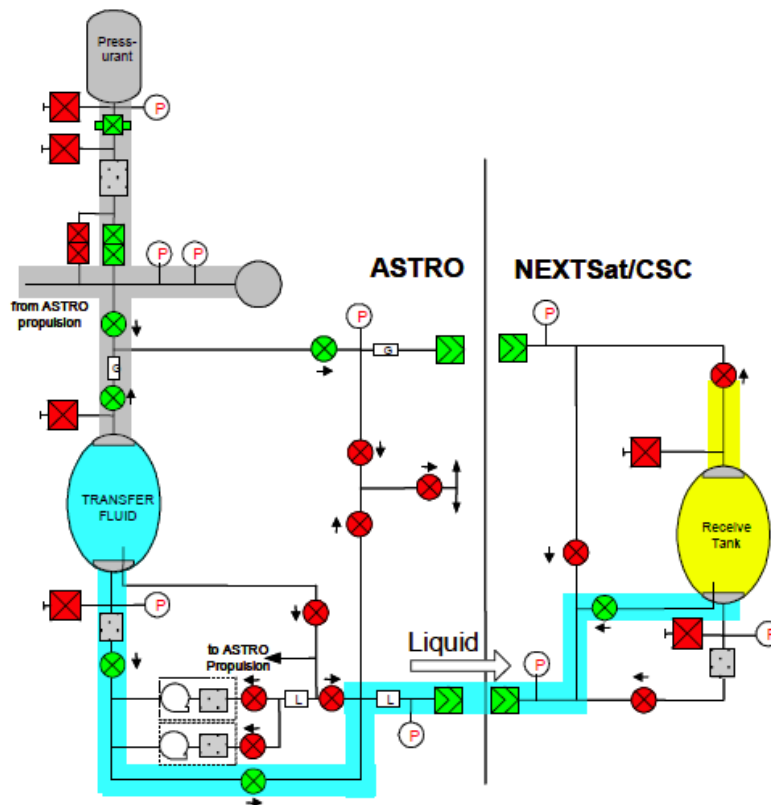
Figure 2.8: Fluid Transfer and Propulsion System Schematic for the Orbital Express Mission [15]



(a) Closed -Loop Fluid Transfer - ASTRO to NEXTSat [15]



(b) Closed -Loop Fluid Transfer - NEXTSat to ASTRO [15]



(c) Ullage Recompression Fluid Transfer – ASTRO to NEXTSat [15]

Figure 2.9: Different fluid transfer paths of the Orbital Express Mission [15]

The Orbital Express system is designed to minimise the hardware required to be added to a client spacecraft, being only a passive-half of the capture mechanism, one to two passive half couplings, one to four isolation valves, one pressure transducer and the associated lines, heaters, structures and multi-layer insulation. It is anticipated by the system designers that this would add between 15 and 25 kg to a client craft. It is foreseen that particularly client tanks with PMD must undergo the most adaption as an additional mode of operation must now be considered, however the potential increase in system weight and cost is always offset by the benefits on on-orbit resupply [15].

While the Progress spacecraft possesses a particularly high flight heritage it has proven rather difficult to find any information regarding the system it uses to transfer UDMH and NTO to the International Space Station, other than the fact that a bladder system is employed. While a number of small tests have been carried out on parabolic flights, or in-orbit for depot systems, servicing craft and transfer methods, the main focus is on developing these technologies for single use missions and in particular for cryogenic propellants, and neither of these applications are overly relevant for the transfer system to be developed.

2.4. Refuelling System: Transfer, Management and Handling Methods

The primary purpose of the system under consideration is to transfer H_2O_2 potentially from depot station or refuelling craft to a receiver vehicle. Thus this section will describe the numerous manners in which this transfer and a number of associated tasks may be accomplished. Besides from purely transferring propellant a number of different aspects must be considered when working with fluids in space. Given the microgravity environment liquids will tend to cling to the exterior of a tanks walls as well as creating spheres of liquid floating through a volume of gas in the tanks centre. This unpredictable nature of the fluids dynamics requires more novel methods for tasks such as transferring the propellant that would be a simple operation under gravity. Beyond purely transferring, the management and handling of the propellant must be considered too. Propellant management covers the area of maintaining propellant

coverage of the outlet of a tank and ensuring that no vapour enters the lines when a transfer method is employed. These management methods are fulfilled using propellant management devices and are passive, ensuring that this function is continually fulfilled. Another issue that may be encountered when utilising fluids in a microgravity environment is that of sloshing and vortexes. These phenomena may effect your vehicle dynamics and vapour ingestion and are also treated using propellant management devices. Propellant handling on the other hand defines methods used to orient over a tank outlet during specific moments. In this manner this method is active, only orienting the propellant at key moments such as during station keeping manoeuvres or other burns, and letting it float and slosh around at other times.

This section will first treat the areas of propellant transfer in Section 2.4.1, management in Section 2.4.2, and handling in Section 2.4.3 before finalising with a overview of propellant thermal control in Section 2.4.4 and propellant mass gauging methods in Section 2.4.5.

2.4.1. Propellant Transfer Methods

Propellant transfer methods will be defined here as the transfer of propellant from one tank, system or vehicle to a secondary tank, system or vehicle. A variety of methods, based on rather dissimilar principles, exists for the purpose of transferring propellant, with different methods being more or less appropriate for different applications. Boretz presents three major requirements that exist on a transfer system, being the total quantity of propellant to be transferred, the time allotted for this transfer to take place, and the type and properties of the propellant to be transferred[7]. In turn these parameters result in further important factors such as the flow rates required between the two systems, the power for the associated mechanisms, the loading accuracy of the second vessel etc. Beyond these purely technical parameters more systems and project based considerations come into account such as reliability, weight, cost, safety, development risk and compatibility with existing systems, infrastructure and regulations. On top of these considerations Boretz also outlines the aspects of the environment these systems will operate in that are critical in their design, being orbital altitude, hard vacuum, solar radiation, micrometeoroids, solar flares, drag make-up and station keeping, and orbital debris[7].

A number of the methods presented here may be used both to transfer propellant from tank to tank, but are also primarily used as methods to transfer propellant from tanks to combustion chambers in propulsion systems. Thus Figure 2.10 is included below as a reference from Sutton in the following discussion.

Tank replacement is one of the more straightforward concepts where an empty vessel is removed from the vehicle to be refilled after which a new full tank is attached in its place. This method requires the use of some form of (quick)disconnect couplings and may or may not require an extra vehicular activity or robotic assistance depending on the system design [7]. No example of this method being used in practise could be found, and when considering the added dry mass imposed by the ability to attach and remove tanks, as well as complexity added by conducting these operations in a space environment, it is logical that this method seems to be given greater consideration for terrestrial applications, such as swapping out the tanks of refuelling vessels on the lunar surface [12].

Bladders and pistons are employed to transfer propellant by means of expulsion. Such "positive expulsion devices" are commonly used for the pressurisation of tanks in pressure fed systems and maintain a mechanical separation between the pressurant and the working fluid. This is can be required for a number of reasons, namely;

- Preventing the pressurant gas from dissolving in the working fluid/propellant. This would dilute the propellant and reduce specific impulse.
- To allow for hot, often reactive, gasses, perhaps produced by a gas generator or through heat exchange with a combustion chamber, to be used as a pressurant. This method may reduce the total mass of the pressurant system and this mechanical separation prevents chemical reactions occurring between the pressurant and the propellant and reduces heat transfer to the propellant.
- In the servicing of some systems a toxic propellant may need to be vented without the risk of operators or other system components being exposed to toxic vapours.

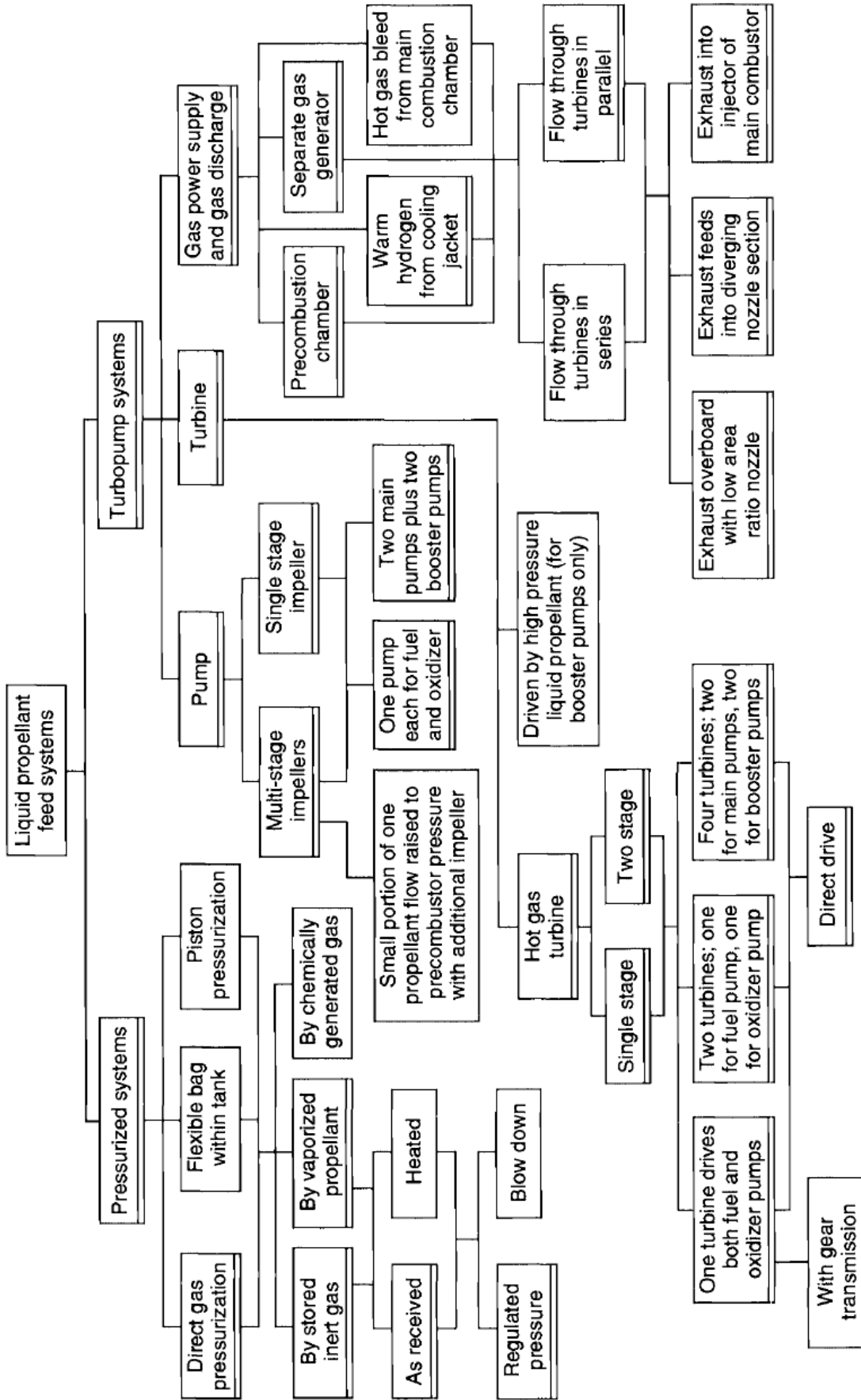


Figure 2.10: Design options of feed systems for liquid propellant rocket engines. The more common types are designated with a double line at the bottom of the box [6.1]

It is worth noting that the use of a piston as an expulsion device means that the centre of gravity is accurately known, and sloshing and vortex effects are easily prevented. It is noted by Boretz that bladders face a number of shortcomings in their permeability by certain pressurant gases such as nitrogen and helium, as well as their production complexity [7]. This source is somewhat older however and thus these may no longer be limiting factors. A number of these positive expulsion devices and their properties are outlined in Table 2.7 and presented in Figure 2.11.

Table 2.7: Comparison of Propellant Expulsion Methods for Spacecraft. Reproduced from [61]

Selection Criteria	Single Elastomeric Diaphragm (hemispherical)	Inflatable Dual Elastomeric Bladder (Spherical)	Foldable Metallic Diaphragm (Hemispherical)	Piston or Bellows	Rolling Diaphragm
Application	Extensive	Extensive	Limited	Extensive in high acceleration vehicles	Limited
Weight (normalised)	1	1.1	1.25	1.2	1
Expulsion Efficiency	Excellent	Good	Good	Excellent	Very Good
Maximum Side Acceleration	Low	Low	Medium	High	Medium
Control of COG	Poor	Limited	Good	Excellent	Good
Long Service Life	Excellent	Excellent	Excellent	Very Good	unproven
Preflight Check	Leak test	Leak test	Leak test	Leak test	Leak test
Disadvantages	Chemical deterioration	Chemical deterioration; fits only into a few tank geometries	High-pressure drop; fits only certain tank geometries; high weight	Potential seal failure; critical tolerances on piston seal; heavy	Weld inspection is difficult; adhesive for bonding to wall can deteriorate

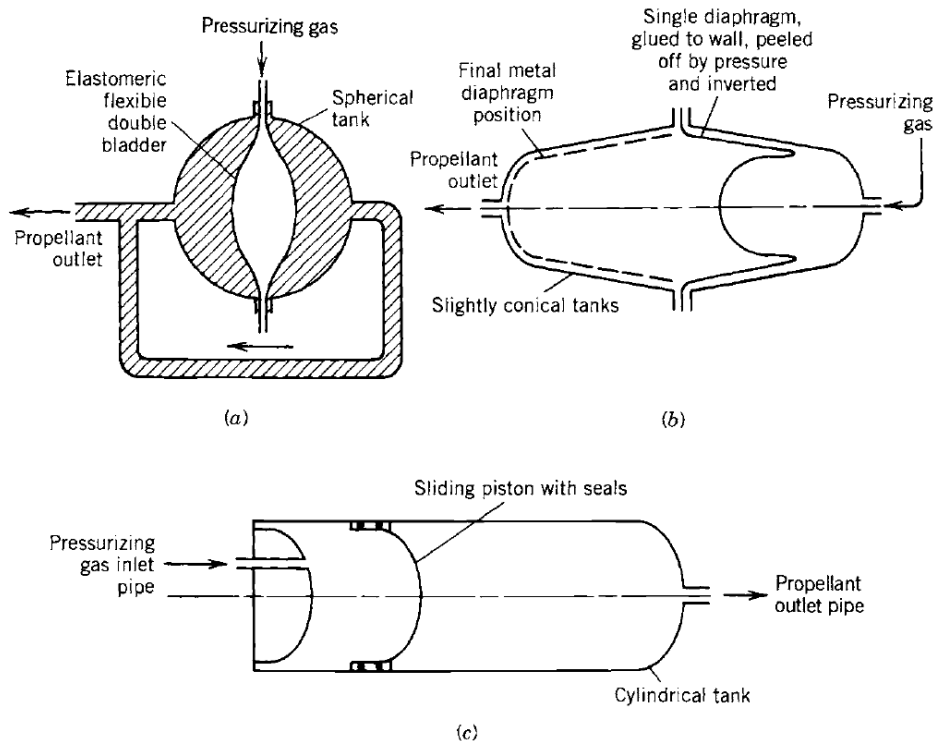


Figure 2.11: Three concepts of propellant tanks with positive expulsion: (a) inflatable dual bladder; (b) rolling, peeling diaphragm; (c) sliding piston. As the propellant volume expands or contracts with changes in ambient temperature, the piston or diaphragm will also move slightly and the ullage volume will change during storage [61]

Another method of propellant transfer is by means of applying a linear or angular acceleration field. This method is portrayed in Figure 2.12 where two vehicles have rendezvoused, coupled their propellant tanks and an acceleration is applied causing the propellant to drain under the influence of artificial gravity. Boretz stresses that in order to achieve reasonable transfer times either significantly larger accelerations must be applied or large cross sectional area transfer lines must be used, limiting this methods usability.

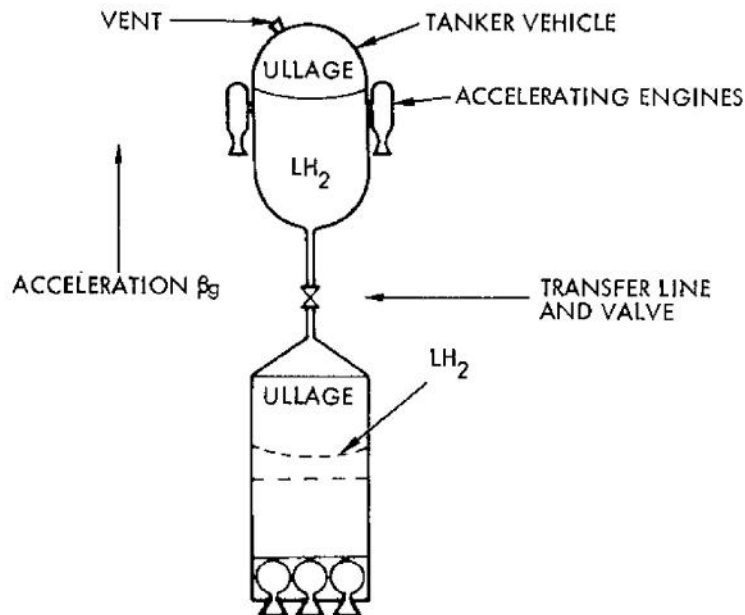


Figure 2.12: Linear acceleration propellant transfer [7]

Propellant may also be transferred using a pump, which in turn may be powered by electric means or using a turbine. Such pumps are often used for high thrust, long duration applications such as booster and sustainer stages of launch vehicles. These pumps also require the propellant to be pressurised in order to prevent cavitation (a parameter referred to as Net Positive Suction Head (NPSH)), however to a lower degree than purely gas pressurant means. Recently a number of microlaunchers have begun using batteries to power these pumps however turbines have been the preferred method for most rocketry applications. These turbines utilise a number of different engine cycles where the hot gasses powering the turbine are either generated separately to the main combustion chamber or tapped off from it, and once these gasses have exited the turbine they are either dumped to the atmosphere, injected into the nozzle or directly into the main combustion chamber. An example of H_2O_2 being used in such a cycle is the V2 missile where decomposed H_2O_2 was used to power the turbine [61].

Gas pressurant may be employed in a number of manners to pressurise and transfer propellant. The most simple form of these methods is to simply use a stored pressurant gas to pressurise the propellant. These gases are normally inert and helium and nitrogen are favoured. These gases must not condense or dissolve in the propellant they are pressurising. Typically these gasses are stored at high pressures resulting in thick walled tanks that result in high pressurising system dry masses for larger vehicles. Secondly a gas may be generated for use as a pressurant by means of a gas generator. The source of this gas may be a solid propellant that is combusted or a liquid propellant, either a monopropellant decomposed through the means of a catalyst, or a bipropellant system with combustion occurring with the two propellants. Compared to a stored gas pressurant system this system offers a reduction in mass however may vary in relative complexity depending on whether a secondary liquid is involved or not. In the use of bipropellant gas generators employed for turbine systems the O/F ratio is often varied in order to result in favourable combustion gas temperatures, typically yielding a fuel rich mixture [61]. This option may be of particular interest for the application at hand given the widespread use of H_2O_2 in monopropellant gas generators in the past. This option may also be used in a variety of permutations for example hot gas generator without a separator, hot gas generator with a separating bladder or

piston, or a hot gas generator powering a turbopump.

Main Tank Injection (MTI) is a pressurisation method possible with hypergolic propellants. In this method oxidiser is injected into a fuel tank or fuel is injected into an oxidiser tank upon which the propellants will ignite and create a small combustion zone. The combustion gases in turn pressurise the tank and a pressure switch is used to regulated the injector as shown in Figure 2.13. The feasibility of this means of pressurisation was proven, including using H_2O_2 reacted with Alumazine, ClF_3 and ClF_5 . This system is remarkable for its low system mass, especially on systems where fuels and oxidisers may be cross-fed to each others tanks, reducing inert system mass drastically, however it is worth noting that some pressure must be present in the system to cause one reactant to flow into the other propellant tank, thus stored gas is not completely eliminated. Lastly this system has not seen adoption outside of its initial tests on a rocket sled platform, according to Bingam et al. this may be attributed to the resistance to change from existing flight vehicle heritage and the psychological resistance towards someone "wanting to build a fire in my tank?" [21].

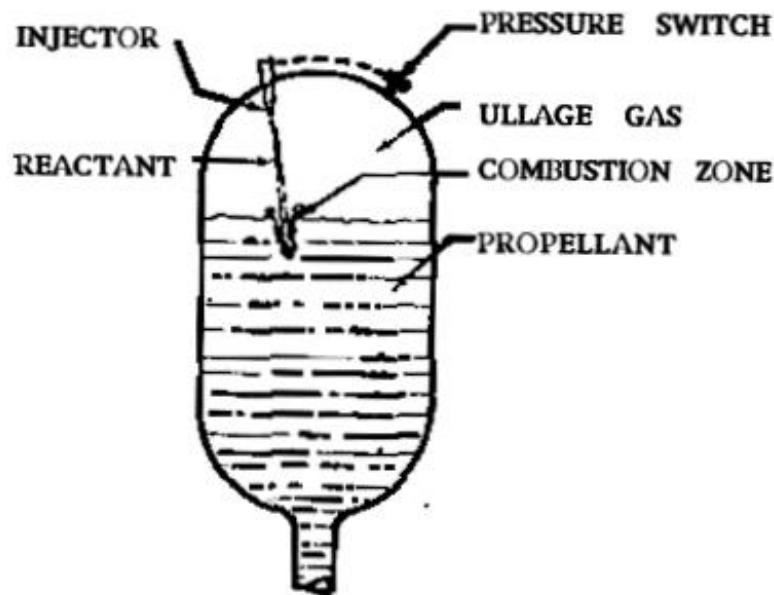


Figure 2.13: Main Tank Injection System Schematic [21]

The last method of gas pressurant to be mentioned is that of boil off or ullage gas pressurant. With this method the propellant that boils off from a cryogenic propellant, or the ullage gas of a non-cryogenic propellant, is heated using solar energy of some other form of thermal energy source, and through a regulator is fed back into the main tank to pressurise it [7].

A final method to mention is that of using strong permanent or electromagnets to orient and transfer propellant, using inherent paramagnetic or diamagnetic properties of the propellant, illustrated in Figure 2.14. Paramagnetic materials are slightly attracted to strong magnetic fields whereas diamagnetic materials are slightly repelled from strong magnetic fields[25]. H_2O_2 is slightly diamagnetic and thus repelled by a magnetic field[57]. The magnetic susceptibility of H_2O_2 may be seen in Figure 2.15. Experiments such as the Magnetically Actuated Propellant Orientation Experiment (MAPO) have been conducted by NASA to validate CFD models established for modelling the behaviour of these fluids in a Zero-G environment under the influence of magnetic fields [46]. These experiments focused on the use of this technique in settling and orienting fluids rather than transferring them.

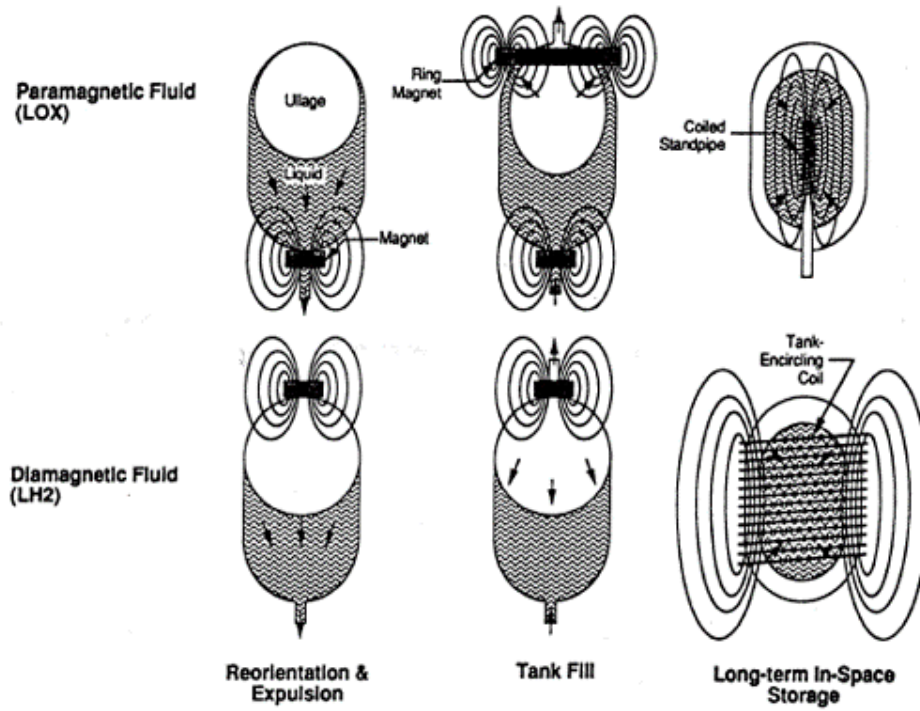


Figure 2.14: Magnetic Propellant Positioning Options for Paramagnetic Propellants (LO₂) and Diamagnetic Propellants (LH₂) [25]

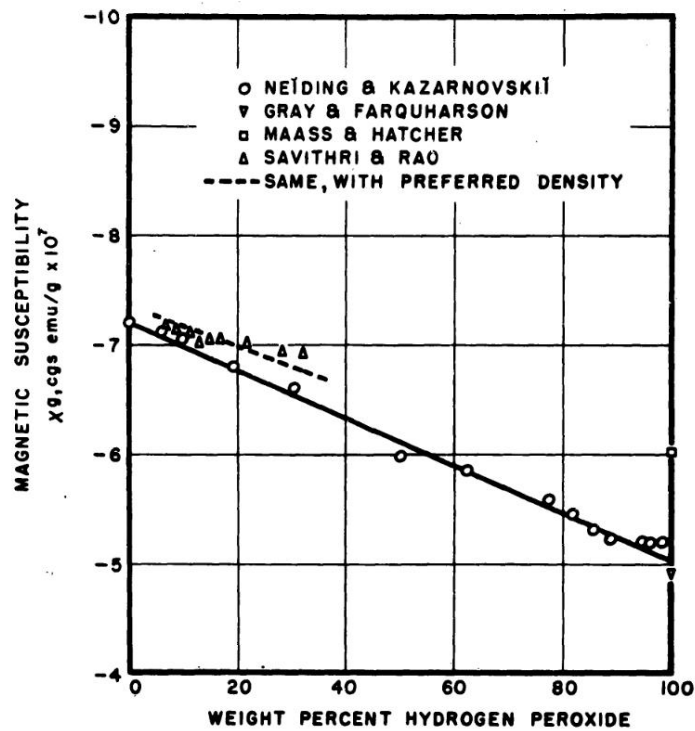


Figure 2.15: Magnetic Susceptibility of H₂O₂ - Water Solutions [57]

Table 2.8 presents a summary of the various methods of propellant transfer.

Table 2.8: Propellant Transfer Methods [7]

Method	Sub-Method	Comments
Tank Replacement		Simple, using existing quick disconnects, larger mass on resupply
Positive Displacement Bladders or Pistons		Eliminates issues of ullage and venting control, porous to certain gasses, materials limited by thermal capabilities of bladder material
Draining by Linear or Angular Acceleration		Flow rate proportional to gravity field induced, propellant is sacrificed for the transfer, low flow rates
Low NPSH transfer Pumps		Other elements necessary to provide NPSH, can achieve higher flow rates
Gas Pressurant	Stored	Inert gas used to pressurise system, ullage control needed
	Gas Generator	Primary or secondary fluid used, requires combustion chamber, cooling of exhaust gas required
	Main Tank Injection	Combustion of hypergolics in tank, low TRL and risky
	Ullage Gas	Boil off gas heated or returned to pressurise system
Dielectrophoresis / EM Fields		Use of magnetic properties of propellant in combination with EM field to induce force on fluid. Low TRL but increasingly investigated.

2.4.2. Propellant Management Devices & Liquid Acquisition Devices

The next set of systems to discuss are Propellant Management Devices (PMDs) and Liquid Acquisition Devices (LADs). Hartwig succinctly states "The purpose of a propellant management device is to separate liquid and gas phases within a propellant tank and to transfer vapour-free propellant from a storage tank to a transfer line en route to either an engine or a receiver depot tank, in any gravitational or thermal environment." [27]. The necessity of PMDs may be illustrated using the Bond number which is a dimensionless parameter that measures the ratio of gravitational forces to surface tension forces, defined by Equation 2.2. Here ρ refers to the liquid density, g is the gravitational acceleration, L_c is the characteristic length of the system and γ_{LV} is the surface tension. Typically during launch the high thrust levels and high-g levels maintain a distinct separation between the propellant and the gas inside of the propellant tanks, in essence this is a high Bond number environment. However in a microgravity environment the surface tension forces become the dominant force, causing a low Bond number. In this scenario liquids wrap around the outer walls of the propellant tanks and leave a gaseous core. If vapour is ingested by a motor then at best it can yield instabilities and at worst a hard start, and this phase mixing presents difficulties to propellant transfer too.

$$Bo = \frac{\rho g L_c^2}{\gamma_{LV}} \quad (2.2)$$

This is the challenge that PMDs are implemented to mitigate. PMDs may be classified into three broad categories, non-capillary type PMDs, partial communication capillary PMDs, and total communication capillary PMDs. Most often a variety of PMDs are implemented in combination to ensure the best performance. This performance may be evaluated using three criteria; PMD mass, required mass flow rate, and expulsion efficiency (EE), defined as the ratio between the volume of residual propellant in the tank to the volume of the empty tank.

One of the first forms of PMD to be explored were the non-capillary types, pistons, diaphragms and bladders, all of which have been discussed in Section 2.4.1. Some of the disadvantages of the three are that pistons are susceptible to leakage and low EE, bladders may require a support structure to prevent folding and lowering of EE, and diaphragms require sealing along the entire circumference of the tank compared to the bladder that is only sealed at a certain inlet. Over all this method does allow for good sloshing control and awareness of CG location, however as these methods span the width of

the tank they can rival the mass of the tank walls and become impractically heavy for larger applications. Examples of diaphragm usage are on the Space Shuttle APU tanks and Cassini's RCS [27].

Traps, baffles, troughs and vortex suppressors are considered partial communication capillary PMDs. An example of a trap as well as the variety of shapes they come in may be seen in Figure 2.16. Traps are closed structures that use porous components such as screens to trap gas outside of the structure and contain as well as provide a quantity of propellant to an application by using surface tension forces. Traps are not able to passively reacquire propellant in low gravity environments, and are most often used on systems that undergo single manoeuvres such as launch or station keeping [34].

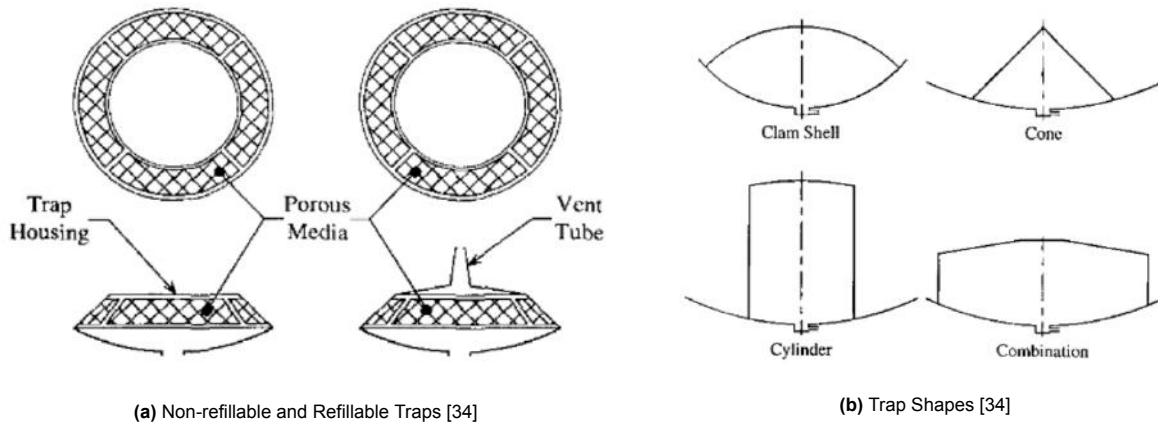


Figure 2.16: Trap types as well as various trap shapes [34]

Troughs on the other hand are open structures that contain and supply a quantity of liquid and may be passively refilled in zero-g. Troughs do not rely on surface tension to retain propellant but rather hydrostatics, and consequently are not acceleration limited [34]. An example of traps and the shapes they may take may be found in Figure 2.17.

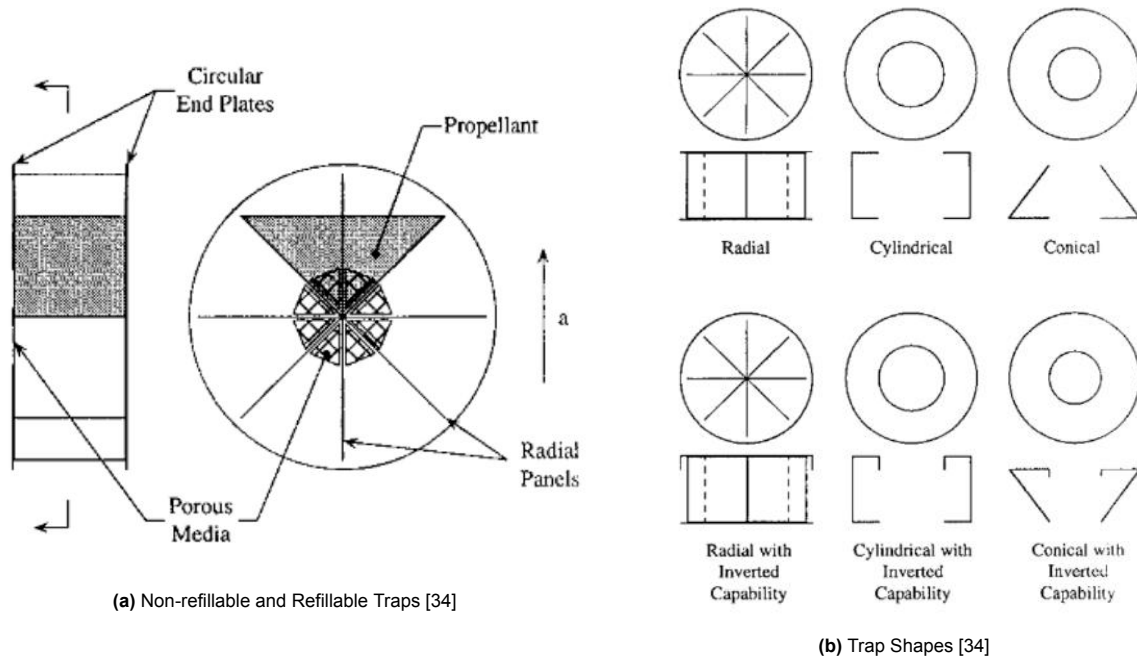


Figure 2.17: Trap types as well as various trap shapes [34]

Baffles are employed in order to prevent sloshing and the adverse effects this may cause on vehicle dynamics while vortex suppressors are used to prevent the formation of vortices at tank outlets with high mass flow. Abramson et al. identify the following causes of oscillations inducing sloshing in tanks [1]:

- Wind gusts during powered flight
- programmed changes of attitude of the vehicle
- control pulses for attitude stabilisation
- separation impulses
- elastic deformations of the vehicle

The magnitude of the force and moment induced by the sloshing depend upon:

- shape of the tank
- properties of the propellants
- damping
- height of the propellant in the tank
- acceleration
- perturbing motion of the tank

Figure 2.18 displays a number of different types of ring baffles utilised inside of cylindrical tanks. Greater consideration will be given to baffles if it is deemed that they are necessary in the system being considered, however as some of the transfer or management methods also fulfil the function of baffles the information presented here is limited.

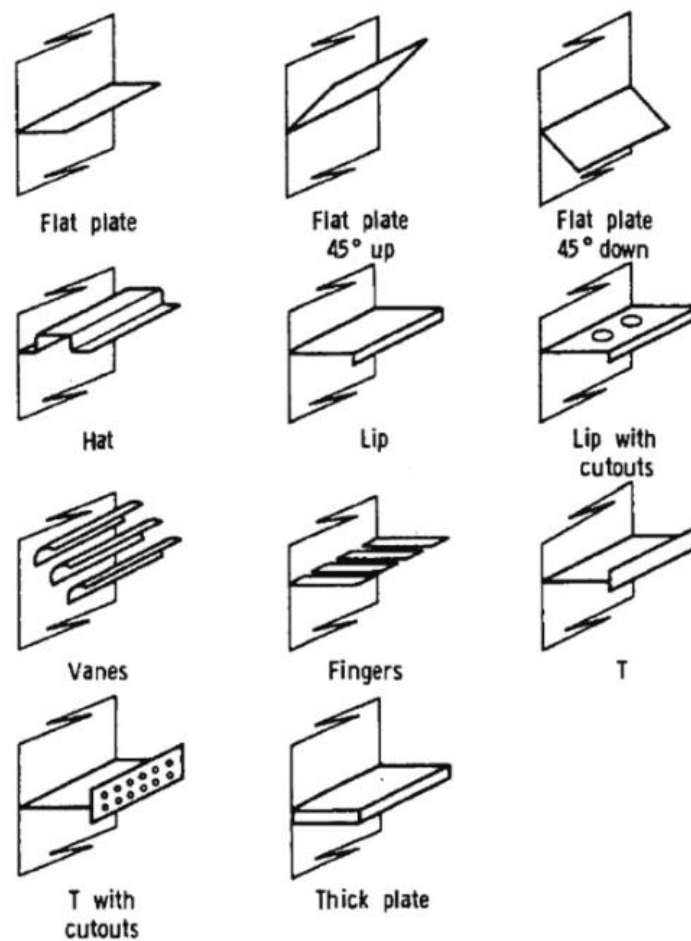


Figure 2.18: Types of ring baffles used for circular cylindrical tanks [31]

Total communication capillary PMDs come in the form of vanes, sponges and screen channels. Vanes may be classified as open acquisition devices, being relatively simple and only allowing for relatively low flow rates while maintaining the advantage of being cheap. Vanes are often fabricated from thin sheet metal, and are mounted in the axial direction perpendicular to the tank walls. This joint between the vane and the wall forms an open path which will be occupied by fluid propellants which form a fillet in this crevice due to surface tension and will flow along the pathway due to capillary forces. Jaekle explains that the primary advantages vanes provide over positive expulsion devices are their low mass, their reliability due to the lack of moving parts, and their material compatibility, given that some vane systems may be fabricated completely from titanium. Conversely positive expulsion devices can deliver high flow rates and can do so regardless of acceleration magnitude and direction. Two common uses of vanes are illustrated in Figure 2.19. Typically hydrazine systems require relatively low thrust thrusters but in a variety of thrust directions. Thus a total communication system, allowing propellant to be acquired from anywhere in the tank is suitable for this application given the low accelerations. For bipropellant application vanes are more often used in systems where there is not a requirement for unlimited flexibility in manoeuvre duration and direction, such as geosynchronous communications satellites. These applications utilise refillable PMDS such as sponges where the vanes acquire propellant during long duration coasting and refill the sponge in preparation for the subsequent manoeuvre. The last factor worth treating regarding vanes is that a number of geometries are possible for the vane cross section, such as a double parallel vane forming a channel, a ribbon vane that is parallel to the tank wall and remains at a stand off distance from it, or a Y shaped vane [35].

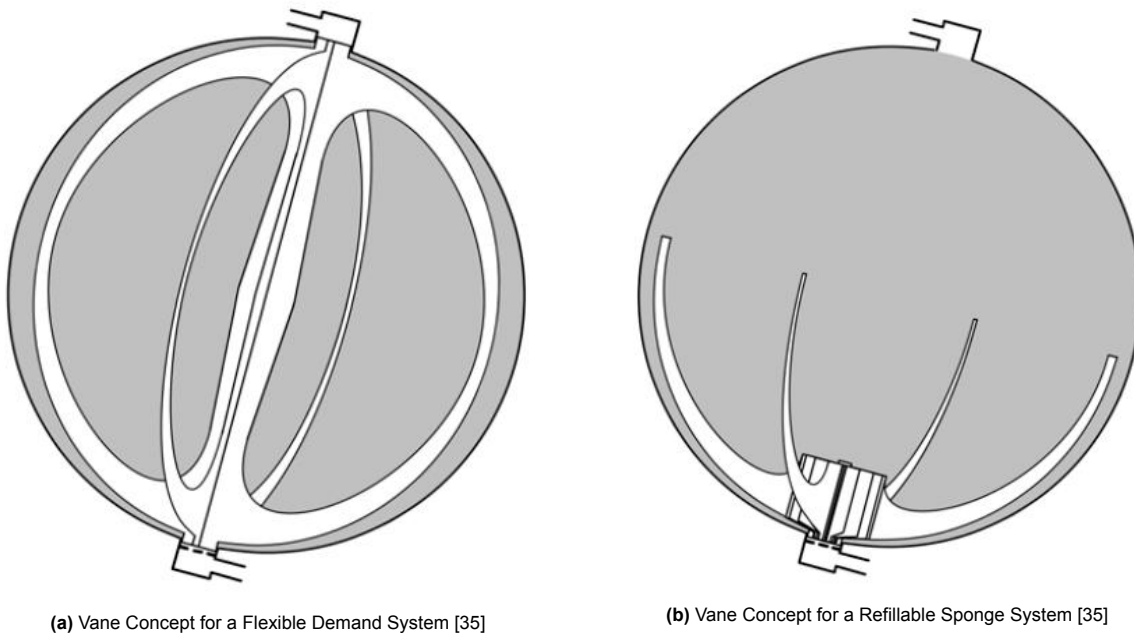


Figure 2.19: A variety of vane configurations [35]

Sponges are a form of refillable PMD that contains and provides a quantity of liquid propellant through the use of surface tension. In a similar manner to vanes, where liquid is held in the crevices where the vane is attached to the tank wall, sponges retain propellant in the crevices between intersecting panels. Figure 2.20 shows a conventional sponge under acceleration in the indicated direction *a*, where a conventional sponge describes a sponge made up of planar sheets divided by a tapered gap.

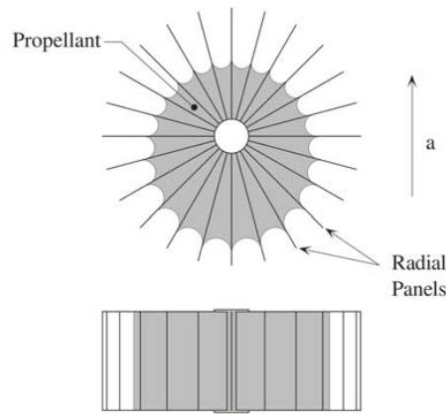
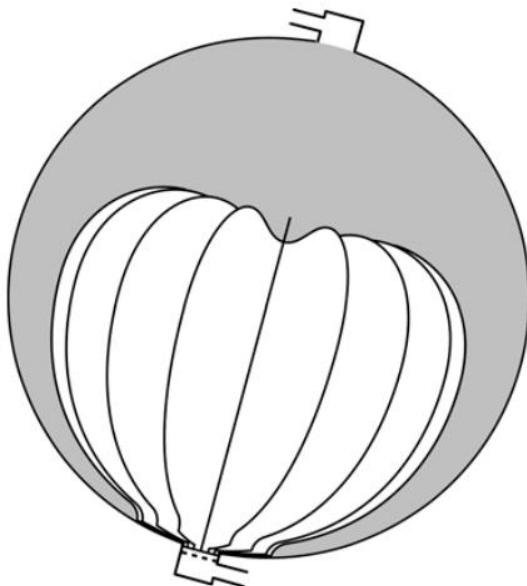
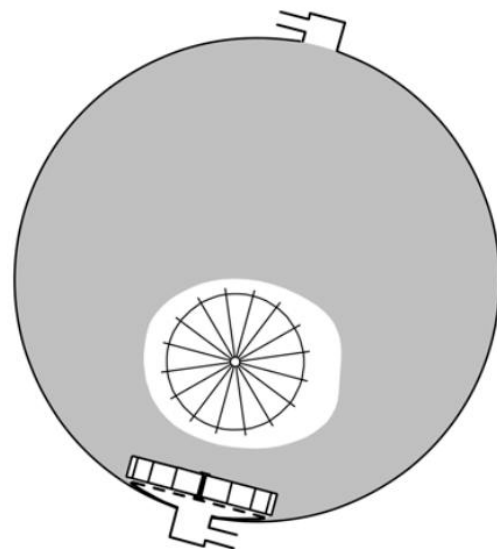


Figure 2.20: A Conventional Sponge with Liquid Attached [33]

Similar to vanes, sponges advantages over positive expulsion devices lay in their simplicity and low mass. Typically sponges are employed in high thrust systems where they supply propellant for ignition and as thrust increases to settle the remainder of the propellant, in systems requiring repeated consumption of a specific quantity of propellant in a standard manoeuvre, and in systems requiring propellant centre of gravity control in zero g. Figure 2.21b shows an example of a sponge PMD used for engine ignition, where a large porous element is placed between the sponge and the outlet to allow for high propellant flow during ignition. Such an ignition system sponge must contain the quantity of propellant necessary to supply the thrust chamber as the thrust reorients the remainder of the propellant in the tank. Figure 2.19b illustrates an example of a sponge application in a specific demand system. This predictable demand for a set quantity of propellant is most common for station keeping manoeuvres of communication satellites. A sponge is a lightweight method of fulfilling this requirement and may be refilled during coasting by vanes. Lastly Figure 2.21a shows a sponge used to control propellant positioning for pointing or orientation reasons. Such a sponge is of a comparable size to the tank itself, and may be used to orient both the propellant as well as the gas pocket, preferably the latter over a venting outlet. Similar to vanes the geometry and configuration of sponges may be varied drastically for a variety of results[33].



(a) Sponge Concept for a Propellant Control System [33]



(b) Sponge Concept for an Ignition System [33]

Figure 2.21: A variety of sponge PMD configurations [33]

Gallery PMDs are the last to be mentioned, and are defined as PMDs utilising an internal or closed flow path for propellant to flow along, the subset of these devices being screen channels and porous elements joined by tubing. Positive expulsion devices possess the same advantage over galleries as they do for vanes and sponges, however galleries are capable of supplying propellant for any duration. The mission flexibility in terms of duration and acceleration direction is the main reason galleries are employed, as compared to other PMDs they are heavy and complex. Figure 2.22a provides an example of a gallery PMD for a flexible demand system, requiring gas free propellant supply while thrusting in directions that do not settle the propellant towards the tank outlet for extended durations. Such a box screen consists of channels with a square cross section, where the channel wall facing the tank walls consist of a porous skin. The finer the porous elements of a channel the higher the acceleration capability of the system, however small pore elements also result on higher flow losses and are more challenging to fabricate, clean and ensure compatibility with [32]. Commonly perforated sheets or weaved meshes are used for these screens however given recent progress in additive manufacturing this may be a suitable application for such a fabrication method. Figure 2.22b illustrates the three primary types of gallery, the screen covered channel, the tube connecting pick up assembly and the liners. Liners are primarily employed in very small tanks and within traps where the challenge of fitting any other solution into such a small volume is too great. Given their high mass and difficulty in maintaining the liner gap they are not recommended for widespread use. Tube connected pick up assemblies are simpler and cheaper to fabricate, however the location of propellant must be predictable to a greater degree than with the liner method. Due to the limited cross section of the tubing connections the transient during start up may be challenging for these galleries contributed to also by the fact that propellant may only be collected in discrete locations. Screen channels allow for improved transient behaviour due to its larger cross sectional area as well as the manner in which it may collect propellant over a greater surface area. As with the previously discussed PMDs the finer geometry and configuration of galleries may be varied, for example screen channel cross sections may be semi-circular, triangular or rounded depending on a variety of requirements and manufacturing considerations. Similarly gallery number and placement may be configured with significant consideration being given to the coordinate system of the satellite, aligning the most common thrust vectors with receiver locations on the gallery.

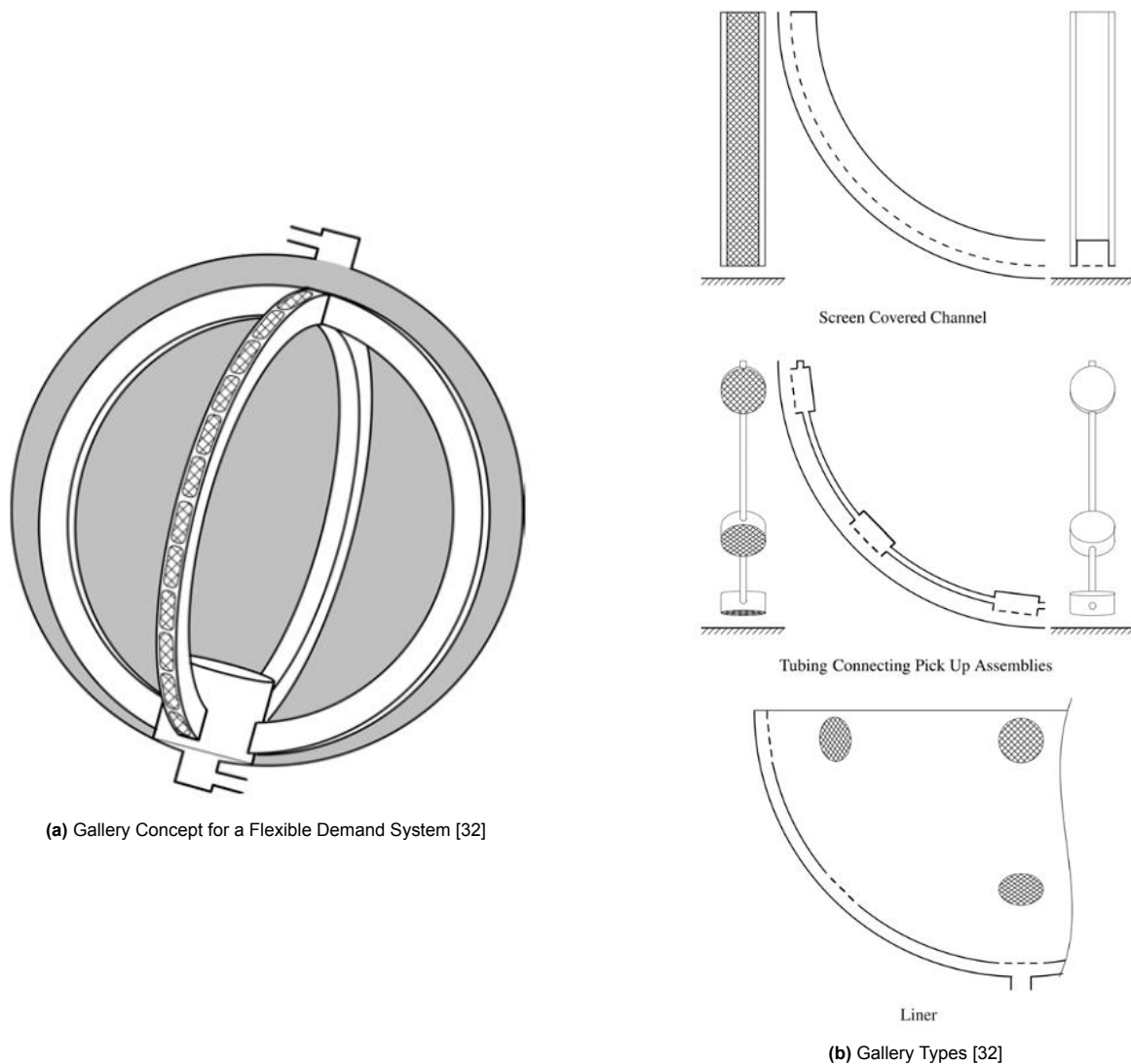


Figure 2.22: Illustrations of a Gallery PMD [32]

2.4.3. Propellant Handling & Settling Methods

While PMDs manage the location of some or all of the propellant in a tank on a continual, passive basis, propellant handling covers the methods that fulfil a generally similar function but in an active, intermittent manner. Table 2.9 presents an overview of such methods as collected by Goff et al. The methods of propulsive settling as well as electromagnetic settling are largely the same as the techniques mentioned in Section 2.4.1 being used for propellant transfer and thus are not elaborated upon any further. Zero G handling refers to methods that allow the liquid to remain in microgravity and use only passive PMDs, so in essence no means of propellant handling, and as PMDs are covered in Section 2.4.2 no further elaboration is provided here. The tether and gravity gradient methods presented by Goff et al. are rather novel and have not been implemented or tested on any scale. Similar to using a centrifugal method where the depot craft may be spun about its centre of gravity, the location of this centre of gravity may be augmented by extending a tether with a counterweight. This method may be extended to make use of the gravity gradient in the system. Rather than spinning the entire assembly the length of the vehicle will cause the axis of lowest moment of inertia to be aligned vertically with the nadir and the small gravitational difference over the length of the vehicle will cause propellant to tend towards the lowest point.

Table 2.9: Propellant Handling and Settling Methods [25]

Method	Advantages	Disadvantages
Zero G Handling	<ul style="list-style-type: none"> • Does not require reaction mass for propellant settling. • Integration with big stations easier • Configuration and orientation independent of operations • Loading/offloading operations identical 	<ul style="list-style-type: none"> • Zero-G thermal control, transfer, and liquid acquisition are low TRL.
Propulsive Settling	<ul style="list-style-type: none"> • Settled cryo handling is high TRL, and simplifies all other depot functions • Settling and reboost functions can be combined. 	<ul style="list-style-type: none"> • Uses reaction mass for settling • Hard to integrate with existing space stations • Constrains tank arrangement to get correct settling effects
Centrifugal Settling	<ul style="list-style-type: none"> • Does not require reaction mass for propellant settling • Settled cryo handling is high TRL, and simplifies all other depot functions 	<ul style="list-style-type: none"> • May require despinning for docking • May need to be combined with another process for transfer ops • Constrains tank arrangement to get correct settling effects
(ED) Tether Settling	<ul style="list-style-type: none"> • Provides reboost and propellant settling without using reaction mass • Can use zero boil-off systems 	<ul style="list-style-type: none"> • Requires moderately large station with significant solar power capability • Low TRL for ED tethers • Challenges docking • Constrains tank arrangement to get correct settling effects
Gravity Gradient Settling	<ul style="list-style-type: none"> • Does not require reaction mass for propellant settling 	<ul style="list-style-type: none"> • Requires very long tether and large overall system • Complex system dynamics • Constrains tank arrangement to get settling effects correctly
Electromagnetic Settling	<ul style="list-style-type: none"> • Does not require reaction mass for propellant settling. • Provides more control over propellant positioning. • More flexibility on tank arrangements and depot layout 	<ul style="list-style-type: none"> • Electromagnetic settling is low TRL • Superconducting electromagnets may add significant weight • Uncertainty if existing electromagnets sufficient for large LH2 tank settling.

2.4.4. Propellant Thermal Control Methods

Besides from purely storing the propellant and possessing the ability to transfer it to visiting customer craft, a propellant depot must be able to control the temperature of a stored propellant. Thermal control systems are necessary on spacecraft due to both the harsh thermal environment imposed by space but also due to the specific thermal ranges some spacecraft components require. Besides components within the system that generate heat, the primary external sources of thermal energy to a spacecraft system are solar flux, albedo flux from nearby planetary bodies, and infrared energy emitted by nearby bodies. This may be represented by Equation 2.3 where q''_{total} is the total rate of thermal flux incoming, α is the absorptivity of the surface, S'' is the solar flux at that location, R_{TOA} is the Earth's radius, ρ_{alb} is the albedo, h is the spacecraft altitude, θ is the solar zenith angle, ε is the emissivity and E'' is the infrared flux emitted by the Earth. Equation 2.4 represents the total thermal energy balance of the spacecraft, where the input energy is the summation of q''_{total} to the various spacecraft surfaces, and the generated energy comes from the internal components producing heat, also illustrated in Figure 2.23. The stored energy depends on the nature of the components in the spacecraft, as well as on the spacecraft mass,

where a higher mass typically provides a larger heat capacitance allowing for smoother changes in the spacecrafts temperature over the course of an orbit or orientation change. The output thermal energy depends on the type of thermal control system employed by different craft [29].

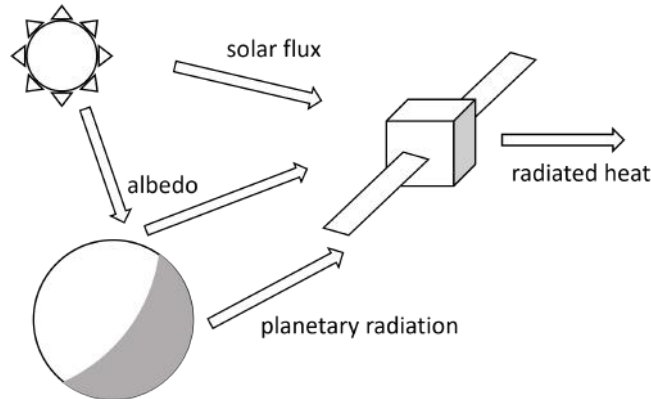


Figure 2.23: Thermal balance of a spacecraft in a planetary orbit

$$q''_{\text{total}} \approx \alpha \cdot S'' + \alpha \cdot \left(\frac{R_{TOA}}{R_{TOA} + h} \right)^2 \cdot \rho_{alb} \cdot S'' \cdot \cos(\theta) + \varepsilon \cdot \left(\frac{R_{TOA}}{R_{TOA} + h} \right)^2 \cdot E'' \quad (2.3)$$

$$\dot{E}_{in} + \dot{E}_{gen} = \dot{E}_{stored} + \dot{E}_{out} \quad (2.4)$$

Thermal control systems may fall in two broad categories, passive and active. Passive systems come in the form of insulation, from multi layer insulation, sunshades, vacuum insulation panels and low conductivity mounts. Active thermal systems come in the form of heat rejection surfaces, heat switches, pumped fluid loops, heat pipes and heat pumps [29]. Depending on the chosen, or combinations thereof, the \dot{E}_{out} is modelled differently. While the design of the potential thermal system for the depot that the propellant transfer system under consideration may be employed in is outside of the scope of this thesis, some basic thermal analysis may be required. ThermXL is an excel add-in that performs thermal analysis of a spacecraft in a discretised nodal system, and is likely the most applicable top level analysis tool to be employed for the system under consideration.

2.4.5. Propellant Mass Gauging Methods

One of the other unique challenges posed by working with propellant in microgravity is that of establishing how much propellant has been transferred as well as how much remains in the depot. For this a propellant mass gauging system is required that is capable of dealing with the potential mixing of vapour and liquid. Boretz lists the following methods as being at varying states of development and providing accuracies between $\pm 1\%$ and $\pm 5\%$ [7]:

- Pressure-Volume Temperature
- Acoustic
- Radioactive Tracer Gas
- Nuclear Radiation Attenuation
- Capacitance
- Positive Displacement
- Density-Volume
- Optical
- Radio Frequency
- Flow Rate Measurement
- Point Sensor

Yendler presents the most prevalent methods of propellant estimation as book-keeping, Pressure-Volume Temperature (PVT), and thermal propellant gauging. Book keeping requires that the system collect information on thruster firing times, the pulse-width, the thrust and mass flow rate. Much of this information must be pre-recorded during ground testing and remain consistent throughout the systems lifetime. A typical accuracy of $\pm 2.5\%$ - $\pm 3.5\%$ is to be expected. The accuracy of this method decreases over time as orifices and other mechanical parts wear, and it cannot distinguish the propellant in individual tanks in a multi-tank system. The PVT method makes use of the ideal gas law to establish the volume of the vapour in the tank based on the temperature and pressure within the tank. The accuracy of this method depends on the tank volume, its deformation, as well as the accuracy of the temperature and pressure sensors and how this accuracy may vary over time. The accuracy of this method decreases with lower propellant masses so therefor deteriorates over the system lifetime. The thermal propellant gauging method measures the thermal capacitance of a vessel holding liquid propellant and pressurant vapour by measuring the temperature response of the tank to a certain heating input. This is then compared to simulated temperature responses. Given the non-uniform positioning of the propellant and vapour in the tank, as well as the discrete locations of the heating system and the non-uniform distribution of the temperature sensors, consideration must be taken to ensure this method is as accurate as possible [76].

2.5. Refuelling System: Peripheral Systems to the Transfer System

This section will briefly describe the systems likely to be present in such a depot that the propellant transfer system will interface with and thus may impose requirements, or may have requirements imposed on them, by the transfer system. Section 2.5.1 first mentions the propellant tanks connected to the subsystem, Section 2.5.2 discusses the refuelling interface allowing other spacecraft to connect to the system, and finally Section 2.5.3 mentions the propulsion system of the propellant depot.

2.5.1. Tanks

Depending on the choice of propellant transfer method, as well as the definition of the system boundaries, the tanks present in the depot, both for H_2O_2 production, concentration, storage and utilisation may be considered part of the system or not. For system configurations where the transfer system lies outside of the tank, then the tanks must be designed with careful consideration for the PMDs that may be required as described in Section 2.4.2, as well as the material and design considerations described in Section 2.2.

2.5.2. Refuelling Interface

As it is an objective of the depot system to provide propellant to customer spacecraft there is a need for a method for a connection to be made between the depot and the customer spacecraft. A number of different institutions and companies have developed interfacing methods for a variety of combinations of electronic and fluid exchange, the first of which to be mentioned here is the ESA initiated ASSIST activity carried out by a consortium from GMV, MOOG, NTUA, DLR, OHB, and TAS. The resulting investigation details the design of both internal and external systems to allow for on-orbit servicing as well as refuelling operations. Figure 2.24 shows the resulting design of the end effector, designed to be installed on the servicing craft on the end of a robotic arm with a camera and LIDAR system that supports the final berthing operations. The system is designed with a complementary berthing fixture to be placed on the customer craft, allowing zero force capture to be performed with the craft rotational constrained, before proceeding with hard lock and other operations such as refuelling. The system has been simulated with a kinematic and dynamic simulator and tested on an air-bearing table. The goal of interface design was to define a standard for the major European space actors so that craft would be equipped with this universal interface [47].

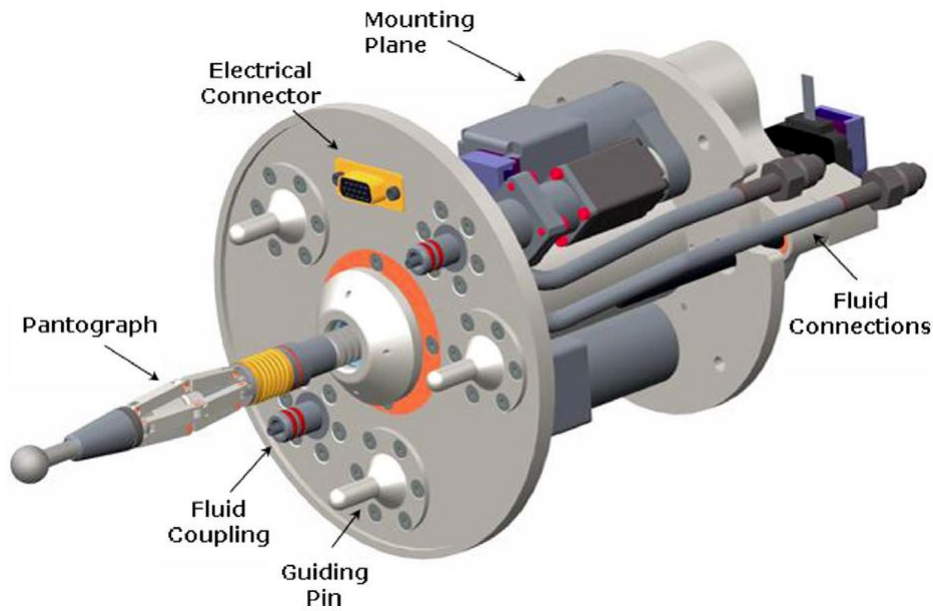


Figure 2.24: Service/Fuelling spacecraft end effector developed by the ASSIST initiative [47]

Another interface method worthy of note is that developed by Orbit Fab a company who is also developing a propellant depot as well as all of the associated systems. Orbit Fab has sought to tackle the issue where interface methods are not installed on spacecraft as there are no servicing spacecraft, and the converse issue, by partnering with a Benchmark Space Systems who's propulsion products are featured in Section 2.1.2 [22]. These systems have a compatible berthing interface allowing the two systems to interact and refuel the customer satellites. The Rapidly Attachable Fluid Transfer Interface (RAFTI) system developed by Orbit Fab may be seen in greater detail in Appendix B and is illustrated in Figure 2.25.



Figure 2.25: Service/Fuelling spacecraft end effector developed by the ASSIST initiative[56]

Lastly the interface method developed by MOOG that the Orbital Express system was based off

of may be seen in Figure 2.26a with the finalised version developed by SpaceDev/Starsys visible in Figure 2.26b.

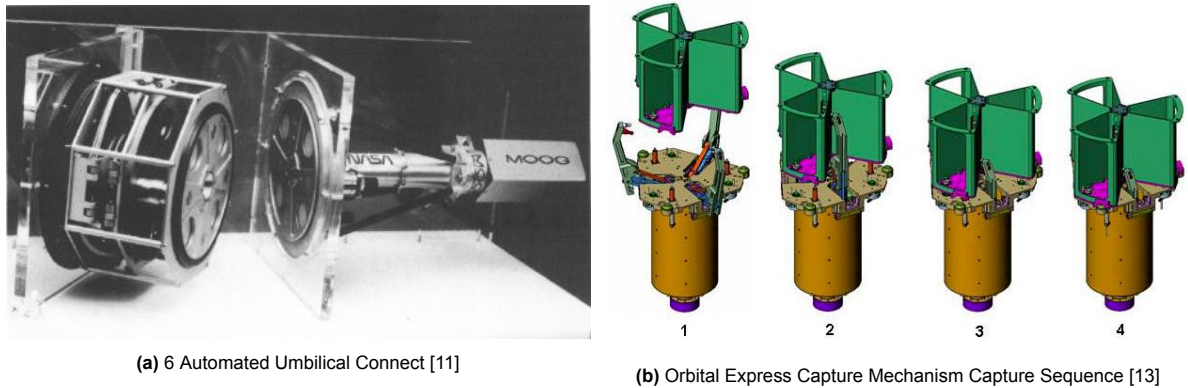


Figure 2.26: The fluid transfer interface developed for and used by the Orbital Express mission

Another thesis student will be working on the development of this interface for the propellant depot in question in parallel to this thesis research.

2.5.3. Propulsion System

A dual mode propulsion system is under development with SolvGE that is planned to provide propulsive capabilities to the depot. This system is capable of firing using solely H_2O_2 as a monopropellant or H_2O_2 and Ethanol as a bipropellant. This system utilises thermal energy to decompose the H_2O_2 allowing for catalysts to be avoided and allow pseudo-hypergolicity [45][8]. This system has only been developed at a sub-scale prototype level and has yet to be hot fired. Further sizing is necessary of this system once the depot has been designed to a greater degree.

2.6. Conclusion

In conclusion hydrogen peroxide is a relatively high density liquid oxidiser with the advantageous capability of decomposing exothermically into water steam and oxygen, as well as being non-toxic and easy to handle. H_2O_2 saw relatively widespread use in the early days of the space age before hydrazine came to dominate due to its superior performance. With the end of hydrazine's usage in sight there are growing numbers of thrusters on the market using 87.5% to 95% H_2O_2 , and fuel cells using 65% and above. H_2O_2 is susceptible to decomposition, but this is minimised through the usage of proper materials, most often aluminium and stainless steel alloys, as well as Teflon based seals.

In terms of existing propellant transfer systems, the most prevalent is that used by the Progress spacecraft to refuel the ISS with UDMH and NTO. More recently Orbital Express mission flew a tandem spacecraft mission that demonstrated a variety of forms of autonomous propellant transfer between orbiting spacecraft. This made use of pressurised pump systems. In the USA the company Orbit Fab is looking to launch propellant depots, using bladder systems for their transfer method, and have released a public interface design for refuelling.

When transferring fluid in-orbit one must also face the challenges of propellant management, as well as settling, and mass gauging. Different forms of technical solutions for these separate problems may solve a multitude of these issues. These solutions include propellant management devices such as vanes and capillary methods, to positive expulsion devices, centrifugal forces and more. Mass gauging can be achieved using book-keeping of fluid usage, pressure volume temperature methods, or thermal gauging among others.

Lastly the propellant transfer system does not exist in isolation and it primarily interfaces with the storage tanks of the refuelling architecture, as well as the propulsion system, and the refuelling interface to the customer segment.

3

Refuelling System Concept

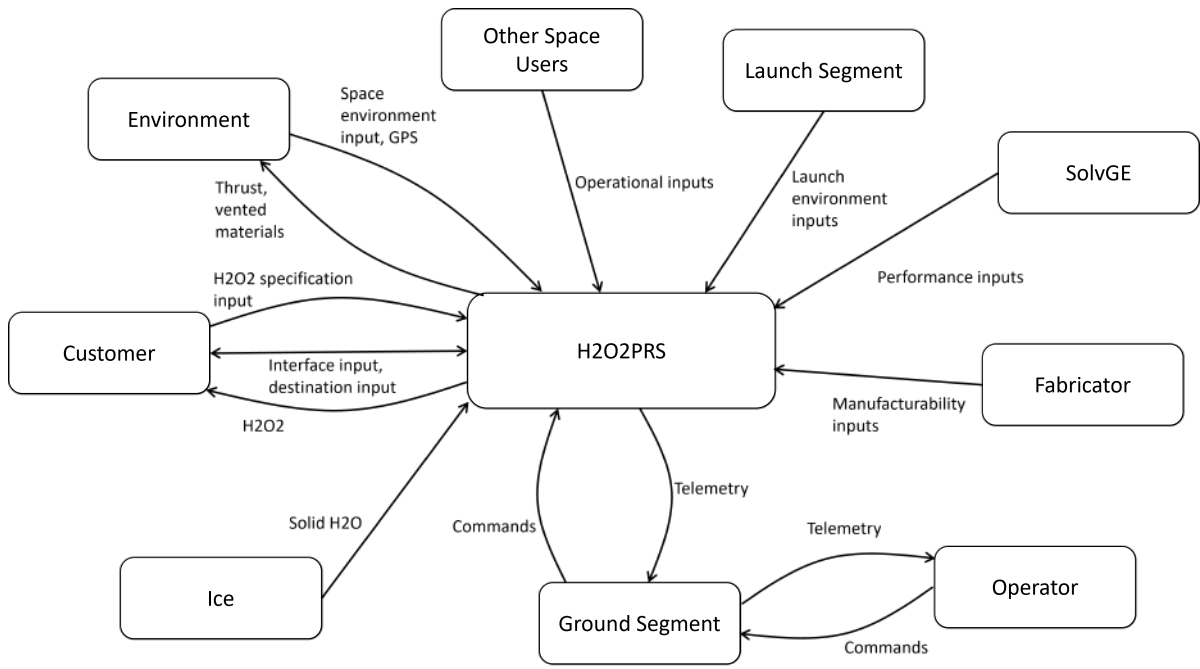
The preceding chapter has shown that there are a number of ways in which to solve the design challenge at hand. In order to ascertain which configuration is best for the specific purpose at hand a preliminary trade off is conducted in this chapter. In order for a trade off to be conducted requirements are first necessary and these are created in Section 3.1, after which the trade off itself is discussed in Section 3.2.

3.1. Requirements

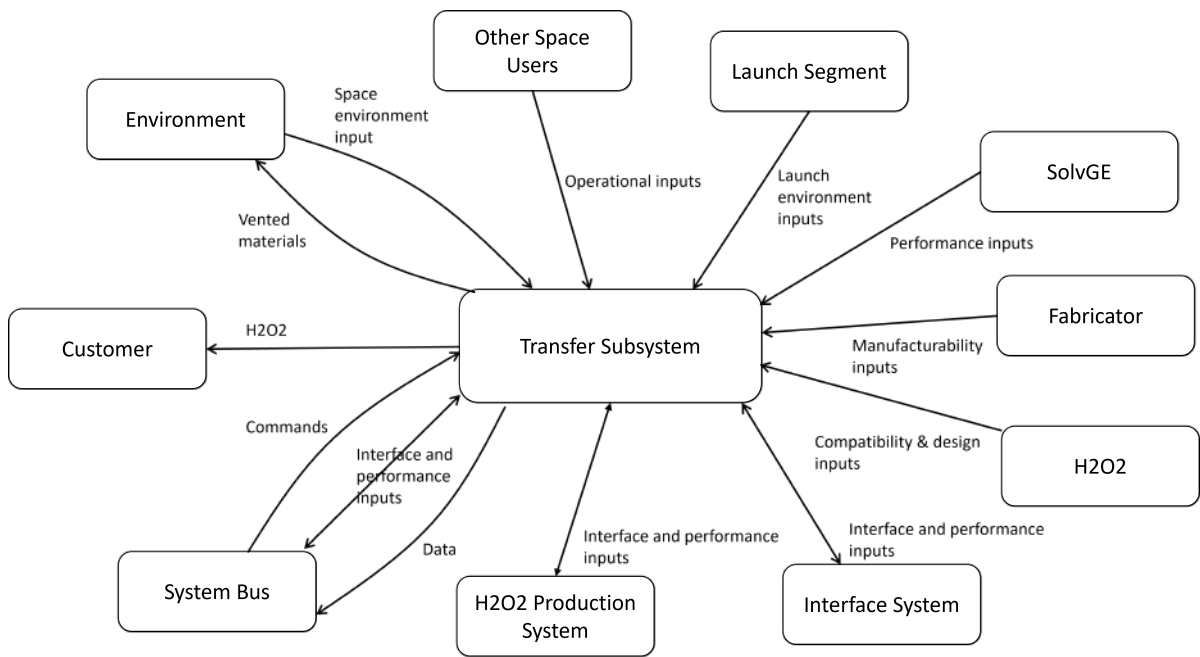
In order to establish the requirements on the system at hand it is first necessary to identify the primary stakeholders in the system and what their desires for the system might be. This is done with the help of context diagrams, shown in Figure 3.1, where the boundaries of the system, as well as how it interacts with other systems are displayed. This is done both for the refuelling architecture as whole as well as specifically the propellant transfer system.

From these context diagrams the stakeholders and their relevant desires may be distilled. The principal stakeholder is SolvGE, the company behind the initiative to explore this form of space architecture. The long term goal for SolvGE with this system would be to employ their H_2O_2 production and concentration technology in such a deep space depot that would utilise locally gathered water as an input and be capable of transferring high concentration H_2O_2 to customer spacecraft. As this would be a commercial initiative by SolvGE it would be in their interest for this depot to be long lived, have a low complexity, and have a low price. SolvGE's primary area of expertise lies in the development of H_2O_2 technologies, thus it maintains a relationship with an external fabrication specialist for design consultation and the production of parts. Be it either this fabricator or another that would eventually produce this depot, it is important for this party that the system is producible, i.e. possible to fabricate with current and cutting edge production techniques. As the depots purpose is to operate in space then it must be launched into space by a launch service provider. This entity will not have any desires for the functionality of the depot however the constraints imposed by this launch service provider will impose requirements on the depot. The depots purpose is to serve a customers, who in turn will desire a certain number of qualities from the system. Among these are that the system possess an interface with which the craft can dock and receive the transferred H_2O_2 . The customers will also expect a reasonable transfer time for this propellant transfer to take place within, as well as desire a specific concentration of H_2O_2 as well as a specific volume to be transferred to their tank. Lastly other users of the space domain, specifically those in proximity to the depots area of operations, will expect the depot not to pose a hazard to them in its activities. These desires from the different stakeholders are summarised Table 3.1 below:

These desires may be formalised as a list of requirements as is presented in Table 3.2. These requirements are generated as conceptual requirements on a full scale system and are used to guide the trade off of refuelling mechanism. The list is not exhaustive and as this thesis will not cover the final development of the full scale system, compliance cannot be validated at this stage.



(a) Context diagram refuelling system



(b) Context diagram propellant transfer system

Figure 3.1: Context diagrams of the refuelling system and the propellant transfer subsystem, illustrating the interaction between the systems and their environments.

Table 3.1: Stakeholder desires

SolvGE	Fabricator	Launch Service Provider	Customer	Other Satellites and Space Users
Longevity	Producible	Launchable	Compatible transfer interface	Does not present a hazard
Low complexity			Reasonable transfer time	
Low cost			Specific concentration level	
Water as input			Specific propellant volume	

Table 3.2: Preliminary System Requirements for the H₂O₂ Depot and Transfer System

Identifier	System Requirement
SYS-01	The system shall be capable of transferring 200 L of H ₂ O ₂ to the receiver vessel
SYS-02	The system shall withstand the loads imposed on it during launch activities with those of the Falcon 9 launch vehicle taken as reference ¹
SYS-03	The system shall withstand the loads imposed in its orbital environment as specified in NASA's Natural Orbital Environment Guidelines for Use in Aerospace Vehicle Development [37]
SYS-04	The system shall incorporate a H ₂ O ₂ production and concentration system that utilises water as a raw material
SYS-05	The system shall be fabricated and operated for as economical a cost as possible
SYS-06	The system shall be capable of interfacing with a receiver vessel
SYS-07	The system shall transfer H ₂ O ₂ at no less than 0.1 kg/s to the receiver vessel
SYS-08	The system shall measure the mass flow of H ₂ O ₂
SYS-09	The system shall be compatible with concentrations of H ₂ O ₂ up to 99%

3.2. Design Trade Off

As the various methods presented in Section 2.4 that may be implemented to fulfil the different functions of propellant transfer, management, handling, and mass gauging, contain varying amounts of overlap in the number of these functions that they may fulfil, Table 3.3 illustrates which solutions can carry out what functions. Green (2) indicates a possibility to fulfil this function, orange (1) indicates potential to fulfil the function indirectly or with modification, and red (0) indicates a lack of ability to fulfil a function. Numbering is provided purely for black/white compatibility and colour blindness. It is evident that some methods are capable of fulfilling purely a single function, such as many of the PMDs, however other methods, in particular the piston, is capable of fulfilling most if not all of the tasks. As it is desirable for this system to be as lightweight, simple, and cost effective as possible, it is therefore desirable to minimise the number of systems used, thus it is favourable to opt for systems that can fulfil a number of functions.

Table 3.3 is purely indicative of what system combinations may be required or desirable. To allow for better insight into what system may be optimal for the application at hand, a trade-off between these different options should be conducted. A trade off must be based on a certain set of criteria, and these are distilled from the system requirements presented in Table 3.2. As has already been discussed this system is to operate in space, and thus must be launched. A significant cost in any space project is the launch of the hardware, which is directly proportional to the mass to be launched. Therefore minimising the launch mass (neither dry nor wet mass is used here as the system may be launched with, none, some, or all of its working fluids) is of the utmost importance and this is included as a trade off criterion. The system complexity is related to the system cost, as well as its likelihood of failure during its lifespan thus this criterion is included. Some of the system options mentioned make the incorporation of system redundancy more or less difficult, and system redundancy in turn allows for increased chances of nominal operations over the system lifetime, thus system redundancy is included as a criterion. The system life/longevity is an important factor as this depot system is envisaged to

Table 3.3: An illustration displaying which of the transfer, PMD and settling systems can fulfil the functions of transfer, management, handling and mass gauging. Green (2) indicates a possibility to fulfil this function, orange (1) indicates potential to fulfil the function indirectly or with modification, and red (0) indicates a lack of ability to fulfil a function. Numbering is provided purely for black/white compatibility and colour blindness.

		Transfer	Management	Handling/Settling	Mass Gauging
Transfer Methods	Bladder	2	1	2	1
	Diaphragm	2	2	2	1
	Piston	2	2	2	2
	Tank replacement	2	0	0	0
	Acceleration	2	2	2	1
	Pump	2	0	0	1
	Stored gas	2	0	1	1
	Gas Generator	2	0	1	1
	Main Tank Injection	2	0	1	1
	Ullage heating	2	0	1	1
	Magnetic Field	2	2	2	1
	PMDs	Traps	0	2	1
Troughs		0	2	1	0
Baffles		0	2	1	0
Anti-vortex		0	2	1	0
Vanes		0	2	1	0
Sponges		0	2	1	0
Screen Channels		0	2	1	0
Settling Methods	Inertial	2	1	2	1
	Tether	2	1	2	1
	Gravity Gradient	2	1	2	1
	Electromagnetic	2	1	2	1

maintain operations supplying H_2O_2 as long as it is supplied with water. Certain transfer methods are capable of transferring propellant at different flow rates, and while it may be possible to achieve similar rates with all options, penalties will be present in terms of mass or power required for some. Equally customers will desire to spend as little time as is necessary away from their crafts nominal operations during fuelling, thus mass flow rate is included as a trade off criterion. As the exact mass of propellant the system should be able to transfer is as of yet undetermined, and some of the transfer options are more suited for smaller or larger masses, thus the scalability of the system is included. As was evaluated in Table 3.3, some of the transfer methods may also fulfil other functions while some require additional systems to be included, and this is evaluated in this criterion. Finally, as will be elaborated upon in Section 4.2 there may be scenarios in which it is desirable to locate the transfer system in different segments of the refuelling architecture and not on the refuelling craft, such as on an orbital depot, and thus the ability of the transfer system to be placed off of the refuelling craft is included as the final criterion.

Regarding the weighting of these criteria, this is done on a scale of one to three, where one designates a less important weight and three designates a more important weight. The system launch mass, and system longevity are considered to be the most important weights as they are significant determinators of the system cost and system lifetime. While poor scoring in other criteria can often be compensated with resources such as cost and time, these criterion are essentially cost and time and thus are paramount. System complexity, the ability of adding redundancy, the necessity of other systems alongside the transfer system, and the ability to locate the transfer system off of the refuelling craft, are all weighted with a two, as they are rather important but not of equal importance to the top two criteria. Finally the mass flow rate and the system scalability criteria are weighted with a one, as these may be considered as more "nice to have" qualities rather than mission driving, and thus are weighted the

lowest.

The systems are scored under these criteria with scores of one, zero, or minus one. This scoring method was used as some of the options are quite comparable in performance under certain criteria and in this scenario they may all be awarded a zero, a baseline score, while those worse and better than these options may be awarded a one and minus one respectively (i.e. lowest total score is the best). The scoring of each design option under each trade off criterion will now be justified.

System Launch Mass: Under the criterion of launch mass the options of piston, pump, acceleration, and ullage heating were given a zero as it was judged that while these methods add a small amount of mass to the overall systems it is not as large as some of the other options presented. For example the acceleration utilise systems already included such as the thrusters while the ullage heating is judged to not add significant mass to the system assuming that the solar energy absorbed by the system may be used. The tank replacement option has been awarded a one as it likely requires the addition of more systems such as tank clamp and release mechanisms and a greater number of interface points in the system, thus increasing the system launch mass. The stored gas options is judged to add significant mass to the system as it require more pressurant gas to be added at take off as well as more tanks and components such as regulators. The main tank injection option would require liquids that are hypergolic with H_2O_2 to be flown at launch and would thus add mass to the take off weight and is thus awarded a one. Lastly the magnetic field option is awarded a one as it is presumed that significant electromagnetic system mass will need to be added to facilitate this option. For the favourable systems, being the bladder, the diaphragm and the gas generator, it was reasoned that former two add very little mass to the tank assembly, while the latter utilises H_2O_2 already carried along with a small gas generator, having a low total system mass and thus being awarded minus one.

System Complexity: The options of bladder, diaphragm, and piston are awarded zero, as while they are not incredibly simple, their basic principle is well understood and they simply require a pressurant gas stored in a secondary vessel regulated with a regulator to deform or displace the separating material. The tank replacement option however is more complex, not being utilised before and requires a number of separate complex processes of launching refilling craft, undocking old tanks, docking new tanks and maintaining sealing interfaces to all function correctly, and is thus awarded a one. The acceleration system is awarded a one, while it is not a complex system in and of itself, it does require the system to accelerate in a certain direction for the duration of the propellant transfer, changing the systems location continually, requiring greater work in planning and executing essentially more manoeuvres adding complexity to the system. The pump is awarded a one as it involves adding a relatively complex system, that adds sealing surfaces and points of failure in both the pump itself as well as its power system. Stored gas is awarded a minus one as it is relatively the most straight forward option with simply a tank and regulator. The gas generator and main tank injection options are both awarded one for adding more feedsystem, and more combustion characteristics to the system, which must be very carefully tested and executed. Ullage heating and magnetic field are both also awarded one as they are rather low TRL system with complex components required for their execution.

System Redundancy: For the bladder, diaphragm, piston and tank replacement options adding redundancy may be done through the addition of redundant storage tanks also containing duplicate membrane methods in the first three cases. This doubles the tank system mass as well as the propellant mass to be carried and is thus awarded a one. The acceleration option may have redundancy added rather easily by adding additional thrusters and thus is awarded a negative one. The pump, stored gas, gas generator may all be made redundant with the addition of a small number of components and thus are awarded negative one. The main tank injection method required the addition of greater quantities of secondary working fluids and likely further complex combustion systems, and is thus awarded a one. Ullage heating and the magnetic field options are systems where the same tanks may be used for redundancy and purely a redundant heating or EM system must be added, which is judged to not be overly complex or heavy, and thus these options are awarded negative one.

System Life/Longevity: The bladder option is awarded a one for system life as the literature available on this method indicates that the repeated cycling of the material used in bladders typically leads to ruptures over time. The diaphragm option is awarded a zero, tanks with diaphragms are likely to last longer than the bladder materials, however the deformation of the material will still fatigue it over time. The piston option is awarded a negative one as it is capable of surviving rather long with only the sealing surfaces wearing which may be designed to account for this. Tank replacement and acceleration are both awarded negative one for the interface points and the thrusters are the main

points that will undergo wear and tear, thus these systems are likely to last rather long. The pump option receives a zero as it is unlikely to wear exceptionally fast if designed not to, however its increased number of parts and complexity means it may not last as long as other options. The stored gas system requires refilling of the pressurant gas however the simplicity of the system means that it is likely to last for quite long and thus this option is awarded a zero. The gas generator and main tank injection both use consumables in the form of the stored gas, the gas generator catalyst and the hypergolic liquids stored in the depot and thus have a defined life span based on the quantity of these consumables on board. Thus these systems are all awarded one. The ullage heating and magnetic field options are awarded zero as these methods are low TRL and it is unknown how long their operational lives may last.

Mass Flow Rate: The bladder, diaphragm and piston options are all awarded zero for their mass flow rates, as in essence these systems may be designed to provide a desired mass flow rate with a relatively minor mass penalty. The tank replacement option is awarded a negative one, as in the moment of replacement the mass is entirely transferred so it can somewhat be considered instantaneous. The acceleration method can yield a rather low mass flow with reasonable accelerations and feed system diameters and is thus awarded a one. A pump is capable of rather high mass flows depending on the power and dimensions of the system, therefore the option is awarded a negative one. The stored gas and gas generator options may easily be made to achieve greater flow rates with the adjustment to the pressure produced through the mass flow through the regulators in these systems with relatively minor mass penalties in the rest of the system, thus receiving scores of negative one. Main tank injection may be capable of achieving high mass flow rates but only through injecting more propellant and achieving higher combustion pressures resulting in complications for the storage tank design, all undesirable consequences, thus this option receives a zero. Ullage heating and magnetic field both receive a one as high mass flows may only be achieved through high temperatures in the ullage or strong magnetic fields, both requiring more system mass which is undesirable.

Scalability: As the scalability assesses the ease with which some of the transfer methods may be scaled, both bladder and diaphragm options are awarded one, as larger tanks will result in larger bladders and diaphragms with difficult material implications for manufacturing given that these options must deform reliably. Piston and tank replacement both receive a zero as the piston may easily be enlarged in diameter and the thruster system may be scaled through greater thrust or more thrusters. The pump option receives a negative one as it is straightforward to size a pump for a larger mass flow rate. The stored gas options score poorly with a one as for a larger system even more stored gas must be launched negatively affecting the system mass. The gas generator methods receive a negative one as scaling the system means there is only slightly more H_2O_2 present to be decomposed to pressurise the system in turn, and only a very minor mass penalty being suffered on a marginally larger gas generator unit. Main tank injection receives a zero as more hypergolic propellant must be launched for a larger system. Ullage heating and magnetic field options both receive negative one as their scaling is rather straightforward with the heating or EM apparatus being enlarged to match the scale.

Necessity of other systems: (See Table 3.3 for reference) Both the bladder and diaphragm options require separate systems for either the management and/or mass gauging functions and are thus both awarded zero. The piston system is the only option that does not require other systems for the management, handling and mass gauging, and it is therefore awarded a negative one. The tank replacement option requires other systems for the management, handling and settling, and is therefore awarded a one. The acceleration method requires only a separate system for the mass gauging and thus receives a zero. The pump, stored gas, gas generator, main tank injection, and ullage heating all require other systems for the functions of management, handling and mass gauging and thus all receive one. Lastly the magnetic field option requires another system only for the mass gauging function, therefore receiving a zero.

Can be located off of the craft: The bladder, diaphragm, and piston options all necessitate a secondary system to allow transfer, and while these items themselves cannot be located outside of the craft, the secondary system may be, and thus these options are awarded a neutral zero. For the tank replacement option, the refuelling craft must be capable of carrying and replacing a filled tank, and while some of these subsystems may be located on other segments the majority of the system will remain on the craft and thus this is awarded a one. The acceleration option requires the craft itself to be manipulated and thus this cannot be located on other systems, receiving a one. The pump system favours well under this criteria as this may be used to force propellant into and suck propellant out

of the craft, thus receiving a negative one. The stored gas, gas generator and main tank injection methods all have the possibility of placing some subsystems outside off the craft however they not be placed entirely on another segment and thus receive a zero. Lastly the ullage heating and magnetic field options require the propellant to be manipulated in the refuelling craft itself and thus cannot be placed off of the craft, thus receiving a one.

Table 3.4 displays the transfer system trade off, with a colour gradient provided in the total score column to illustrate the comparative scores. It may be seen that the piston system emerges as the optimal choice with a very low score of minus three, with the pump method following closely at negative two, then the diaphragm and gas generator bunched with the acceleration and stored gas at values of zero and one respectively, and finally the bladder, ullage heating, tank replacement, magnetic field, and main tank injection scoring poorest of all. In terms of sensitivity, if the weights are set to one then the ranking of the options is practically identical, with the scores being 2, 1, -1, 3, 2, -2, 0, -1, 5, 3, and 3, thus the general grouping of the optimal outcome is maintained. However it should be noted that this method only assesses the optimal solution using a single system, and does not in any way consider combining systems such as stored gas or gas generator and a bladder, diaphragm or piston, or combining a pump and stored gas. This assessment is best conducted qualitatively rather than through more specific permutations and combinations being traded off against each other.

What may be concluded is that the piston is particularly useful as it fulfils many functions of transferring the propellant, maintaining its orientation in one segment of the tank, and measuring the location of the piston allow the propellant mass to be gauged. The system may be moved through a variety of means, be they mechanical actuators or a pressure on one side. Pressurising the piston may also be achieved through a number of methods, either a gas generator using H_2O_2 or another fuel or using stored gas, as well as using the pumped method with a smaller back pressure provided by another means, or using entirely the stored gas method. All of these methods of actuating the piston also scored well in this trade off, thus they will be further considered in combination with the piston method. Another major advantage that the piston possesses is that it maintains separation between the propellant and the pressurant gas. In a sustainable off-Earth propellant resupply architecture it is likely that the easy to produce pressurant gasses are not compatible, or undesirable to have in contact with peroxide. In this manner byproducts of the H_2O_2 production process such as oxygen gas could be used as the stored gas without absorption or comparability issues.

3.3. Conclusion

In order to assess an optimal method for transfer H_2O_2 in space requirements must first be created, and this may be done based on the desires of the primary stakeholders in the project, these being SolvGE, the fabricator, the launch service provider, the customer and other satellites and space users. The requirements distilled from these stakeholders cover the system longevity, complexity, and cost, the fact that water must be used as an input, that the system is producible and launchable, that the system has an interface that can be mated with, that the transfer time, concentration and propellant volume are satisfactory to the customer, and that the system does not pose a hazard to other space users. When assessing the propellant transfer systems it is worth noting which of these can also fulfil functions of propellant management, handling and mass gauging, with the piston being able to fulfil all of these functions. From the aforementioned requirements some trade-off criteria can be established, namely system launch mass, system complexity, system redundancy, system longevity, mass flow rate, scalability, the necessity of other systems, and the ability of the system to be located off of the refuelling craft. From this trade off it is deemed that the piston method is the optimal transfer method, though it must be used in conjunction with another method such as the stored gas, gas generator or pump options in order to actuate the piston. These three combinations shall be investigated further.

Table 3.4: Trade-off of in-space propellant transfer methods

Weight	Criteria	Bladder	Diaphragm	Piston	Tank Replacement	Acceleration	Pump	Stored Gas	Gas Generator	Main Tank Injection	Ullage Heating	Magnetic Field
3	System Launch Mass	-1	-1	0	1	0	0	1	-1	1	0	1
2	System Complexity	0	0	0	1	1	1	-1	1	1	1	1
2	Ability for redundancy	1	1	1	1	-1	-1	-1	-1	1	0	0
3	System Life	1	0	-1	-1	-1	0	0	1	1	0	0
1	Mass Flow Rate	0	0	0	-1	1	-1	-1	-1	0	1	1
1	Scalability	1	1	0	0	1	-1	1	-1	0	-1	-1
2	Necessity of other systems	0	0	-1	1	0	1	1	1	1	1	0
2	Can be located off of the craft	0	0	0	1	1	-1	0	0	0	1	1
	Total	3	0	-3	7	1	-2	1	0	12	6	7

4

Refuelling Architecture

The refuelling system in question does not exist in isolation, it must interface with the servicer's refuelling segments as well as the customer vehicle. This entire system, from the collection of the raw material of water ice, to the production of H_2O_2 , to the transfer of the propellant to the customer, is referred to as the refuelling architecture. This chapter first considers the optimal location of the various segments of this architecture, be it on a planetary body or in a certain orbit. The outcome of this assessment will better inform the choice of specific propellant transfer mechanism. Next first order sizing of a Single Stage to Orbit propellant refuelling craft is conducted. This sizing gives us the mass envelope of the vehicle the propellant transfer system in question must fit within. Finally some first order mass sizing of three variants of the chosen transfer system is conducted. These values help define the design space for the transfer mechanism and the refuelling craft as whole, and will later be used in Chapter 8 in combination with the testing results to assess the feasibility of this transfer method and concept in general.

4.1. Segment Location

The manner in which the H_2O_2 supply system is organised has a large impact on the design of the propellant transfer system. For example if the propellant transfer occurs on a planetary surface with a significant gravitational force then the issues presented in Section 2.4.2 where propellant management devices are necessary may be neglected. Similarly if the refuelling architecture is comprised of multiple vehicles or locations, for example where the propellant is produced in one location, then transferred across the planetary surface in a secondary vehicle, and then brought to orbit in a resupply craft, and finally transferred in orbit, then a number of transfers must occur in different environments, potentially resulting in a different optimal design.

Table 4.1 displays the variety of options for how the segments of the refuelling architecture may be located, where option one has the majority of the operations on a planetary bodies surface, and option six has the majority of the operations in space. It is assumed at this stage that as the intended customer base is in-orbit vehicles then delivery will take place in-orbit. Figure 4.1 displays options one and six from Table 4.1 pictorially.

Table 4.1: Segment location possibilities

Step	Mine Ice	Liquify	Electrolysis	H ₂ O ₂ Production	H ₂ O ₂ Concentration	H ₂ O ₂ Storage	H ₂ O ₂ Delivery
Option No.							
1	Lunar/Martian/Planetary Surface						
2	Lunar/Martian/Planetary Surface						
3	Lunar/Martian/Planetary Surface						
4	Lunar/Martian/Planetary Surface						
5	Lunar/Martian/Planetary Surface						
6	Low Earth/Martian/Lunar Orbit, L1, L2						

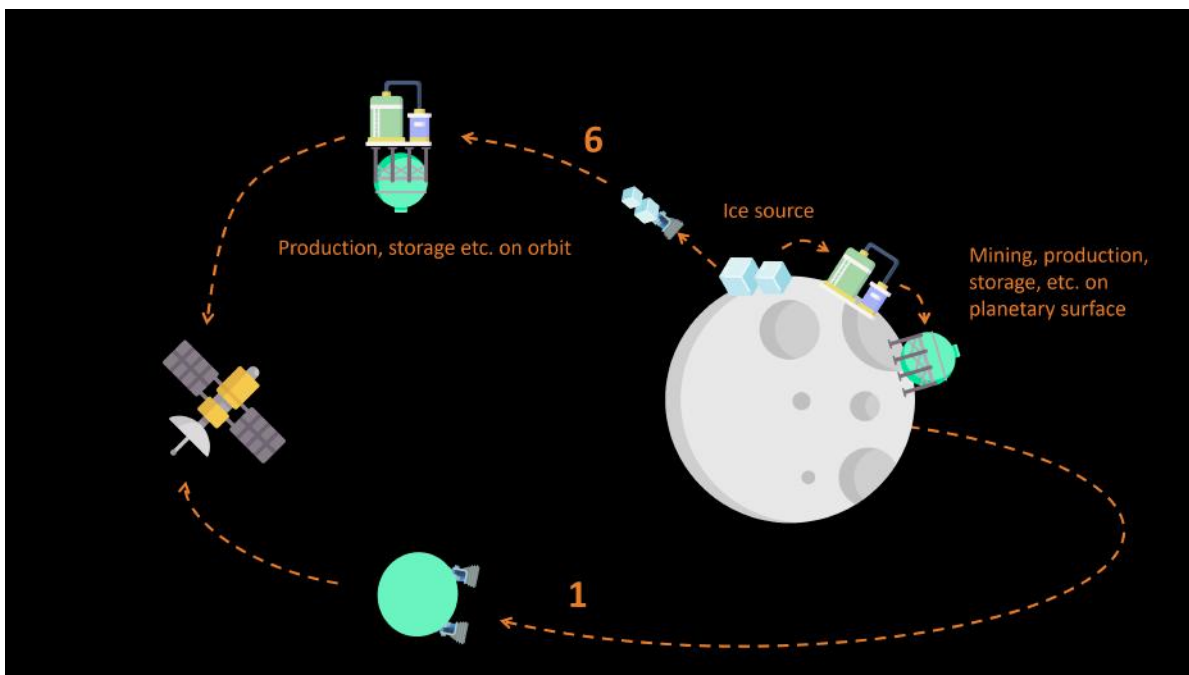


Figure 4.1: Segment location example showing options one and six from Table 4.1

As a baseline for the design of the propellant transfer system in question it is assumed that the primary use of the system would be in a refuelling architecture option number one. In this manner the payload of H₂O₂ is in its final, most energy dense, and thus lowest mass, form, which is desirable when launching items into orbit. The compatibility of the transfer system with other options in Table 4.1 is not neglected entirely but its main application is assumed as option six.

Figure 4.2 clarifies the nomenclature for this hypothetical refuelling architecture. The systems located on a planetary surface used for mining the water ice, liquefying it, producing H₂O₂, concentrating it, and storing it until a customer requires it, are referred to as the production segment. The customer is the vehicle that the propellant is to be transferred to. Finally the refuelling craft is the vehicle that ferries the H₂O₂ from the planetary surface in to orbit, rendezvouses with the customer, transfers the H₂O₂ and then returns to the planetary surface for the subsequent cycle.

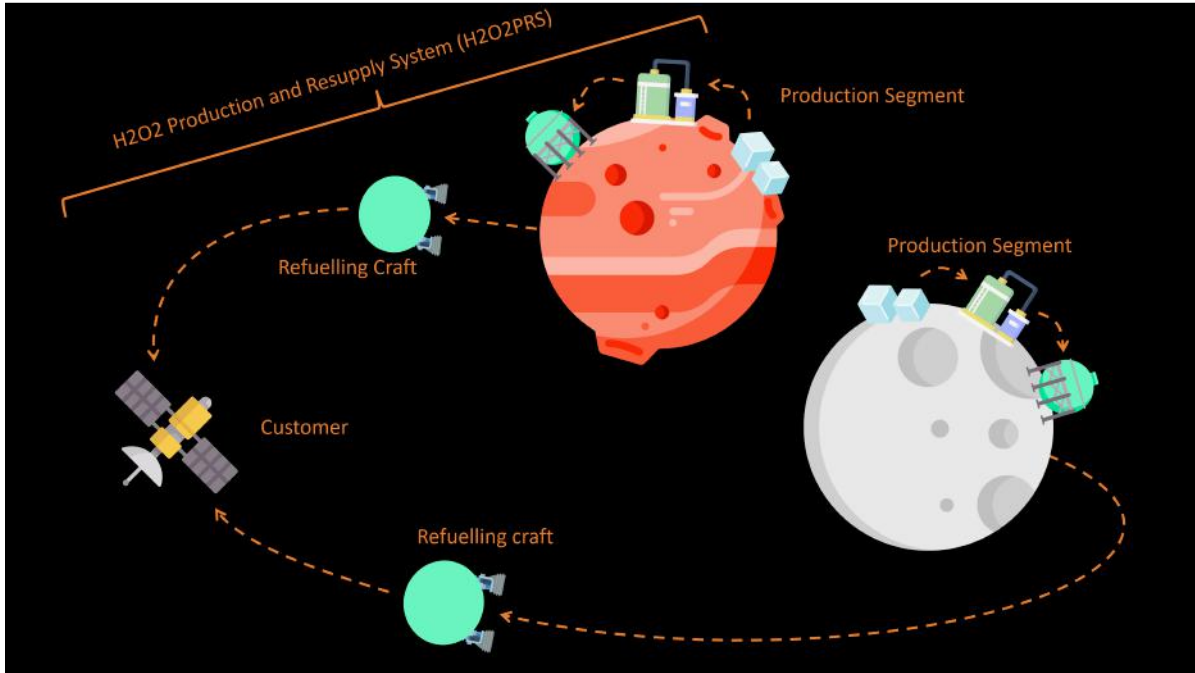


Figure 4.2: Naming of segments with chosen locations

4.2. Resupply Craft Sizing

As it has been decided that the production segment for the refuelling architecture in question will be located on a planetary surface, and only after the H_2O_2 has been produced and concentrated will it then be transferred to the customer, it is interesting to gain some initial insight into both the sizing and thus the feasibility of this refuelling craft that will carry out this transport. This sizing will be conducted in a top down manner, where instead of summing the mass of individual components, the components such as the structure and the payload will be generalised as ratios of the total mass. Subsequently a bottom up mass estimation of the transfer system is conducted in Section 4.3.

This sizing will only be conducted at a top level manner to gauge the feasibility of carrying a certain quantity of H_2O_2 from the surface of various planetary bodies to a variety of expected customer locations, with some basic assumptions made regarding the refuelling craft and its propulsion. This feasibility will be assessed by calculating the structural coefficient of a single stage to orbit (SSTO) craft for a variety of gross lift off weights (GLOW) and observing whether the craft would lay in a feasible range for these parameters.

The equation governing this sizing is the Tsiolkovsky rocket equation, Equation 4.1, where Δv is the velocity increment in m/s required to perform a certain manoeuvre, I_{sp} is the specific impulse of the propellant(s) used by the resupply craft, g is the gravitational acceleration on the Earth's surface, $9.81 m/s^2$, and m_0 and m_1 are the masses of the craft before and after executing the manoeuvre in question. As shown in Equation 4.2 and Equation 4.3, the initial, or GLOW, is made up of the structural mass, the propellant mass, and the payload mass, whereas the final mass is made up of only the structural mass and the payload mass. The structural coefficient λ is the ratio between the structural mass and the summation of the structural mass and the payload mass, as shown in Equation 4.4.

$$\Delta v = I_{sp} g \ln \frac{m_0}{m_1} \quad (4.1)$$

$$m_0 = m_s + m_p + m_{pl} = GLOW \quad (4.2)$$

$$m_1 = m_s + m_{pl} \quad (4.3)$$

$$\lambda = \frac{m_s}{m_s + m_p} = \text{structural coefficient} \quad (4.4)$$

Figure 4.3 displays the flight profile of the refuelling craft considered when carrying out this sizing. In this scenario two different burns or manoeuvres are executed. During the first manoeuvre the resupply craft launches from the planetary surface, carrying with it the mass of propellant required to complete the ascent (M_{p_a}), the mass of H_2O_2 to be transferred to the customer craft ($M_{H_2O_2}$), and the mass of propellant required to complete the descent afterwards (M_{p_d}). During the first manoeuvre the $M_{H_2O_2}$ and M_{p_a} are treated as payload mass. After this burn has finished and M_{p_a} is consumed, $M_{H_2O_2}$ is then also subtracted from the craft mass, assuming it has been transferred to the customer. Finally the second manoeuvre, returning to the planetary surface is executed, with no payload mass remaining, and M_{p_d} is consumed. This method of sizing the refuelling craft neglects a number of factors, including the propellant required for course corrections, for manoeuvring in proximity with the customer craft and rendezvousing with it, trapped propellant etc. however it suffices for an initial first order sizing.

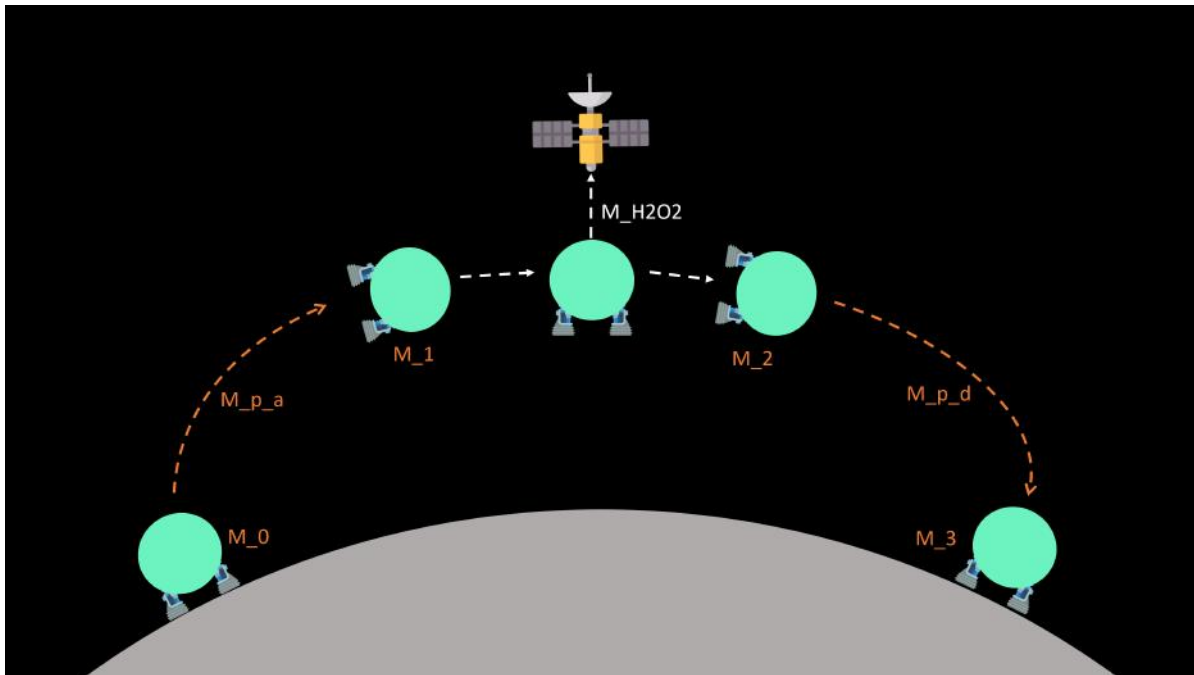


Figure 4.3: Refuelling Craft Flight Profile

The delta-V required to travel from certain planetary bodies to other locations in the solar system are known, and a variety of these may be seen in Figure 4.4. The planetary bodies used in this sizing are chosen based off of those that are confirmed or suspected to contain water ice which may be used as a feed stock for the H_2O_2 production process, namely Earth's moon, Mars, and the Martian moons Phobos and Deimos. For each of these locations a customer location must be chosen. For the Moon both Earth-Moon Lagrange Point 1 (EML-1) and Earth-Moon Lagrange Point 2 (EML-2) are locations where customer vessels may be permanently located or used a loitering point to be refuelled before embarking on the remainder of a mission. From the Moon Low Lunar Orbit (LLO) is also a potential location for customers. From Mars the primary location of customer craft is chosen as Low Martian Orbit (LMO) circa 200 km. And similarly from Deimos and Phobos LMO is chosen as the most likely customer location. Table 4.2 presents tabulated delta-V data for these aforementioned refuelling routes, and additionally the delta-V required from the Martian moons to both EML-1 and EML-2, as it may be seen that especially for EML-2, interestingly less delta-V is required than to travel from the Lunar surface. These additional routes will not be evaluated during this sizing but are mentioned here to highlight their potential beneficial exploitation which is recommended for further investigation. It should be noted that for the Mars surface to LMO route, the delta V requirement for the descent is halved as it is assumed that aerobraking can be utilised to decrease the remainder of the velocity. The remainder of the routes require the same delta-V for descent as for ascent.

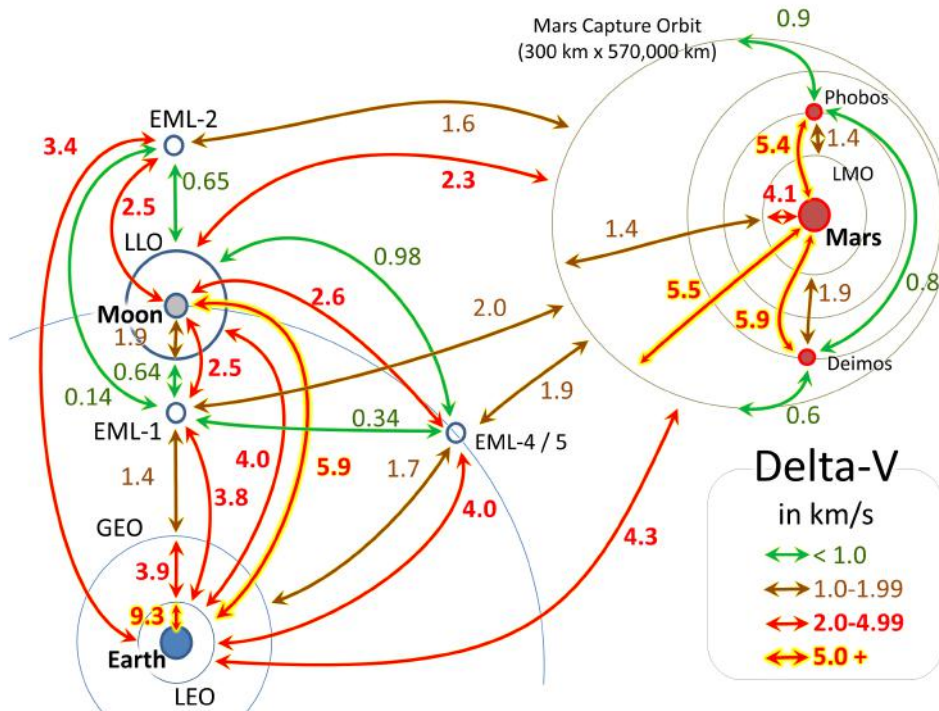


Figure 4.4: Delta-V Map of the Earth, Moon, and Mars System. chart by R. Penn¹

Table 4.2: Tabulated delta-V data for likely refuelling routes and additional routes of interest

Route	delta V [km/s]
Moon surface to EML-1	2.52
Moon surface to EML-2	2.53
Moon surface to LLO	1.9
Mars surface to LMO	4.1
Phobos surface to LMO	1.4
Deimos surface to LMO	1.9
Phobos surface to EML-1	2.9
Phobos surface to EML-2	2.5
Deimos surface to EML-1	2.6
Deimos surface to EML-2	2.2

Here it is worth briefly discussing the payload mass, or resupply propellant quantity, that is to be taken. As the refuelling craft of this thesis will operate as a commercial venture, it is beneficial for it to be able to refuel the most suitable amount to potential customers. Figure 4.5 presents the propellant mass of a variety of satellites, recorded versus their year of launch. No clear trend is present and this data misses data points from recent years. As refuelling is most likely to be done with cooperative customers, as in those equipped with refuelling ports, likely satellites constructed in the coming years, it is more of interest to analyse the trends in future propellant loads. Two examples of spacecraft that may require refuelling in the coming decade are the James Webb space telescope (JWST), and the Galileo constellation of the European Union. JWST possesses a refuelling port, and carries 240 L of propellant on board. The Galileo satellites do not currently carry refuelling ports but there is the potential for them to be added in the future, and these satellites carry 93 kg of propellant on board. The propellant load

¹hopsblog-hop.blogspot.co.uk

of these satellites is clearly lower than those of Figure 4.5. It is decided to take 200L of propellant as a reference value for the investigation in this thesis, as it has margin on the value for the Galileo satellites and is close to the value of the JWST. It is also just above the greatest propellant volume used by any of the propulsion systems surveyed in Table 2.1. With the density of high concentration H_2O_2 this 200 L of propellant is equivalent to 290 kg.

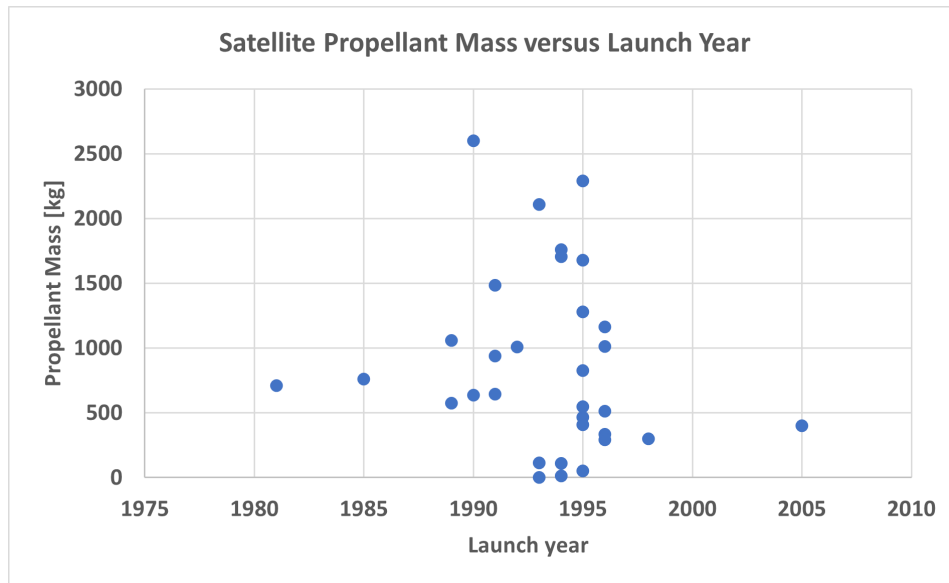


Figure 4.5: Satellite propellant mass versus year of launch. Reproduced from Zandbergen[78]

Plots of the GLOW vs Structural Coefficient are generated for each route by taking the delta-V required, as well as the payload mass of $290kg$, and with a variety of values for I_{sp} and M_3 the mass of the craft before and after the various manoeuvres may be calculated. For the choice of I_{sp} H_2O_2 was assumed as the oxidiser given the ability to produce it on location, while for fuels two that may be produced through ISRU methods from water ice or using CO_2 (mainly present on Mars) of LH_2 and CH_4 were used and kerosene was also included due to its prolific use though how it may be supplied/produced elsewhere in the solar system is less clear. These combinations provide I_{sp} values of $319s$ for H_2O_2 -Kerosene, $342s$ for H_2O_2 - CH_4 , and $378s$ for H_2O_2 - LH_2 . Thus the analysis is run for I_{sp} values of $300s$, $320s$, and $340s$ as these are deemed to be more feasible to reach. An example of the values output from this sizing may be seen in Table 4.3. Here it may be seen that a value is taken for M_3 from which the remainder of the masses may be calculated. For each new row the value of M_3 is doubled. This sizing is conducted for each route and each I_{sp} value yielding Figure 4.6 and Figure 4.7.

Table 4.3: GLOW and structural fraction calculation for the Moon surface to EML-1 route with an I_{sp} of 300 s and a payload of 290 kg

delta V [km/s]	m_3 [kg]	m_2 [kg]	m_pd [kg]	m_1 [kg]	m_0 [kg]	m_pa [kg]	struc frac [-]
2.52	7.2	17.0	9.8	307.0	722.8	415.8	0.0167
2.52	14.5	34.0	19.6	324.0	762.9	438.9	0.03057
2.52	28.9	68.1	39.2	358.1	843.0	485.0	0.052282
2.52	57.8	136.1	78.3	426.1	1003.3	577.2	0.081069
2.52	115.7	272.3	156.6	562.3	1323.8	761.5	0.111869
2.52	231.3	544.6	313.3	834.6	1964.9	1130.3	0.138102
2.52	462.6	1089.2	626.5	1379.2	3247.0	1867.9	0.156445
2.52	925.2	2178.3	1253.1	2468.3	5811.3	3343.0	0.167574
2.52	1850.5	4356.6	2506.2	4646.6	10939.9	6293.2	0.173754
2.52	3700.9	8713.3	5012.4	9003.3	21196.9	12193.7	0.177018
2.52	7401.8	17426.5	10024.7	17716.5	41711.1	23994.6	0.178697
2.52	14803.6	34853.1	20049.5	35143.1	82739.5	47596.4	0.179548
2.52	29607.3	69706.2	40098.9	69996.2	164796.2	94800.0	0.179977
2.52	59214.5	139412.3	80197.8	139702.3	328909.6	189207.3	0.180192
2.52	118429.0	278824.6	160395.6	279114.6	657136.5	378021.8	0.180299
2.52	236858.1	557649.3	320791.2	557939.3	1313590.2	755650.9	0.180353

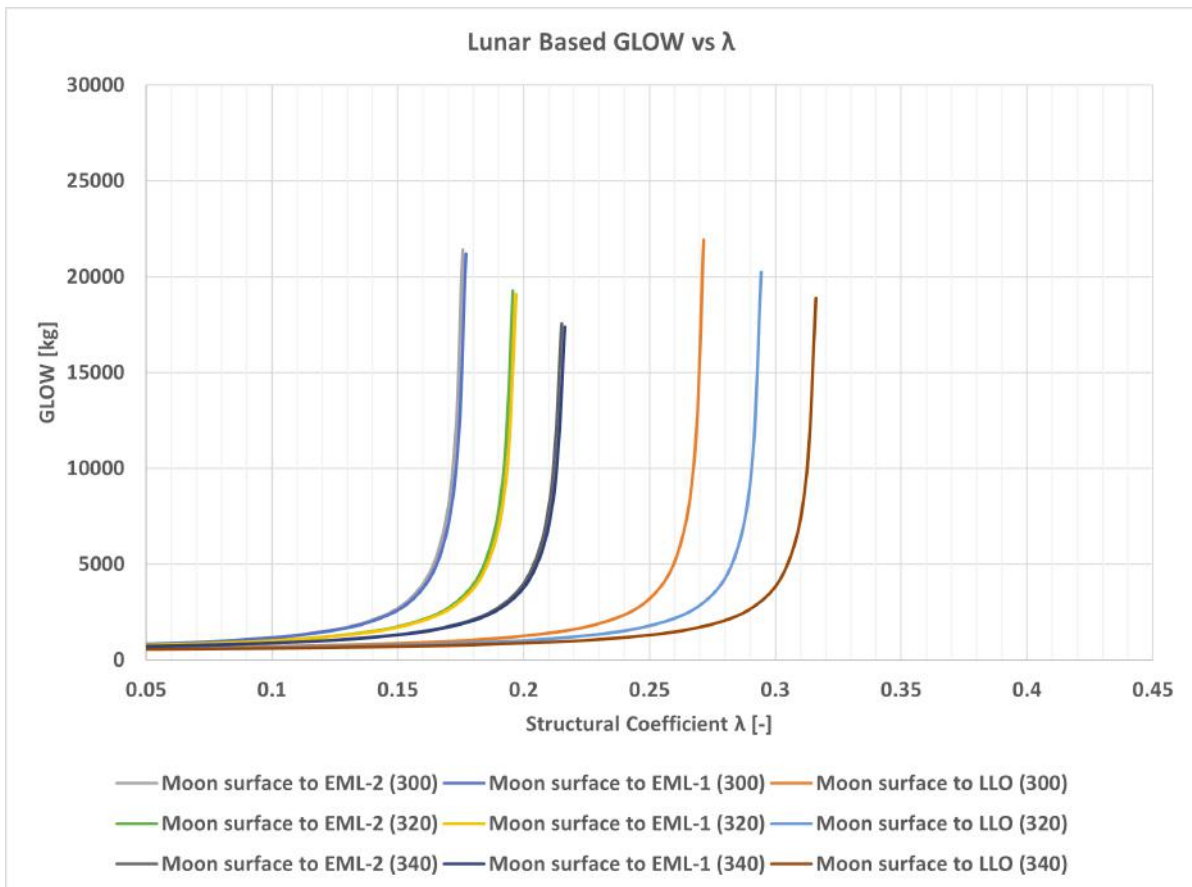


Figure 4.6: LOW vs λ for a variety of Lunar based production destinations and I_{sp} values of 300s, 320s, and 340s

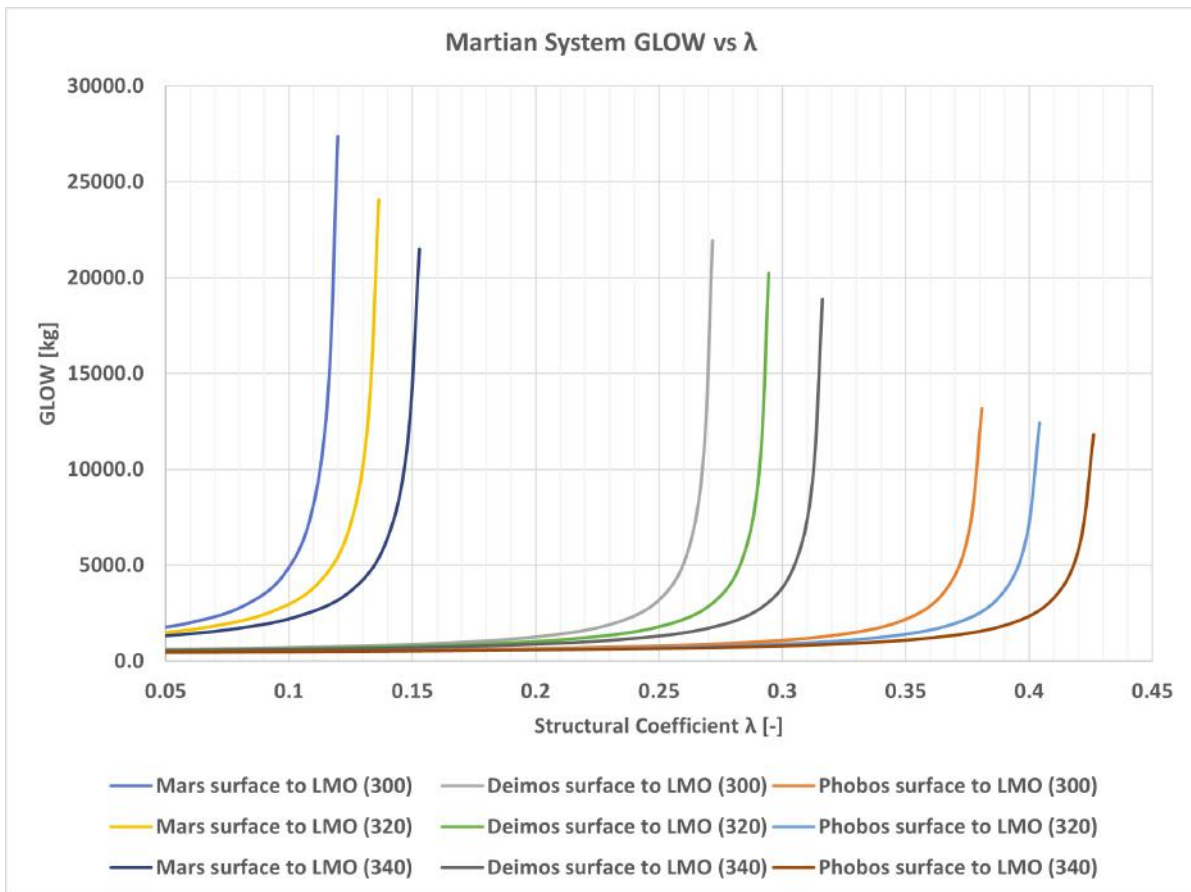


Figure 4.7: GLOW vs λ for a variety of Martian system based production destinations and I_{sp} values of 300s, 320s, and 340s

Figure 4.6 and Figure 4.7 illustrate a number of things. Current material technology imposes a limit on the value of λ of 0.1, below which structures are not feasible. All points for the various routes and I_{sp} lie above a λ of 0.1 meaning that with this as a lower bound they are feasible. However this value is an absolute minimum, and while it may be possible to approach this for optimised launch vehicles, especially multi-stage vehicles, it is less likely that this is achievable for lower heritage, SSTO vehicles. Thus Table 4.4 presents the mass data and calculated structural coefficients for a variety of vehicles, with the Falcon 9 included to show the low value for modern launchers, and the remainder are historical, current or proposed Lunar landers, which are a closer vehicle to what is being considered. The average of these structural coefficients for the representative craft is 0.33, increasing to 0.37 when the Starship HLS, an optimistic outlier, is excluded, but dropping to 0.29 when the LK Soviet Lander, a heavy outlier is excluded.

Table 4.4: Calculated structural coefficient for a variety of vehicles, primarily Lunar ferry vehicles

Vehicle	m _{prop} [kg]	m _{dry} [kg]	m ₀ [kg]	m _{payl} [kg]	λ [-]
Falcon 9	488370	29500	517870	22000	0.06
Lunar Lander	11480	4920	16400		0.30
Lunar Lander Ascent	2550	2150	4700		0.46
LK Soviet Lander	2400	3160	5560		0.57
Chang'e 3	2460	1320	3780		0.35
Starship HLS	1500000	110000	1710000	100000	0.07
Lockheed Lander	40000	22000	63000	1000	0.35
Blue Origin HLS	9000	2250	14650	3400	0.20

If the higher of these structural coefficient averages is taken as the cut off point for a feasible refuelling craft then the only route that would appear to be possible would be the Phobos to LMO option. After this route both the Deimos to LMO and Lunar surface to LLO routes are equally feasible in terms of structural coefficient. Next come the Lunar surface to EML-1 and EML-2 routes, with the most challenging route being the Martian surface to LMO. All of these routes do lie above the theoretical limit of structural coefficients of 0.1, and well above the apparent values for the Falcon 9 and Starship HLS values of 0.6 and 0.7 respectively. It is likely for such a new form of vehicle initial versions lack the low structural coefficient of optimised models and thus either the Lunar surface to LLO or the Martian moons routes would first be tested. During this craft development, once an achievable structural coefficient has been identified, the resulting GLOW and transportable propellant amount may be estimated.

Overall it may be concluded that an SSTO refuelling architecture as outlined in Figure 4.2 and Figure 4.3 appears viable. As with all spacecraft, the vehicle dry mass will be of critical importance to its viability thus the development of propulsion, structural, GNC systems etc. must be done with this in mind. With this minimisation of dry mass in mind it should be investigated if the transfer system can be placed on the depot or production segment, however on routes where no depot is present and transfer must be done directly to the customer this cannot be done. In this way the transfer mechanism must be versatile and capable of being located within multiple systems.

4.3. Mass Sizing of Transfer Mechanism Variations

With the conclusion of Section 4.2 being that the transfer mechanism should be located on the depot or production segment if possible, three possible locations for the transfer system can be identified, on the production segment, on the depot or on the production craft, as shown in Figure 4.8. It is assumed that the mass penalty of having the propellant transfer system located on the customer craft would be too great of a price to pay. The case that will be focused on is the placing of the transfer system on the transfer craft. While this is the most challenging to the structural coefficient of the vehicle it is also the most versatile of the placements, as transfer can always be conducted irrespective of if a depot is used or not. The mechanism will thus be designed for this case.

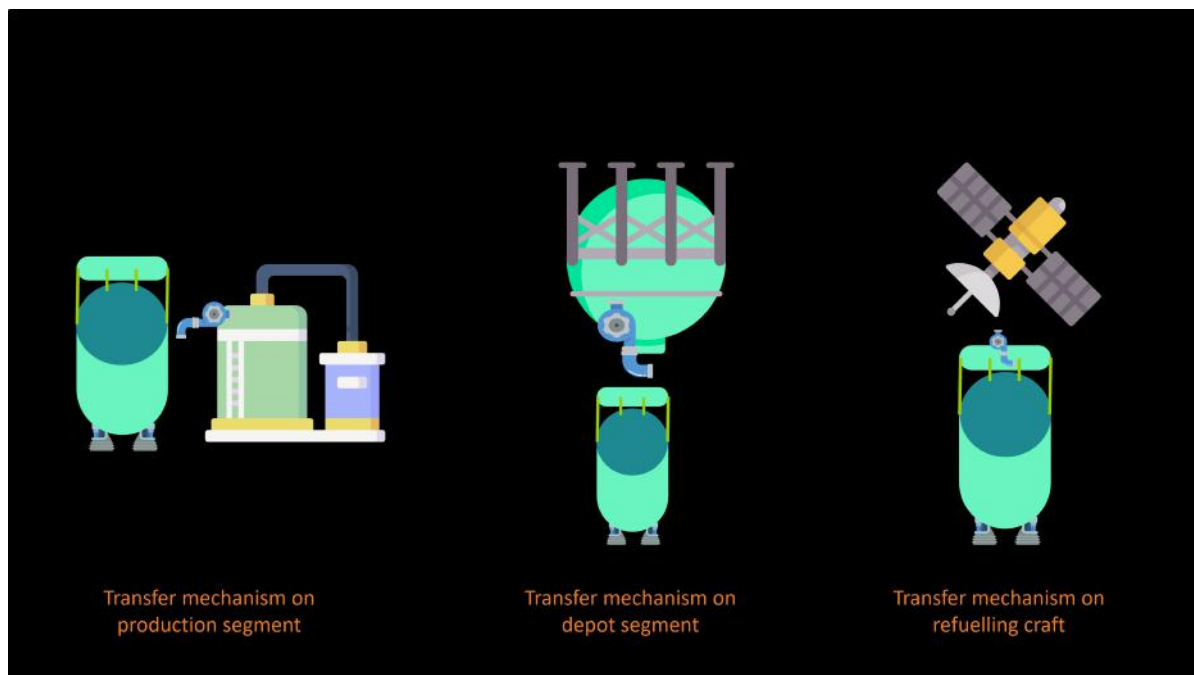


Figure 4.8: Possible placement of the transfer mechanism

Section 3.2 highlights the applicability of a number of other transfer systems in tandem with the piston system, namely using a gas generator to decompose a small amount of the H_2O_2 in order to provide pressure for the transfer, or using a pump to provide pressure. A comparison of total system mass for the three options of using purely pressurant gas for the transfer, using a gas generator to

decompose H₂O₂ for the transfer, and of using pressurant gas and an electric pump for the transfer. In all three scenarios pressurant gas must still be carried to resupply the customer with. The initial inputs used for this sizing are the pressure the propellant tank is to be pressurised to $P_{f_{prop}}$, the final allowable pressure of the pressurant gas tank $P_{f_{gas}}$, and the initial pressure of the pressurant gas tank $P_{i_{tank}}$. Additionally some constants are required such as the yield strength and the density of the material the vessels is to be made from σ , ρ_{wall} , the density of the propellant ρ_{prop} , the temperature of the pressurant gas T_{gas} , the molecular mass of the pressurant gas M , and the specific heat ratio of the pressurant gas γ . The two parameters that may be varied for the purpose of the system mass sizing are the volume of propellant to be transferred V_{prop} and the desired propellant transfer rate \dot{m} .

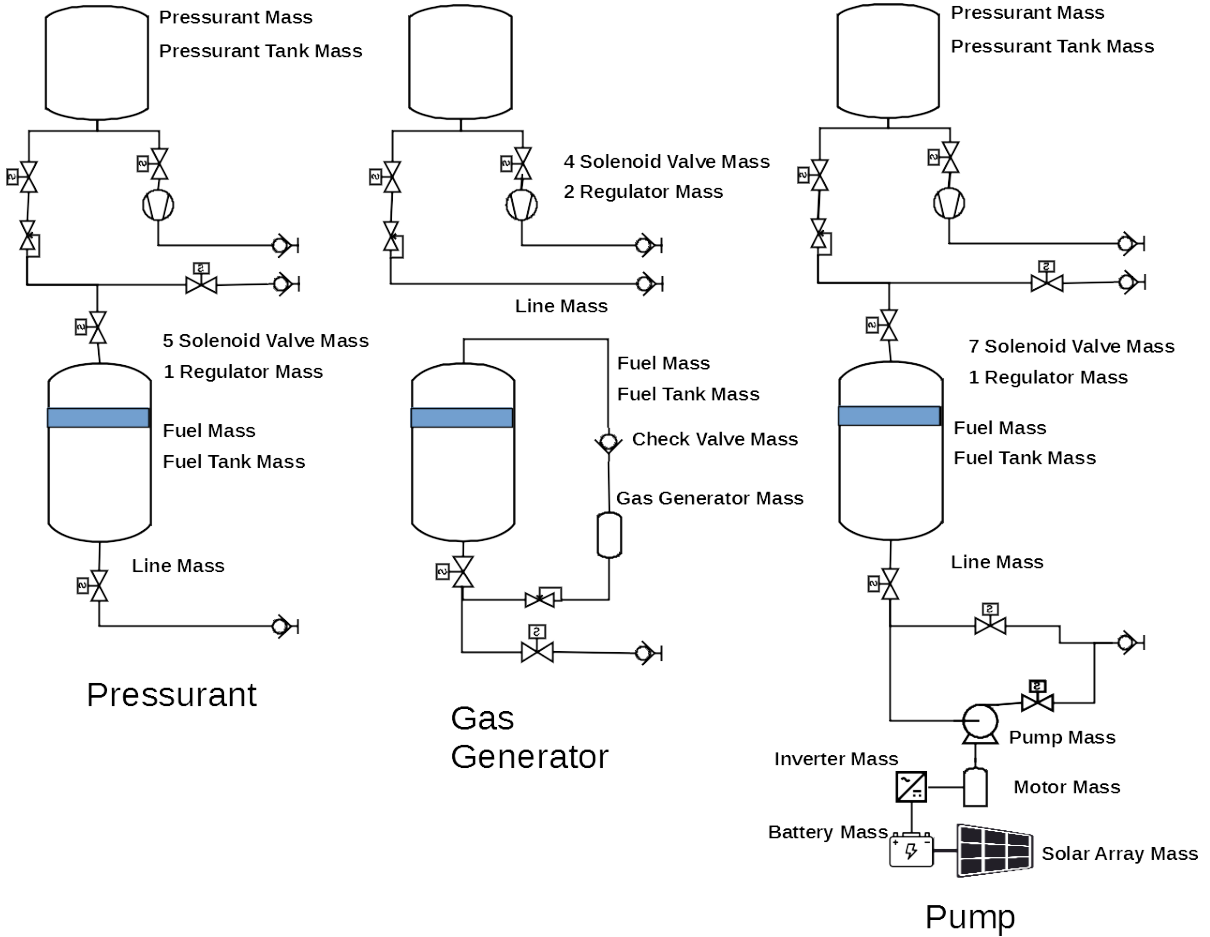


Figure 4.9: Schematic of the system layouts used for comparative mass sizing

First the masses of the propellant and the propellant tank, as well as the mass and volume of the pressurant gas are calculated. With an input volume of propellant the mass may be calculated using the propellant density. The pressurant gas mass is calculated using Equation 4.5 from which the gas volume may be calculated using the ideal gas law. With the volume to be contained in both the pressurant and propellant tanks known the radius of the tank may be calculated assuming the tank to be a sphere, and using a constant safety factor of four for all sizing the tank wall thickness may be calculated using the material strength. The minimum producible skin thickness for the tanks is limited to 0.1 mm[60], if a value lower than this is required then 0.1 mm is taken. In such a scenario the safety factor will be higher than four and this resulting safety factor is also calculated. With the value of tank wall thickness known then the tank mass may be generated by multiplying the tank area by the wall thickness and the tank material density. This same procedure is conducted for the propellant tank.

$$M_{gas} = \frac{P_{tank} \cdot V_{tank}}{R \cdot T_i} \cdot \left[\frac{\gamma}{1 - (P_f/P_i)} \right] \quad (4.5)$$

The next component to have its mass estimated are the feed lines. Firstly the feed line pipe diameter is established using Equation 4.6, where \dot{m} is the mass flow through the line, ρ is the flow density in kg/m^3 , and v is the flow velocity in m/s. The flow velocity is set at 9 m/s for this sizing, the upper bound of the recommended range[42]. Next the piping length is estimated. For the purposes of this sizing the piping length is taken as a multiple of the propellant tank radius, with the multiplier estimated based off of the feed system layouts shown in Figure 4.9. For the regulated pressure option a multiplier of five is used, for the gas generator option ten is taken, and for the pump option one is taken. The thickness of the piping is established using the same relation as for the tanks, but for the piping the final pressure in the tank is taken as the internal pressure, and three is used as a safety factor. Again the minimum thickness is taken as .1 mm and the pipe mass is found by multiplying the surface area by the thickness of the walls and the wall material density. The pressure drop over the piping is briefly assessed in order to establish whether it is significant enough to be accounted for in this top level mass sizing. For this Equation 4.7, Equation 4.8 and Equation 4.9 are used. Equation 4.7, where ρ is the fluid density, v is the flow velocity, D is the pipe diameter, and μ is the dynamic viscosity of the fluid which is taken as 0.0012141 kg/ms for H_2O_2 . With the Reynolds number calculated the appropriate friction coefficient may be selected from Equation 4.8, and applied to Equation 4.9, Darcy–Weisbach equation. The highest pressure drop observed in this sizing is 0.124 bar which is deemed to be low and thus it is neglected.

$$D_{pip} = \sqrt{\frac{4 \dot{m}}{\pi \rho v}} \quad (4.6)$$

$$Re = \frac{\rho v D}{\mu} \quad (4.7)$$

$$f = \begin{cases} \frac{64}{Re}, & Re \leq 2000 \\ 0.3164 Re^{-0.25}, & 2000 < Re \leq 10^5 \\ 0.0032 + 0.221 Re^{-0.237}, & Re \geq 10^5 \end{cases} \quad (4.8)$$

$$\Delta p_{pip} = f \left(\frac{l_{pip}}{D_{pip}} \right) \frac{1}{2} \rho v^2 \quad (4.9)$$

For the gas generator system both the mass of the gas generator as well as the additional H_2O_2 required to operate it must be estimated. The gas generator system mass is set at 0.1 kg for each configuration in order to avoid overly complex sizing at this stage. This value was chosen based off of the masses of several similarly sized gas generators from the General Kinetics Inc. gas generator catalogue [23]. A number of methods were trialled to estimate the mass of H_2O_2 required to run the gas generator and pressurise the main run tank. A mass balance of the tank liquid output and the tank gaseous input was trialled however the complexity due to estimating the gas generator exhaust product temperature made this method unfeasible as it was estimating very low H_2O_2 mass flows. Instead a value from Whitehead was used where 2% of the main H_2O_2 flow is diverted to the gas generator and thus this additional amount of peroxide must also be stored in the tank. Lastly check valve mass for each flow rate was taken from supplier data sheets[30].

In order to size the pump system and supporting hardware the method employed by Lee [42] is used. The following components are considered of the pump itself, the electric motor to drive the pump, the power inverter, the battery to store the power for the system and the additional solar array mass required for this option compared to the other options. The required pump power is given by Equation 4.10 where ΔP_P is the pressure increased the pump creates, \dot{m} the mass flow through the pump, ρ the density of the liquid flowing through the pump, and η_P the pump efficiency, taken as 61% which is the same value Lee uses. Equations Equation 4.11, and Equation 4.12, define the specific velocity, N_s , and the specific diameter, D_s , respectively where ω is the rotational speed, Q the volumetric flow rate, H the pump head rise, and D_{out} the outlet diameter. Equation 4.13 relates N_s and D_s through the Cordier diagram, an empirical relation. Equation 4.14 gives the outlet velocity of the pump u_{out} and finally Equation 4.15 gives the pump mass based on the pump diameter.

$$P_p = \frac{\Delta P_p \dot{m}}{\rho \eta_p} \quad (4.10)$$

$$N_s = \frac{\omega\sqrt{Q}}{(gH)^{3/4}} \quad (4.11)$$

$$D_s = \frac{D_{out}(gH)^{1/4}}{\sqrt{Q}} \quad (4.12)$$

$$N_s = 3.72 \cdot D_s^{-1.1429} \quad (4.13)$$

$$u_{out} = \omega \frac{D_{out}}{2} \quad (4.14)$$

$$m_p = 0.4703 \times \exp(0.01072 \times D_p) \quad (4.15)$$

Next the electric motor that drives the pump may be analysed. Equation 4.16 gives the motor power density, $\delta_{P,m}$ which relates the motor power output $P_{m,out}$, and the motor mass, m_m . The input power required by the pump is equivalent to the output power from the motor and thus Equation 4.17 shows how the motor mass may be found based on the required pump power. The motor power density $\delta_{P,m}$ is taken as $0.875kW/kg$, the same value used by Lee.

$$\delta_{P,m} = \frac{P_{m,out}}{m_m} \quad (4.16)$$

$$m_m = \frac{1}{\delta_{P,m}} P_{m,out} = \frac{1}{\delta_{P,m}} P_p \quad (4.17)$$

Similar to the motor the inverter mass may be estimated using its power density δ_{inv} and Equation 4.18 where $P_{inv,out}$ is the inverter output power and m_{inv} is the inverter mass. η_m , the motor efficiency, which relates the inverter output power and the motor output power, allows us to obtain the invert mass using Equation 4.19. The motor efficiency is taken as 87%.

$$\delta_{inv} = \frac{P_{inv,out}}{m_{inv}} \quad (4.18)$$

$$m_{inv} = \frac{1}{\delta_{P,inv}} P_{inv,out} = \frac{1}{\delta_{P,inv}\eta_m} P_{m,out} \quad (4.19)$$

Two parameters are important for estimating the battery mass, namely the power density $\delta_{P,b}$ and the energy density $\delta_{E,b}$ whose equations may be found in Equation 4.20 and Equation 4.21 respectively. Here κ_b is a structural margin applied to the battery pack accounting for sub-component masses, assumed to be 1.2, η_{inv} is the inverter efficiency (85%), η_E is the battery efficiency (92.5%), $P_{inv,out}$ is the inverter power out and t_b is the duration over which the pump must be powered. This pump duration is calculated based on the total mass of propellant to be transferred and the transfer rate selected. Both the mass estimate based on power density and the mass estimate based on energy density are calculated and the larger value of the two is taken for a conservative estimate.

$$m_{b,P} = \frac{\kappa_b}{\delta_{P,b}} P_b = \frac{\kappa_b}{\delta_{P,b}\eta_{inv}} P_{inv,out} \quad (4.20)$$

$$m_{b,E} = \frac{\kappa_b}{\delta_{E,b}} E_b = \frac{\kappa_b}{\delta_{E,b}\eta_E\eta_{inv}} P_{inv,out}t_b \quad (4.21)$$

$$m_b = \max(m_{b,P}, m_{b,E}) \quad (4.22)$$

Solar array mass may be found according to Equation 4.23 where $(P_{Sp})_{SA}$ the specific power of the array in W/kg and P_{SA} is the power output required of the array. The value of $115 W/kg$ is taken for the specific power, that of TJ GaAs ultraflex arrays, a mid-range array model, at the beginning of solar array life. Values for end of life should be used during actual design work however this suffices for sizing comparison at this stage. This value is corrected for operations in a Martian orbit of $1.5 AU$.

$$M_{SA} = \frac{P_{SA}}{(P_{Sp})_{SA}} \quad (4.23)$$

The remaining components that require their mass to be estimated are the solenoid valves and the pressure regulators. From Figure 4.9 the number of pressure regulators and solenoid valves in each configuration may be established. These values were also taken from relevant supplier data sheets and while not chosen in a detailed manner their masses have a relatively low impact on the overall mass estimation.

Table 4.5 displays the resultant masses of each component of the three configurations for the 200L transferred at 0.1 kg/s variation. The results for the other settings may be found in Appendix C. For the components where the number implemented varies per configuration the number in each configuration is shown in brackets. The output component masses for all four variations of 200L and 1000L, and 0.1kg/s and 1 kg/s are plotted in Figure 4.11. Note that in these plots the propellant/fuel mass to be transferred is by far the largest mass, and thus the plots are truncated to primarily display the other component masses in the system.

Table 4.5: Mass of sub-components of transfer systems using pressurant gas, gas generator, and pumped, for 200L transferred at .1 kg/s

Mass	Pressurant	Gas Generator	Pumped
Propellant Mass	290.000	295.800	290.000
Propellant Tank Mass	7.452	7.551	7.452
Pressurant Mass	2.224	1.112	1.479
Pressurant Tank Mass	19.213	9.606	12.776
Solenoid Mass	(5) 2.000	(4) 1.600	(7) 2.800
Regulator Mass	(1) 0.400	(2) 0.800	(1) 0.400
Line Mass	0.286	0.576	0.858
Pump Mass			0.470
Motor Mass			0.033
Inverter Mass			0.001
Battery Mass			0.187
Solar Array Mass			0.760
Gas Generator Mass		0.100	
Check Valve		0.400	

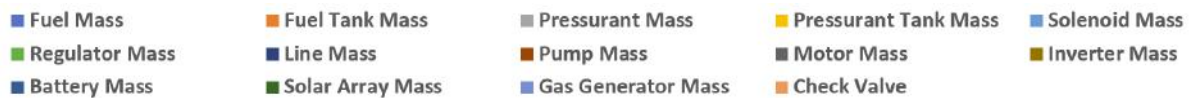
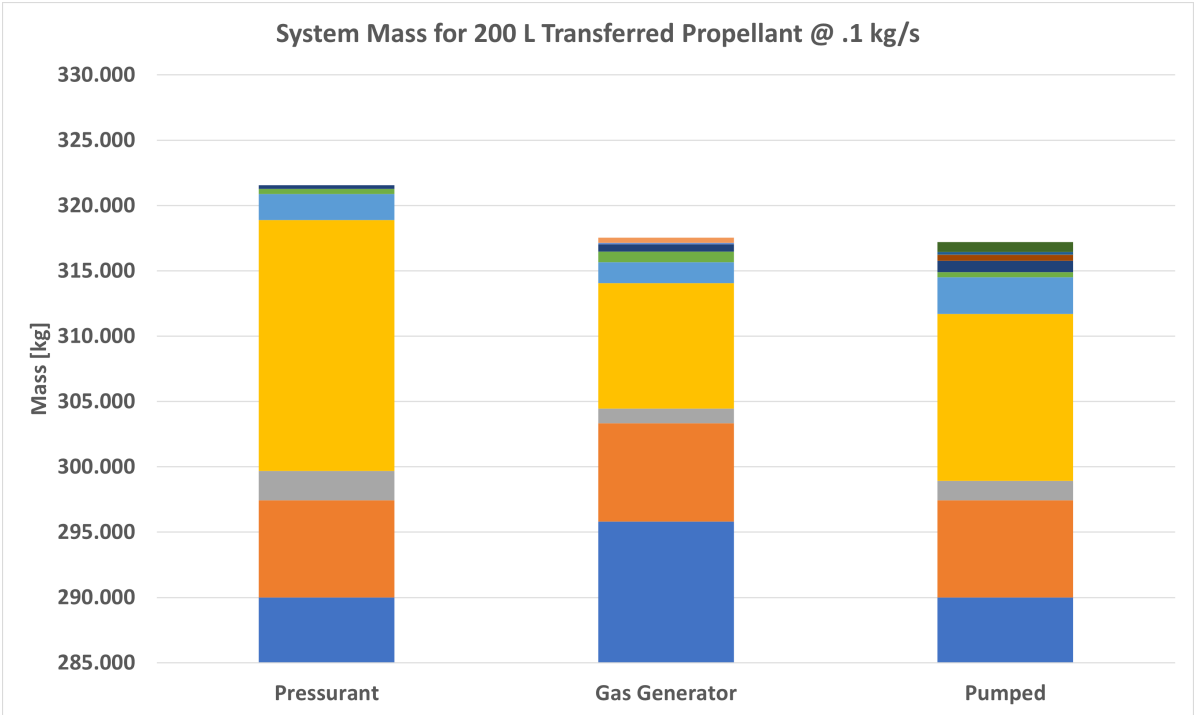
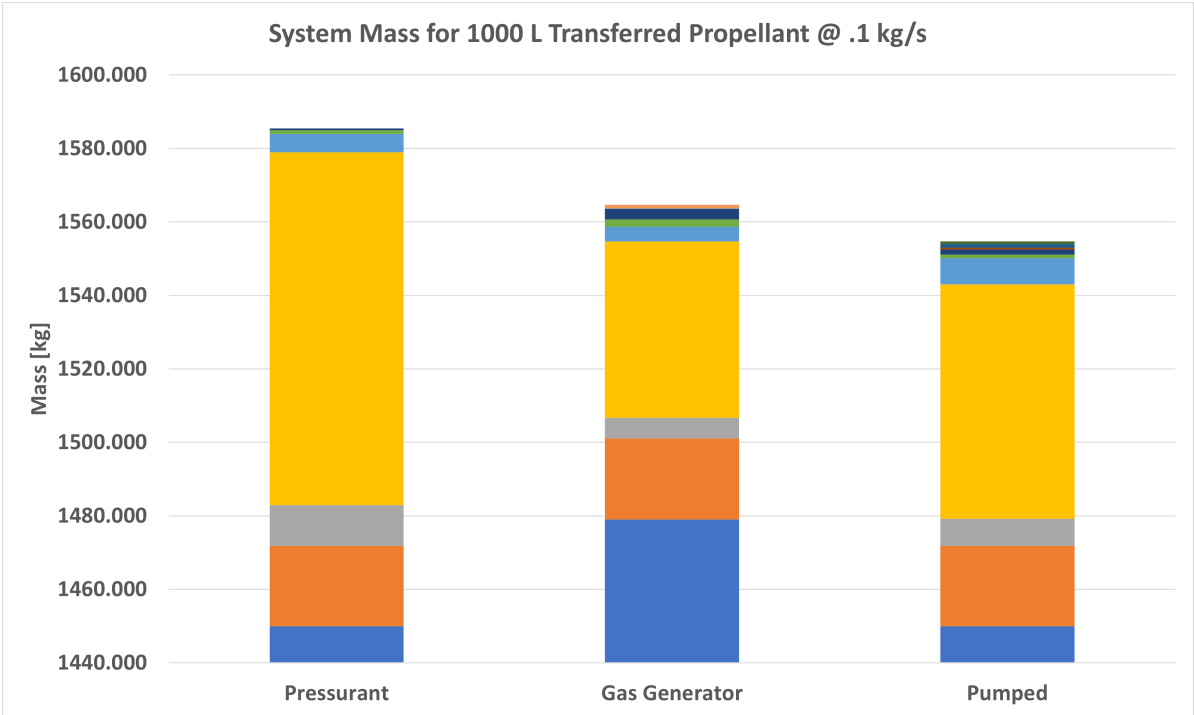


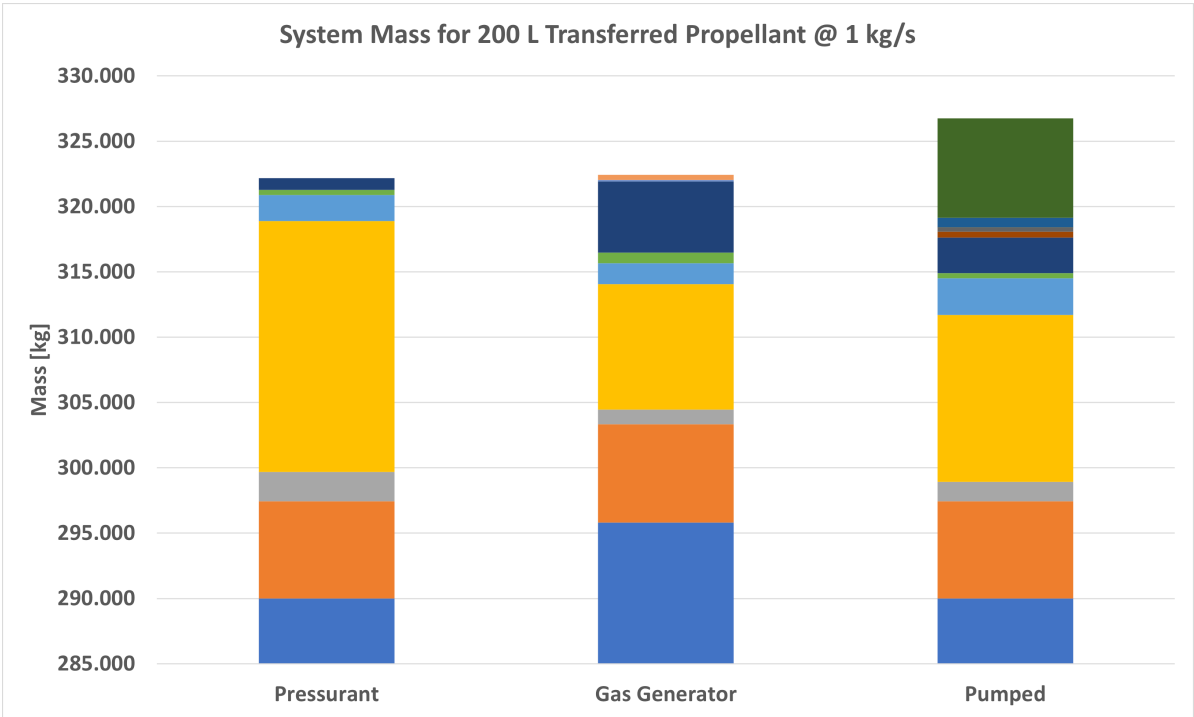
Figure 4.10: Symbol legend for Piping and Instrumentation Diagrams



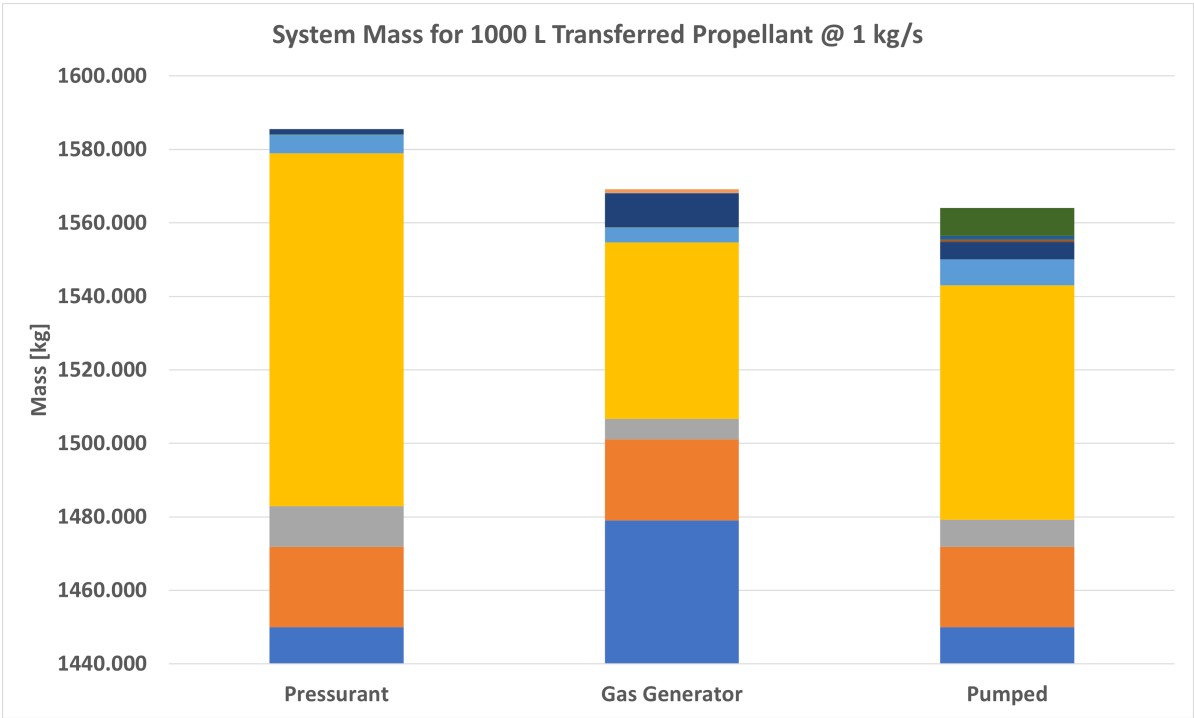
(a) Component Mass for 200L Transferred at 0.1 kg/s



(b) Component Mass for 1000L Transferred at 0.1 kg/s



(c) Component Mass for 200L Transferred at 1 kg/s



(d) Component Mass for 1000L Transferred at 1 kg/s

Figure 4.11: Mass sizing of three different piston based transfer methods at varying propellant volume and transfer rates

One of the first observations that may be made on the plots in Figure 4.11 is that the outcome of this mass comparison is very sensitive to the assumptions it is based on. For example the assumption that the pump configuration requires such an addition of electrical power that the mass of the power generation and power train equipment should be modelled leads to significant changes in the overall mass. Similarly some potential influencing factors are neglected, such as the heating effect of the gas generator system, potentially requiring adjustments to the piping and valving, and other in depth considerations about peripheral systems to these transfer methods. It is clear from comparing Figure 4.11a and Figure 4.11b that the transfer rate is a driving influencer on the mass of the solar arrays and pumping system as well as driving the feed line mass in the gas generator variation, both results of the assumptions the mass models are founded on. After the mass of the propellant to be transferred, the mass of the propellant tank and the mass of the pressurant tank are the second largest contributors to the overall system mass. The mass of these tanks is mainly driven by the minimum producible thickness as well as the applied safety factor, and these masses are likely to change if the material is changed from metal to potentially composite structures. While it could be said that different transfer configurations are likely more appropriate for different transfer scenarios, what can clearly be concluded is that compared to the propellant mass the configuration specific masses are very low, for example comparing the configurations of the 1000L system, the total mass variation between them is close to 20 kg, less than 2% of the total system mass, with a similar percentage difference present on the 200L systems. As the piston system may be supplemented for various applications with the addition of the gas generator or pump, and these additions have a low relative impact on the total system mass, purely the general pressurant actuated piston will be focused on for the testing conducted. The pressurant tank mass, as the second largest mass contributor in every configuration presented, is driven by the quantity of pressurant that is required, and the pressure it is stored at. Thus the experimental set up of this piston transfer system will gather data on the pressurant mass required to refine the estimate employed.

4.4. Conclusion

While the different operations contained within an in-space refuelling architecture may be conducted in a variety of locations, it is assumed for the sake of this work that the majority, being the mining of water ice, its liquefaction and the production of H_2O_2 , and the storage, are all conducted on a planetary or Lunar surface. Solely the delivery of the H_2O_2 is carried out in-orbit, and thus the propellant transfer system must operate in a low-G environment to receive the H_2O_2 from the production segment, and also in a zero-G environment to transfer the H_2O_2 to the customer.

An initial sizing of an SSTO refuelling craft, launching from a variety of locations with water ice, and using a variety of propellant combinations, provides a design envelope within which the propellant transfer system may be placed. This sizing illustrates that depending on the achievable structural coefficients, the most accessible refuelling route is from Phobos to LMO, followed by Deimos to LMO and Lunar surface to LLO routes. The criticality of the mass of this refuelling vehicle means that it may be of interest in some applications for the propellant transfer mechanism to be located off of the refuelling craft, such as on both the production segment and on an orbiting depot, shaving mass off the refuelling craft itself and making a certain refuelling route feasible.

A mass sizing comparison is conducted for the three piston transfer methods of stored gas, pumped and a gas generator. This sizing is conducted for a transferred propellant volume of both 200L and 1000L, at transfer rates of 0.1 kg/s and 100 kg/s. It is found that for the different permutations of the transferred amount and the transfer rate, the lightest transfer method varies, however for all permutations the relative total mass variation is less than 2%. The major mass components are firstly the propellant to be transferred, there after the pressurant tanks mass, the propellant tank mass, and the pressurant mass. This high pressurant tank mass is due to the presumed high storage pressure and pressurant quantity assumed. Thus this will be further investigated through testing.

5

Piston Design and Experimental Test Set Up

With the findings of Chapter 3 and Chapter 4 that the optimal transfer method for this application is a piston system using either stored gas, pumping, or a gas generator to actuate the piston, and that the pressurant gas mass and storage pressure greatly influence the transfer system mass, a test set up will be devised to further investigate the piston functioning and pressurant parameters. First the technical implementation of a piston transfer system in a refuelling craft will be discussed in Section 5.1 before the design of the test set up is elaborated on in Section 5.2.

A variety of Piping and Instrumentation Diagrams (PID) are presented in this section, for the sake of clarity the symbol legend for these diagrams is given in Figure 5.1 rather than showing it in each PID.

Symbol legend			
	Check valve		Pressure regulator
	Hand-actuated valve		Pressure sensor
	Solenoid-actuated valve		Pressure relief valve
			Quick disconnect
			General compressor
			Pressure vessel
			General pump

Figure 5.1: Symbol legend for Piping and Instrumentation Diagrams

5.1. Piston Transfer System Design

While Chapter 3 concluded that a piston system is the optimal transfer method for this application, how it is integrated in a refuelling system has not yet been treated. In addition Section 2.4.1 highlighted a number of challenges facing piston systems, the mitigation for which will be discussed in this section.

As briefly alluded to in Section 2.3, and Figure 2.9 there are a number of transfer methods that are more or less applicable to different customer tanks. Here the methods discussed are no longer the physical driver behind the transfer of the propellant from one craft to the other, but instead the operational method employed by the two systems. An overview of these methods is given in Table 5.1 reproduced from Eberhardt et. al [16].

Adiabatic ullage compression is applicable solely to blow down tank systems, and involves the forcing of propellant into the customer tanking, re-compressing the expanded ullage. Compressive heating effects on the ullage can complicate this method that is otherwise rather straight forward, and may be conducted with just the use of stored pressurant gas. Ullage exchange is applicable to pressure regulated surface tension tanks and requires a closed loop between the supplier and customer tank. This method requires a pump to be utilised as it is a constant pressure process, where the pumped propellant displaces ullage gas back into the supplier tank. The vent/fill/repressurise method

is applicable to both diaphragm and surface tension tanks, and presumes that the customer tank can maintain the separation between the liquid and the vapour, to allow for liquid free tank venting. This method moves the propellant to the customer tank by reducing pressure through venting and avoids any compression heating effects. However for blowdown systems the ullage would have to be repressurised somehow. Finally the drain/vent/no-vent fill/repressurise method is applicable to complicated PMD tanks that must be completely emptied before being filled due to the nature of the PMD, and allows filling to start from a known volume, and minimises unintentional venting of liquid. After the propellant has been drained to a catch tank on the servicer craft, the receiving tank is then vented in a controlled manner to prevent propellant freezing, before a no-vent transfer method is used to transfer the defined amount of propellant. All of these methods except the ullage exchange method do not require a pump and may be carried out solely using stored gas or a gas generator.

Table 5.1: Fluid transfer method applicability, reproduced from [16]

Transfer Methods	Monopropellant				Bipropellant		
	Blowdown		Regulated		Regulated		Blowdown
	Diap.	S.T.	Diap.	S.T.	S.T.	Bellows	S.T.
Adiabatic Ullage Compression	•	•					•
Ullage Exchange				•*	•*		
Vent/Fill/Repressurise	•		•	•*	•*	•	
Drain/Vent/Fill/Repressurise		•		•	•		•
Diap. - Diaphragm Tank S.T. - Surface Tension Tank *Not applicable to complex surface tension devices							

Ideally a refuelling craft would employ a transfer system that could cater to the various different customer tanks as to not exclude potential customers. Figure 5.2 and Figure 5.3 display two potential system layouts that are capable of various modes of propellant transfer, with the transfer hardware being placed in the refuelling craft and exterior to the refuelling craft respectively. Both Figure 5.2 and Figure 5.3 allow for all of the transfer methods previously mentioned with the exception of drain/vent/no-vent fill/repressurise as this method requires the addition of a holding tank. Regardless of the transfer methods used, and the location of the transfer hardware, the piston and tanks remain relatively unaffected and thus the design of a test set up to investigate the piston functioning and pressurant parameters may be carried out without regard for the exact transfer method used.

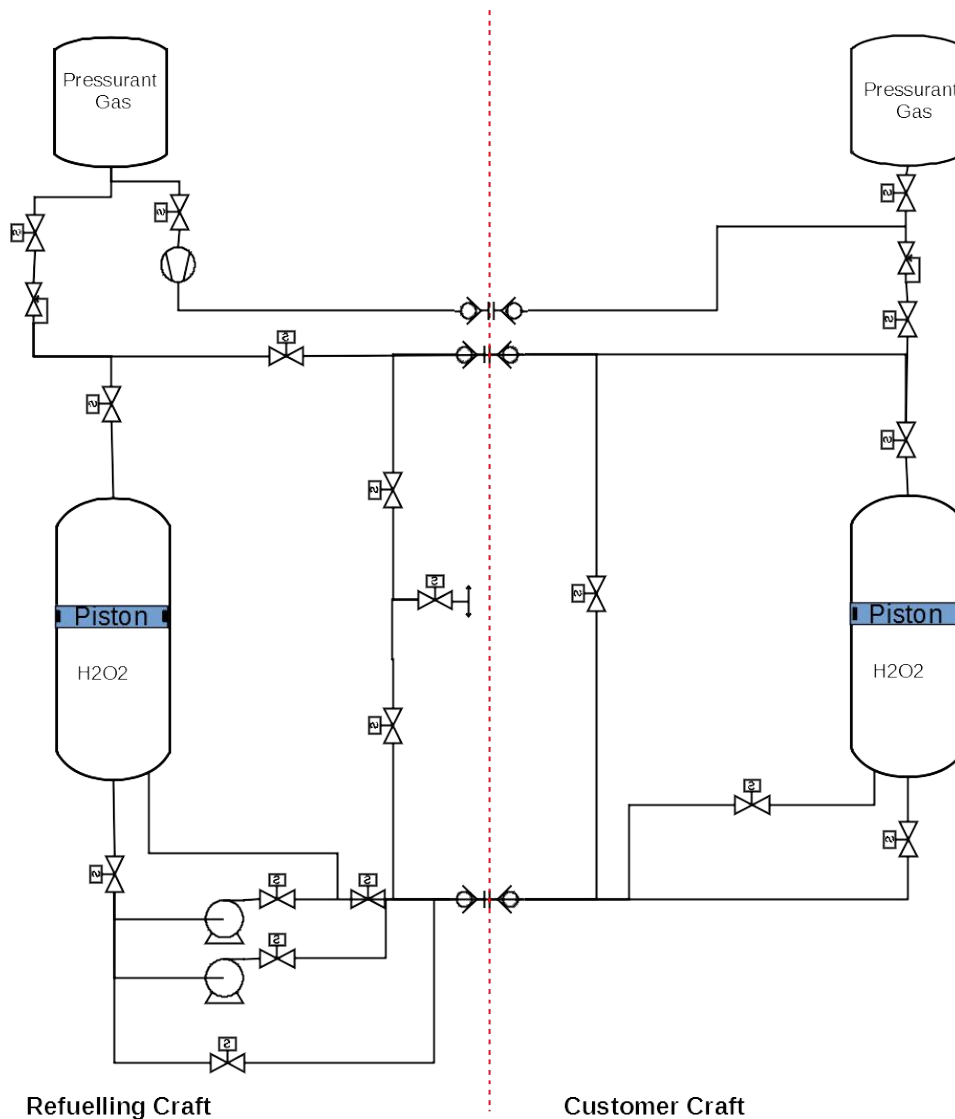


Figure 5.2: Concept Architecture of Propellant Transfer System with Transfer Mechanism Inside of Refuelling Craft

Section 2.4.1 highlighted a number of challenges facing piston systems, namely leakage around the piston head, from the gas side to the liquid side, or vice versa, and also the issue of piston heads becoming stuck or jammed inside of the piston cylinder causing the system to fail. As little literature could be sourced on the topic of piston design, a meeting was organised with Jan Boomsma, and Ruben Evenblij, engineers at Angst + Pfister BV, a company specialising in sealing and fluidic technologies. They outlined some of the principles of piston functioning and the capabilities of modern piston sealing. Pistons are either single or double acting meaning that it can either exert a pressure or force in a single direction or in both direction of extension and retraction. As the primary use of pistons in industry is for actuating systems using pneumatic or hydraulic means most seals are designed around these applications. Figure 5.4a displays the various forms of seal used on a heavy duty hydraulic cylinder, many of which are impacted by whether the piston is dual or single acting. The relevant seals for the piston transfer system are the piston seal and the piston guide rings (as well as static seals elsewhere on the test set up). The purpose of the piston seal is to prevent the leakage of fluid or gas between the two compartments of the piston, while the purpose of the guide ring is to prevent contact between the piston head and the cylinder walls, to counter the side loads exerted on the piston head, and to keep the piston head centred in the cylinder. As the piston used for propellant transfer is not being used to exert a force through a rod for the purpose of mechanical work the rod related seals shall not be mentioned further. Additionally, a guide rod running through the central axis of a piston cylinder may be used to stabilise a piston head and prevent it from jamming, however in the opinion of the Angst +

Pfister engineers this element is not needed if the design of guide rings is done correctly.

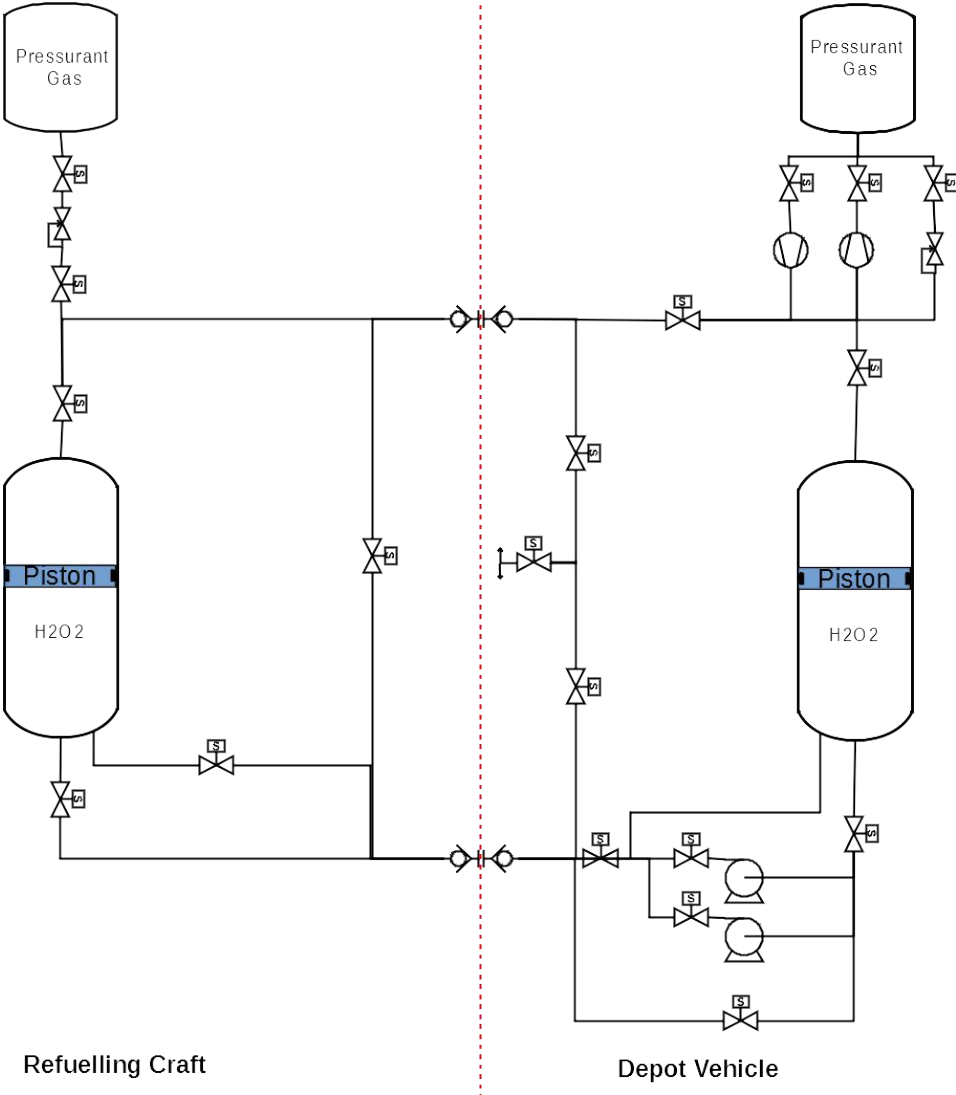


Figure 5.3: Concept Architecture of Propellant Transfer System with Transfer Mechanism Outside of Refuelling Craft

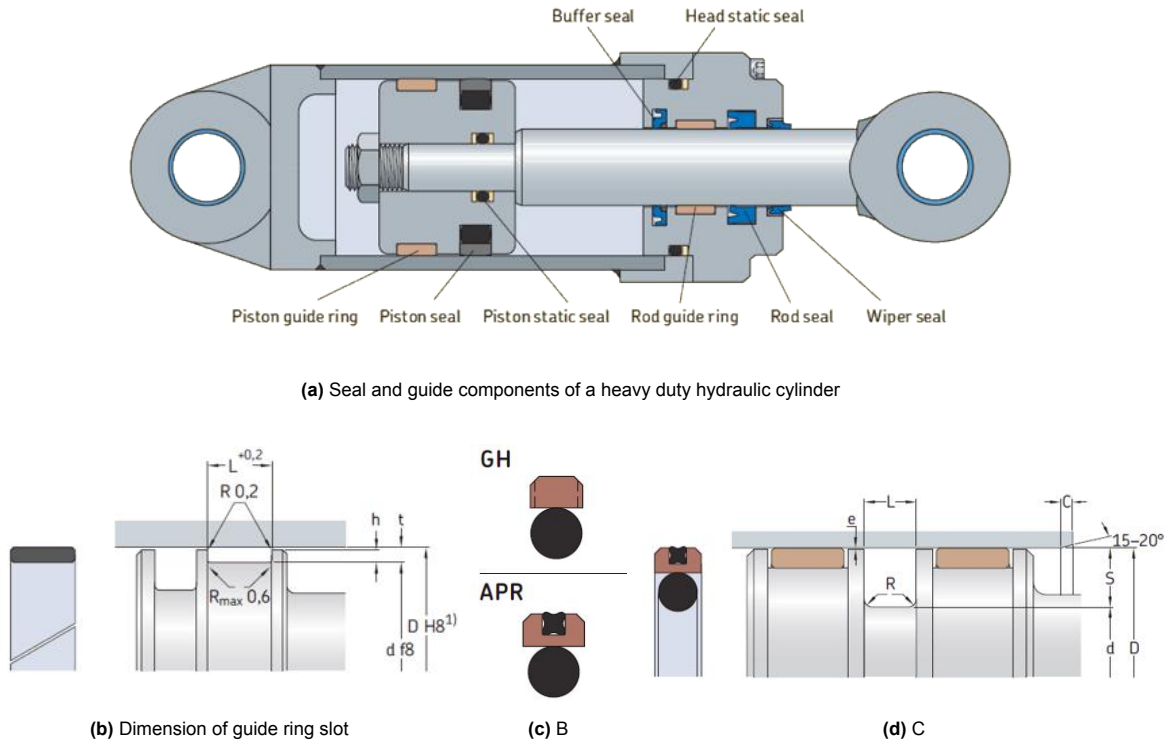


Figure 5.4: Piston sealing element details taken from SKF hydraulic seals catalogue [58]

The most appropriate commonly produced seal material for this application involving H_2O_2 is PTFE. Not only is PTFE compatible with H_2O_2 it is also self lubricating. Guide rings from PTFE are fabricated by using strips of so called guide tape and then cutting it with the appropriate length and geometry to be wrapped into an accommodating slot, the dimensions of which are shown in Figure 5.4b. Piston seals made of PTFE come in a range of standard sizes, however as PTFE is not capable of forming a seal on its own, what is known as an energising element must also be included in this piston seal. This comes most often in the form of a standard rubber o-ring placed below the PTFE sealing element that compressed the PTFE against the cylinder wall. As rubber is not compatible with H_2O_2 an FKM ring will be substituted. A variety of cross sections of sealing elements may be employed, as shown in Figure 5.4c. Configuration GH is described as "PTFE slide ring, nitrile rubber energiser; low breakaway friction; suitable for medium duty applications", with APR being the same with the addition of and "incorporated nitrile rubber X-ring for improved sealing performance". Despite the improved sealing of the APR configuration the incompatibility of the nitrile rubber x-ring means the GH configuration is the only one that may be used on this set up. The piston seal must follow the dimensions outlined in Figure 5.4d which will be elaborated on in Section 5.2.

Porter et al provide a summary of the design trends for piston design as positive expulsion devices [53]. The cross section of the piston perpendicular to the direction of translation is normally circular for each of fit and sealing. As pistons are susceptible to having the piston head become jammed or cocked to one side occasionally a centre guide is employed, most often with flat piston heads rather than concave or convex ones. Pistons are normally designed to have a length to diameter ratio of 5/8 to prevent this cocking issue. The drawback of sliding seals in a piston is that during static stages the seal must continually push against the piston wall. Some materials flow into the cylinder walls in these conditions and increase the resulting static friction. Recent work has focused on developing bellows assemblies to seal the piston rather than conventional seals. Other research has gone into inflatable seals that can continually be pressurised to seal the piston head and the cylinder. These advanced sealing methods are beyond the scope of the current thesis but may be investigated for further work.

5.2. Piston Test Set Up

In order to further investigate the piston functioning and pressurant parameters a test set up is devised. This subsection presents the philosophy behind the design of this set up as well as the design and selection of the individual components.

Figure 5.5 presents the PID of the test set up. The two primary components are the high pressure tank used to store the compressed pressurant gas, and the piston, holding the propellant to be transferred as well as the piston head assembly. Both of these vessels are fitted with pressure relief valves, allowing the vessel to relieve pressure safely in the event of over pressurisation, as well as pressure sensors, for recording the pressure within throughout the testing. Attached to the high pressure tank is a regulator, or pressure reducing valve. By adjusting this pressure regulator the pressure in the piston may be adjusted and set to a certain level. The line emerging from the high pressure tank has a hand valve that may be used to isolate it when it is being filled or when setting the pressure in the system. There is also a pressure sensor placed right after the regulator to record the pressure the system is set at. Before entering the piston the line from the high pressure tank passes through a solenoid valve, labelled as the gas valve. As this is a solenoid valve it may be electronically controlled to accurately initiate a test expulsion. Between this solenoid valve and the piston the line splits, leading to a bypass line of the piston as well as another solenoid. This solenoid is the bleed valve, allowing the pressure in the system to be safely vented by electronic control. The bypass line is included in the scenario that during further testing a customer or receiver tank is added, and thus this bypass would allow for the ullage recompression mentioned in Section 5.1 to be tested. A hand valve on this line allows it to be isolated when not in use. Emerging from the piston are two lines, one being a fill line and the other the expulsion lines for the propellant. The fill line has a hand valve allowing it to be closed when the system is filled with propellant, and the fill line has a electronically actuated valve to allow for precisely timed control during testing. The hardware implementation for each of these component will now be presented in turn as well as some peripheral components used.

Figure 5.6 is presented here to clarify terminology regarding the piston assembly. At each end of the piston is an endcap that is used to hold the pressure within the piston. The walls of the piston are referred to as the cylinder, and the element separating the gas from the liquid, that translates within the cylinder is the piston head.

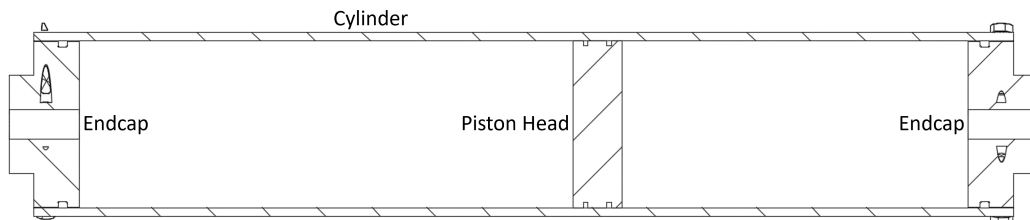


Figure 5.6: Labelled section view of piston assembly

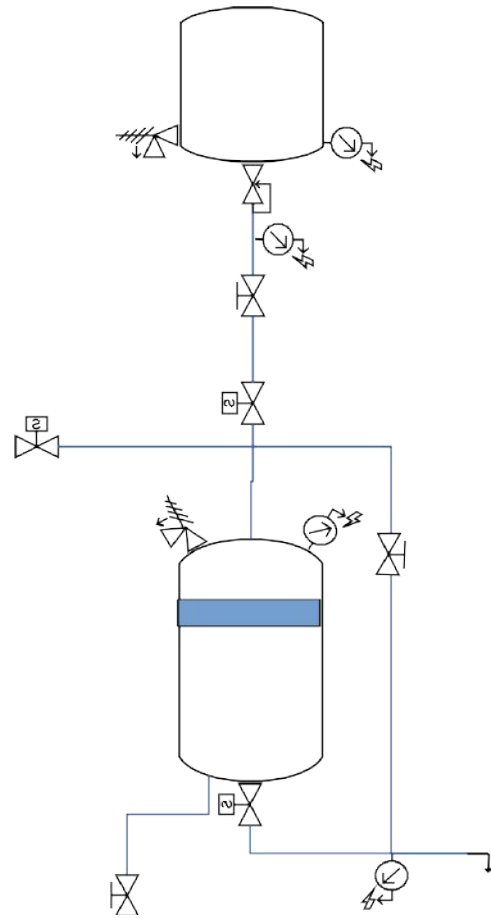


Figure 5.5: PID of piston test set up

5.2.1. High Pressure Tank

A variety of high pressure tanks were considered for this set up, with the main requirement being that they hold enough volume to transfer one litre of liquid from the piston and can withstand pressures of up to 100 bar. The chosen tank was a second hand Tippmann 13 ci (0.2 L) paintball tank (Figure 5.7), which is rated for use to 3000 psi (200 bar). The tank contains an internal regulator which steps the output pressure down to 850 psi (58 bar). The outlet manifold has two pressure relief valves, one in the high pressure segment and one in the low pressure segment, as well as an pressure dial and an 8 mm quick connect fill nipple. The analogue pressure dial is removed and a digital pressure sensor is placed at this port.



Figure 5.7: Paintball tank used as high pressure tank

5.2.2. Regulator

The paintball tank used for the high pressure tank comes with a built in pressure regulator made of a piston assembly with a stack of belleville washer springs that close the regulator outlet when the outlet pressure exceeds 850 psi. Any adjustment to the configuration of these spring washers only results in a higher outlet pressure and it is desirable for this test set up to be operated at lower pressures than this 58 bar. Thus the built in regulator assembly was removed from the tank and it was opted to use an additional adjustable regulator. While an electronically controlled regulator would be ideal to allow for the regulated pressure to be precisely set and maintained, the cost proved prohibitive, and thus a cheaper manually adjustable regulator was sourced, pictured in Figure 5.8. This regulator threads on to the .825x14 National Gas Outlet threads of the paintball tank outlet, and in turn the outlet of the regulator is a male 1/4 Gas thread. A knob on the regulator is used to adjust the regulated pressure while an analogue pressure dial is also present to read the outlet pressure.



Figure 5.8: Adjustable regulator

5.2.3. Valves

The manual valves on the system are ball valves, pictured in Figure 5.9a with a max operating pressure of 63 bar and a small cross sectional diameter of 7 mm. The gas valve on the set up is a solenoid pictured in Figure 5.9b with a maximum operating pressure of 4 bar and a kv value of $0.4 \text{ m}^3/\text{h}$. This kv value was selected to minimise the pressure drop over the valve. The bleed valve is a solenoid valve pictured in Figure 5.9c with a maximum operating pressure of 6 bar and a kv value of $0.23 \text{ m}^3/\text{h}$. All of these valves have 1/4 Gas female connections and the solenoids operate at 24 V and are normally closed.

When assessing solenoid valves for the liquid valve the combined requirements of having a valve body and sealing materials compatible with H_2O_2 (stainless steel and FKM), as well as a kv value that would minimise the pressure drop over the valve, meant that the valve options were prohibitively expensive. Thus an alternative valve was designed, where a manual ball valve would be actuated using a servo. A high torque servo was selected that can be driven with up to 6.8 V, and a 3D printed

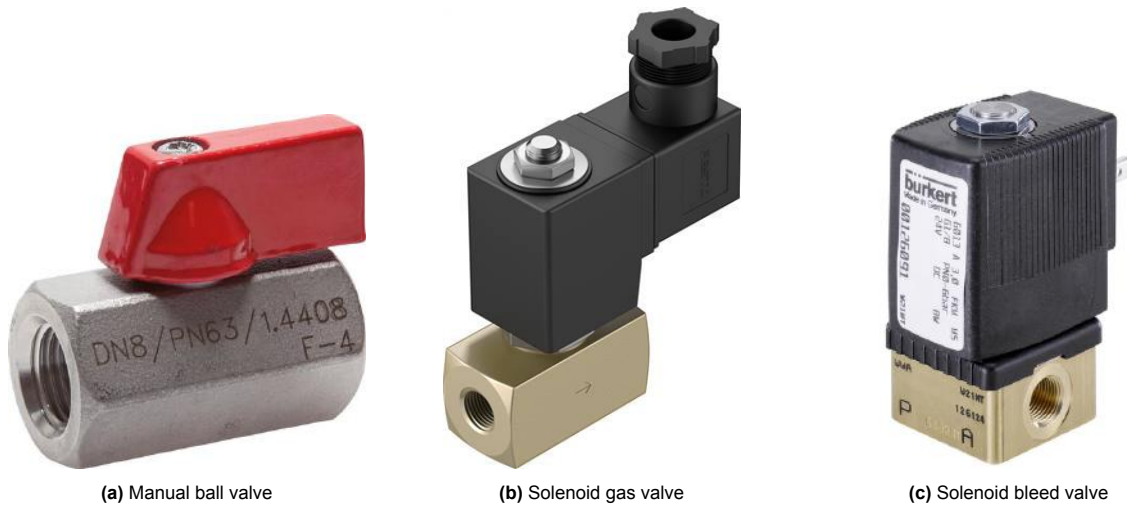


Figure 5.9: Various valves used in the set up

housing and adaptor were designed that would mate the metal servo horn to the ball valve lever, and hold the whole assembly together, all hold together with bolts. This assembly is pictured in Figure 5.10. Lastly the pressure relief valve installed on the piston was a TÜV safety valve set to 9 bar with a 1/4 Gas male fitting.

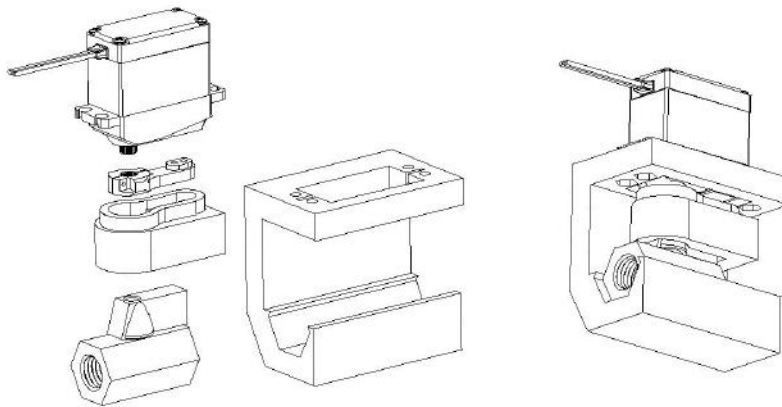


Figure 5.10: Exploded and isometric view of servo-valve CAD assembly. The left hand image shows the servo valve, the servo horn, the adaptor to the valve, and the ball valve, as well as the housing of the assembly in an exploded view. The right hand figure shows the assembly.

5.2.4. Sensors

The low pressure sensors used on the set up are pictured in Figure 5.11a and are rated to 80 PSI (5.8 bar), while the high pressure sensor is pictured in Figure 5.11b and is rated to 100 bar. Both of these sensors operate off of a 5 V DC power source and output a 0.4-4.5 V output signal. As the high pressure sensor uses the same 0.4-4.5 V over a much larger measurement range of 0-100 bar the resolution of this sensor is substantially lower than that of low pressure sensors.



Figure 5.11: Various pressure sensors used in the set up

5.2.5. Lines and Fittings

As the pressure regulator is attached directly to the high pressure tank the remainder of the system only experiences the lower regulated pressure. Thus to minimise cost and allow flexibility in the arrangement of the components, PVC pneumatic tubing is employed (Figure 5.12a). This tubing has an external diameter of 6 mm and an internal diameter of 4mm. As well as being compatible with H_2O_2 this tubing can withstand 7.5 bar. This tubing is connected through push in fittings (Figure 5.12b) to the 1/4 Gas connectors of the valves and other components. These fittings have FKM seals and are made of nickle plated brass. The remainder of the components are connected using double nipple male to male 1/4 Gas connections (Figure 5.12c) and three or four way connector pieces (Figure 5.12d). PVC gaskets were used at all surface to surface sealing surfaces, while conventional Teflon tape was used at thread seal locations.

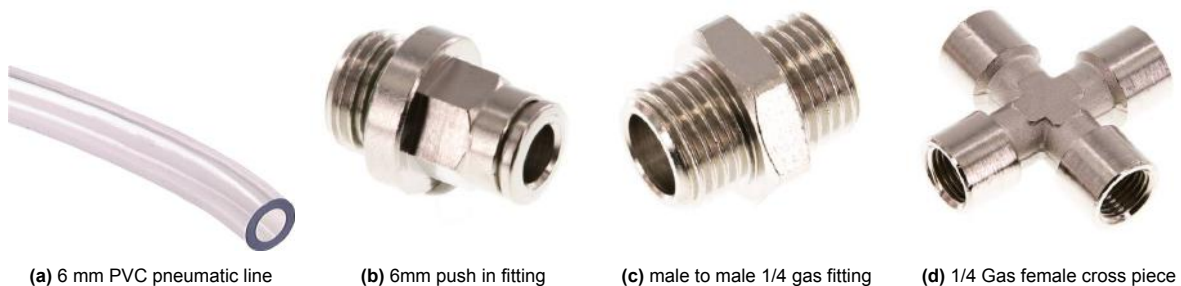


Figure 5.12: Various lines and fittings

5.2.6. Piston

Given the high cost of the seals present in the piston assembly, the piston system is designed around the availability of commercially available seals. As one of the issues to be examined during testing is that of the piston head leaking or jamming, it is desirable to have a transparent piston allowing for observation of the piston head during operation. Therefore two versions of the piston will be designed and fabricated, one with a metallic cylinder and one with a transparent PVC cylinder. In order to be able to use the same piston head in both cylinders the interior diameter must be the same for both, and this must match the outer diameter of a commercially available piston seal. This combination is found for a PVC cylinder of 57 mm inner diameter, 63 mm outer diameter, and an aluminium cylinder of 57 mm inner diameter and 60 mm outer diameter. When the volume of one litre is stored within these cylinders, the piston length to diameter ratio presented by Porter to prevent jamming is satisfied [53]. The author

has experience fabricating cylindrical pressure vessels with radially bolted endcaps, and thus the piston cylinder will be fabricated in a similar manner, with radially bolted aluminium endcaps. The cylinders are sized to contain a one litre transferable volume of propellant, accounting for the volume occupied by the piston head.

For the piston head itself it is chosen to have a single piston seal with a guide ring made of guide tape placed both above and below the piston seal. Multiple piston seals may be used to further reduce the leakage rate however at the sacrifice of increasing the friction between the head and the cylinder. The piston seal that best fits the selected cylinders is pictured in Figure 5.14a with an external diameter of 57 mm, an internal diameter of 46 mm and a width of 4.2 mm. The outer sealing element is made of Eriflon ER 39, a bronze PTFE and the inner NBR ring is replaced with an FKM ring of the same dimensions. The guide ring chosen is made from the guide strip shown in Figure 5.14b, a thickness of 2.5 mm and a width of 5.5 mm, also made of ER 39. The ends of the strip are cut at 30°. The piston head designed to accommodate these elements is presented in Figure D.2.

The piston cylinder will act as a pressure vessel and therefore calculations have to be conducted to establish the pressures it may be safely operated at. There are three failure modes for a radially bolted tank to be considered, the first being radial burst of the tank walls, the second being shear failure of the bolts securing the top and bottom endcaps to the wall, and lastly the shear out of the wall where the bolts tear-out through the tank ends. The desired failure mode is for the wall to shear out surrounding the upper endcap. In this way if the tank fails the results is a slow failure where the bolts can be seen to be tearing out, and then the pressure is relieved through venting of pressurised gas through the resulting tear out holes. This prevents either a rapid and energetic failure such as a radial burst, and keeps the H_2O_2 contained within the intact parts of the cylinder.

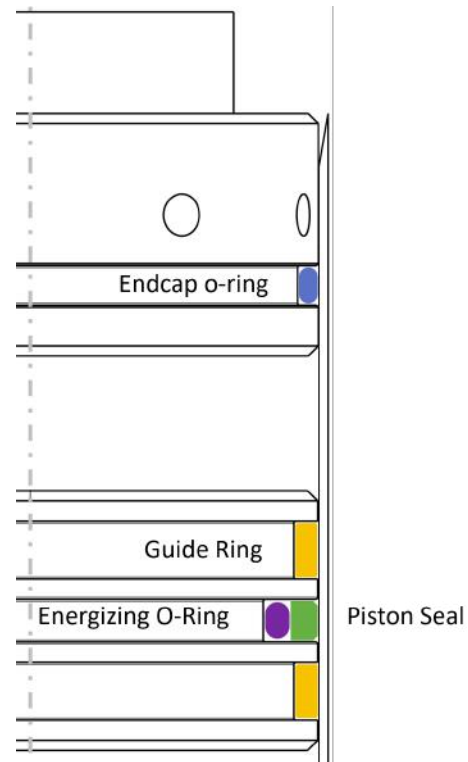


Figure 5.13: Section view of piston showing seals on endcap and piston head



(a) Piston Seal



(b) Guide Strip

Figure 5.14: Sealing elements of the piston head

As the availability of seals and materials fixes the dimensions of the cylinder, the pressure at which the various failures occur will be calculated to establish the best number and placement of bolts to ensure the desired failure order. Equation 5.1 presents the equation for the pressure at which the

radial failure of the tank will occur. Equation 5.2 yields the pressure at which the bolts will shear, where n is the number of bolts used to secure the endcap and 0.58 is the von Mises stress given by $1/\sqrt{3}$. Equation 5.3 gives the pressure at which the cylinder walls shear out, adjusted from Kulak et al.[39]. L is the distance between the end of the cylinder and the bolt hole centre line and L_{ch} is the length of the cylinder is chamfered. This addition of the chamfer length is required compared to the formula given by Kulak et al. as this chamfer that is required for the insertion of the piston head without damaging the seals removes material from the cylinder wall above the bolts and causes them to shear out at a lower pressure. This version of the formula accounts for that reduction in wall area.

$$\sigma_y = \frac{Pr}{t} \Rightarrow P = \frac{\sigma_y t}{r} \quad (5.1)$$

$$\sigma_y = \frac{PA_{\text{tank}}}{0.58nA_{\text{bolt}}} = \frac{4Pr_{\text{tank}}^2}{0.58nD_{\text{bolt}}^2} \Rightarrow P = \frac{0.58nD_{\text{bolt}}^2 \sigma_y}{4r_{\text{tank}}^2} \quad (5.2)$$

$$P = \frac{n \cdot (2t) (L - L_{ch}/2 - D_{\text{bolt}}/2) (0.58\sigma_y)}{\pi r_{\text{tank}}^2} \quad (5.3)$$

The properties for the two different piston cylinders, as well as the chosen M5 bolts, along with Equation 5.1, Equation 5.2, and Equation 5.3 yield the results conveyed in Table 5.2. Here it may be seen that with nine radial bolts the PVC piston will experience bolt shear out at just below 15 bar and the aluminium piston at just above 42 bar, with the other failure modes following much far above. As it is unlikely the test set up will ever be pressurised to higher than five bar the margin allowed by this design is ample.

Table 5.2: Calculations of failure modes for PVC and aluminium piston cylinder

Parameter	PVC	Aluminium	Unit
OD	63	60	mm
t	3	1.5	mm
ID	57	57	mm
IR	28.5	28.5	mm
sigma_ult	5.40E+07	2.90E+08	Pa
sigma_yield	4.40E+07	2.50E+08	Pa
sigma_ult_8.8steelbolt	8.30E+08	8.30E+08	Pa
sigma_yield_8.8steelbolt	6.60E+08	6.60E+08	Pa
Von Mies	0.58	0.58	-
L	8	8	mm
L_chamf	5	5	mm
d bolt min	4.2	4.2	mm
d bolt max	5	5	mm
d bolt hole	5.5	5.5	mm
no bolts	9	9	-
P_radial_burst	46.315789	131.57895	bar
P_bolt_shear	187.05241	187.05241	bar
P_case_failure	14.851405	42.19149	bar

The last element to be chosen for the piston cylinder assembly is the o-rings that seal the top and bottom endcaps. The o-ring calculators provided by Eriks¹ and Parker² were used to establish that an FKM o-ring of 52 mm internal diameter and a thickness of 3 mm, along with the groove dimensions portrayed in Figure D.1, will suffice to contain the pressure in the piston.

An overview of the fabrication steps for the piston assembly may be seen in Figure 5.15. First the aluminium and PVC cylinders were clamped, and as the piece is quite slender it had to be supported by a secondary clamp and the alignment checked. The ends of the cylinders were then faced before

¹<https://oringcalculator.eriksgroup.com/>

²<https://solutions.parker.com/ORingSelector>

being chamfered. The endcaps and piston heads were then produced according to the tolerances in the drawings present in Appendix D and these tolerances were checked with a micrometer. Lastly the radial holes securing the endcaps in the piston cylinders were drilled on a column drill and tapped. Lastly the aluminium piston cylinder was sandblasted to remove blemishes left from the production process.

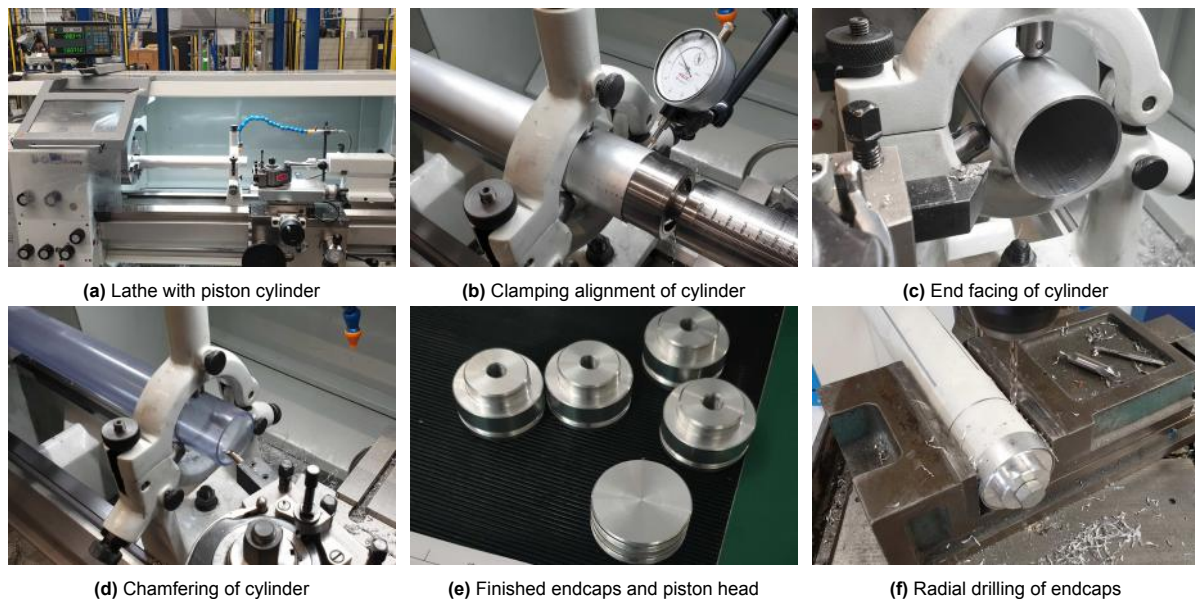


Figure 5.15: Fabrication of the piston assembly

5.2.7. Other Hardware

A variety of other pieces of equipment are used to support the test set up. A three stage stirrup hand pump, capable of reaching 4500 psi (300 bar), is used for pressurising the high pressure tank to the test pressure required. A laboratory power supply is used to power the servo valve during tests. A peristaltic pump is used to pump the fluid into the piston through the fill port, which in turn displaces the piston head upwards inside of the piston cylinder. A variety of 3D printed fixtures are used to hold the valves and other components in place on an aluminium extrusion framework.

5.2.8. Data Acquisition and Control

The data acquisition and control system for this set up is composed of an Arduino Uno as well as a NI LabVIEW programme. The Arduino was chosen due to the authors experience with it and LabVIEW allows for a readily understandable interface with safer operations as a results. The Arduino Uno is plugged into a power supply and connected to a laptop, and provides 5 V DC power to the four sensors, as well as reading out their output signal to an analogue pin. While the servovalve is powered by an external power supply the pulse width modulated signal to drive it is provided by a digital pin on the Arduino. A 24 V DC power converter is used to power the two solenoid valves, and the Arduino controls these by means of 5V relays, also controlled using digital pins. A secondary Arduino Nano is used to power these 5V relays as their power consumption while the total system is operating causes power supply issues with the sensors if a relay was actuated. A common ground is made between both Arduinos and a breadboard is used to connect all components allowing for the connections to be readily adjusted.

A programme is created on LabVIEW using the LINX interface with Arduino, allowing the user to input the ports that the sensors and valves are connected to, and when the programme is running a live read out of these sensors is visible and the valve states may be viewed and controlled. These controls and readouts are superimposed on a diagram of the test set up. The sensor values, as well as the valve states and the time are written to a TDMS file, the standard format for NI software. The user interface of the programme may be seen in Figure 5.16 and zoomed out overview of the backend block diagram may be seen in Figure 5.17.

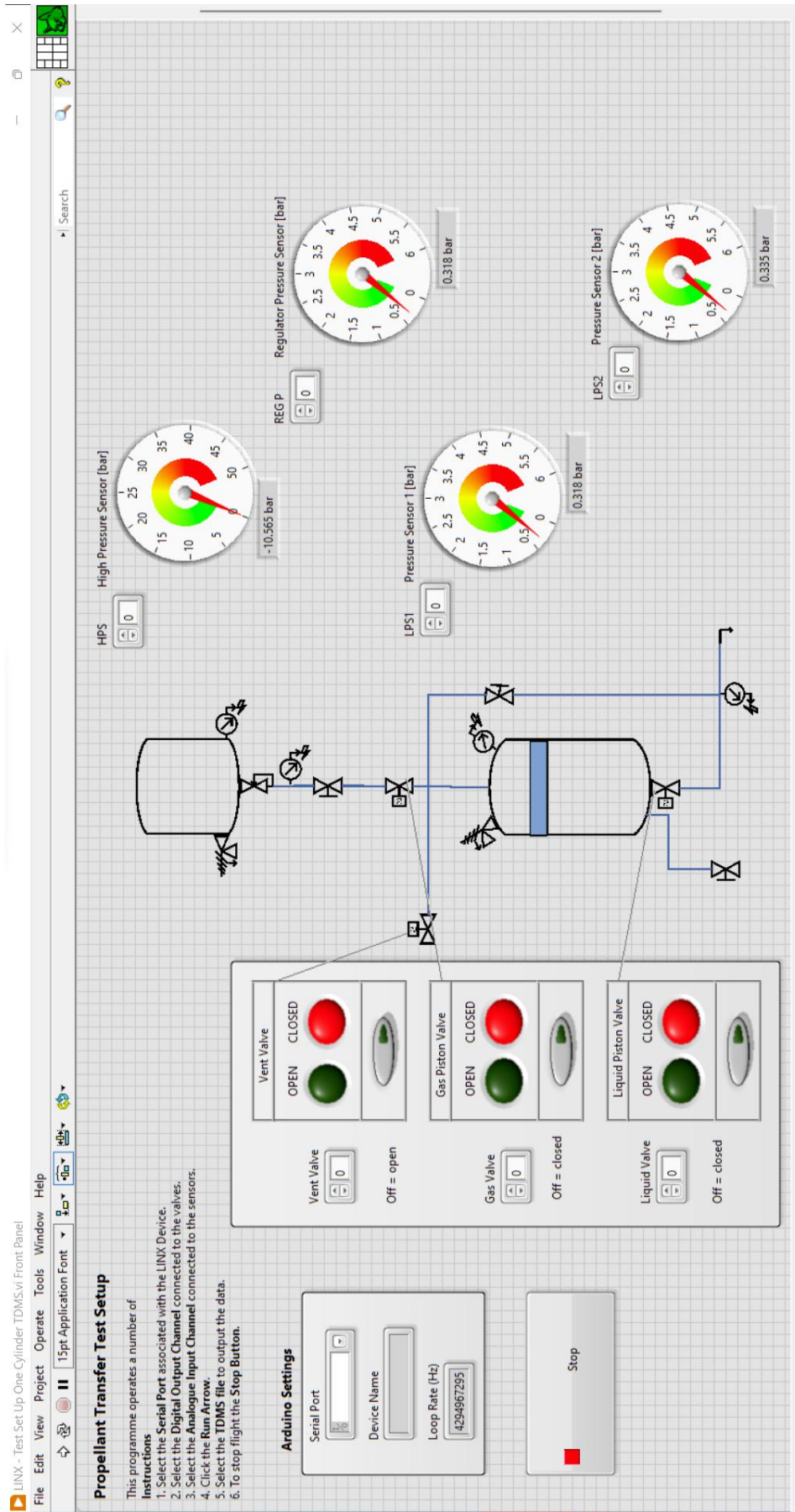


Figure 5.16: Front panel of LabVIEW interface

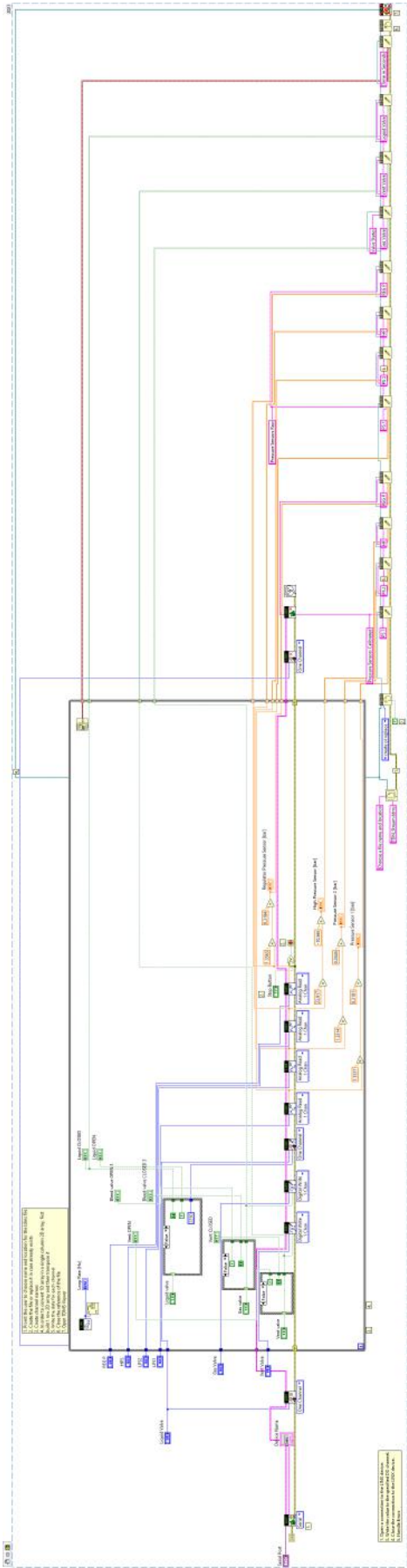


Figure 5.17: Block diagram of LabVIEW programme

The finished and assembled test set up assembly may be seen from various angles in Figure 5.18.

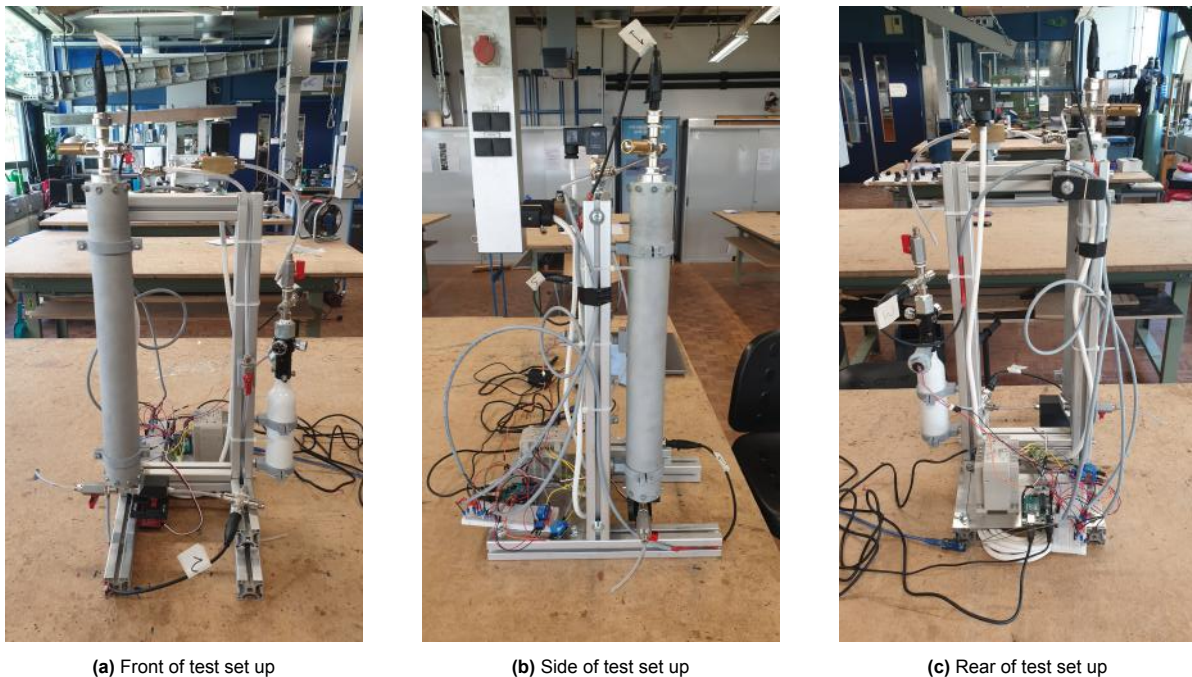


Figure 5.18: Multiple views of the assembled test set up

As the exact layout of the PID figures and the physical arrangement of the test setup do not exactly align, Figure 5.19 presents as close as possible an alignment of the physical and PID layouts.

5.3. Conclusion

There are a number of propellant transfer procedures that are more or less applicable to different forms of customer propellant tanks. These are adiabatic ullage compression, ullage exchange, vent/fill/repressurise, and drain/vent/fill/repressurise. Customer propellant tanks that are of a blowdown or regulated system, or that use a diaphragm or capillary type propellant management device, are only compatible with some of these transfer procedures. Ideally a refuelling craft could cater to all forms of customer system.

A double acting hydraulic piston, which is a comparable system to the piston propellant transfer method, employs a piston seal to seal the piston head, and guide rings to sustain the side forces on the piston head to prevent it becoming stuck. The most appropriate piston seal material for the application at hand is PTFE, which due to its stiffness cannot function as a seal on its own and instead requires an energising element in the form of an FKM o-ring. Similarly the guide rings will be made of PTFE guide tape.

A test set up is devised to investigate the pressure parameters and functioning of a piston transfer system. A high pressure paintball tank is used as a pressurant tank, with an adjustable regulator, a variety of manual, solenoid, and servo valves, and is fitted with a high pressure sensor on the tank and low pressure sensors throughout the rest of the system. A PVC and an aluminium piston assembly are designed capable of withstanding the operating pressures of the system and with the same internal diameter to allow for the same off the shelf piston seals to be used. The transparent PVC piston is meant for initial tests and observations of the leaks around the piston head. FKM o-rings are used on the endcaps of the piston assembly for sealing. A 300 bar hand pump is used for pressurising the tank, and the components of the set up are mounted on an aluminium extrusion frame. Data acquisition and control are carried out using NI Labview running on an Arduino Uno, and a secondary Arduino Nano supplies 5 V power to the sensors and a mains power to 24 V DC power converter powers the solenoids. Data from the pressure sensors is logged in its raw and calibrated form along with the valve states.

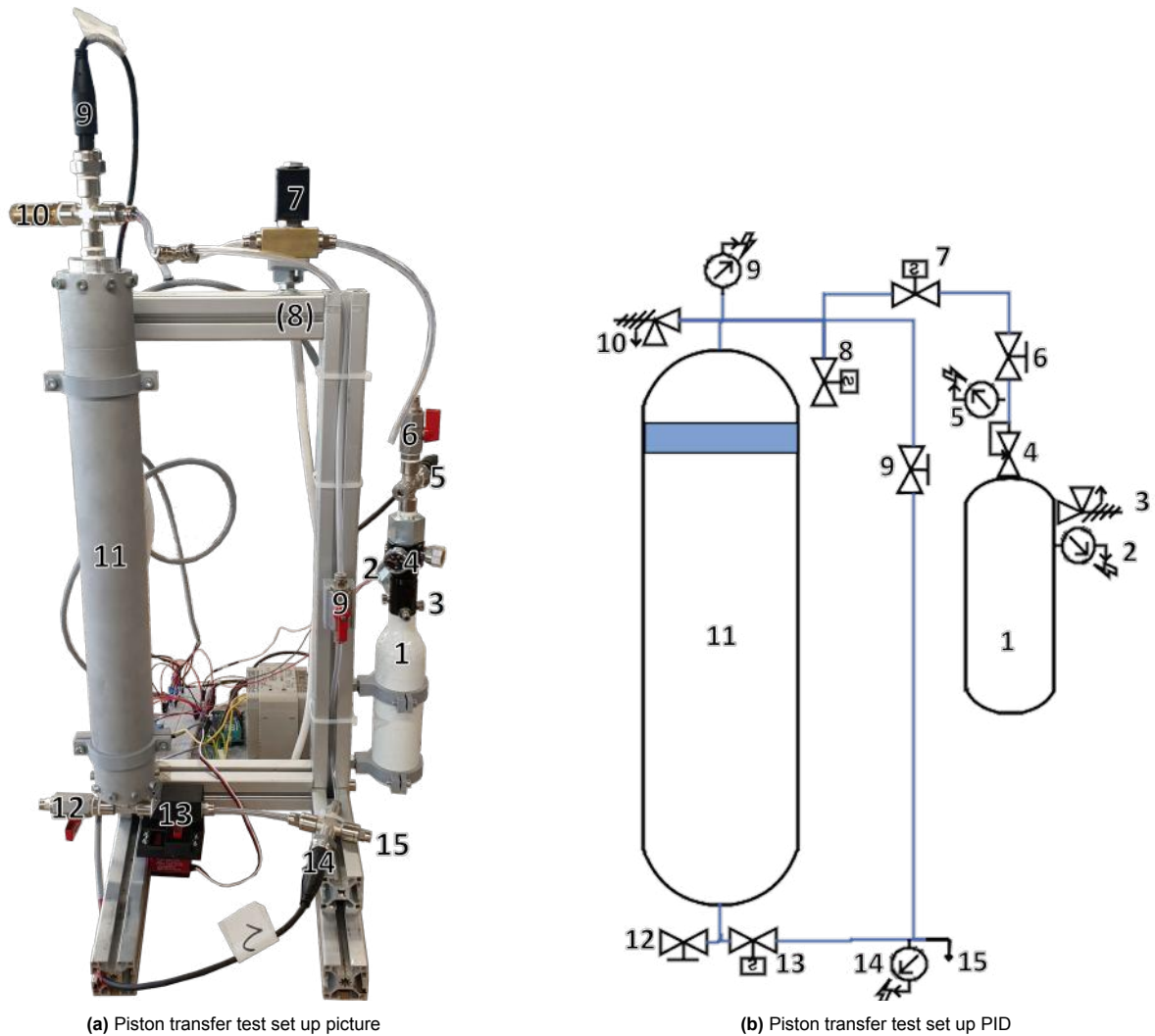


Figure 5.19: Side by side comparison of transfer test set up picture and PID. The components are labelled as follows; 1 - high pressure tank, 2 - high pressure pressure sensor, 3- high pressure relief valve, 4 - pressure regulator, 5 - pressure sensor, 6 - manual ball valve, 7 - solenoid gas valve, 8 - solenoid bleed valve (obscured by test frame in picture), 9 - pressure sensor, 10 - pressure relief valve, 11 - piston assembly, 12 - manual fill ball valve, 13 - liquid servo valve, 14 - pressure sensor, 15 - outlet.

6

Testing

With the test set up complete, and the goal of examining the piston functioning and pressurant parameters, testing may now be carried out. Table 6.1 outlines the requirements of the testing based off of areas of investigation highlighted in the previous chapters. This chapter will firstly discuss the systematic approach to testing, followed by details of the challenges encountered during testing and how they were remedied. The actual results of this testing are presented in Chapter 8.

Table 6.1: Requirements on testing of the H₂O₂ transfer system

Identifier	System Requirement
TEST-01	Testing shall investigate the reliable functioning of the piston
TEST-02	Testing shall investigate the variation in pressurant gas mass required with the addition of the piston head
TEST-03	Testing shall investigate the dependence of pressurant gas mass required as a function of the storage and regulated pressure
TEST-04	Testing shall investigate the functioning of the piston transfer system with H ₂ O ₂
TEST-05	Testing shall investigate the functioning of the piston transfer system inverted

6.1. Test Plan

In order to test the functioning of the piston, and observe the effect of different pressurant parameters, a systematic approach is required towards the testing. Firstly a number of unit tests may be done on separate components and parts of the system in order to verify their functioning individually before tackling the system as a whole. This is detailed in Section 6.3. In order to observe the initial functioning of the system it is planned to first conduct simple tests with the transparent PVC piston assembly, as in this way any leakage of gas or liquid around the piston head, or issues with the piston head becoming stuck, can be easily observed. Thereafter the aluminium piston assembly may be tested, and as this system is likely more representative of a final in-space system, with more realistic friction between the piston head and the cylinder for example, this aluminium assembly will be used for the systematic testing of the pressurant parameters.

Ideally all testing of the system may be conducted in the workshop of the TU Delft Aerospace faculty, with convenient access to power and working surfaces. The pressures that systems can operate at in this workspace are limited as it is a confined space with other students working, and thus the limit set for the high pressure tank is 40 bar, and for the remainder of the system 2.5 bar. The lower bound of pressures that are interesting to test at is established during preliminary testing of the system and is found to be 5 bar for the high pressure tank and 1.5 bar for the rest of the system. Thus it is proposed that the system will be operated with pressures of 5, 10, 20 and 40 bar in the high pressure tank, and with 1.5, 2, and 2.5 bar in the remainder of the system. Expulsions with the system should be carried out at least twice at each combination of pressure settings. As it is interesting to observe the amount of pressurant required to overcome the friction forces presented by the piston head, these tests will also be conducted both with, and without the piston head inserted into the cylinder.

Conducting these tests within the workshop space also means that the majority of the tests will be done with deionised water in the system rather than hydrogen peroxide. Finally the system will be tested in an inverted position, with the logic that if the system can function with an adverse 1 G acceleration, then it can likely also function in a 0 G environment. These combination of testing parameters are summarised in Table 6.2

6.2. Challenges Encountered

Two significant challenges were encountered during testing that disrupted the intended test plan. The first of these was that the PVC piston cylinders could not fit the endcaps of piston head, and the second was that the piston seal leaked. These two issues are discussed in turn in this section.

The PVC tube that was procured was presumably formed by extruding and thus when measured upon arrival some parts of the tube have an inner diameter greater than 57 mm while others are slightly larger. It was hoped when the endcaps and piston head were inserted they would deform the cylinder better into shape, and that after the piston head had been forced through the mid sections of the cylinder it would also improve. The endcaps could readily be forced into position at the top and bottom of the cylinder allowing the radial holes to be drilled. However it was found to be near impossible to force the piston head through the cylinder. PVC has a glass transition temperature just above 80 °C and thus it was attempted to heat the cylinder evenly and then force through the piston head, reforming the cylinder. This did not succeed, the piston head became stuck at an angle in numerous locations, causing local deformation of the cylinder walls well beyond tolerance. Additionally when the cylinder cooled, it contracted and returned to its previous unevenness. Perhaps if this method was attempted with a metal rod or cylinder with an outer diameter of 57 mm, and some form of jig to ensure the metal rod could be forced evenly down the centre of the heated PVC tube, and then left in while it cools and removed after, maybe this could succeed. However given the time constraints on this work this was not attempted and instead the focus was shifted to just testing with the aluminium cylinder, and the piston head functioning could perhaps be observed through the endcaps between tests.

When the piston head was finished and being checked for the fit inside of the piston cylinder it was found that the piston seal consistently leaked. Firstly placing the piston seal on to the piston head was found to be a considerable challenge. The FKM o-ring can be easily deformed and placed into the piston seal slot, with a piece of thread placed underneath it being drawn around it to remove twist. The PTFE sealing element however is very difficult to deform and normally required a specialised tool that forces the seal along a taper shaft, expanding it before it is pushed over the lip of the shaft and into the slot. A custom tool was designed for this, which may be seen placing the piston seal in Figure 6.1a, Figure 6.1b, and Figure 6.1c, which functioned well. Unlike in the instructions provided by the manufacturers when the PTFE ring moved off the of the shaft it did not quickly reform into its original shape, and it remained significantly deformed with a larger inner diameter, Figure 6.1d. This was counteracted by using electrical tape to tightly wrap the seal and exert a distributed force on the PTFE, Figure 6.1e. After leaving the seal for a week it had sufficiently reformed its shape to be inserted into the cylinder.

The guide tape was installed and then with some force required the piston head could be pushed into the cylinder, smoothly passing the chamfer and radial holes as shown in Figure 6.1f. Care was

	High Pressure Tank [bar]	Regulated Pressure [bar]	No. tests	Note
No piston head	5	1.5	x2	
	5	2.0	x2	
	5	2.5	x2	
	10	1.5	x2	
	10	2.0	x2	
	10	2.5	x2	
	20	1.5	x2	
	20	2.0	x2	
	20	2.5	x2	
	40	1.5	x2	
	40	2.0	x2	
With piston head	5	1.5	x2	
	5	2.0	x2	
	5	2.5	x2	
	10	1.5	x2	
	10	2.0	x2	
	10	2.5	x2	
	20	1.5	x2	
	20	2.0	x2	
	20	2.5	x2	
	40	1.5	x2	
	40	2.0	x2	
	40	2.5	x2	
	20	2.5	x2	With H2O2
	20	2.5	x2	
	10	2.0	x2	Inverted
10	2.0	x2		

Table 6.2: Systematic Testing Plan

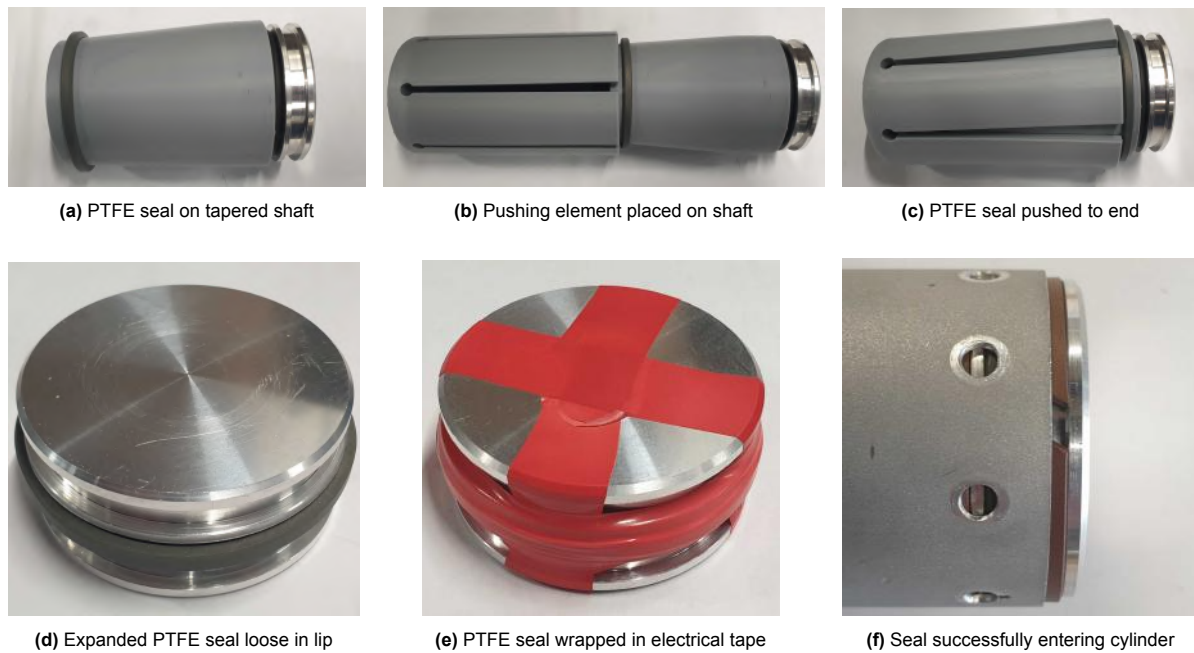


Figure 6.1: Procedure followed to assemble piston head

taken to stop the piston head from entering under an angle or from digging into the radial holes for the endcap bolts. With the piston head inserted the bottom endcap was loosely secured in place with some bolts however without a seal as only the sealing behaviour of the piston seal was to be investigated. Regulated pressure was supplied from the workshop compressed air supply to the top of the cylinder. The bottom of the cylinder was immersed in water in order to view if the air pressure was leaking past the piston seal. Unfortunately bubbles could be observed emerging from the bottom of the cylinder meaning the piston seal was leaking. A number of steps were attempted in order to remedy this leak. This piston head was removed and inspected for damage. Upon removal some streaks or distinctive lines can be seen on the sealing surface, Figure 6.2a. As these lines run up and down it is presumed they are due to debris in the piston of the surface left from the extruding process that formed the cylinder. The spare piston head was used and a new set of guide strips as well as a new piston seal were installed. The piston head assembly as well as the cylinder interior were sprayed with PTFE lubricant to assist in the insertion and sliding of the piston. This also leaked. There was a chance that as the piston head was close to the end of the tube when it was pushed up against the bottom endcap, that this area may be deformed due to machining. A piece of metal stock installed between the endcap and the piston head to keep the piston head secured in almost the centre of the cylinder lengthways. The leak testing was attempted again, with the piston head secured at two different locations in the cylinder and still leaks were present. Lastly two piston heads were installed at once and the test repeated again, and the leak was found to still be present. With the piston head inside of the cylinder a test was done with the cylinder removed from the water, and instead the piston head was observed as the pressure was increased. The leak was seen to occur at one location on the piston head, as may be seen in Figure 6.2b, even as the piston head moved up and down the length of the cylinder. Based on this observation it is perhaps the case that the extruding process that formed the tube left ridges and troughs on the surface, and a particularly large trough is allowing the piston seal to leak. This could potentially be remedied by having a machined surface on the cylinder interior.



Figure 6.2: Damage to the piston seal and leak location visible

When the second piston head was tested in the centre of the cylinder and above the bottom endcap, the pressure was recorded, a hand valve was used to isolate the cylinder and the leak rate as the piston head over time may be observed. This does assume that no leaks occur from anywhere else in the assembly. The resulting plot may be seen in Figure 6.3. It may be seen that the leak rate depends on the pressure difference between the pressure in the cylinder and the atmospheric pressure on the other side of the piston head. The bottom two lines are from the piston head being held in the centre of the cylinder and the upper two are with the piston head directly above the endcap. The largest leak rate recorded in the tests corresponds to 0.22 mbarL/s . This leak rate is relatively high however given the unsuccessful attempts to mitigate it, and the time and cost involved in trialling a machined piston cylinder, it is decided to proceed with testing with the given leak rates, and the effect on the results will be estimated.

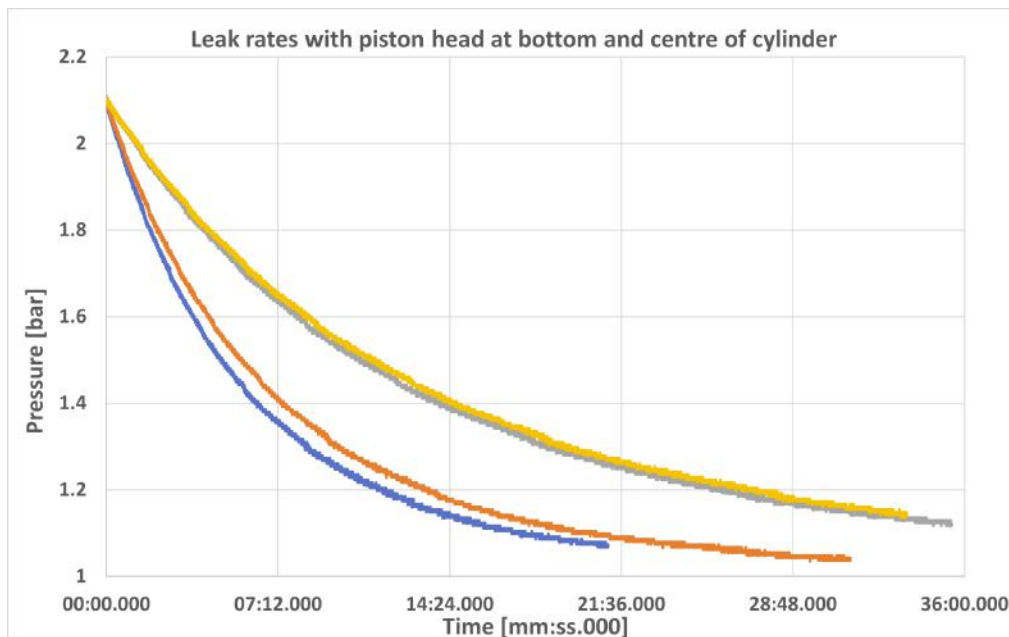


Figure 6.3: Leak rates with piston head at bottom and centre of cylinder. The bottom two lines are from the piston head being held in the centre of the cylinder and the upper two are with the piston head directly above the endcap.

The last topic of note for this section is the challenge in inserting the endcaps in place with the FKM o-rings installed. As FKM is a harder material than rubber it proved quite difficult to insert the endcaps with the FKM o-rings protruding. When sufficient force was applied to insert the endcap it was found that as the o-ring passed the empty radial holes for securing the bulkhead, the ring emerged through the holes and had chunks cut out of it as it continued to move past the bottom of the holes, as may be seen in Figure 6.4a and Figure 6.4b. This was counteracted by using aluminium tape to line the inside of the piston cylinder, meaning the tape prevented the o-rings from peaking out through the radial holes as it was pushed past, shown in Figure 6.4d. It could be seen that some minor damage still occurred to the rings in some spots, however an attempt to stop this completely by applying more aluminium tape to the endcap and the o-ring was not successful due to the tight tolerances between the endcap and the piston cylinder, Figure 6.4c. Later upon removal of the endcaps the rings were seen to be in relatively good condition and no leaking was ever observed around the o-rings on the endcaps, Figure 6.4e.



Figure 6.4: Endcap o-ring damage and remedy

6.3. Initial and Unit Testing

6.3.1. Leak Testing

One of the first tests of the system to be conducted is leak testing. For this the system may be pressurised to various levels using either the high pressure hand pump or the workshop compressed air supply. With the system pressurised leak detection spray is applied to potential leak sites, and the presence and rate of bubbles at these sites provide an indication of the leak size. A number of the connections at the top and bottom of the piston assembly leaked surrounding the PVC gaskets which could be remedied by tightening. The regulator assembly at the outlet of the high pressure tank had a large number of leaks present, due to the number of connections and poor sealing surfaces, as can be seen in figure Figure 6.5a. The leaks at the connections that did not need to be regularly disconnected could be sealed by using LOCTITE 542 thread sealant. This was applied and left cure before the leakage was again tested and none were found. For connections that required occasional disassembly, such as the attachment of the high pressure sensor to the tank, an alternative solution was required. The leakage at this site was caused due to the small diameter difference between the threaded part of this sensor

and the main body of the sensor. This small difference left little flat area for a gasket or dowty seal to be compressed by. This was solved by machining a larger washer or flange that was glued to the body of the pressure sensor, allowing for sufficient area to compress a dowty seal and seal this connection, Figure 6.5b and Figure 6.5c.

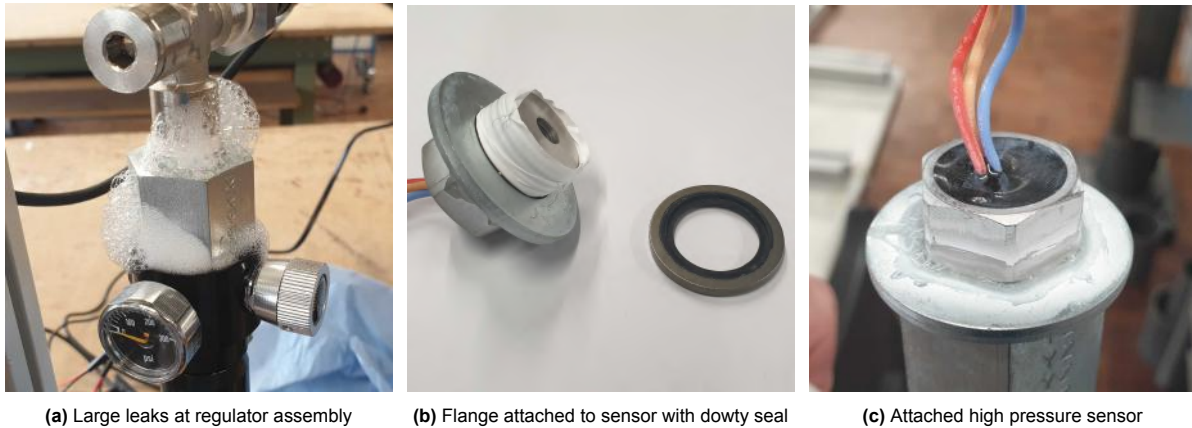
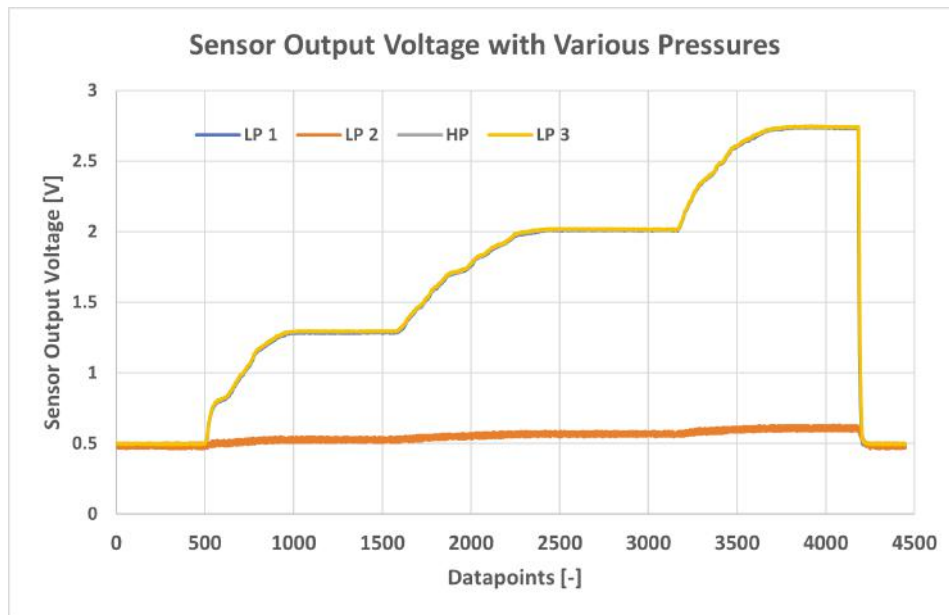


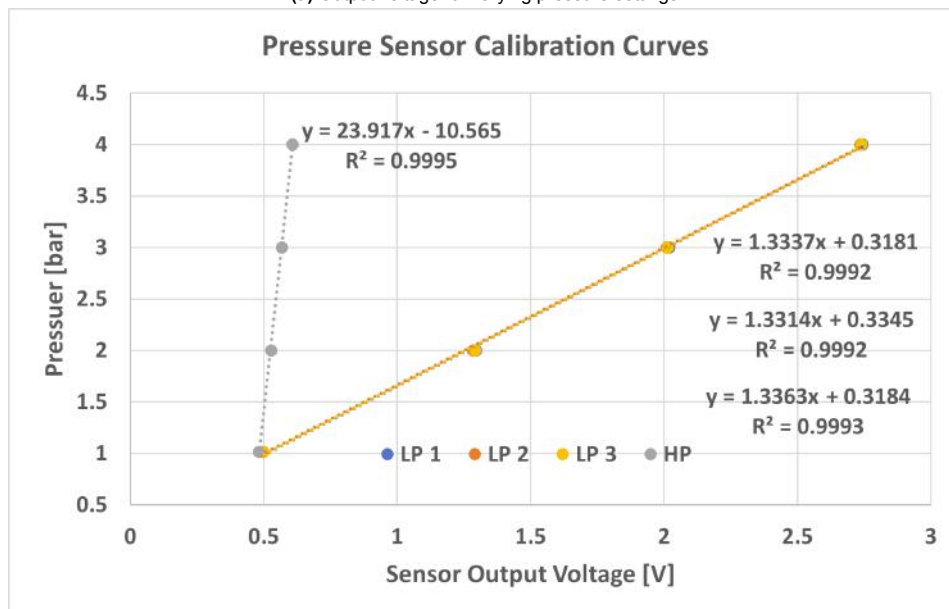
Figure 6.5: Leak locations and leak remedies

6.3.2. Sensor Calibration

As the pressure sensors were supplied without a calibration curve this had to be performed in order to relate the measured pressure and the sensor output voltages. This was done by connecting all pressure sensors to a length of PVC line, and using a workshop regulator to supply varying levels of pressure from the workshop compressed air line to the sensors. The analogue pressure dial on the regulator was used to set the pressure to atmospheric, then two, three, and four bar, Figure 6.6a. Post processing of the recorded output voltage of the sensors provided the average voltage when the sensors were experiencing these pressure settings. These averaged voltage values could be plotted against the pressure they were measured at, and with a linear trend line plotted on these points the calibration curve of the pressure sensors is obtained, Figure 6.6b. These linear lines show a very good fit, exceeding an R^2 value of 0.999 for all sensors. The coefficients of these lines was used in the LabVIEW software described in Section 5.2.8 to display the pressure in the system in real time, as well as to log both the output voltage of the sensors and the calibrated values. Unfortunately the high pressure sensor could not be calibrated at higher values but this was not observed to present any issues during the conduction of the tests.



(a) Output voltage for varying pressure settings



(b) Calibration curve of pressure sensors

Figure 6.6: Calibration of pressure sensors

6.3.3. Compatibility Testing

In order to observe whether the selected materials and components are compatible with H_2O_2 before conducting the testing with H_2O_2 , a compatibility test is performed. This is done by placing a sample of each of the materials in contact with H_2O_2 in a beaker along with 30% concentration H_2O_2 . A piece of the guide strips, the endcap containing a piston seal, as well as one of the FKM endcap o-rings are placed in one beaker, while another beaker contains the end of an aluminium piston cylinder, Figure 6.7a. As any incompatibility between H_2O_2 and the materials will result in H_2O_2 decomposing, this may be readily observed in the form of bubbles. No initial bubble formation was observed so the samples were left to sit for a week. Upon returning to the samples the piston cylinder had no bubbles forming and after removal from the beaker and drying there was no visual change to the surface, both machined and un-machined. However the second beaker contained quite a bit of bubble formation, Figure 6.7b. On the FKM o-ring, the aluminium endcap, and the piston seal there was a small amount of bubbles formed that were clinging to the surface, however when observed over a few minutes no

new bubbles were forming and thus it may be the case that the decomposition was caused by grease and handling of the materials before the test. However the guide tape had numerous bubbles actively forming showing that even after a week decomposition was still occurring on its surface. This guide tape is reportedly made from EP 39, a PTFE containing bronze. According to the compatibility charts shown in Appendix A the PTFE has a rating of A, or "Suitable", and the bronze has a rating of B, or "Good, minor effect, slight corrosion". This level of decomposition appeared worse than this rating and thus this specific components should likely be reassessed for further work on this topic, however for a short duration expulsion test with H_2O_2 the level of decomposition observed is deemed to be acceptable.

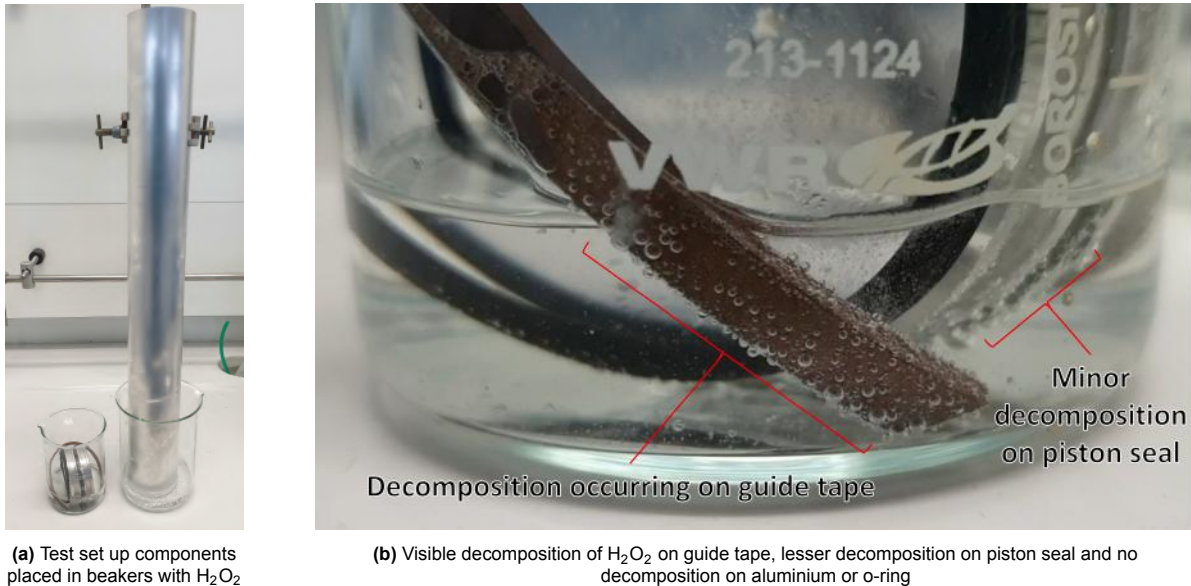


Figure 6.7: Compatibility testing of test set up components with 30% H_2O_2

6.3.4. Friction Testing

Chapter 7 details a model made of the test set up in order to mimic the outcome of the expulsion tests and to assist in estimating the masses of a scaled up version of this system. One of the key components in this model is the friction that acts on the piston head as this will add to the amount of pressurant gas required to displace the propellant. In order to estimate the parameters of the friction to include in the model two forms of test were conducted. Firstly to investigate the breakaway friction between the piston head and the interior of the piston cylinder, the piston head was placed inside of the cylinder, after which the air pressure supplied by the workshop supply of compressed air and a regulator attached to the piston assembly was increased until the piston began to move. The pressure in the upper half of the cylinder was recorded in order to note the pressure at which the piston head began to move. The second form of test conducted involved pushing the piston head all the way to the top of the cylinder, and then securing the lower endcap in place. The workshop compressed air was regulated to a certain pressure setting after which a hand valve to the piston was opened. The pressure in the upper endcap of the piston was recorded and in this way the pressure required to move the piston head as well as the duration of travel along the piston length was recorded, and may be seen in Figure 6.8. The values obtained in this testing were used in Section 7.2.

6.4. Systematic Testing

6.4.1. Without Piston Head

The initial method employed when carrying out expulsion tests was to close the gas valve between the high pressure tank the piston, then adjust the regulator to the desired pressure for the test, and open the solenoid electronically to start the expulsion. However when the solenoid valve is opened the pressure in the system drops substantially from the level that has been set and does not recover. This was checked at various regulated pressure settings, and also by adding a five meter length of line as a reservoir before the gas valve, however when the gas valve is opened the same substantial drop occurs. Instead the method used for testing was to open the gas valve, and when setting the regulated

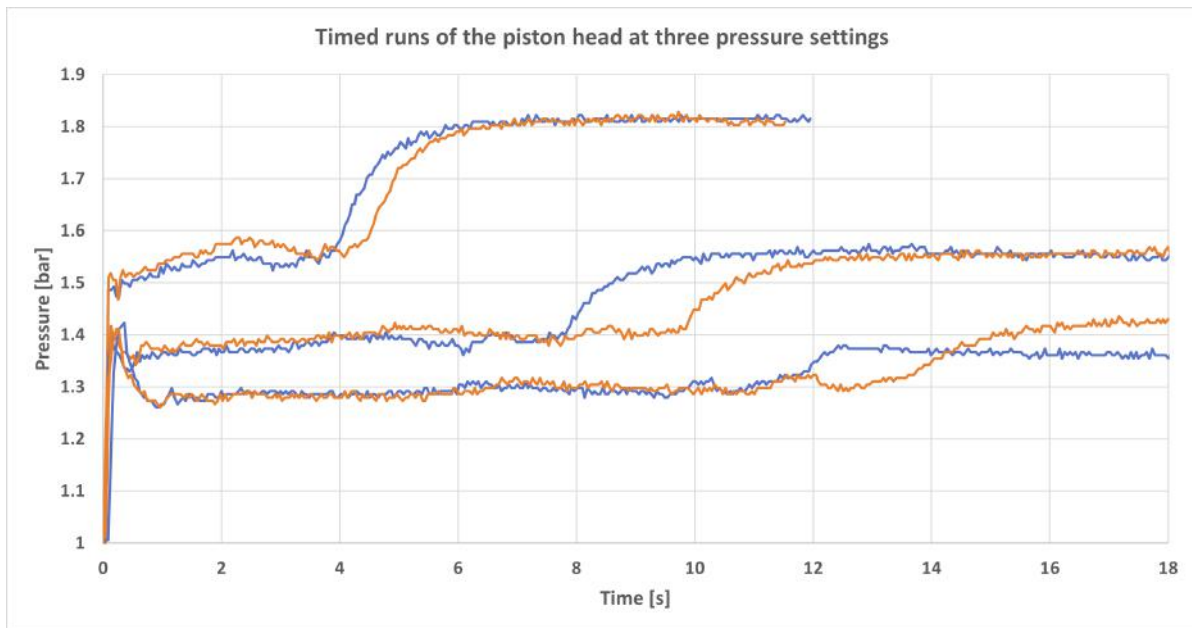


Figure 6.8: Timed runs of the piston head at three different pressure settings of 1.3 bar, 1.4 bar, and 1.5 bar, with two runs at each pressure setting

pressure the whole line leading from the high pressure tank up until the piston head is pressurised. With this method the test is started by opening the liquid servo-valve. The test is stopped by observing when the liquid finishes emerging from the drain line at which moment the liquid valve is closed to electronically store that time stamp.

Another issue that was found was that when testing at the five bar in the high pressure tank setting the quantity of gas in the pressurant tank was just on the threshold of what was sufficient to fully expel the water in the piston. If the tank was set to slightly above five bar then the test was successful. For each regulated pressure setting of 1.5, 2.0 and 2.5 bar with the high pressure tank at 5 bar, one test was unsuccessful, as may be seen in the testing log in Table E.1. One challenge encountered when running these expulsion tests was that the dial used to set the pressure on the adjustable regulator proved to be extremely sensitive to small adjustments. Typically when the dial was set to a certain position the pressure would climb and then slowly level off to a certain value. Often this value would fall short of the desired regulator pressure setting and thus even when the dial was adjusted the smallest possible increment the pressure would jump and often climb past the desired pressure setting. This led occasionally to a situation where the expulsion was started with the pressure still climbing somewhat. These cases are noted in Appendix E. In addition filling of the high pressure tank with the hand pump made it difficult to achieve an exact pressure setting without overshooting. In general an accuracy of ± 0.1 bar was achieved for the regulated pressure and ± 0.5 bar for the high pressure tank.

6.4.2. With Piston Head

With the testing without the piston head complete, the bottom endcap was removed to allow the insertion of the piston head. Due to the tight fit a significant amount of force was required to remove the endcap, when this was achieved some aluminium tape debris could be observed on the inner part of the piston cylinder as well as on the endcap, however despite the difficulty in inserting and removing the endcap, the FKM o-ring appeared unharmed, a good sign for the sealing. With the surfaces cleaned the piston head was inserted, after which the endcap was reinserted and bolted in place. A pressure test to 2.5 bar proved the system remained leak tight at the endcaps. The filling procedure for the tests without the piston head has involved disconnecting a line at the top of the empty piston to atmosphere, allowing the air in the piston to vent. When the water was nearly entirely pumped in the line from the feed stock beaker would begin to pump in air bubbles as the last millilitres of water were sucked in. This did not pose an issue with the non-piston head tests as this air could simply bubbled up through the piston and vent through the top disconnected line. However caution was required following this same procedure for the tests with the piston heads as in this scenario the disconnected line at the top allowed the air to

vent as the piston head was displaced upwards, however once the head had reached the top, and if the pump was introducing air bubbles into the fill line, the volume below the piston head would become pressurised and either water or air bubbles would likely leak around to the upper side of the piston head. The pumping pressure of the peristaltic pump was measured to ensure this could not cause an over-pressure. The pump was found to supply a pressure of 2 bar and be able to suck the system down to a pressure of 0.3 bar, all conditions the system can withstand.

The testing log for the piston head tests may be found in Table E.2. The filling issue mentioned above did present a phenomena where once almost all of the water had been filled into the cylinder, the pump was turned off and the hand valve on the fill line was closed. As some air had been pumped into the system, if the detached line at the top of the piston was reattached, the pressure would slowly start to rise above the piston head due to the gas leaking around it. This was combated by keeping that line detached for a number of minutes after filling in order to allow for the pressure to vent pas the piston head. The expulsion testing with the piston head had a number of unexpected phenomena occur that were likely due to the leaking around the piston head. Sometimes bubbles would emerge from the drain line during the testing, or when the piston head had been heard to hit the bottom endcap liquid flow would continue, presumably from above the piston head. During the piston head tests, as well as with the previous tests without the piston head, for the tests with a 40 bar high pressure tank and 2.5 bar regulated pressure, at the end of the expulsion when the liquid valve was closed pressure would rise rapidly in the piston cylinder, often above 3 bar, thus for some of these tests the test was ended by opening the vent valve or by closing the manual valve to the high pressure tank. During the piston head testing occasionally after the water had been pumped in the top connector was removed and the piston head could be observed flush with the top endcap as in Figure 6.9. Additionally during the expulsion it could be heard when the the piston head contacted with the bottom bulkhead, most times coinciding with the end of the expulsion. These two observations demonstrate the smooth and consistent functioning of the piston head as it easily travelled along the cylinder and never became stuck.

6.4.3. Inverted

Inverted tests were conducted by first filling the high pressure tank to the desired pressure, then pumping the litre of deionised water into the piston. With the system ready to test it was then carefully brought to the edge of the work surface before being rotated downwards and held in place by an assistant, pictured in Figure 6.10. With the system in place the outlet line was placed in a beaker level with the system in an attempt to negate the pressure difference if the beaker was placed on the table surface or the floor. After the regulated pressure was set in this inverted position the expulsion was initiated and run until completion. These



Figure 6.9: Piston head visible at top endcap after water filling



Figure 6.10: Assistant holding test set up inverted

tests were conducted at 20 bar and 2.5 bar in the high pressure tank and system respectively in order to ensure a complete expulsion and also in order to have good non-inverted test data to compare to. Notes on these tests may be found in Table E.3.

6.4.4. H₂O₂ Testing

In order to test the set up with H₂O₂ it had to be relocated to the large fume hood of the DASML chemistry laboratory. The system was elevated on a number of stands within a tray that would capture any potential leakage or spillage, pictured in Figure 6.11. A separator was also placed between the control and sensing electronics and the fluid part of the system. The system first had the high pressure tank filled to the desired level, after which the peristaltic pump was used to fill the piston with one litre of 30% concentration H₂O₂. The regulator was used to set the system to the desired regulator pressure, after which the door of the fume hood was closed and an expulsion ran. Notes on these tests may be found in Table E.3.

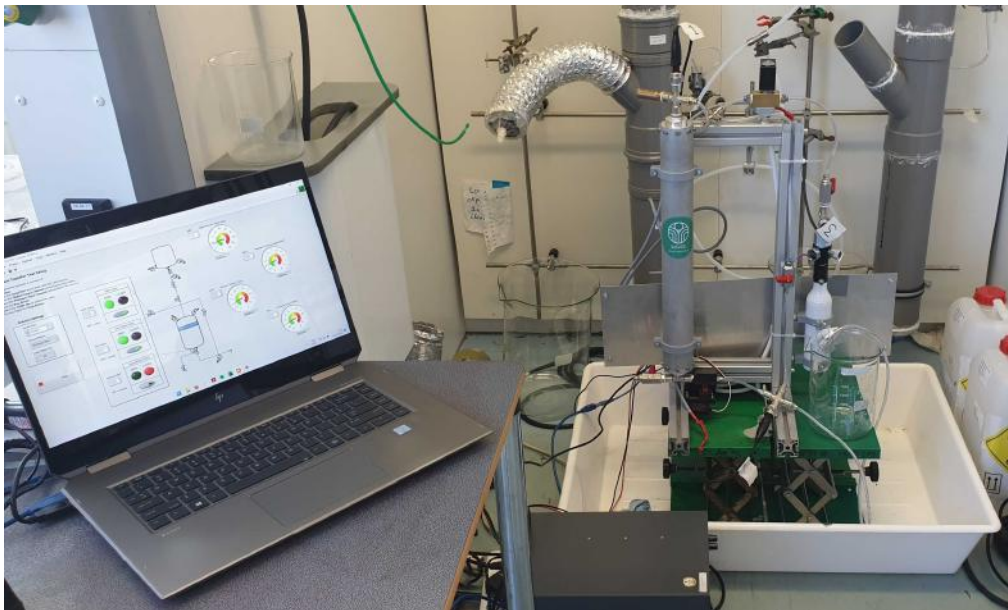


Figure 6.11: Test set up in large fume hood of chemistry lab for 30 % H₂O₂ testing

6.5. Conclusion

A test plan is devised to systematically test the pressure parameters and functioning of the piston. Half of the testing will occur without the piston head, and then the same tests will be performed with the piston head, in order to observe the increased pressure required. Tests will be performed with the high pressure tank at pressures of 5, 10, 20 and 40 bar, and with the system regulated to 1.5, 2.0 and 2.5 bar. Each test configuration will be tested twice for repeatability. In addition to these tests completed with one litre of water to be transferred, tests will be conducted with the test set up inverted, to observe the effect of microgravity on the set up, and with H₂O₂ as the fluid to be transferred to observe the compatibility.

A number of challenges were encountered during the initial testing, namely that the PVC cylinder did not fit the piston head and endcaps, despite numerous attempts to reform the inner diameter to the correct size, and secondly that the piston head was found to leak in the aluminium cylinder. A number of remedies to this leak were attempted to no avail. The leak is likely due to the roughness of the extruded cylinders inner surface. The leak rate is characterised to establish if it is likely to contribute significantly to the test results.

The remainder of the system is leak tested and the leaks found are fixed by tightening connections, or applying LOCTITE thread sealant. The pressure sensors are calibrated using the workshop air supply and a pressure regulator. The compatibility of the test set up components are tested with 30% H₂O₂ for the duration of a week. It is found that the aluminium components have no reaction, similarly

for the FKM o-rings. The PTFE in the guide tape and the piston seal however show decomposition occurring even after a week, despite the materials being classified as compatible, thus this choice of components should be reassessed for further work. Tests are also carried out to characterise the friction between the piston head and the piston cylinder to inform the creation of a model of the test set up.

The systematic testing was carried out by first pressurising the tank to the desired level, the litre of deionised water was then pumped into the cylinder through the fill valve. The pressure in the set up was then set using the pressure regulator. A transfer test was initiated by opening the liquid servo valve, and the test was concluded when gas was seen entering the drain line by closing the liquid servo valve, after which the tank was closed and pressure in the system was vented. Testing at 5 bar in the tank proved to have insufficient pressurant gas to complete the transfer. These tests were again replicated with the piston head but the results also showed incomplete transfers. This same testing procedure was followed for testing with the piston head, where the piston head was displaced upwards by the liquid being filled into the set up. Proper functioning of the piston head was confirmed visually by inspecting it through the upper endcap. Issues with the testing included the sensitivity of the regulator when setting the pressure, as well as allowing the pressure caused below the piston head by pumping to be relieved before the piston head tests were begun. The piston head never became stuck or jammed during testing, proving its smooth functioning.

The inverted testing, where the set up was suspected over the edge of a work surface and the same testing procedure was followed, has no issues of note. Similarly the testing using H₂O₂ went smoothly.

Table 6.3 displays how the requirements that were initially set out for the testing of the prototype transfer systems have been fulfilled.

Table 6.3: Compliance with requirements on testing of the H₂O₂ transfer system

Identifier	System Requirement	Compliance
TEST-01	Testing shall investigate the reliable functioning of the piston	Leak testing exposed a minor leak around the piston head that could not be remedied. Otherwise smooth functioning of the piston head during all testing, with no jamming, was observed.
TEST-02	Testing shall investigate the variation in pressurant gas mass required with the addition of the piston head	Conducting tests with the same pressurant settings both with and without the piston head installed has shown the additional pressurant mass required when the piston head is added.
TEST-03	Testing shall investigate the dependence of pressurant gas mass required as a function of the storage and regulated pressure	By varying the storage and regulated pressure the dependence of pressurant gas mass consumed on the related pressure settings for each transfer has been recorded
TEST-04	Testing shall investigate the functioning of the piston transfer system with H ₂ O ₂	By conducting transfer tests with 1 L of 30% H ₂ O ₂ this requirement has been fulfilled.
TEST-05	Testing shall investigate the functioning of the piston transfer system inverted	By conducting two transfer tests with the test set up inverted this requirement has been fulfilled.

7

Model

The purpose of the model is to provide a digital twin of the system, capable of accurately representing the behaviour of the system in terms of mass flow, pressure, and heat transfer, allowing a sizing of a flight scale system to be performed based on the test data gathered. A number of modelling environments were considered for this purpose. Aspen and DWSIM are two programmes useful for modelling chemical processes, with Aspen being a proprietary software and DWSIM being open source. As the primary focus of this model is not the chemical processes occurring within the system but instead the thermodynamic processes, these programmes were not pursued. OpenModelica and Matlab-Simscape are two programmes focused on the thermodynamic and mechanical activities within systems, again with the former being open source and the latter being proprietary. Given the lack of support for the open-source option and the familiarity of the author with Matlab it was chosen to implement the model of the system in question in Matlab-Simscape. This section will elaborate on how the model works, how it has been developed and the challenges faced in that development.

7.1. Foundation of Model

Matlab-Simscape works off of a block diagram type system, where each block represents a physical components or an attribute of a component. Each of these blocks have parameters that may be set, either as constants, or relationships to other values, or as control inputs. A solver configuration block connected to the remainder of the block diagram determines the solver parameters the solution must meet. The system is set to run for a certain time interval, or until a certain criteria or value is met by some part of the system.

Figure 7.1 displays the majority of the blocks used in the various models developed for this research, where G refers to gas, and IL refers to isothermal liquid. At the core of all of the models is the Double-Acting Actuator (G-IL) block (Figure 7.1a), representing a linear actuator with a gas in one chamber and an isothermal liquid in the other, with the pressure difference between the chambers governing the movement of the piston head. This represents the piston in the propellant transfer system. The Constant Volume Chamber (G) (Figure 7.1b) is a fixed volume with a gas stored at certain conditions, and in the model it is used to represent the pressurant storage tank. The pipes containing gas and liquid in the propellant transfer system are represented by the Pipe (G) (Figure 7.1c) and Pipe (IL) (Figure 7.1d) blocks respectively. Matlab-Simscape contains a standard Pressure Reducing Valve (G), or pressure regulator, block (Figure 7.1e) that may be used to set the pressure in the system. Some of the models developed in this thesis employ this regulator blocks and other develop more in depth models of the pressure regulator.

The Translational Friction block (Figure 7.1f) represents friction in a translating mechanical system, which is employed in this context to model the friction between the piston head and the cylinder walls. Similarly the Translational Damper block (Figure 7.1g) is utilised to represent the damping of the movement of the piston head due to the liquid dynamics in the system. As some models were employed in this thesis to gauge the effects of temperature changes during operation of the system, primarily from the warmer compressed gas in the high pressure tank, as well as the cooled gas used to pressurise the system as it expands through the regulator, the Thermal Mass block (Figure 7.1h) is used with the corre-

sponding ports on the piston, piping and high pressure tank blocks. The Reservoir (G) (Figure 7.1i) and Reservoir (IL) (Figure 7.1j) blocks are used as references conditions in order to measure the pressure in the system and to implement ambient conditions where needed. The liquid reference is also used as the sink for the fluid flow from the system. Similarly the Mechanical Translational Reference block (Figure 7.1k) is used as a mechanically fixed point for the translational parts of the system. Lastly the Gate Valve (IL) block (Figure 7.1l) is employed as the liquid servo valve from the test set up, controlled by a preset signal to enforce the opening and initiation of an expulsion in the model.

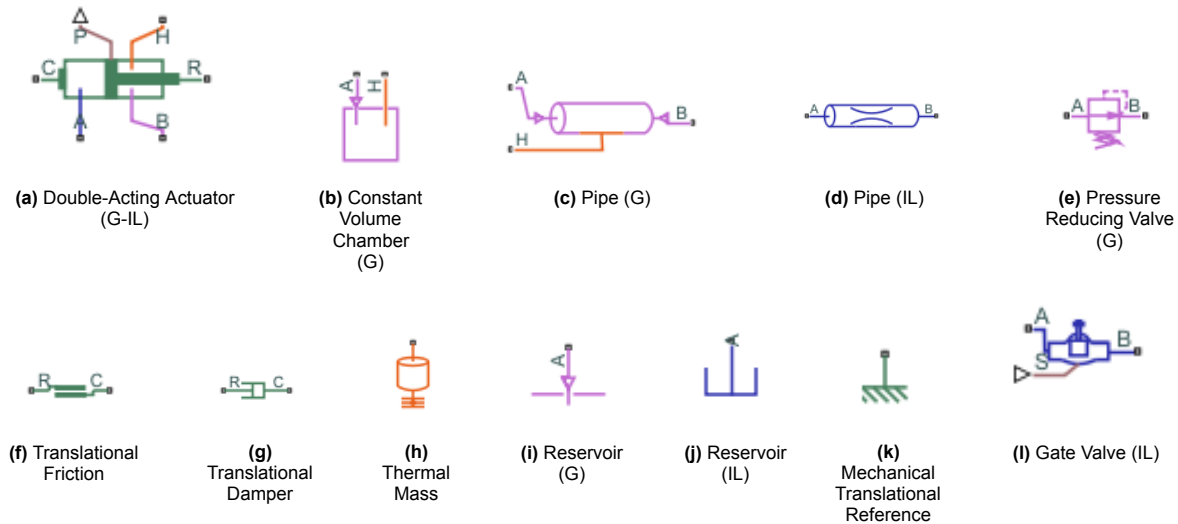


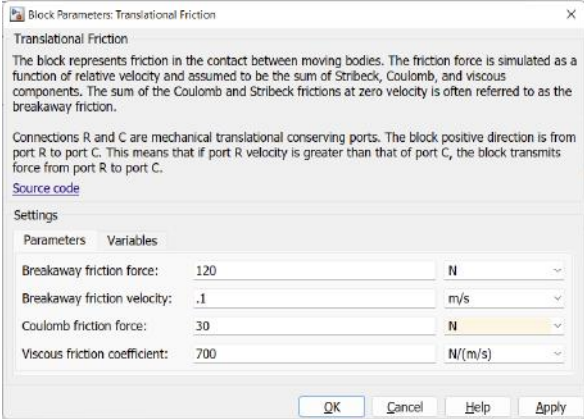
Figure 7.1: Various blocks used in Matlab-Simscape model

These blocks were used to assemble a number of models as well as a final unified model which will be described in the following sections.

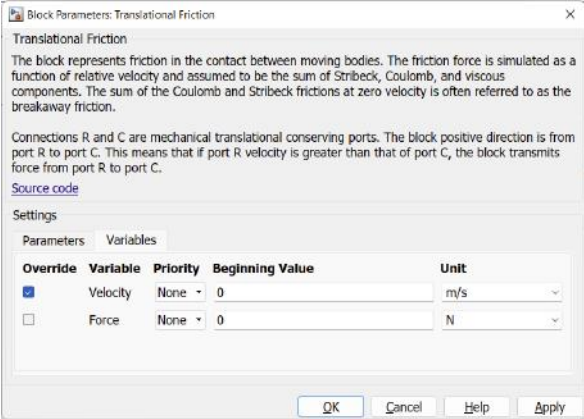
7.2. Tuning of Piston Friction Model

Rather than attempting to create a model of the entire system and tune it to match the performance of the test set in its entirety, it was decided to tune subsections of the model individually and then superimpose these different parts to form the unified model. One of the main subsections this was done for was the friction of the piston. As described in Section 6.3.4, two forms of test were conducted to establish the various parameters of the friction block. The parameters of this block that may be adjusted are shown in Figure 7.2a, and the values for initial variables that may be chosen are shown in Figure 7.2b. Figure 7.2c displays how the friction force is modelled as a function of the relative velocity, in this case of the piston head, and how this relates to the parameters that may be adjusted. As the breakaway friction force is a single parameter this was established by inserting the piston head into the cylinder, and then increasing the pressure of the supplied air to the cylinder until the piston head began to move. This was done a number of times and averaged. Using the area of the piston head this pressure value was converted to the breakaway friction force of 120 N . Literature did not present values for the other friction parameters between PTFE and aluminium surfaces, therefore testing was carried out to find the optimal values to fit the model to the functioning of the test set ups. The test data portrayed in Figure 6.8 was used to fit the model.

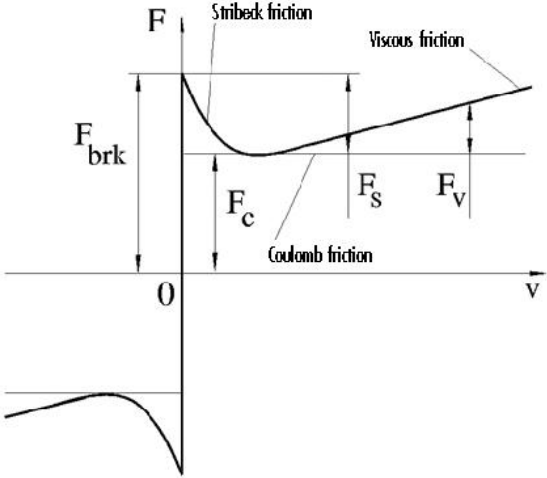
The model made for establishing these friction parameters may be found in Figure 7.3. This model uses a controlled pressure source to move the piston with the friction applied across the piston head. The test terminates when the piston head reaches the end of the cylinder. Note that this is a different actuator block with only a gaseous input and no liquid chamber as the bottom of the piston was open to atmospheric conditions in this testing. Initial attempts at tuning this model to the test data involved setting a constant pressure value at the source however these model runs did not appear representative of the test results. Instead the recorded data from the pressure sensor at the top of the cylinder from each of these tests runs was used as the control input to the pressure source, and a good fit with the test results was achieved. This yielded the values of breakaway friction velocity of 0.1 m/s , a Coulomb friction force of 30 N , and a viscous friction coefficient of 700 N/(m/s) .



(a) Matlab-Simulink friction block - Parameters



(b) Matlab-Simulink friction block - Variables



(c) Friction force as a function of relative velocity

Figure 7.2: Details of Matlab-Simulink friction block

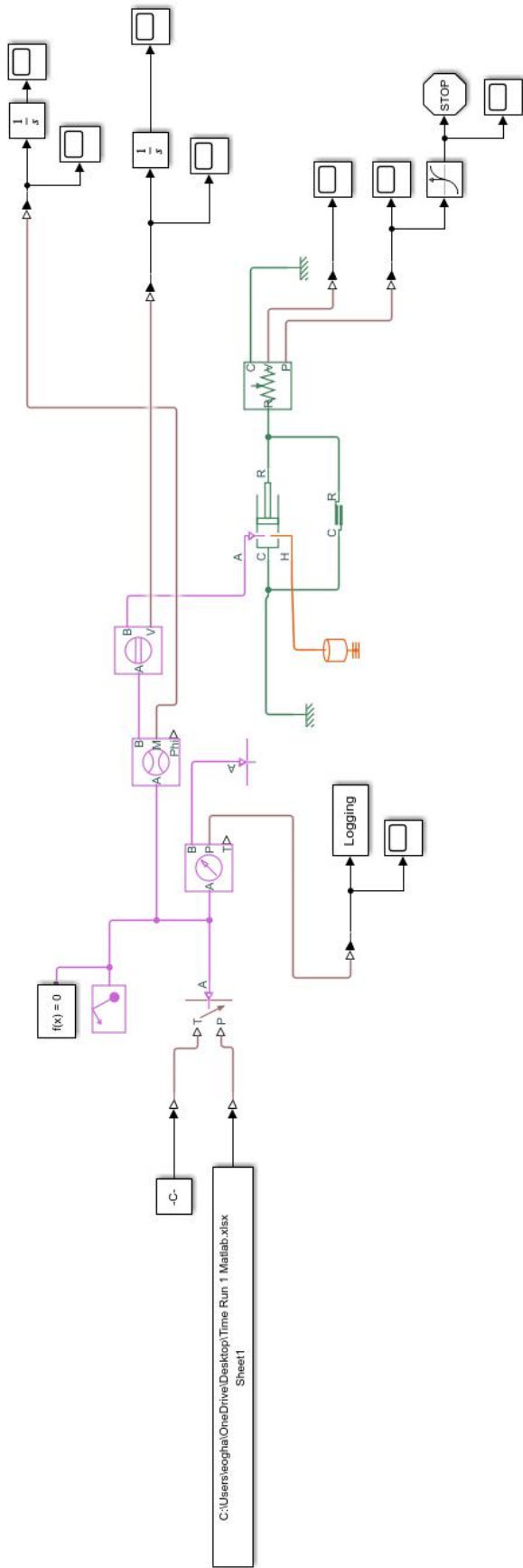


Figure 7.3: Model used for tuning of piston head friction

7.3. Model with Standard Regulator Block

Figure 7.4 displays the initial attempt to create a total model of the test set up. This model contains the constant volume chamber as the high pressure tank, with a pipe leading to the regulator, then another pipe with a variety of blocks implemented to measure the flow properties at this location. The next gas pipe leads into the piston, with has a mechanical reference point attached to either end, as well as the friction working over the piston head. A measurement of the piston head longitudinal displacement is used to terminate the test when the piston is empty. The liquid half of the piston leads into a pipe with a gate valve functioning as the servo-valve, controlled by a step function. This then leads to a reference condition outlet for the system.

The initial tests with this model to assess whether it produced feasible results highlighted a number of shortcomings with the model. Firstly the regulator block did not behave as would be expected and did not mimic the behaviour of the pressure in the cylinder during testing. Despite refinement of the parameters the behaviour of the regulator could not be mimicked. Unfortunately no specifications for the regulator could be sourced from the manufacturer to refine the parameters used. Thus a custom sub-model of the regulator system was created and is described in Section 7.4. The absence of thermal mass blocks caused strange behaviour from the gas element blocks that have thermal conserving ports. Thus thermal masses had to be added at these locations with mass and specific heat values for these components. The liquid outlet of the system led to a reference point with a pressure equalling that of the atmosphere. This forced an unrealistic boundary and caused a scenario where there was a large, non-physical pressure drop over the gate valve. This was remedied by adding a pipe after the gate valve as well as an orifice that the pressure drop could occur over, and thus a non-realistic boundary would not be enforced.

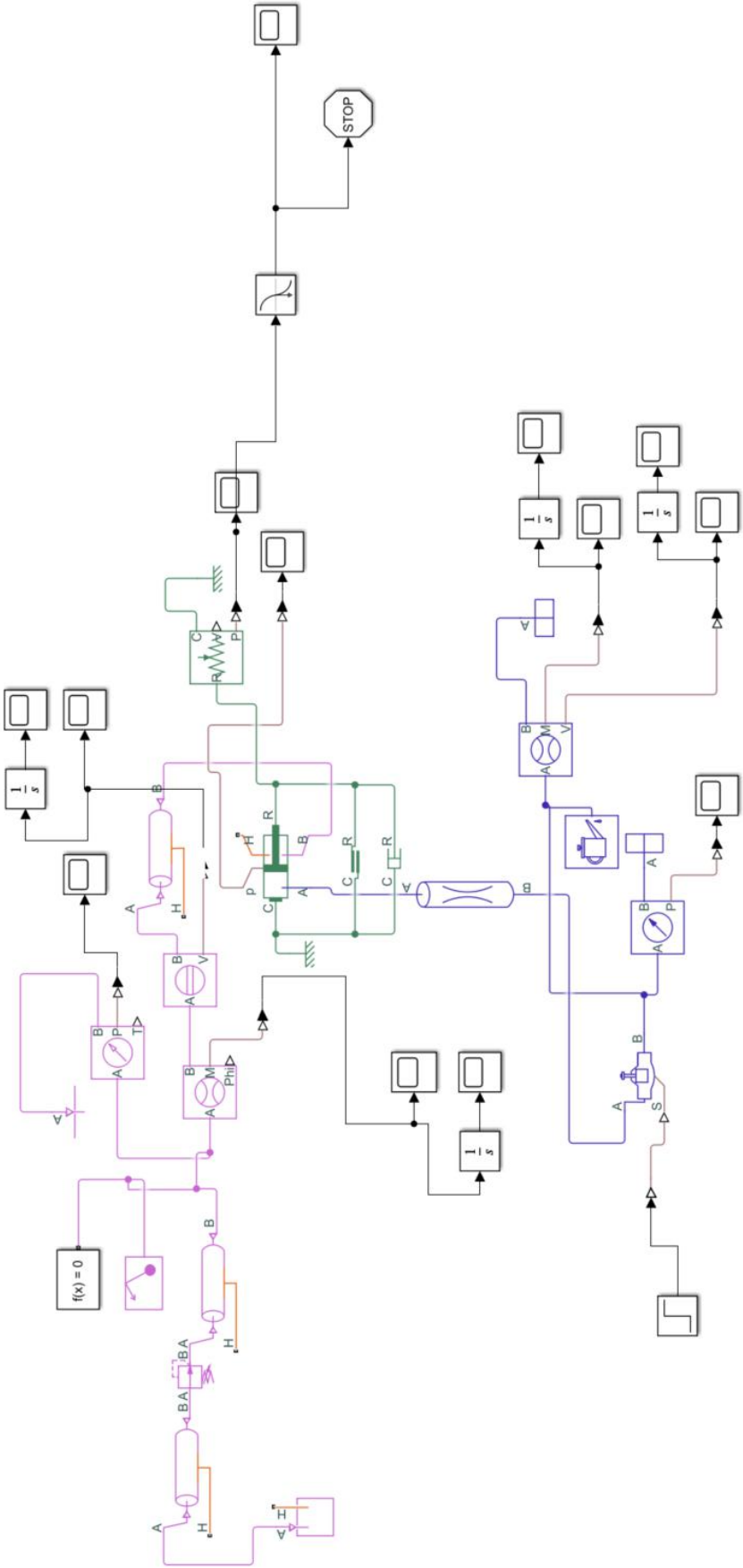
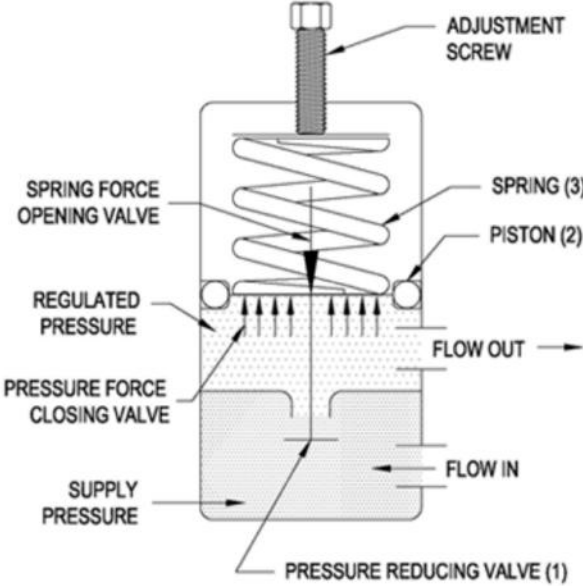


Figure 7.4: Model of system using standard regulator block



PRESSURE REGULATOR SCHEMATIC
SHOWING FORCES ACTING ON
THE INDIVIDUAL ELEMENTS

Figure 7.6: Cut through of a pressure regulator showing principles of functioning¹

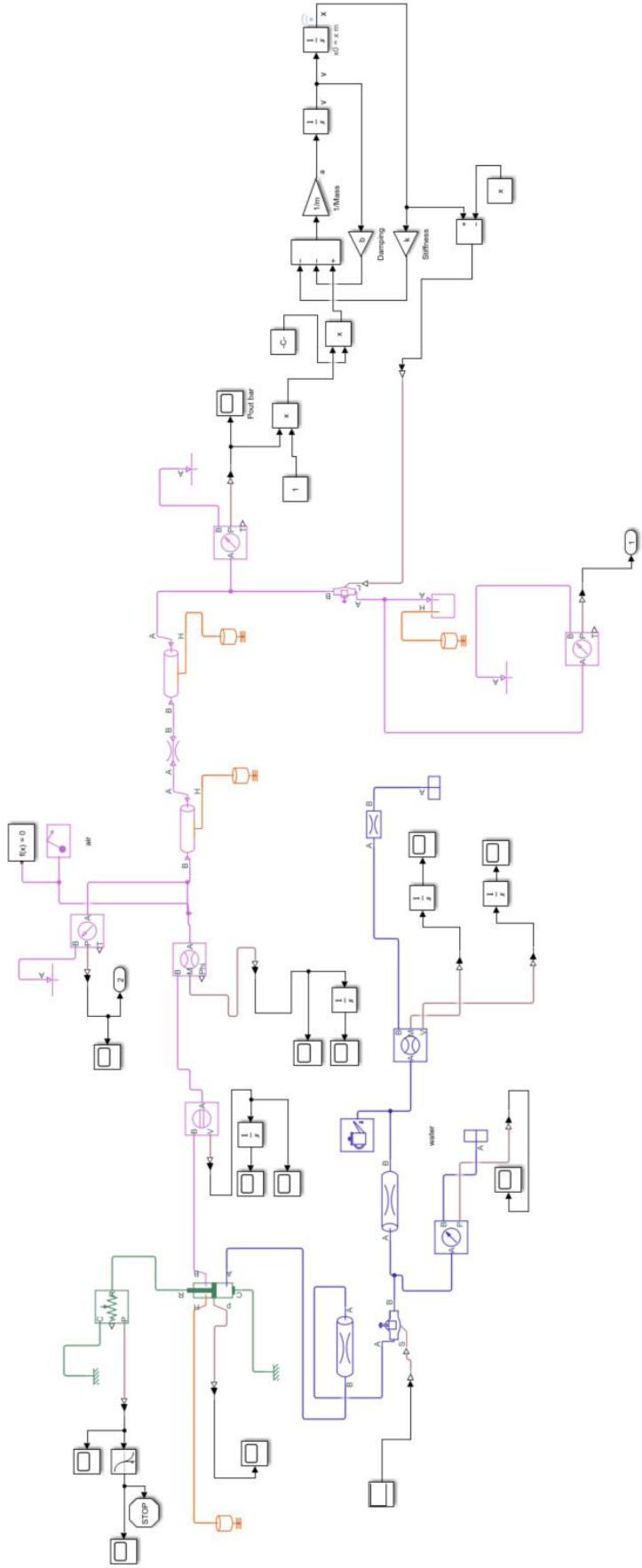


Figure 7.7: Model of system using custom Simulink regulator model

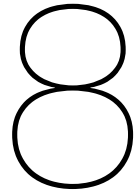
7.5. Conclusion

A model is created to act as a digital twin to the test set up, with the goal being that if the model correctly mirrors the tests, then it will function as an accurate method of scaling this behaviour to a large scale system. This model is created in Matlab-Simscape due to its pre-made blocks that readily represent existing mechanical components. These blocks have parameters that may be set as constants, such as the volume of a chamber, or in relation to some other parameter in the system. With certain boundary conditions and triggering events such as valves opening, the conduction of a transfer test may be mimicked and the parameters throughout the system during a transfer calculated.

Rather than tuning the entire model to match the set up in one go, this is done in parts, with one of these main parts being the friction applied across the piston head. The unit testing done during initial piston testing provided values for the breakaway friction of the piston head, as well as timed runs of the piston head along the length of the cylinder at different pressure settings. With this data the parameters in the Matlab-Simscape friction block are tweaked until the piston translation with the same pressure as recorded during testing matches well to the test data.

A model of the full test set up is made, using a constant volume chamber as the high pressure tank, and using a double acting actuator with gas in one chamber and an isothermal liquid in the other as the piston. The general behaviour of this initial model does not match the tests conducted and this is due to how the pressure regulator, or pressure reducing valve block is behaving. The regulated pressure in the tests is seen to drop quickly once the servo valve is opened, for it to then slowly recover, sometimes to a greater value than the initial pressure setting. The Matlab-Simscape block does not reproduce this behaviour even at a variety of settings, likely due to it being better suited for representing more stable, less dynamic systems.

As the inner workings of a pressure regulator function using a spring, orifice and piston system, it is trialled to replace the standard regulator block with a custom mass/spring/damper model. The parameters in this model, of the mass, the spring stiffness and the damping coefficient are tuned by using the parameter estimation app to vary them and match the values of cylinder and tank pressure to those actually recorded during testing. Unfortunately this method can only be applied to one data set at a time, and it is found that even if a satisfactory replication of one data set is achieved, this is not consistent with other test settings, thus it is unlikely the model is worth pursuing further during this thesis.



Results and Implications for Large Scale System

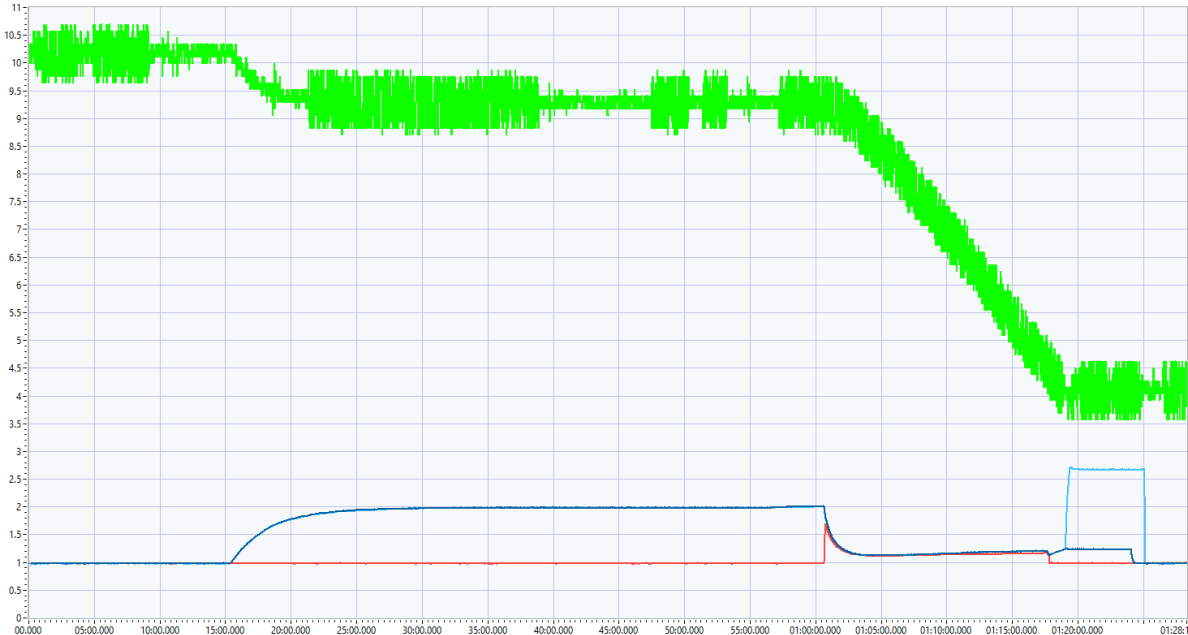
This chapter covers the post processing of the test data generated, as well as the conclusions that may be drawn from this data, followed by the synthesis of these conclusions with the previous work on transfer mechanism and refuelling craft sizing.

8.1. Post Processing and Plotting Test Data

This section describes the post processing carried out on the data obtained during the testing described in Chapter 6 as well as the method employed to produce the plots of this data that will be discussed.

Figure 8.1 displays an image of the raw data gathered from a typical test of the set up with Figure 8.1a showing calibrated pressure data and Figure 8.1b showing the valve states during testing. This data requires post processing to eliminate noise and other sources of unrealistic disturbances in the test data, which is particularly evident in the high pressure data, as well as to trim the data to the periods of interest. Appendix G contains the python code that was developed for this purpose.

Firstly regarding the trimming of the data, the valve state of the liquid servo valve was used as the main indicator of the duration of a test. This valve was opened in order to begin the liquid transferring, and it was closed as soon as gas appeared in the outlet line to stop the test. The changing of this valve state may be seen as the light green line in Figure 8.1b. Before this valve is opened the pressure traces only tracks the filling of the high pressure tank, as well as the pressurisation of the system using the regulator. After the servo valve is closed the pressure can be seen to rise in the regulator line as the hand valve is closed to isolate the cylinder. Finally the bleed valve is opened to allow the system to vent. After inspecting the data it was found that the range in the delay between the servo valve being actuated and the pressure beginning to drop in the cylinder is between 0.00 and 0.25 seconds, meaning this moment exactly in the data is taken as the test beginning. The test end is taken as the exact moment that the servo valve is closed.



(a) Preview of calibrated pressure data from expulsion test



(b) Preview of valve state data from expulsion test

Figure 8.1: Example of previewed test data

Regarding the filtering of the data, it is worth discussing the potential sources for the noise before pursuing a certain form of filtering. As there is particularly remarkable noise on the high pressure data the set up was analysed during the testing to see if this noise could be removed. It was suspected that due to the proximity between the high pressure sensor and the mains power to 24 V DC power converter used for the valves, that some element of the electrical system was causing this noise. Despite attempts to isolate the sensor from this system the noise persisted. Noise from mains electrical power can often be introduced at the 60 Hz frequency, however given that the test data was recorded at 20 Hz this is not easy to distinguish. Figure 8.2 displays a Fourier transform of the data gathered during a typical expulsion test showing no distinct peak of noise that may be filtered with a low pass filter.

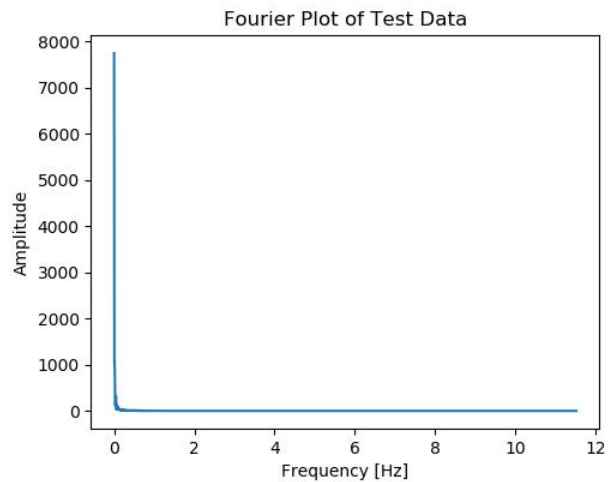


Figure 8.2: Fourier plot of typical test data

A variety of filters and smoothing methods were trialled in the post processing, namely a low-pass filter, a locally weighted scatter plot smoothing and a Savitzky-Golay filter. The low pass filter was ineffective as presumed, with the data still oscillating around the the presumed true value. The locally weighted scatter plot smoothing introduced non-physical trends in the data where it was evident these should not be present. The best results were achieved with the Savitzky-Golay filter. This filter method requires a choice of the window of data for a low order polynomial to be fitted to, as well as a choice of the polynomial order. As the choice of these values is dependent on the phenomena and data they are filtering their selection was done by refining the values until a close representation of the raw data was achieved in combination with good smoothing. For the high pressure data the window of points was 301, while for the low pressure data the window was much smaller at 11. The polynomial order for all data streams was chosen as two. This lead to the best representation of the phenomena that were at play without over manipulating the data.

8.2. Ideal Gas Mass Assumption

The primary parameter of interest to be extracted from the test data is the mass of pressurant gas required to transfer the litre of propellant. As the test set up did not employ a load cell or mass balance the mass had to be inferred from the pressure measurements recorded. The ideal gas law, $PV = nRT$, relates the P the pressure in Pascal, and V the volume in m^3 , to the number of moles, the gas constant R in $m^3 \cdot Pa / K \cdot mol$ and the temperature T in kelvin. As the volume of the high pressure tank is known, the temperature is assumed not to change (though this may be accounted for to allow for greater accuracy), the gas constant remains constant, and the pressure is recorded, we can establish the number of moles of gas in the tank. Using the molar mass of the gas, in this case air, then the mass of gas inside of the tank may be established. The accuracy of this method has been tested by measuring the pressure of the gas inside of the tank and also measuring the mass of the tank at discrete moments when it is under pressure and empty, using a mass balance. The mass balance employed had an accuracy of 0.1 g, while the low pressure sensors on the set up have an accuracy of 0.004 bar. Table 8.1 displays a comparison of the mass measured by the mass balance and calculated based on the ideal gas law, yielding an accuracy of 0.65 %, quite sufficient for the purposes of this thesis.

Table 8.1: Example comparison of ideal gas law mass change and measured mass change

Pressure [Pa]	Mass Measured [g]	Delta Mass Measured [g]	Delta Mass Calculated [g]	Relative Accuracy [%]
2.255E+06	1050.3			
		4.0	4.03	0.65
6.650E+05	1046.3			

8.3. Results

Figure 8.3 is an example of the plots produced using the filtering described in Section 8.1. The plots for each test are included in Appendix F. As the tests including the piston head at five bar had no successful transfers, and the tests without the piston head only had a 50% success rate, plots for this pressure setting are not included. This particular plot is included here as an example as it illustrates the challenging phenomena with the pressure regulator that the Matlab-Simscape model struggled to represent. As is the case in all of the plots, the two green lines represent the low pressure sensors and may be read off from the left hand axis, while the blue line represents the high pressure sensor which may be read off from the right hand axis. The upper low pressure line is the sensor placed at the top of the piston cylinder, while the lower line is the pressure sensor placed at the outlet of the test set up. When the text begins with the servo valve opening it can be seen that the pressure within the cylinder begins to drop, until around the four second mark where it starts to recover. Similarly the pressure at the outlet spikes before also dropping and recovering at a similar rate. What is interesting is that the pressure recovers beyond the original setting of 1.5 bar.

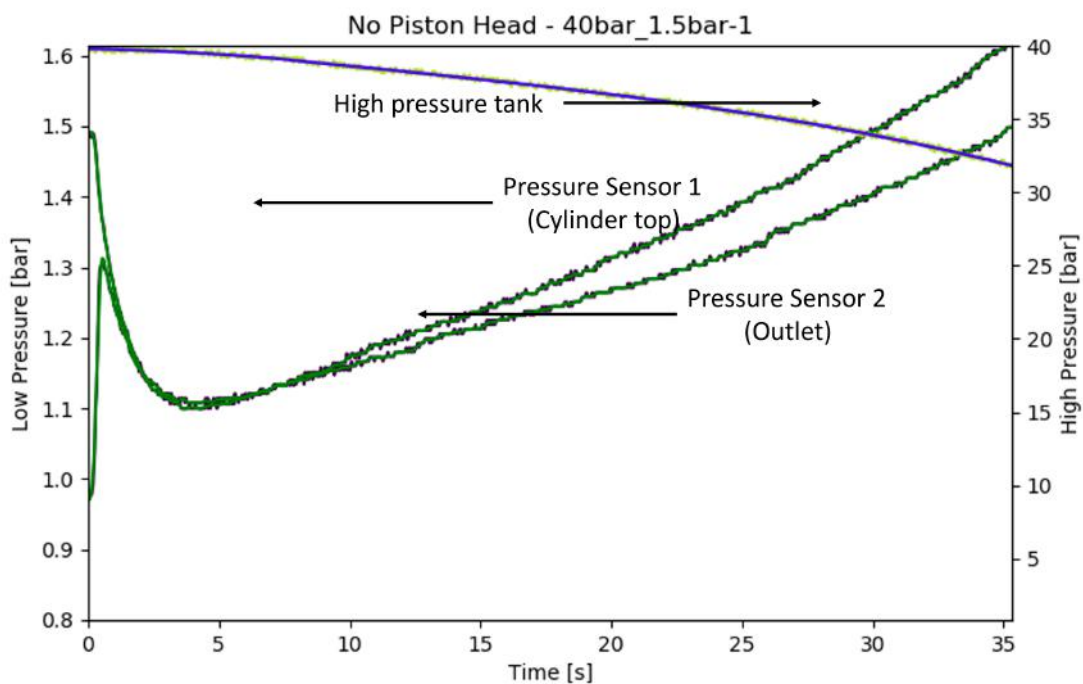


Figure 8.3: Pressure data from test - No Piston Head - 40bar_1.5bar-1 including data labels and axis indicators

Pressure regulators are known to behave differently in dynamic environments, and with this test set up where the back pressure of the regulator in the high pressure tank is dropping, and the liquid volume is decreasing, clearly the dynamic effects are causing this phenomenon in the piston cylinder. As the Matlab-Simscape block functions more as an ideal regulator this behaviour is not captured. These conditions where the pressure in the piston cylinder varies considerably during the transfer, also differ from the assumption in the method employed by Sutton to estimate pressurant gas mass, as it is assumed that the propellant volume is pressurised to a constant value. For the purposes of establishing the pressurant mass used during the test expulsions only the initial and final value of pressure in the high pressure tank is required and this is unaffected by the regulator dynamics. Using the procedure described in Section 8.2 the pressurant mass expelled during each test is calculated, and the tabulated results are presented in Table 8.2. Note that the pressure settings for the tabulated tests below are not the systematic pressure settings but the pressure settings that were actually achieved in the set up during the testing.

From these tables the trend in pressurant mass is clear, with the increasing mass required for higher tank pressure and higher regulator pressure. These trends are better illustrated in Figure 8.4a

and Figure 8.4b, where these pressurant masses are plotted on a scatter plots against the beginning pressures in the tank and cylinder, for tests with and without the piston head respectively. These scatter plots also feature a plane of best fit for the data they contain, with the R-squared value for the fit of these planes varying between 0.88 and 0.91.

Table 8.2: Pressurant mass expelled for the different tests completed

(a) Pressurant mass expelled during testing without piston head

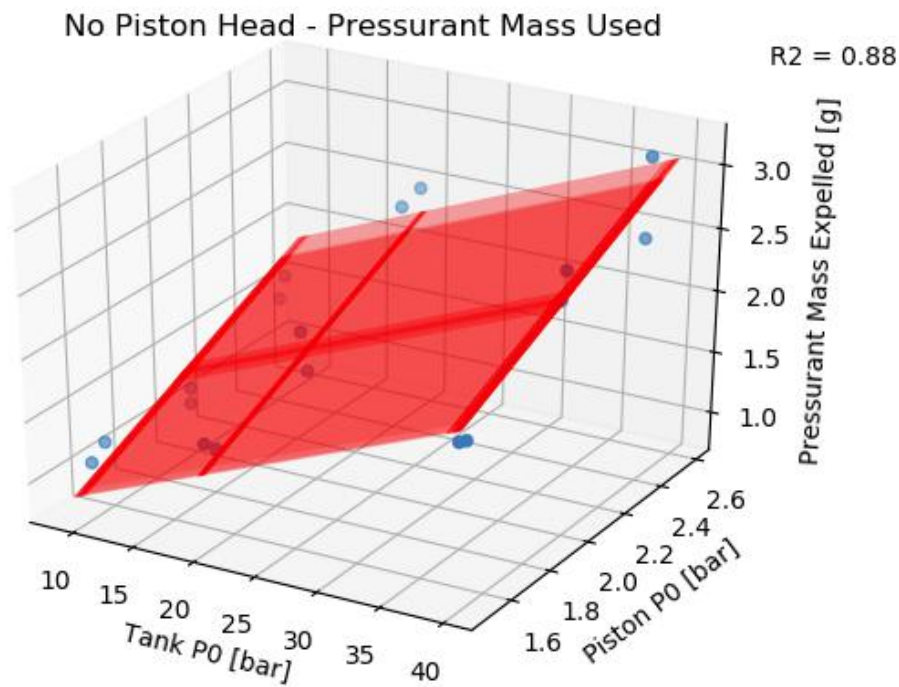
	High Pressure Tank [bar]	Regulated Pressure [bar]	Pressurant Mass Expelled [g]	Transfer Duration [s]
No piston head	9.72	1.52	1.12	66.71
	9.63	1.58	1.22	53.43
	9.11	2.02	1.05	57.27
	9.38	2.01	1.20	44.14
	8.69	2.49	1.42	29.95
	9.04	2.50	1.61	27.11
	19.71	1.54	1.44	45.50
	19.60	1.49	1.53	42.55
	19.22	2.01	1.55	34.72
	19.50	1.96	1.92	28.24
	19.12	2.59	2.44	21.71
	19.06	2.50	2.38	22.20
	39.79	1.48	2.02	35.32
	39.94	1.51	2.00	33.95
	39.25	2.05	2.73	21.67
	39.74	1.99	2.57	23.02
	38.77	2.50	2.52	22.04
	38.85	2.51	3.15	17.93

(b) Pressurant mass expelled during testing with piston head

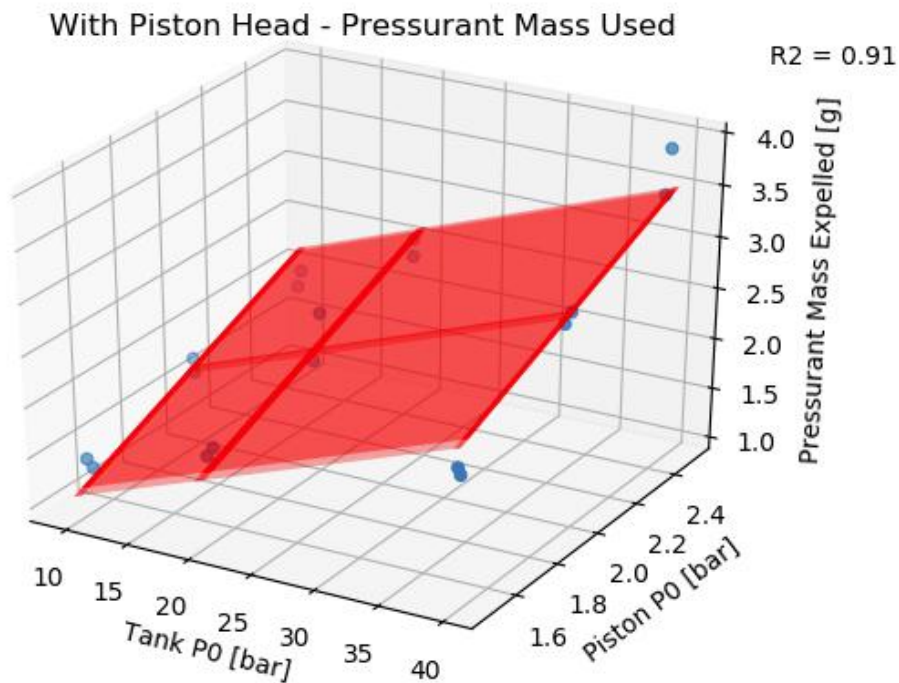
	High Pressure Tank [bar]	Regulated Pressure [bar]	Pressurant Mass Expelled [g]	Transfer Duration [s]
With piston head	9.79	1.50	1.42	149.35
	9.93	1.52	1.31	355.79
	9.49	2.00	1.58	56.31
	9.58	1.99	1.73	46.18
	9.48	2.51	1.94	30.98
	9.27	2.50	1.78	37.49
	19.71	1.50	1.74	74.49
	20.07	1.51	1.82	66.95
	19.61	1.99	1.99	44.26
	19.63	2.02	2.41	32.55
	19.39	2.48	2.37	29.33
	19.25	2.49	2.53	27.62
	39.96	1.47	2.18	54.12
	39.66	1.47	2.24	53.66
	39.62	2.00	2.97	27.98
	39.69	1.97	2.91	28.54
	39.50	2.47	3.48	20.94
	39.38	2.50	3.88	19.32

(c) Pressurant mass expelled during testing with piston head using inverted test set up and H₂O₂

	High Pressure Tank [bar]	Regulated Pressure [bar]	Pressurant Mass Expelled [g]	Transfer Duration [s]
Inverted	18.78	2.37	2.52	38.8
	19.58	2.46	2.96	27.92
With H ₂ O ₂	9.41	2.08	1.64	81.31
	9.40	1.99	1.64	73.35



(a) Scatter plot of pressurant mass used for tests without piston head, including plane of best fit. The equation of the plane of best fit is $-0.0298964 \cdot A - 0.663737 \cdot B + 0.747368 \cdot C + 0.608299 = 0$



(b) Scatter plot of pressurant mass used for tests with piston head, including plane of best fit. The equation of the plane of best fit is $-0.0306257 \cdot A - 0.72114 \cdot B + 0.692112 \cdot C + 0.591945 = 0$

Figure 8.4: Scatter plots of pressurant mass used for tests with and without piston head

In order to better observe the difference in required pressurant mass caused by the presence of the piston head in the system Figure 8.5 is produced, portraying the percentage increase in pressurant mass at the various pressure settings calculated using $\% = (M_{PressWithPistonHead} - M_{PressWithoutPistonHead}) / M_{PressWithPistonHead}$. From this plot it can be seen that the percentage increase in pressurant mass is much smaller at higher tank pressures and at higher cylinder pressures. Additionally it appears to converge towards the 17% difference present for the 40 bar tests. The value that such a plot would converge towards for a different cylinder set up would likely differ due to different levels of piston friction. This is an important parameter for further work on this topic. If this value can be minimised then the extra pressurant mass to be carried in comparison to a simple tank system reduces, reducing the total system mass.

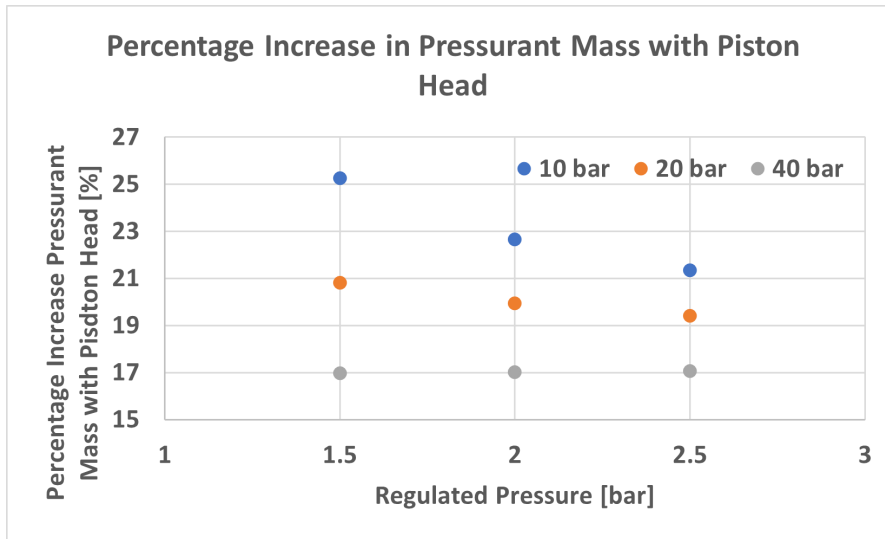
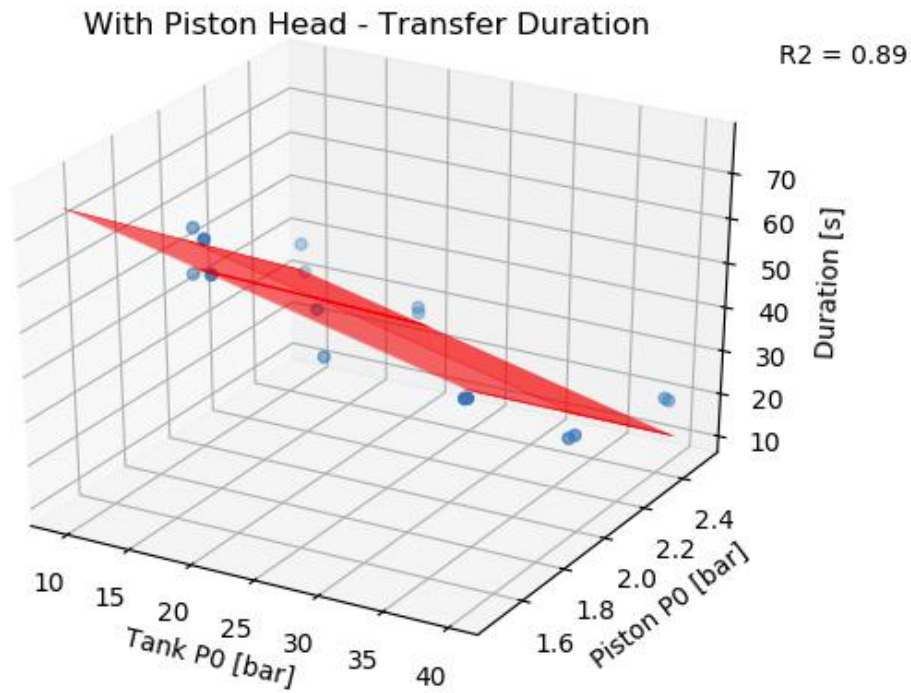
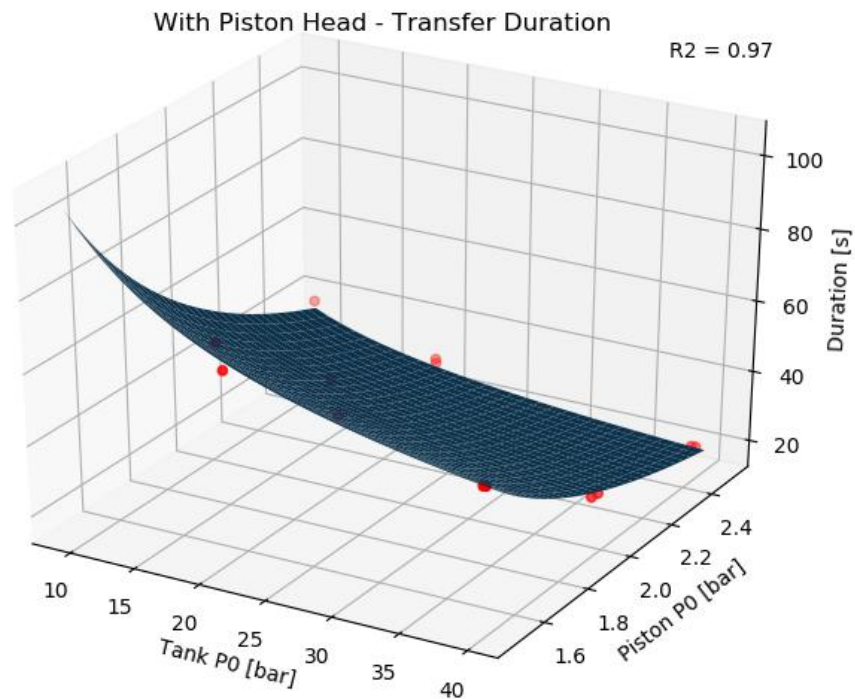


Figure 8.5: Plot of percentage pressurant mass increase due to piston head

Table 8.2 also includes the transfer duration for each test, with the primary trend being that for higher pressure tests the transfer is completed faster. In order to convert these transfer durations to transfer rates, the time duration in seconds is divided into the transferred quantity of one litre, yielding rates from 0.015 L/s at the slowest to 0.052 L/s at the fastest. The targeted 0.1 kg/s was not achieved in this testing. Figure 8.6a and Figure 8.6b display scatter plots of the transfer duration for tests with the piston head, with a plane and paraboloid fitted respectively. In these plots the first two tests with the piston head, at 10 bar and 1.5 bar, are excluded, as their transfer times are significant outliers.



(a) Scatter plot of transfer duration for tests with piston head, including plane of best fit, and excluding two outlier points. The equation of the plane of best fit is $0.0154299 \cdot A + 0.999612 \cdot B + 0.0231913 \cdot C - 3.37624 = 0$



(b) Scatter plot of transfer duration for tests with piston head, including parabolic surface of best fit, and excluding two outlier points. The equation of the surface of best fit is $593.421 \cdot (A^{-0.44102}) \cdot (B^{-0.44102}) = C$

Figure 8.6: Scatter plots of transfer duration excluding two outlier points with two forms of best fit surfaces

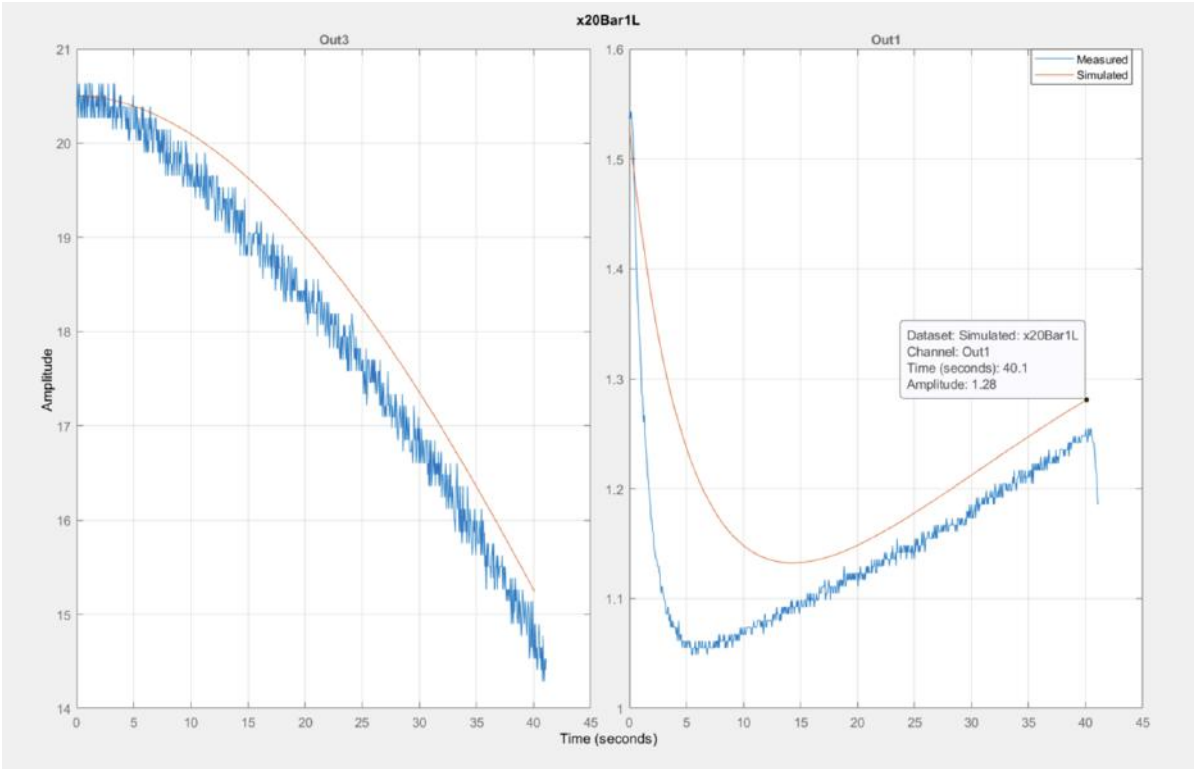
In order to achieve a transfer rate of 0.1 L/s, equivalent to 0.1 kg/s for water, the transfer duration must reach ten seconds. If the parabolic surface of fit from Figure 8.6b is taken, as it has a better R squared, then at a tank pressure of 200 bar as used during the initial refuelling craft sizing, and a regulated pressure of 2.5 bar, the transfer duration is 9.16 seconds, satisfying the transfer rate. Note the plane fit of proves a poor Figure 8.6a proves a poor extrapolation method here as the transfer durations become negative for higher pressures.

With regards to the tests carried out with the test set up inverted and with H_2O_2 as the transferred fluid, the pressurant mass required may be compared to the equivalent point on the trend plane of Figure 8.4b. In terms of a percentage comparison, it is found that in the inverted position, on average 9.02 % more pressurant mass was required for the inverted set up. This is likely due to the fact that the pressure created in the cylinder in the normal orientation due to gravity is assisting the fluid transfer, while in the inverted orientation is working against the transfer. For the tests using H_2O_2 it is found that on average 2.38% less pressurant mass is required, potentially due to the low levels of decomposition occurring that generate pressure in the cylinder. As for both of these comparisons, only two tests were performed, and there is also a limited number of the nominal tests performed, these above conclusions are not strongly supported, but they are in agreement with what theory would suggest.

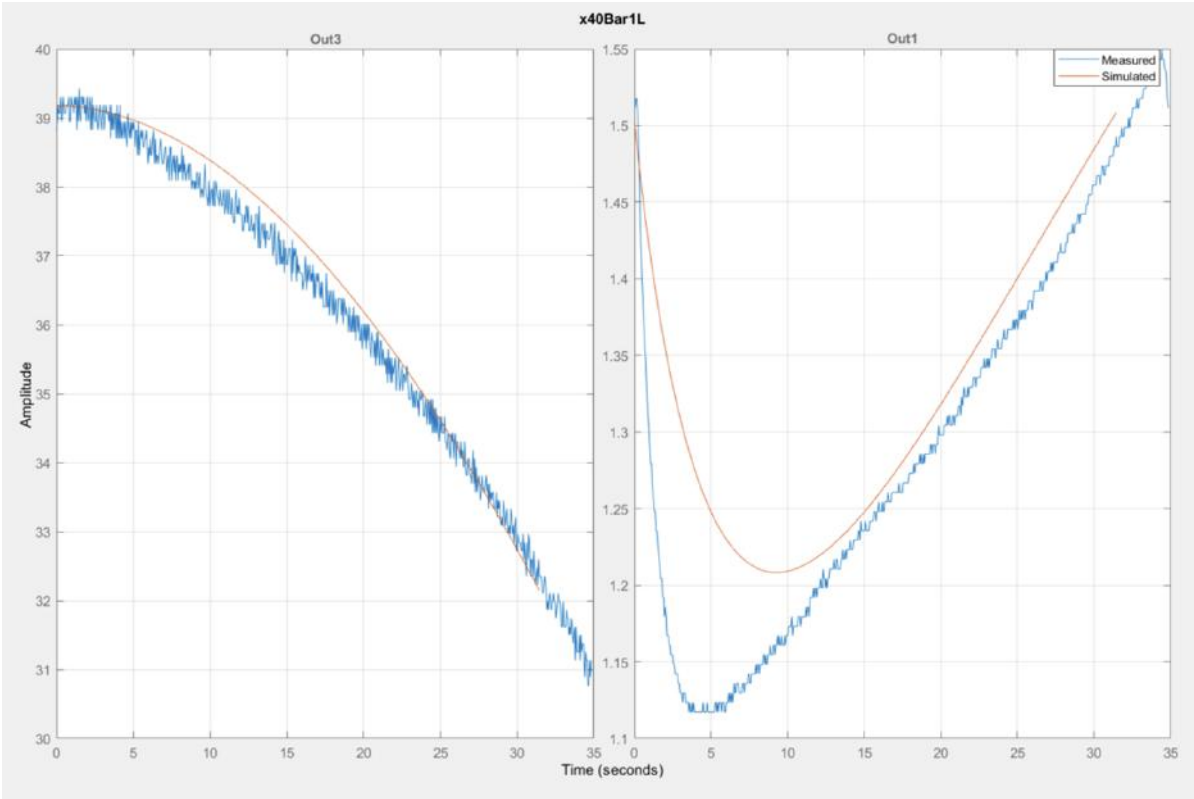
8.4. Comparison to Model

The tuning of the Matlab-Simscape mode, described in Chapter 7, yielded mixed results. This tuning allowed the parameters of the mass-spring-damper system controlling the regulator to be varied in an effort to match the resulting modelled pressure in the tank and in the cylinder to the recorded test results. Unfortunately the model could only be tuned to a single set of test results. The best matching results between the tests and the model were achieved at the settings of 20 bar and 40 bar, as may be seen in Figure 8.7a and Figure 8.7b. The same matching could not be achieved for the 10 bar and 5 bar tests. In these plots the general trends of the data are consistent, however the exact behaviour of the downstream pressure in the cylinder does not drop to the same value, and the duration of the tests and model runs remain different. Outside of these data streams the model also outputs the pressurant mass that has left the high pressure tank. This may be compared to the calculated pressurant mass usage from the corresponding tests. The model pressurant mass used varied from 15%-18% less than that recorded during the testing. Similarly the transfer duration of the model varied from 2%-53% less than the duration of test transfers.

These inconsistencies between the model and the test data mean that the model will not be a useful extrapolation method between the test data and the first order sizing of a large scale system. These difference are likely to be primarily due to the modelling of the regulator dynamics discussed in Section 7.4. For example if Figure 8.7a is taken, on the low pressure plot, as the model pressure does not drop as low as for the test data, there is more pressure in the cylinder, and thus the fluid transfer rate remains higher, and the test completes faster with less pressurant gas expended. Better modelling of the regulator in these dynamic regimes is clearly needed for better representative models to be developed and thus the model is not employed in this thesis for any further purposes.



(a) Matlab-Simscape plots of model and test data superimposed for 20 bar, 1.5 bar test



(b) Matlab-Simscape plots of model and test data superimposed for 40 bar, 1.5 bar test

Figure 8.7: Plots of model and test data superimposed

8.5. Sizing of Full Scale System

As the model proved to be a poor method to extrapolate the parameters of the system to a full scale set up, the trends identified in the test data may be employed instead. The previous sizing of the transfer mechanism in Section 4.3 used Equation 4.6 from Sutton to estimate the mass of pressurant gas required. This estimate does not provide for the real world effects that have been observed in the testing caused by regulators of the addition of a piston head. This method from Sutton estimated a pressurant gas mass of 1.112 kg would be required to transfer 200 L of propellant, with a regulated pressure of 3 bar and a high pressure of 200 bar. If the trend relation for pressurant mass without a piston head from Figure 8.4a is used then 9.851 g of pressurant mass is required for transferring one litre, and linearly scaling to 200L yields a pressurant mass of 1.970 kg is found. Following the same method for the trend with a piston head from Figure 8.4b yields a mass of 11.120 g for one litre and 2.224 kg of mass for 200L. Lastly if the relation for transfer duration from Figure 8.6b is used at the 3 bar and 200 bar settings, a transfer rate of 0.157 L/s is found, exceeding the 0.1 L/s currently employed and required.

With this value for the pressurant mass required, the initial sizing of the transfer mechanism made in Section 4.3 may be refined. Using the transfer method of pressurant gas, at the 200 L at 0.1 kg/s settings, the pressurant gas mass required for just the transfer, is again doubled to account for the pressurant to be transferred to the customer craft, yielding a value of 4.448 kg. Following the same method as previously employed for the rest of the transfer system, a total mass for the transfer system of 343.010 kg is found.

To re-contextualise this value using the same method of delta-V assessment employed in Section 4.2, with this mass of a transfer system, a refuelling vehicle with the same gross lift off weight as that of the Apollo Lunar lander (16400 kg), with an I_{sp} of 340s, and with a realistic structural mass fraction of 0.3 (averaged from that of the Lunar lander, the proposed Lockheed Lunar lander, the proposed Blue Origin Lunar lander, and the Chinese Chang'e 3 lander), would be a viable method of refueling spacecraft in low Lunar orbit when launched from the Moon. Even more so, this vehicle would also be able to refuel spacecraft in low Martian orbit when launched from Deimos, and when launched from Phobos to low Martian orbit an even greater margin exists on the required I_{sp} and structural mass fraction, making this a viable concept.

8.6. Conclusion

Post processing of the test data was carried out in Python. The delay between opening the liquid servo valve and the beginning of fluid flow proved to be small enough that the test data could be trimmed to start at this instant, and the test end was taken as the moment the liquid valve was closed. Noise in the system, particularly in the high pressure sensor data, likely originated from the sensor cables proximity to high power lines supplying the solenoid valves with 24 V. The most effective filter for these data streams was found to be a Savitzky-Golay filter which locally interpolates a polynomial to a certain window of points.

As the primary parameter of interest to extract from the test data is the pressurant mass required for a certain transfer, but the primary recorded source of data is the pressure values in the system, the ideal gas law is employed to convert from pressure to mass. The accuracy of this method is tested using a mass balance to measure the change in mass in the high pressure tank while the ideal gas law is also used to estimate the change in mass. This method is found to be accurate within 0.65%.

Plots are produced of each test, and the trends in the pressurant mass required as well as the transfer duration may be observed. It is found that the pressurant mass required for tests both with and without the piston head show a good fit to a planar surface. The additional pressurant mass required for the piston head tests in comparison with the tests that do not use a piston head, varies between 25% and 17%, and with increasing pressure settings the trend appears to converge to 17%. Only the transfer duration of the piston head tests is examined, and it is found that the trend of these values fits well to a 3D paraboloid. The inverted tests required 9.02% more pressurant mass, likely due to the fact that the gravity gradient was slightly countering the force exerted by the pressure on the piston head. The tests using H_2O_2 were found to require 2.38% less pressurant mass as the potential decomposition in the piston cylinder assembly may have increased the pressure in the regulated section of the set up.

Despite attempts to tune the parameters of the model regulator to fit data in the model to recorded data from single tests, the Matlab-Simscape model continued to show poor agreement with the over

all test data. The failure of the model regulator to match the dynamics of the one employed in the test set up mean that both the transfer duration and the required pressurant mass are underestimated, and this the model is not of use for extrapolation of these test results to a large scale system.

The trends identified in the test data may instead be used to scale the pressure parameters to a full scale system. The settings employed for the initial transfer method comparison, of 200L to be transferred, with the high pressure at 200 bar and the regulated pressure of 3 bar, are used. With the trend identified for pressurant mass with a piston head, it is found that 11.120 g of pressurant are required for transferring one litre, and linearly scaling to 200 L gives 2.224 kg of pressurant. At these pressure settings, the trend observed for transfer duration yields a transfer rate of 0.157 L/s, which exceeds the requirement of 0.1 L/s. The values yield a total propellant transfer system mass of 343.010 kg for a system transferring 200L. When placed on a refuelling craft with the gross lift off mass equivalent to that of the Apollo Lunar lander this craft could viably refuel spacecraft both in Lunar and Martian orbits when launched from the moon, Phobos or Deimos respectively.

9

Conclusion

The current trend among in-orbit refuelling initiatives, such as Orbit-Fab in the US, is to refuel satellites primarily with hydrazine, using refuelling missions launched from the Earth's surface or as secondary objectives of launcher kick-stages. This approach not only supplies spacecraft with a toxic and soon to be outlawed propellant, but in utilising a launch from the Earth's gravity well, refuels them in an unsustainable manner. Based on this gap, both in research and the market, the following research objective was formed;

To investigate the feasibility of an in-situ H_2O_2 refuelling architecture and reusable refuelling craft, with the inclusion of a novel H_2O_2 propellant transfer mechanism, through top level sizing and prototype testing

Which was then split into a number of research questions, the answers for which are presented below. Due to shortcomings in the model development it was not utilised to extrapolate the findings of the testing to a large scale set up, and instead the trends observed during testing were used, as illustrated in Figure 9.1. This chapter presents the summarised answers to the previously posed research questions, as well as recommendations for further work.

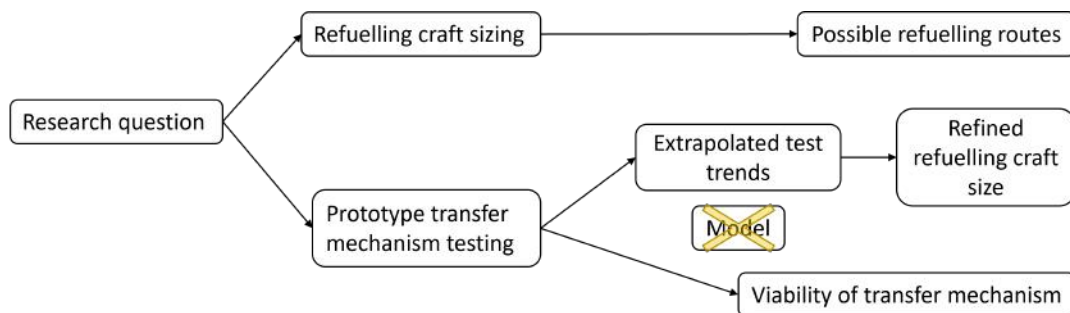


Figure 9.1: Research question implemented approach flow diagram

1. What refuelling craft mass is viable and on what routes in the solar system?

As this proposed refuelling architecture originates at sources of water in the solar system, the Moon, Mars and the Martian moons are assessed as refuelling bases. It is found that a craft with a reasonable structural mass fraction of 0.3, and an I_{sp} of 330 s - 340 s could viably launch from the Moon to low Lunar orbit, and from Deimos and Phobos to low Martian orbit, to refuel spacecraft. A spacecraft capable of refuelling 200 L of H_2O_2 with the pressurant mass determined from the testing in this thesis, would weigh approximately the same as the gross lift of mass of the Apollo Lunar lander (16000 kg).

2. What is the optimal transfer mechanism for a sustainable propellant resupply system?

The optimal transfer mechanism is established based off of criteria founded on the desires of refuelling customers, the refuelling company and other stakeholders, and is deemed to be a piston based transfer method. A piston is capable of transferring the propellant, as well as maintaining its orientation in the storage tank in a zero-G environment, and also assisting in gauging the mass of propellant. The piston must be used in conjunction with another method such as the stored gas, gas generator or pump options in order to actuate the piston.

(a) What systems must the transfer mechanism be used in conjunction with, and how sensitive are these configurations to changes in system requirements?

A mass comparison is carried out between the piston being actuated using pressurant gas, a H_2O_2 powered gas generator, and a pump in conjunction with pressurant gas, using different volumes of propellant to be transferred (200 L and 1000 L), at different transfer rates (0.1 kg/s and 1.0 kg/s). It is found that for the different permutations of the transferred amount and the transfer rate, the lightest transfer method varies, however for all permutations the relative total mass variation is less than 2%. Thus the most appropriate transfer system for different scenarios likely varies and may be tailored.

(b) What challenges face the transfer mechanism and can they be overcome?

The main challenges faced by the piston transfer system are that of jamming or cocking within the piston cylinder, and leakage occurring around the piston head. Through consultation with experts, utilising guide tape, and with careful design approaches, using the correct L/D ratio the issue of piston jamming was never encountered. This should be tested over longer durations to observe the longevity of the system with high cycle numbers. The fabricated piston head was found to leak when assembled with the chosen piston seals. Despite retesting with new components, and PTFE sealing sprays this issue persisted. likely with improved fabrication methods this issue can be mitigated.

(c) Can the transfer system function in a representative environment?

When consulting experts regarding zero-G testing it was suggested that if a system can perform nominally in an inverted orientation then it is likely to perform well in-orbit. Additionally as the system is designed to transfer H_2O_2 this is also trialled to prove the compatibility of the system. In an inverted orientation, it is found that 9.02% more pressurant mass is required due to the adverse gravity gradient, and the required pressurant mass in-orbit is likely within this range. The tests using H_2O_2 were found to require 2.38% less pressurant mass as the potential decomposition in the piston cylinder assembly may have increased the pressure. Improved selection of materials in future iterations can reduce this decomposition phenomenon.

9.1. Recommendations

A variety of recommendations may be made in order to remedy challenges encountered during this work and in order to better facilitate further research on this topic;

- The adjustable pressure regulator used during the prototype transfer mechanism testing caused issues due to its unexpected behaviour and replicating this behaviour in the model. For further research a more sophisticated pressure regulator should be used, ideally one that comes with a detailed data sheet. Furthermore before integrating this regulator in the test set up, unit tests should be done with it in order to characterise its behaviour.
- The sealing of the piston head in the piston cylinder leaked during testing. Changing the method in which the piston cylinder is fabricated, and rather than having a raw extruded finish having the interior of the cylinder machined to tolerance would likely help in remedying this. Additionally the more novel forms of piston seal such as inflatable ones should be further investigated to assess their viability for repeated use.
- The radial bolting of the endcap components in this set up caused issues during piston head insertion and endcap assembly. This form of interface should be replaced with a flanged endcap style for testing to prevent these issues, and a welded assembly for flight models for weight savings.
- One drawback of piston systems is that they typically are heavier than an equivalent simple tank. This thesis did not focus on mass optimisation of the piston assembly however for a flight version the focus will have to be placed on this quality too, potentially through formable piston head designs and other innovations.
- Current proposed propellant transfer systems are designed for single or a handful of uses, for a truly sustainable long term refuelling architecture transfer mechanisms must be capable of high cycle numbers.
- This research showed that for some forms of customer spacecraft a pump is needed to resupply propellant, and also that this piston may be actuated through pressurant gas or even a gas generator. This research did not explore these permutations of the transfer system design, and thus future work should investigate where these methods are most appropriate and how best they might be integrated with the piston.
- Lastly this research also showed that the piston transfer mechanism can be of used when gauging the propellant mass in the system. Methods through which this property could be exploited were not explored in this research, and thus in future methods to measure the displacement of the piston head, and therefor the propellant mass should be investigated.

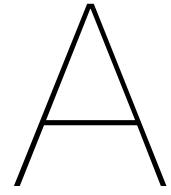
References

- [1] HN Abramson et al. *Propellant Slosh Loads*. Tech. rep. NASA - ASASP-8009, Aug. 1968.
- [2] W E Anderson et al. "Peroxide Propulsion at the Turn of the Century". In: 2013.
- [3] Donald R Bellman and Gene J Matranga. *Design And Operational Characteristics Of A Lunar-Landing Research Vehicle*. Tech. rep. Edwards California: Flight Research Centre, Sept. 1965.
- [4] Benchmark Space Systems. *Integrated Propulsion Products*. 2021. URL: <https://www.benchmarkspacesystems.com/products/propulsion#halcyon-datasheet>.
- [5] Richard M Bentley. *Design And Development Of The Syncom Communications Satellite*. Tech. rep. El Segundo: Hughes Aircraft Company, Space Systems Division, 1965.
- [6] T. Bewer et al. "Novel method for investigation of two-phase flow in liquid feed direct methanol fuel cells using an aqueous H₂O₂ solution". In: *Journal of Power Sources* 125.1 (Jan. 2004), pp. 1–9.
- [7] J. E. Boretz. "Orbital refueling techniques". In: *5th Propulsion Joint Specialist, 1969*. American Institute of Aeronautics and Astronautics Inc, AIAA, 1969. DOI: 10.2514/6.1969-564.
- [8] T Borsboom. "The design and testing of an injector for an advanced hypergolic dual-mode propulsion system". PhD thesis. 2021.
- [9] Calvin R. James and Wilton P. Lock. *Operation Experience with the X-15 Reaction Control and Reaction Augmentation Systems*. Tech. rep. Edwards, California: Flight Research Center, July 1965.
- [10] Dianxue Cao et al. "A direct NaBH₄–H₂O₂ fuel cell using Ni foam supported Au nanoparticles as electrodes". In: *International Journal of Hydrogen Energy* 35.2 (Jan. 2010), pp. 807–813.
- [11] Joseph M Cardin. "A Modular Approach to On-Orbit Servicing". In: *Journal of Aerospace* 98 (1989), pp. 1214–1224.
- [12] Sophia Casanova et al. "Enabling Deep Space Exploration with an In-Space Propellant Depot Supplied from Lunar Ice". In: *American Institute of Aeronautics and Astronautics* (2017).
- [13] Scott Christiansen and Troy Nilson. *Docking System for Autonomous, Un-manned Docking Operations*. Tech. rep. Louisville: Spacedev/Starsys, 2007.
- [14] D Davis et al. *Fire, Explosion, Compatibility and Safety Hazards of Hydrogen Peroxide*. Tech. rep. Las Cruces: White Sands Test Facility, Jan. 2005.
- [15] Neil F. Dipprey and Scott J. Rotenberger. "Orbital express propellant resupply servicing". In: *39th AIAA/ASME/SAE/ASEE Joint Propulsion Conference and Exhibit*. American Institute of Aeronautics and Astronautics Inc., 2003.
- [16] R. Eberhardt, T. Tracey, and W. Bailey. "Orbital spacecraft resupply technology". In: *AIAA/ASME/SAE/ASEE 22nd Joint Propulsion Conference*. American Institute of Aeronautics and Astronautics (AIAA), June 1986. DOI: 10.2514/6.1986-1604.
- [17] W.H. Erelke. *Hydrogen Peroxide Handbook - Technical Report AFRPL-TR-67-144*. Tech. rep. California: Chemical and Material Sciences Department - Rocketdyne, July 1967.
- [18] Daniel Faber. *Material Transfer Interfaces for Space Vehicles, and Associated Systems and Methods*. 2021.
- [19] Daniel Faber. *Systems and Methods for Creating and Automating an Enclosed Volume with a Flexible Fuel Tank and Propellant Metering for Machine Operations*. 2021.
- [20] Daniel Faber. *Systems and Methods for Delivering, Storing, and Processing Materials in Space*. 2019.

- [21] Dale A Fester and Paul E Bingham. "Main Tank Injection (MTI) Pressurization Of Liquid Rocket Propellant Tanks". In: *54th International Astronautical Congress of the International Astronautical Federation, the International Academy of Astronautics, and the International Institute of Space Law*. Bremen, 2003.
- [22] J Foust. *Orbit Fab and Benchmark Space Systems to partner on in-space refueling technologies - SpaceNews*. Feb. 2021. URL: <https://spacenews.com/orbit-fab-and-benchmark-space-systems-to-partner-on-in-space-refueling-technologies/>.
- [23] *Gas Generator Catalog 2004*. Tech. rep. General kinetics Inc., 2004.
- [24] W. Goette. "Centaur D-1T Propulsion and Propellant Systems". In: *AIAA/SAE 9th Propulsion Conference*. Las Vegas: American Institute of Aeronautics and Astronautics (AIAA), Nov. 1973.
- [25] Jonathan A. Goff et al. "Realistic near-term propellant depots: Implementation of a critical space-faring capability". In: *AIAA Space 2009 Conference and Exposition*. 2009.
- [26] Robert H. Greene. "Early Bird Placement in a Stationary Orbit: Launch and Control System Maneuvers". In: 19 (Jan. 1966), pp. 9–42. ISSN: 0079-6050.
- [27] Jason W. Hartwig. "Propellant management devices for low-gravity fluid management: Past, present, and future applications". In: *Journal of Spacecraft and Rockets* 54.4 (2017), pp. 808–824.
- [28] Øistein Hasvold et al. "Power sources for autonomous underwater vehicles". In: *Journal of Power Sources* 162.2 (Nov. 2006), pp. 935–942.
- [29] Derek W. Hengeveld et al. "Review of modern spacecraft thermal control technologies". In: *HVAC and R Research* 16.2 (2010), pp. 189–220.
- [30] *High-Pressure Check Valves*. URL: www.resato.com/documents/96463/16402961/High+pressure+check+valves+datasheet+download+English.pdf/dd8e2c74-b4f0-eda2-95ee-546168cc0db0.
- [31] A Iaco Veris. *Fundamental Concepts of Liquid-Propellant Rocket Engines*. Rome: Springer, 2019. URL: <http://www.springer.com/series/8613>.
- [32] D E Jaekle. "Propellant Management Device Conceptual Design and Analysis: Galleries ". In: *33rd AIAA / ASME / SAE / ASEE Joint Propulsion Conference & Exhibit*. Seattle, 1997.
- [33] D E Jaekle. "Propellant Management Device Conceptual Design and Analysis: Sponges ". In: *AIAA/SAE/ASME/ASEE 29th Joint Propulsion Conference and Exhibit*. Andover, Massachusetts, 1993.
- [34] D E Jaekle. "Propellant Management Device Conceptual Design and Analysis: Traps and Troughs". In: *31st AIAA / ASME / SAE / ASEE Joint Propulsion Conference and Exhibit*. San Diego, 1995.
- [35] D E Jaekle. "Propellant Management Device Conceptual Design and Analysis: Vanes ". In: *AIAA / ASME / SAE / ASEE 27th Joint Propulsion Conference*. Sacramento, CA, 1991.
- [36] James E. Love and Wendell H. Stillwell. *The Hydrogen peroxide Rocket Reaction Control System for the X-1B Research Airplane*. Tech. rep. Edwards, California: NASA Flight Research Centre, Dec. 1959.
- [37] B Jeffrey Anderson, Editor Marshall, and Robert E Smith. *Natural Orbital Environment Guidelines for Use in Aerospace Vehicle Development*. Tech. rep. 1994.
- [38] Xia Jing et al. "The open circuit potential of hydrogen peroxide at noble and glassy carbon electrodes in acidic and basic electrolytes". In: *Journal of Electroanalytical Chemistry* 658.1-2 (July 2011), pp. 46–51.
- [39] Geoffrey L. Kulak et al. *Guide to design criteria for bolted and riveted joints*. Wiley, 1987, p. 333. ISBN: 0471837911.
- [40] Laboratory of Advanced Jet Propulsion. *Rocket Engine using Hydrogen Peroxide*. 2021. URL: <http://www.lajp.org.ua/r-d-projects/rocket-engine-using-hydrogen-peroxide>.
- [41] Shao Jiang Lao et al. "A development of direct hydrazine/hydrogen peroxide fuel cell". In: *Journal of Power Sources* 195.13 (July 2010), pp. 4135–4138.

- [42] Juyeon Lee et al. "Performance Analysis and Mass Estimation of a Small-Sized Liquid Rocket Engine with Electric-Pump Cycle". In: *International Journal of Aeronautical and Space Sciences* 22.1 (Feb. 2021), pp. 94–107. ISSN: 20932480. DOI: 10.1007/s42405-020-00325-z.
- [43] Logan McKee. *Hydrogen Peroxide for Propulsive Power -Production and use by the Germans During World War II*. 1947.
- [44] Nie Luo et al. "Hydrogen-peroxide-based fuel cells for space power systems". In: *Journal of Propulsion and Power* 24.3 (2008), pp. 583–589.
- [45] Jaime Quesada Mañas. "Propellant grade hydrogen peroxide production and thermo pseudo hypergolicity investigation for dual mode green propulsion systems". PhD thesis. 2020.
- [46] J J Martin and J B Holt. *Magnetically Actuated Propellant Orientation Experiment, Controlling Fluid Motion With Magnetic Fields in a Low-Gravity Environment (MSFC Center Director's Discretionary Fund Final Report, Project No. 93-18)*. Tech. rep. Alabama: Marshall Space Flight Center - NASA, Mar. 2000.
- [47] Alberto Medina et al. "Towards a standardized grasping and refuelling on-orbit servicing for geo spacecraft". In: *Acta Astronautica* 134 (May 2017), pp. 1–10.
- [48] George H Miley et al. "Advanced NaBH₄/H₂O₂ Fuel Cell for Space Applications". In: *AIP Conference Proceedings* 1103.1 (2009), pp. 157–163. DOI: 10.1063/1.3115491. URL: <https://aip.scitation.org/doi/abs/10.1063/1.3115491>.
- [49] Nammo. *220N Monopropellant Thruster - Nammo | Nammo*. 2021. URL: <https://www.nammo.com/product/220n-h2o2-thruster/>.
- [50] Nammo. *30kN Hybrid Engine - Nammo | Nammo*. 2021. URL: <https://www.nammo.com/product/30kn-hybrid-engine/>.
- [51] Parabilis Space Technologie. *H₂O₂ Handling Safety Overview*. 2017.
- [52] Albert C Piccirillo. *The Me 163B Komet, Development and Operational Experience*. Tech. rep. 1997, pp. 1828–1845.
- [53] R N Porter and H B Stanford. *Propellant Expulsion in Unmanned Spacecraft*. Tech. rep. 1965, pp. 93–126.
- [54] Daniel N. Prater and John J. Rusek. "Energy density of a methanol/hydrogen-peroxide fuel cell". In: *Applied Energy* 74.1-2 (Jan. 2003), pp. 135–140.
- [55] A. E. Sanli and Aylin Aytac. "Response to Disselkamp: Direct peroxide/peroxide fuel cell as a novel type fuel cell". In: *International Journal of Hydrogen Energy* 36.1 (Jan. 2011), pp. 869–875.
- [56] J Schiel. *FuelGEO — Orbit Fab*. Dec. 2021. URL: <https://www.orbitfab.com/fuelgeo>.
- [57] W.C. Schumb, C.N. Satterfield, and R.L. Wentworth. *Hydrogen Peroxide - A Monograph Prepared with Support from the Office of Naval Research*. Tech. rep. Cambridge: Massachusetts Institute of Technology, Dec. 1953.
- [58] SKF. *Hydraulic seals*. Tech. rep. 2014.
- [59] Solvay. *H₂O₂ Passivation Procedure*. 2019. URL: www.solvay.com.
- [60] *Space engineering Mechanical-Part 2: Structural*. Tech. rep. 2000.
- [61] George P. (George Paul) Sutton and Oscar. Biblarz. *Rocket Propulsion Elements*. John Wiley & Sons, 2001, p. 751. ISBN: 0471326429.
- [62] T4I. *Bi-Propellant - T4I - Technology for Propulsion and Innovation*. 2021. URL: <https://www.t4innovation.com/bi-propellant/>.
- [63] T4I. *Hybrid Propellant - T4I - Technology for Propulsion and Innovation*. 2021. URL: <https://www.t4innovation.com/hybrid-propellant/>.
- [64] T4I. *Monopropellant - T4I - Technology for Propulsion and Innovation*. 2021. URL: <https://www.t4innovation.com/mono-propellant/>.
- [65] B. Tartakovsky and S. R. Guiot. "A Comparison of Air and Hydrogen Peroxide Oxygenated Microbial Fuel Cell Reactors". In: *Biotechnology Progress* 22.1 (Jan. 2006), pp. 241–246.

- [66] Leonardo Urbinati. "Inflatable Structures for Space Applications". PhD thesis. Politecnico di Torino, 2020.
- [67] M. Ventura and P. Mullens. "The use of hydrogen peroxide for propulsion and power". In: *35th Joint Propulsion Conference and Exhibit*. American Institute of Aeronautics and Astronautics Inc, AIAA, 1999.
- [68] M. C. Ventura and E. J. Wernimont. "History of the Reaction Motors super performance 90% H₂O₂/kerosene LR-40 rocket engine". In: *37th Joint Propulsion Conference and Exhibit*. 2001.
- [69] Forest He Wainscott. *The Syncom 111 Launch*. Tech. rep. Goddard Space Flight Center, Apr. 1966.
- [70] Walter C. Schumb, Charles N. Satterfield, and Ralph L. Wentworh. *Hydrogen Peroxide*. Vol. ACS Monograph 261. 3. New York: Reinhold Publishing Corporation, 1956.
- [71] John Terry White. *Boom and Zoom: The History of the NF-104A AST*. Tech. rep. 2005.
- [72] Fachhochschule Wiener. *Green Advanced Space Propulsion (GRASP) - The Final Report*. Tech. rep. Fachhochschuler Wiener Neustadt fur Wirtschaft und Technik, Nov. 2011.
- [73] Yusuke Yamada et al. "Protonated iron-phthalocyanine complex used for cathode material of a hydrogen peroxide fuel cell operated under acidic conditions". In: *Energy & Environmental Science* 4.8 (Aug. 2011), pp. 2822–2825.
- [74] Shin ichi Yamazaki et al. "A fuel cell with selective electrocatalysts using hydrogen peroxide as both an electron acceptor and a fuel". In: *Journal of Power Sources* 178.1 (Mar. 2008), pp. 20–25.
- [75] Weiqian Yang et al. "Nanostructured palladium-silver coated nickel foam cathode for magnesium-hydrogen peroxide fuel cells". In: *Electrochimica Acta* 52.1 (Oct. 2006), pp. 9–14.
- [76] B. Yendler. "Review of propellant gauging methods". In: *Collection of Technical Papers - 44th AIAA Aerospace Sciences Meeting*. Vol. 15. American Institute of Aeronautics and Astronautics Inc., 2006, pp. 11245–11251.
- [77] Lanhua Yi et al. "High activity of Au–Cu/C electrocatalyst as anodic catalyst for direct borohydride-hydrogen peroxide fuel cell". In: *International Journal of Hydrogen Energy* 36.24 (Dec. 2011), pp. 15775–15782.
- [78] B.T.C Zandbergen. *AE1222-II: Aerospace Design & Systems Engineering Elements I Part: Spacecraft (bus) design and sizing*. Tech. rep. 2018.



H₂O₂ Material Compatibility

Hydrogen Peroxide Material Compatibility Chart

All wetted surfaces should be made of materials that are compatible with hydrogen peroxide. The wetted area or surface of a part, component, vessel or piping is a surface which is in permanent contact with or is permanently exposed to the process fluid (liquid or gas).

Less than 8% concentration H₂O₂ is considered a non-hazardous substance. Typically encountered versions are baking soda-peroxide toothpaste (0.5%), contact lens sterilizer (2%), over-the-counter drug store Hydrogen Peroxide (3%), liquid detergent non-chlorine bleach (5%) and hair bleach (7.5%).

At 8% to 28% H₂O₂ is rated as a Class 1 Oxidizer. At these concentrations H₂O₂ is usually encountered as a swimming pool chemical used for pool shock treatments.

In the range of 28.1% to 52% concentrations, H₂O₂ is rated as a Class 2 Oxidizer, a Corrosive and a Class 1 Unstable (reactive) substance. At these concentrations, H₂O₂ is considered industrial strength grade.

Concentrations from 52.1% to 91% are rated as Class 3 Oxidizers, Corrosive and Class 3 Unstable (reactive) substances. H₂O₂ at these concentrations are used for specialty chemical processes. At concentrations above 70%, H₂O₂ is usually designated as high-test peroxide (HTP).

Concentrations of H₂O₂ greater than 91% are currently used as rocket propellant. At these concentrations, H₂O₂ is rated as a Class 4 Oxidizer, Corrosive and a Class 3 Unstable (reactive) substance.

Material	Compatibility 10% H ₂ O ₂	Compatibility 30% H ₂ O ₂	Compatibility 50% H ₂ O ₂	Compatibility 100% H ₂ O ₂ (HTC)
Chemical resistance data is based on 72° F (22° C) unless otherwise noted				
A- Suitable				
B - Good, minor effect, slight corrosion or discoloration				
F - Fair, moderate effect, not recommended for continuous use;				
softening, loss of strength, and/or swelling may occur				
X - Do Not Use - severe effect, not recommended for ANY use				
NA - Information Not Available				
304 stainless steel	B ¹	B ¹	B ¹	B ¹
316 stainless steel	B	B	A ¹	A ¹
416 stainless steel	B	B	F	X
440C stainless steel	B	B	A	X
ABS plastic	A	A	A	A

It is the sole responsibility of the system designer and user to select products suitable for their specific application requirements and to ensure proper installation, operation, and maintenance of these products. Material compatibility, product ratings and application details should be considered in the selection. Improper selection or use of products described herein can cause personal injury or product damage. In applications where exposure to harmful chemicals is frequent, of long duration or in high concentrations, additional testing is recommended.



End your search, simplify your supply chain
ISO 9001:2015 Certified Companies

4091 S. Eliot St., Englewood, CO 80110-4396
Phone 303-781-8486 | Fax 303-761-7939
Ismedspec.com

© Copyright 2020 IS MED Specialties

Hydrogen Peroxide Material Compatibility Chart

ver 09-Jul-2020

Material	Compatibility 10% H ₂ O ₂	Compatibility 30% H ₂ O ₂	Compatibility 50% H ₂ O ₂	Compatibility 100% H ₂ O ₂ (HTC)
Chemical resistance data is based on 72° F (22° C) unless otherwise noted				
A- Suitable				
B - Good, minor effect, slight corrosion or discoloration				
F - Fair, moderate effect, not recommended for continuous use;				
softening, loss of strength, and/or swelling may occur				
X - Do Not Use - severe effect, not recommended for ANY use				
NA - Information Not Available				
1 - Satisfactory to 120°F (48° C)				
2 - Satisfactory for O-rings, diaphragms or gaskets				
3 - Temporary use only				
Acetal (Delrin®)	X	X	X	X
Acrylic (PMMA)	B	F	NA	X
Alloy 20 (Carpenter 20)	F	B	B	X
Aluminum	A	A	A	A
Brass	X	X	X	X
Bronze	B	B	B	B
Buna N (Nitrile)	X	X	X	X
Carbon graphite	F	F	F	F
Carbon steel	X	X	X	X
Cast iron	F	X	X	X
Ceramic Al ₂ O ₃	A	A	A	A
Ceramic magnet	A	A	A	A
Copper	X	X	X	X
CPVC	A	A	A	A
EPDM	A	B	B	X
Epoxy (epoxide polymers)	F	B	B	X
FKM (fluoroelastomers, Viton®)	A	A	A	A
Hastelloy-C®	A	A	A	A
HDPE	A	A	A	X
Hypalon®	X	X	X	X
Hytre® (polyester elastomer)	X	X	X	X
LDPE	A	F ¹	F ¹	F ¹
Natural rubber	B	F	F	F
Neoprene	X	X	X	X
NORYL®	A ¹	A ¹	A	A

It is the sole responsibility of the system designer and user to select products suitable for their specific application requirements and to ensure proper installation, operation, and maintenance of these products. Material compatibility, product ratings and application details should be considered in the selection. Improper selection or use of products described herein can cause personal injury or product damage. In applications where exposure to harmful chemicals is frequent, of long duration or in high concentrations, additional testing is recommended.



End your search, simplify your supply chain
ISO 9001:2015 Certified Companies

4091 S. Eliot St., Englewood, CO 80110-4396
Phone 303-781-8486 | Fax 303-761-7939
Ismedspec.com

© Copyright 2020 IS MED Specialties

Hydrogen Peroxide Material Compatibility Chart

ver 09-Jul-2020

Material	Compatibility 10% H ₂ O ₂	Compatibility 30% H ₂ O ₂	Compatibility 50% H ₂ O ₂	Compatibility 100% H ₂ O ₂ (HTC)
Chemical resistance data is based on 72° F (22° C) unless otherwise noted				
A- Suitable				
B - Good, minor effect, slight corrosion or discoloration				
F - Fair, moderate effect, not recommended for continuous use;				
softening, loss of strength, and/or swelling may occur				
X - Do Not Use - severe effect, not recommended for ANY use				
NA - Information Not Available				
Nylon (polyamides)	F	X	X	X
PCTFE (Kel-F® and Neoflon®)	A ¹	A ¹	A ¹	X
PFA (perfluoroalkoxy alkanes)	A	A	A	A
Polycarbonate	A ¹	A ¹	A ¹	A
Polypropylene	A	B	B	B
PP-363 (plasticized vinyl) ²	A	A	A	X
PPS (Ryton®)	A	A	F	F
PTFE (Garlock Glyon® 3500) ²	A	A	A	X
PTFE (Teflon®), virgin ²	A	A	A	A
PVC	A	A	A	A
PVDF (Hylar®)	A ¹	A ¹	X	X
PVDF (Kynar®)	A	A	A	A
PVDF (Solef®)	A ¹	A ¹	X	X
Silicone	A	B	B	B
SPR (styrene butadiene rubber)	X	X	X	X
Thiokol™ (polysulfide polymers)	X	X	X	X
Titanium ³	A	B	B	B
TPE (thermoplastic elastomers)	X	X	X	X
TPU (thermoplastic polyurethanes)	X	X	X	X
Tygon®	B	B	B	B
Tungsten carbide	X	X	X	X
Viton® A ²	A	A	A	A

It is the sole responsibility of the system designer and user to select products suitable for their specific application requirements and to ensure proper installation, operation, and maintenance of these products. Material compatibility, product ratings and application details should be considered in the selection. Improper selection or use of products described herein can cause personal injury or product damage. In applications where exposure to harmful chemicals is frequent, of long duration or in high concentrations, additional testing is recommended.



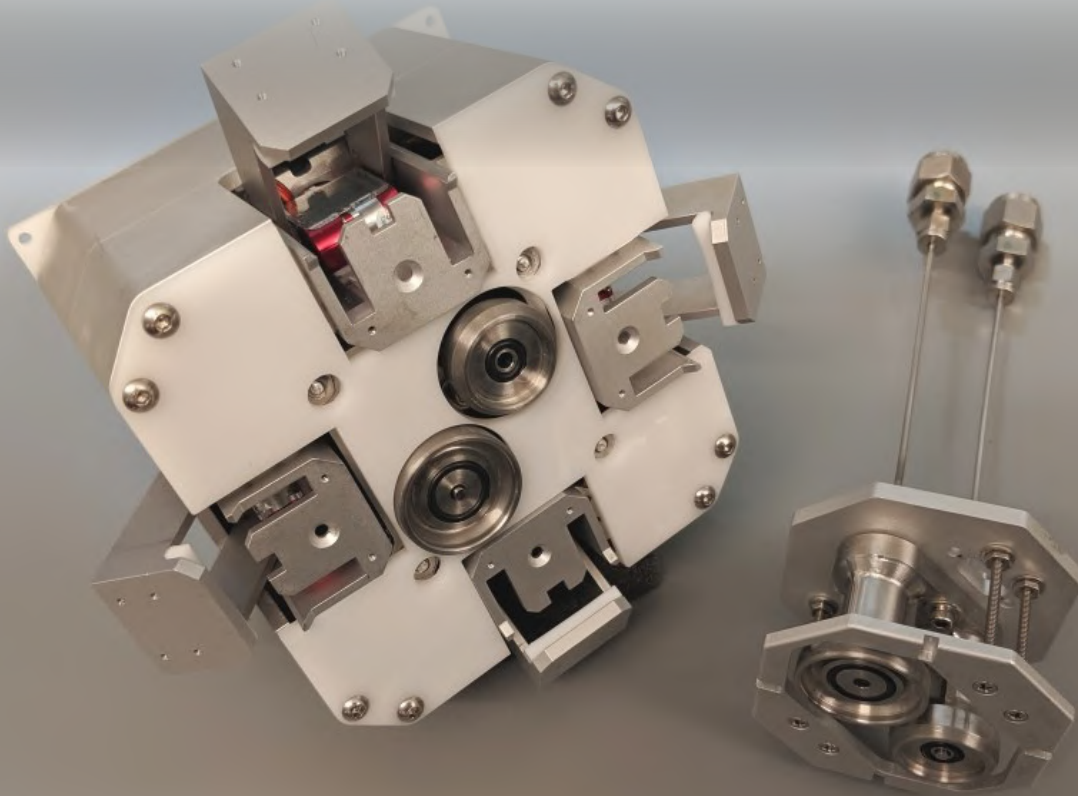
End your search, simplify your supply chain
ISO 9001:2015 Certified Companies

4091 S. Eliot St., Englewood, CO 80110-4396
Phone 303-781-8486 | Fax 303-761-7939
Ismedspec.com

© Copyright 2020 IS MED Specialties

B

Peripheral Systems



Satellite fill-and-drain valves combined with a simplified docking interface, enabling autonomous ground and on-orbit fueling.

Designed for:

- On Orbit Refueling.
- Fill and Drain Operations.
- Docking and On Orbit Servicing.
- Fail Safe and Safe Fail spacecraft docking interface.

Features:

- Peak power draw 10 W.
- Flow rate of 1 L/min @ 15 psi delta-P.
- 500 and 3,000 psi operating pressure.
- Triple redundant external seal leakage during ground fueling.
- Intelligent electrical interface that supports secure inter-satellite handshaking.



RAFTI

Rapidly Attachable Fluid Transfer Interface

Patent Pending

Fill and Drain

The Rapidly Attachable Fluid Transfer Interface (RAFTI) provides cost effective, reliable satellite fill and drain functions during ground operations. The service valve side is low profile, comparable to existing solutions. The rugged latching mechanism and triple seal design ensures a safe propellant transfer. RAFTI is designed for ease of use while exceeding industry range safety requirements. Redundant data logging allows for remote monitoring.

On Orbit Refueling

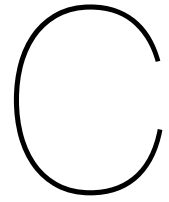
RAFTI is designed to allow reliable propellant transfers in the harshest space environments, making it ideal for mission operations at any orbit. High and low pressure variants are compatible with common modern propellants and pressurants with external leakages less than 1×10^{-6} scc/s. RAFTI is configurable to be normally-open or normally-closed in case of power loss, allowing for fail-safe and safe-fail operations for any mission profile.

Docking

RAFTI supports both primary docking or secondary attachment of two spacecraft. The double action latch mechanism accommodates significant misalignment on all axes during the docking process, allowing for self aligning operations without the need for complex robotic arms. High clamping force accommodates high pressure fluid connections and satellite body movements. Improved reliability by minimizing sliding surfaces and avoiding motors or gears.



Parameter	Low Pressure	High Pressure
Max. Operating Pressure	500 psig	3,000 psig
Proof Pressure	1,000 psig	4,500 psig
Internal Leakage (GHe)	$< 1 \times 10^{-6}$ scc/s	$< 1 \times 10^{-6}$ scc/s
Docking Misalignment	+/- 10mm (X,Y), +/- 10 degrees (X,Y), +/- 20 degrees (Z)	+/- 10mm (X,Y), +/- 10 degrees (X,Y), +/- 20 degrees (Z)
External Leakage	$< 1 \times 10^{-6}$ scc/s	$< 1 \times 10^{-6}$ scc/s
Cycle Life	>1,000 cycles	>1,000 cycles
Operating Temp Range	-40 to 120 °C	-40 to 120 °C
Weight (grams)	150 g (Service Valve) 500 g (Coupling Half)	200 g (Service Valve) 750 g (Coupling Half)
Size	60mm dia x 45mm (Service Valve) 100mm x 100mm x 50mm (Space Coupling Half) (Controller electronics not included)	60mm dia x 45mm (Service Valve) 100mm x 100mm x 50mm (Space Coupling Half) (Controller electronics not included)
Random Vibration	NASA GEVs	NASA GEVs
Pyro-shock	NASA GEVs	NASA GEVs
Media	MMH, UDMH, Water, H ₂ O ₂ , Methanol, Kerosene, Green Monoprops, Isopropyl Alcohol, HFE, N ₂ O ₄	Nitrogen, Helium, Xenon, Krypton



Refuelling Architecture

Table C.1: Mass of sub-components of transfer systems using pressurant gas, gas generator, and pumped, for 200L transferred at 0.1 kg/s

Mass	Pressurant	Gas Generator	Pumped
Propellant Mass	290.000	295.800	290.000
Propellant Tank Mass	7.452	7.551	7.452
Pressurant Mass	2.224	1.112	1.479
Pressurant Tank Mass	19.213	9.606	12.776
Solenoid Mass	(5) 2.000	(4) 1.600	(7) 2.800
Regulator Mass	(1) 0.400	(2) 0.800	(1) 0.400
Line Mass	0.286	0.576	0.858
Pump Mass			0.470
Motor Mass			0.033
Inverter Mass			0.001
Battery Mass			0.187
Solar Array Mass			0.760
Gas Generator Mass		0.100	
Check Valve		0.400	

Table C.2: Mass of sub-components of transfer systems using pressurant gas, gas generator, and pumped, for 200L transferred at 1.0 kg/s

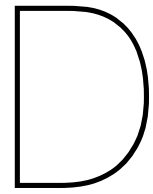
Mass	Pressurant	Gas Generator	Pumped
Propellant Mass	290.000	295.800	290.000
Propellant Tank Mass	7.452	7.551	7.452
Pressurant Mass	2.224	1.112	1.479
Pressurant Tank Mass	19.213	9.606	12.776
Solenoid Mass	(5) 2.000	(4) 1.600	(7) 2.800
Regulator Mass	(1) 0.400	(2) 0.800	(1) 0.400
Line Mass	0.904	5.461	2.713
Pump Mass			0.470
Motor Mass			0.328
Inverter Mass			0.006
Battery Mass			0.717
Solar Array Mass			7.603
Gas Generator Mass		0.100	
Check Valve		0.400	

Table C.3: Mass of sub-components of transfer systems using pressurant gas, gas generator, and pumped, for 1000L transferred at 0.1 kg/s

Mass	Pressurant	Gas Generator	Pumped
Propellant Mass	1450.000	1479.000	1450.000
Propellant Tank Mass	21.791	22.080	21.791
Pressurant Mass	11.120	5.560	7.395
Pressurant Tank Mass	96.063	48.032	63.881
Solenoid Mass	(5) 5.000	(4) 4.000	(7) 7.000
Regulator Mass	(1) 1.000	(2) 2.000	(1) 1.000
Line Mass	0.489	2.953	1.467
Pump Mass			0.470
Motor Mass			0.033
Inverter Mass			0.001
Battery Mass			.937
Solar Array Mass			0.760
Gas Generator Mass		0.100	
Check Valve		1.000	

Table C.4: Mass of sub-components of transfer systems using pressurant gas, gas generator, and pumped, for 1000L transferred at 1.0 kg/s

Mass	Pressurant	Gas Generator	Pumped
Propellant Mass	1450.000	1479.000	1450.000
Propellant Tank Mass	21.791	22.080	21.791
Pressurant Mass	11.120	5.560	7.395
Pressurant Tank Mass	96.063	48.032	63.881
Solenoid Mass	(5) 5.000	(4) 4.000	(7) 7.000
Regulator Mass	(1) 1.000	(2) 2.000	(1) 1.000
Line Mass	1.546	9.338	4.638
Pump Mass			0.470
Motor Mass			0.328
Inverter Mass			0.006
Battery Mass			.937
Solar Array Mass			7.603
Gas Generator Mass		0.100	
Check Valve		1.000	



Engineering Drawings

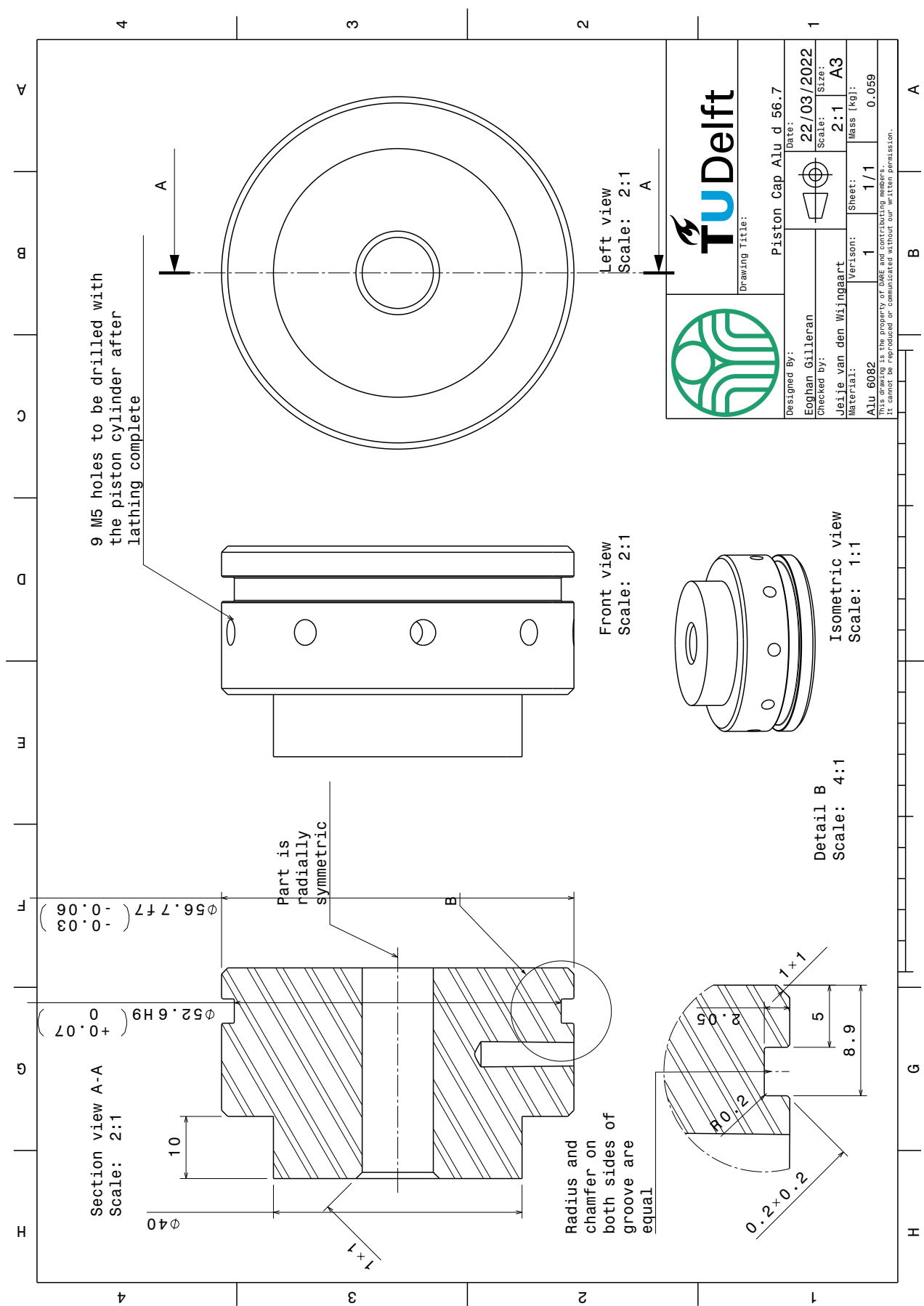


Figure D.1: Piston endcap technical drawing

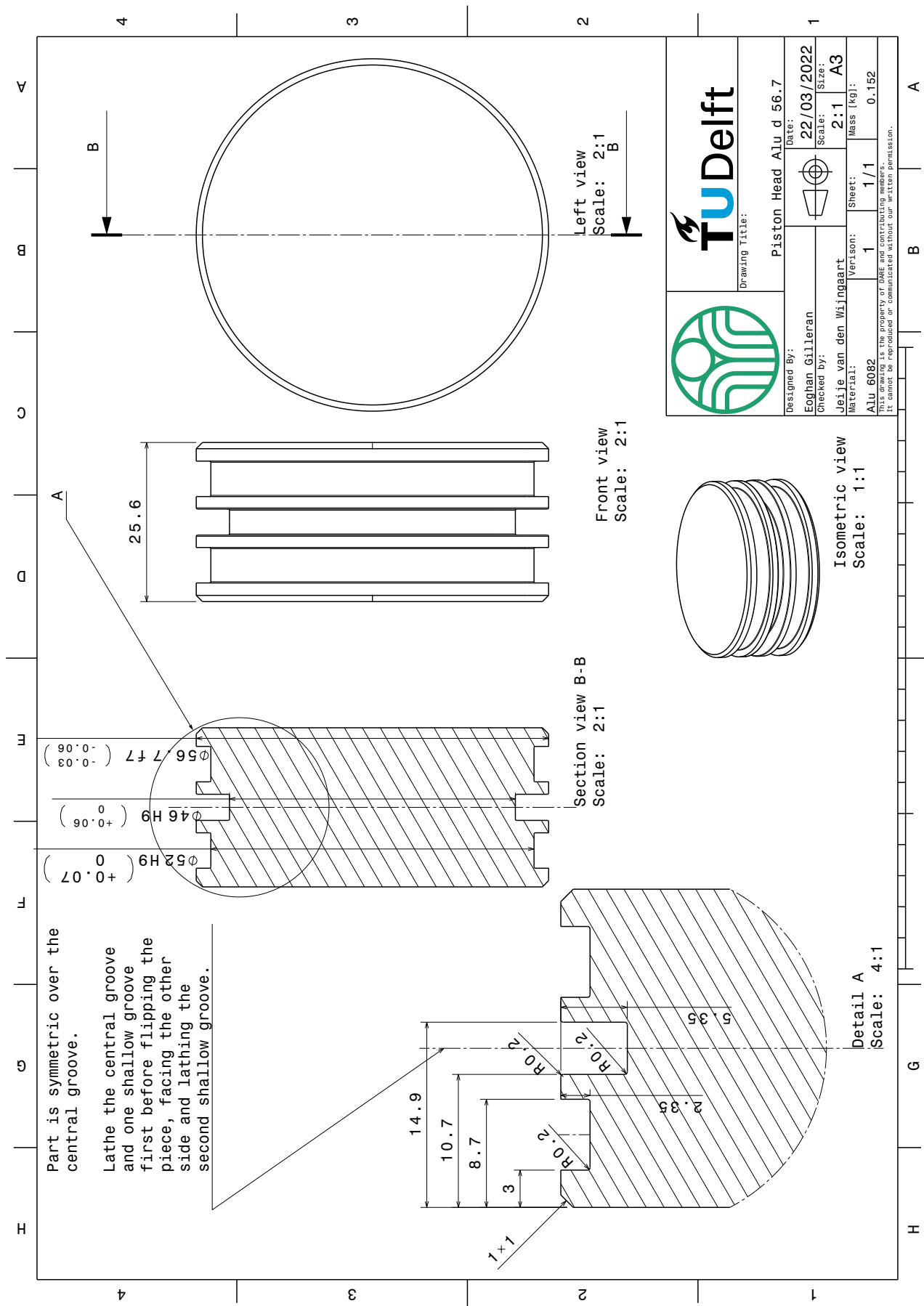


Figure D.2: Piston head technical drawing

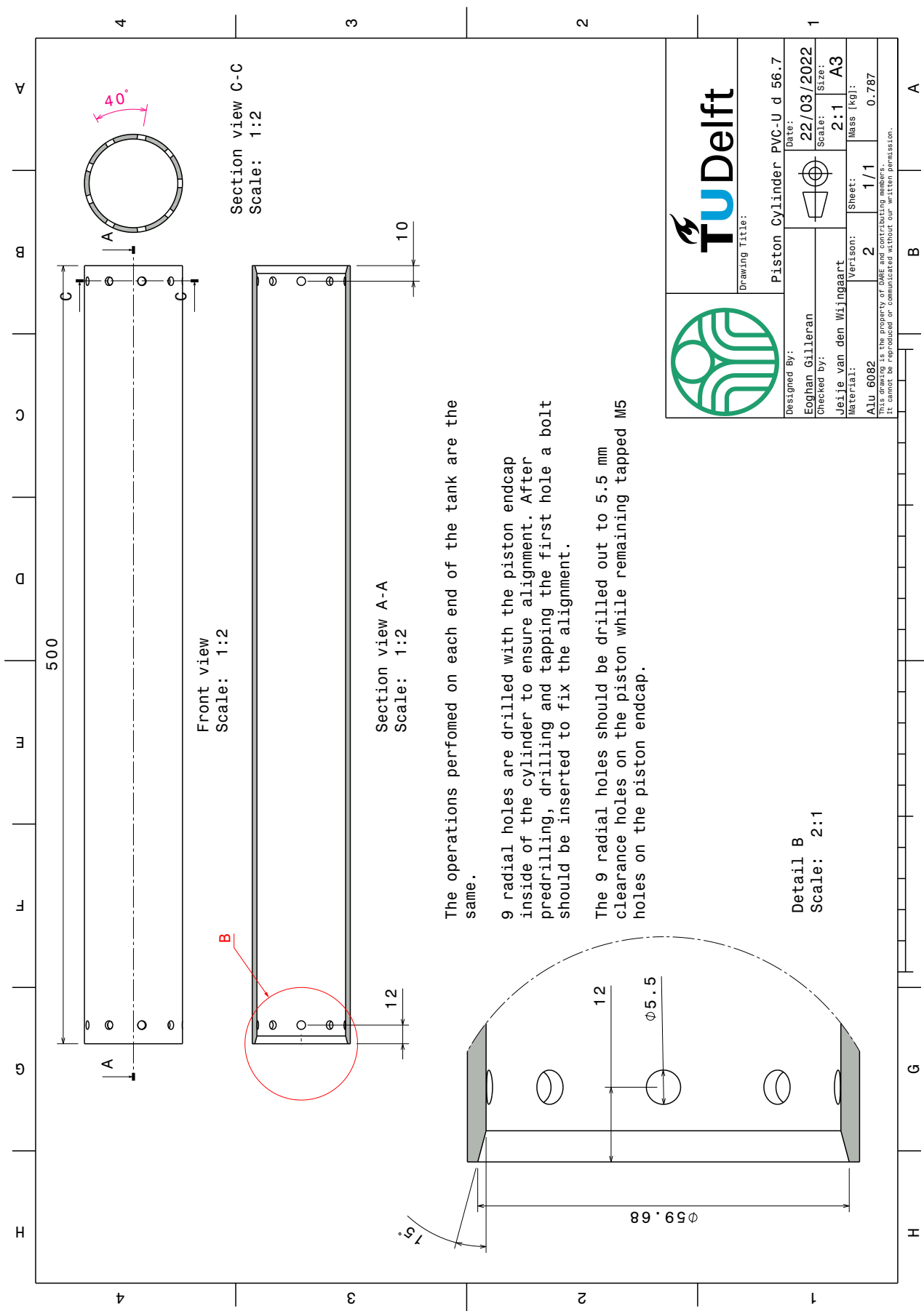


Figure D.3: Piston cylinder technical drawing

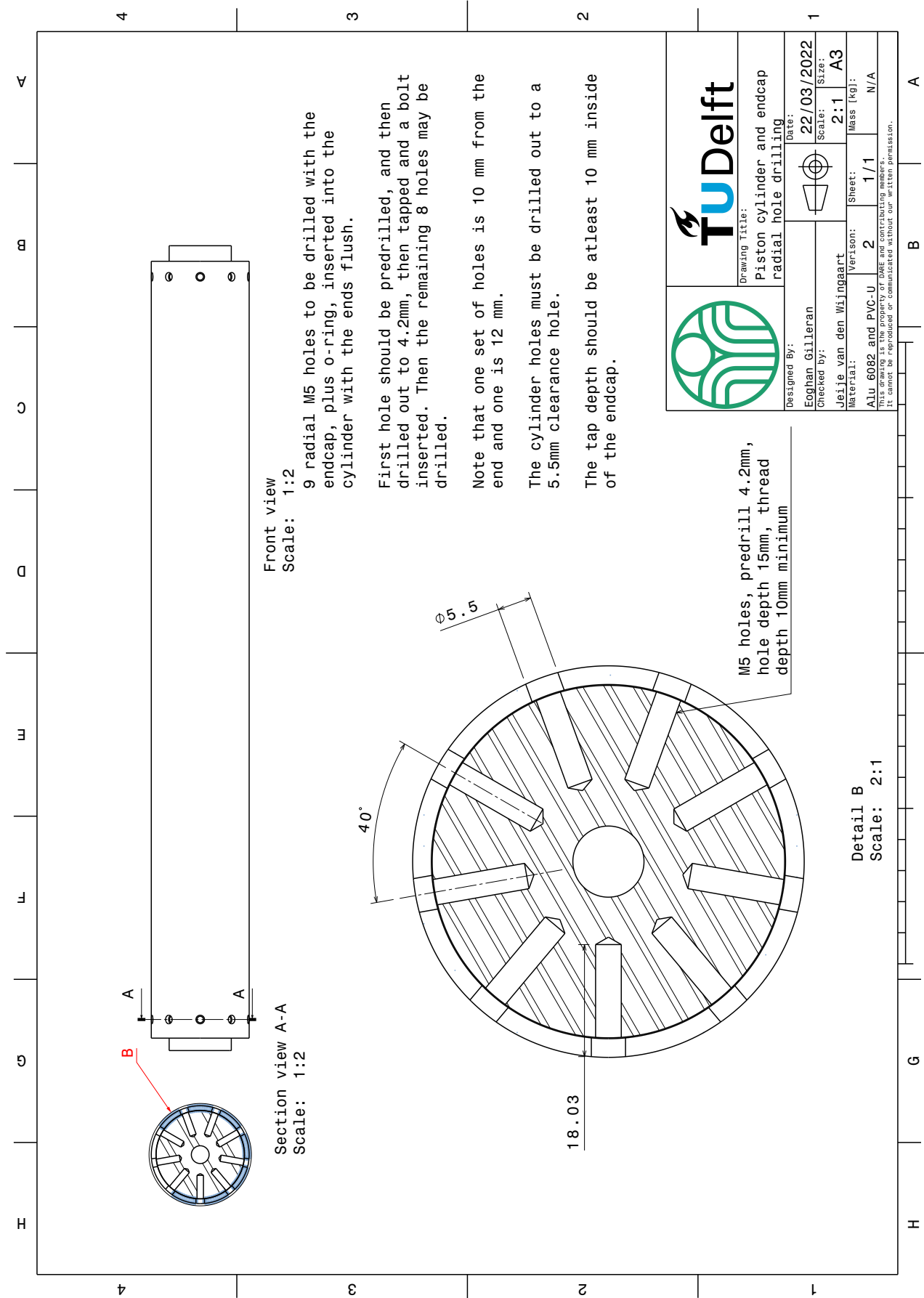
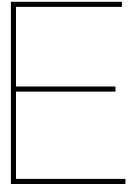


Figure D.4: Piston production process technical drawing



Transfer Test Test Logs

	High Pressure Tank [bar]	Regulated Pressure [bar]	Test Outcome	Comments
Without piston head	5	1.5	Partial (Stopped)	Started a little above 1.5 bar with the pressure still slowly climbing. The flow rate started fast and slowed drastically towards the end, stopping between 900ml and 1L with a slow drip. Test stopped.
	5	1.5	Success	HP had more like 5.5 bar to start, P1 was climbing when the expulsion started, successful start, flow continued stronger until the end. Stopped test when air bubbled exits tube into beaker.
	5	2	Partial (Stopped)	Started flow with reg pressure rising. HP was well below 5 when system was pressurised. Initial flow much faster, stopped test when dripping slowed, between 900 and 1000 mL.
	5	2	Success	Similar behaviour to second 1.5 bar test. Closed liquid valve when bubbled reaches beaker.
	5	2.5	Partial (Stopped)	Pressure line failed before test, refilled tank. Very fast flow initially, dropped off at end, stopped test with drip/no flow between 900 and 1L.
	5	2.5	Success	Took a while waiting for the regulated pressure to hit 2.5. Fast flow at start, slower at end, full expulsion.
	10	1.5	Success	Reg pressure was levelling around 1.3, turned some more, ended up climbing fast past 1.5, started just after 1.5. Expulsion fast, slowed down, then sped up, less distinct end of expulsion, closed valve when gas heard exiting, ended up with slightly less than 1L in beaker
	10	1.5	Success	Same as previous test, same regulator behaviour, reg pressure was rising when test started, pressure dipped then rose again. 4.3 bar after test in HP tank.
	10	2	Success	Reg pressure was climbing a lot when passing 2.0, otherwise good test
	10	2	Success	Took a while to set regulator, likely better data than previous test, otherwise all good
	10	2.5	Success	Had to replace both connectors on the gas valve as they kept popping during multiple attempts on this run. The run itself was ok, reg rising medium speed as expulsion started, end hard to distinguish
	10	2.5	Success	Success, reg rising still a bit when run started
	20	1.5	Success	Success, reg climbing a little too fast when the test started
	20	1.5	Success	All good
	20	2	Success	All good
	20	2	Success	Had a little less than 1L left at end, also end value of HP seemed low
	20	2.5	Success	Reg pressure was rising still a fair bit as the test started, looked like it might stabilise around 2.6
	20	2.5	Success	Success, pressure seemed low at the end
	40	1.5	Success	All good, started run with reg of 1.49, climbed high during run, quite energetic at end
	40	1.5	Success	Good, started run at 1.516, higher than this at end again
	40	2	Success	All good, suspected there was a leak from the tank assembly during this and the last test as the pressure dropped a little after filling and I thought I could hear a hiss. Used leak detections pray on the hp tank and couldn't find anything
	40	2	Success	Reg climbing when test started, not too bad, high pressure at end
	40	2.5	Success	For end of expulsion I closed the liquid valve and then unscrewed the regulator knob immediately to stop the pressure, then vented, so I didn't close the hand valve
40	2.5	Success	Fast flow at end, climbing a little when started, not super great. Closed liquid valve and then closed regulator then vented. Interesting to see the pressure that the tank stabilises slowly.	

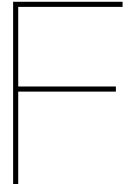
Table E.1: Test log of tests without piston head

	High Pressure Tank [bar]	Regulated Pressure [bar]	Test Outcome	Comments
With piston head	5	1.5	Partial (Stopped)	Air bubbles moving through line occasionally during expulsion, ran very slow, flow rate very dependent on height of outlet. Stopped when flow dripping slowly between 750 and 1000. Pumped tank up again, flow went from liquid to gas to liquid. Suspect that piston was not moving for some of expulsion, also maybe reason for weird behaviour at the end.
	5	1.5	Partial (Stopped)	Same as last test, same liquid, gas liquid at the end
	5	2	Partial (Stopped)	Overshot 1.5 bar went for 2 bar, could see when pumping tank and looking at LP1 that the residual pressure from pumping the liquid in caused the gas at the top to leak around the seal and slowly increase the pressure at LP1 and RegP. When test run at 2 bar the flow was slow and stopped at drip between 900 mL and 1L. Refilled tank to allow emptying of cylinder, increased regulator setting with liquid valve still open. Went from liquid flow to gas flow then back to liquid flow. Unsure if the piston was moving or if the pressure was just leaking around it
	5	2	Partial (Stopped)	Same as before, weird behaviour
	5	2.5	Partial (Stopped)	Similar to before. Slowed to drip between 750 and 1000, stopped, added more pressure twice with bike pump to empty tank
	5	2.5	Partial (Stopped)	Same as before, weird behaviour
	10	2	Success	without piston head. Closed liquid valve then hand valve, then vented pressure and opened hand valve.
	10	2	Success	Same success as before
	10	2.5	Success	Fine
	10	2.5	Success	Fine, had to rebuild pump before it would work, lines popped from hand bypass valve multiple times too. Run itself fine.
	10	1.5	Success	Very slow run but completed in the end
	10	1.5	Success	closed
	20	1.5	Success	Success, low flow at the start, then slowly sped up, little less than a litre out
	20	1.5	Success	Success, similar to before, need to investigate the HP recovery thing
	20	2	Success	Success, all good. After test pressure builds a little again in P1 even with regulator closed, unsure why, maybe trapped pressure with piston
	20	2	Success	Pressure rising when test started a fair built, might be the cause of the fast flow at the end and low HP pressure at the end
	20	2.5	Success	Failed run before this where the regulator stopped at 2.4 bar. Vented pressure and added more Hp, reran and ran fine. At the end there is a burst of gas and then it slows, I think the burst is from the gas that is below the piston before the run starts.
	20	2.5	Success	All good. Vented through the liquid valve at the end and there was still more liquid, little strange, held 2.something pressure above the piston head though
	40	1.5	Success	HP. Run fine, left liquid valve open to see drop in gas flow at end, also vented through liquid valve then vent valve
	40	1.5	Success	Success, same as before, vented through liquid valve
	40	2	Success	All good, fast flow, high pressure at end, some venting though manual bypass valve
	40	2	Success	All good
	40	2.5	Success	Good run. Very fast flow, almost hit 3 bar reg P at end of run, when gas came through I closed regulator knob and let pressure keep venting through liquid valve. Then finally vented. Liquid valve not useful for timing on this one
	40	2.5	Success	Pressure climbing a little when runs tarted, same as last, above 3 bar at end, closed reg P know instead of closing liquid valve. Then vented through hand valve and vent valve. Spilled some before test so topped back to 1 L

Table E.2: Test log of tests with piston head

	High Pressure Tank [bar]	Regulated Pressure [bar]	Test Outcome	Comments
Inverted	20	2.5	Success	Went fine, system disconnected when moving so pressure settings were lost, conducted at non systematic settings
	20	2.5	Success	Worked well, worked at set pressure, no gas flow at end, seemed like piston just hit end properly, let open for a second or two to vent gas, vented with manual bypass valve
With H2O2	10	2	Success	Beaker placed below run set up, run went fine, reg pressure climbing when test started. Maybe decomposition in cylinder
	10	2	Success	Beaker placed level with set up. Pressure stable when test started

Table E.3: Test log of inverted tests and tests using H₂O₂



Transfer Test Plotted Results

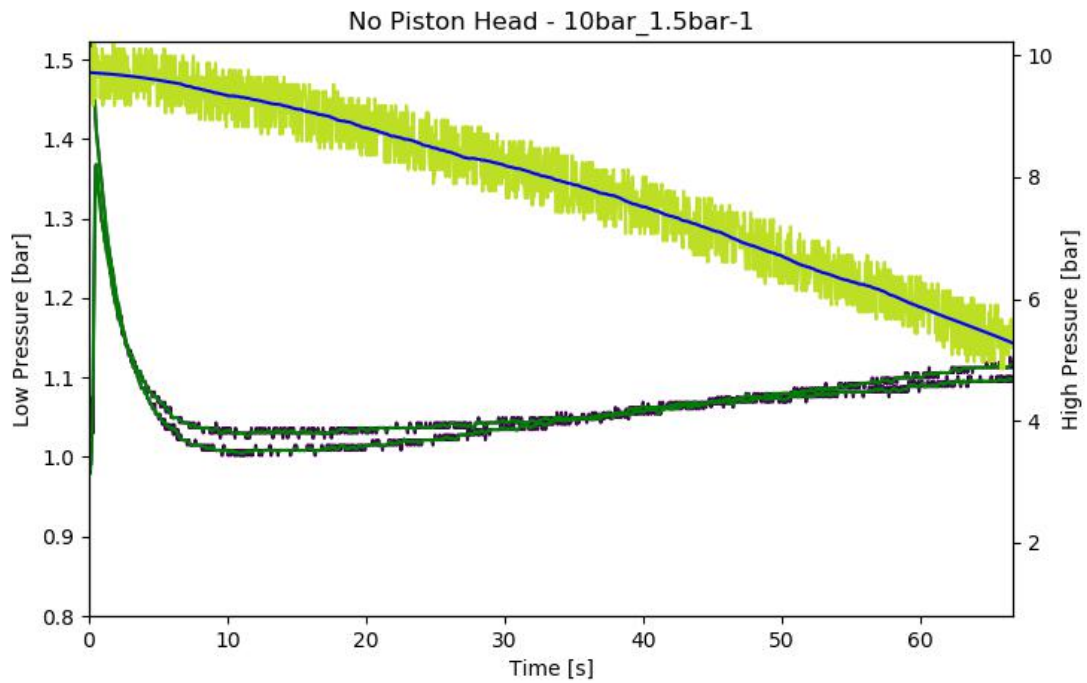


Figure F.1: Pressure data from test - No Piston Head - 10bar_1.5bar-1

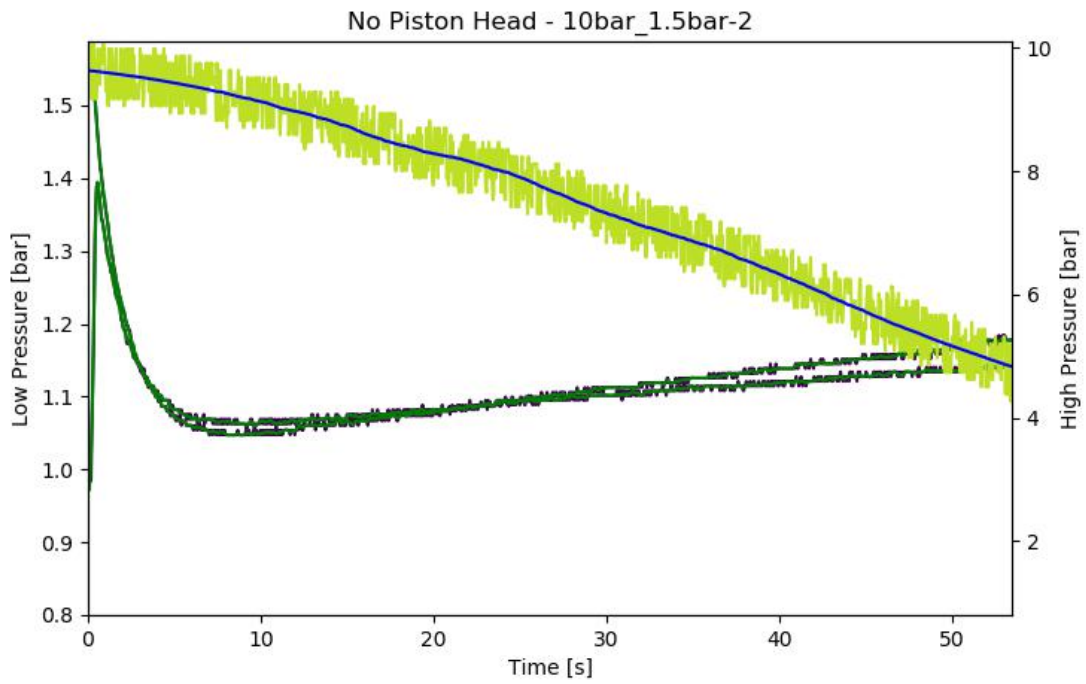


Figure F.2: Pressure data from test - No Piston Head - 10bar_1.5bar-2

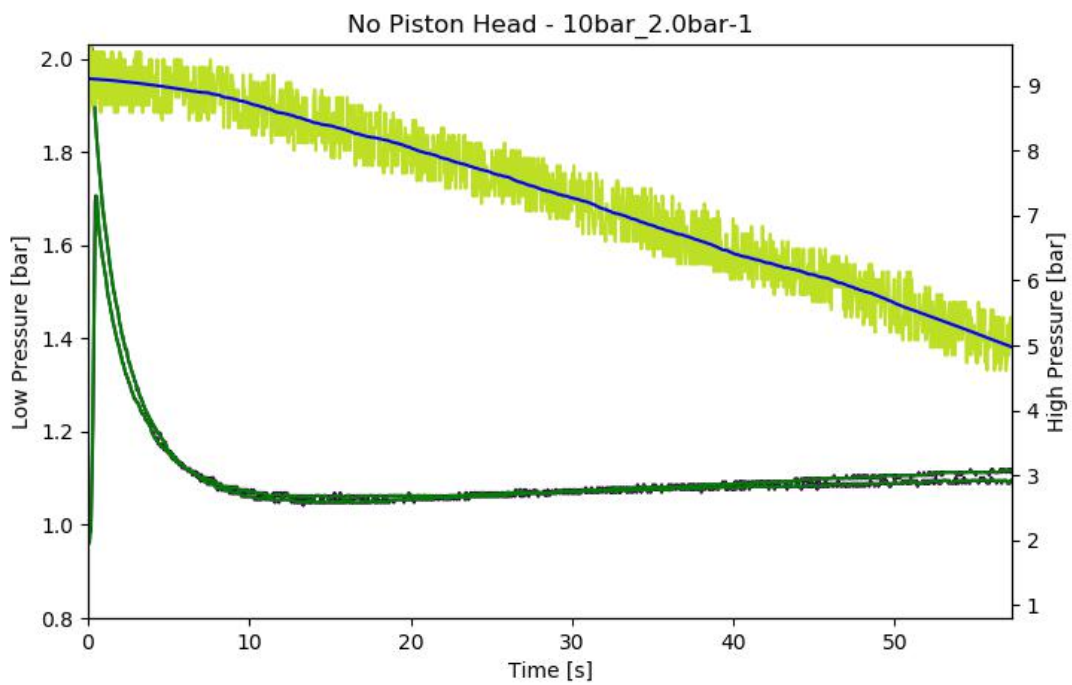


Figure F.3: Pressure data from test - No Piston Head - 10bar_2.0bar-1

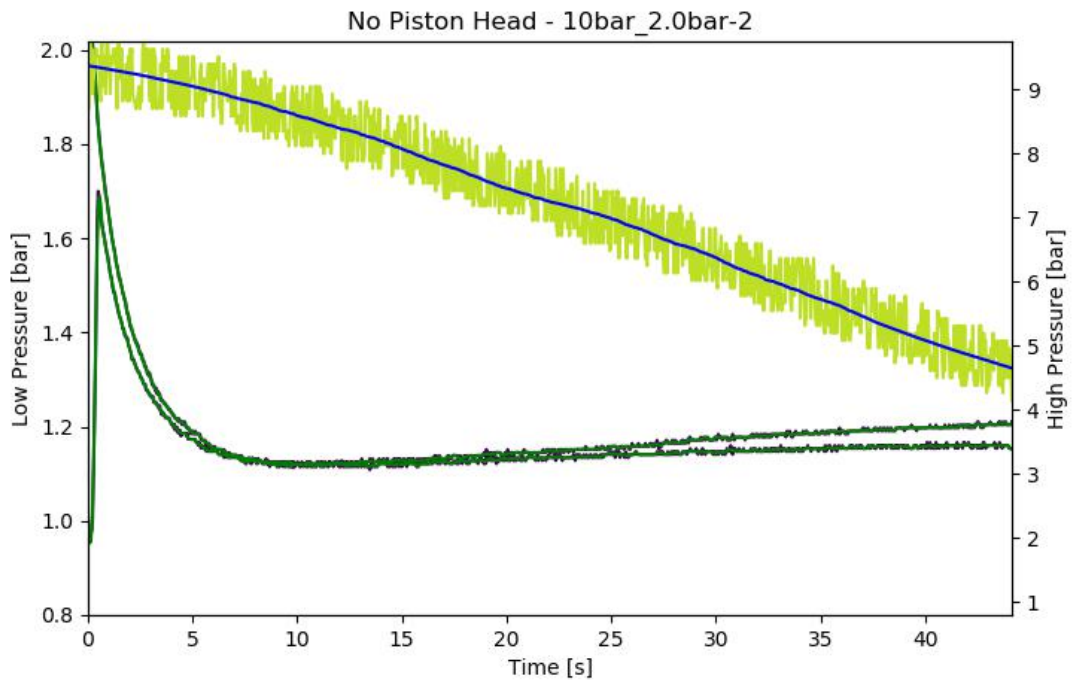


Figure F.4: Pressure data from test - No Piston Head - 10bar_2.0bar-2

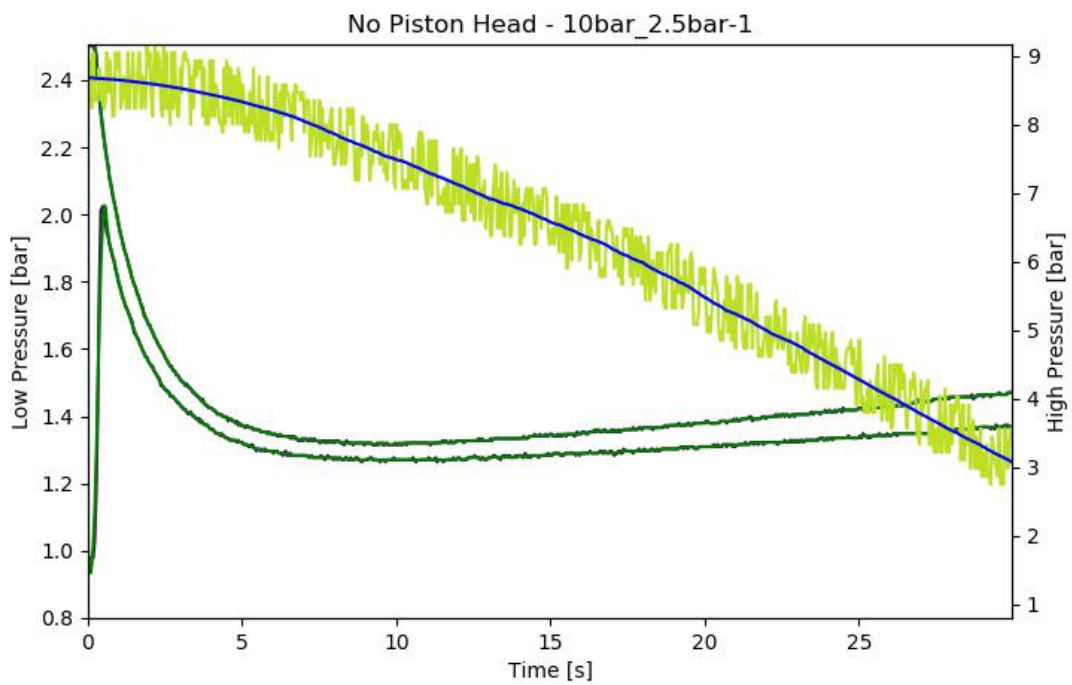


Figure F.5: Pressure data from test - No Piston Head - 10bar_2.5bar-1

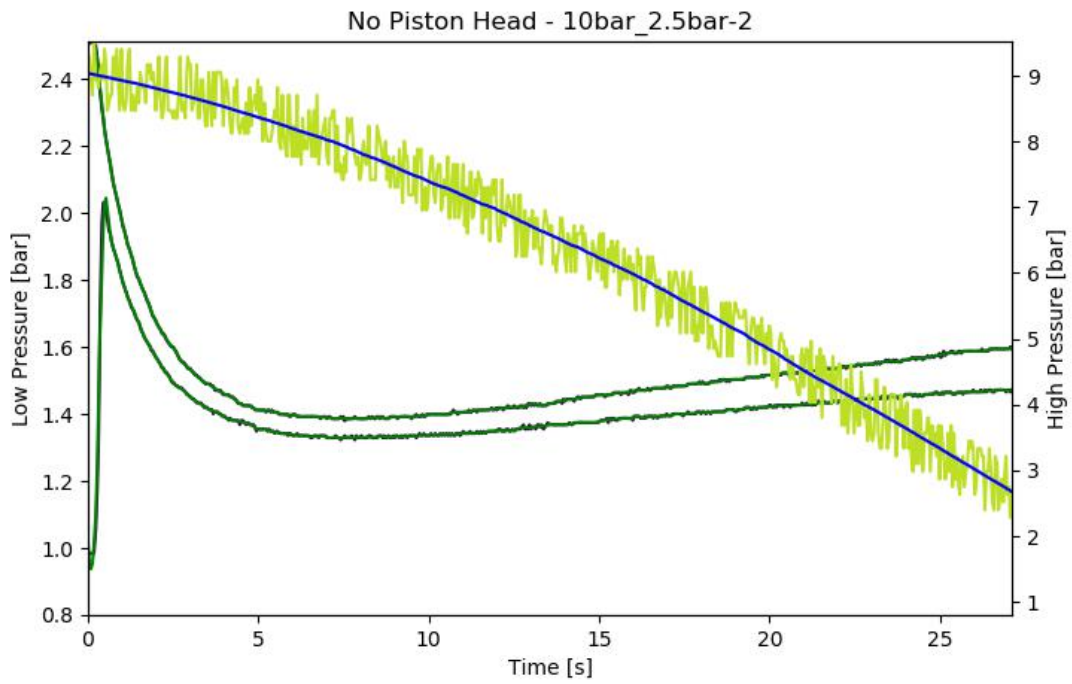


Figure F.6: Pressure data from test - No Piston Head - 10bar_2.5bar-2

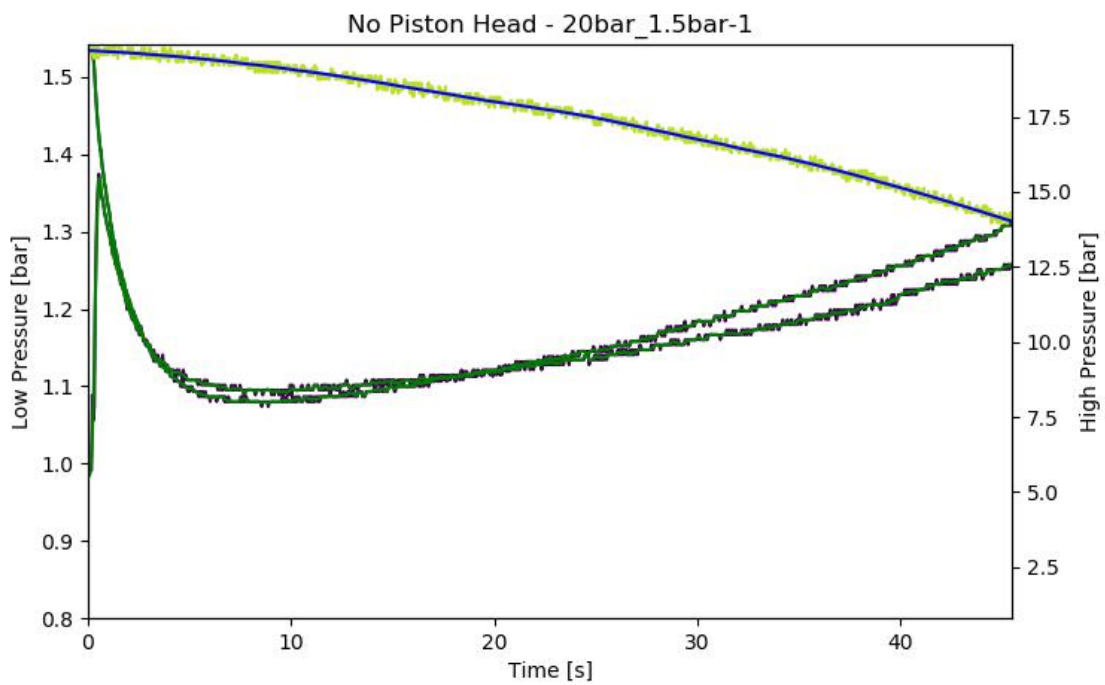


Figure F.7: Pressure data from test - No Piston Head - 20bar_1.5bar-1

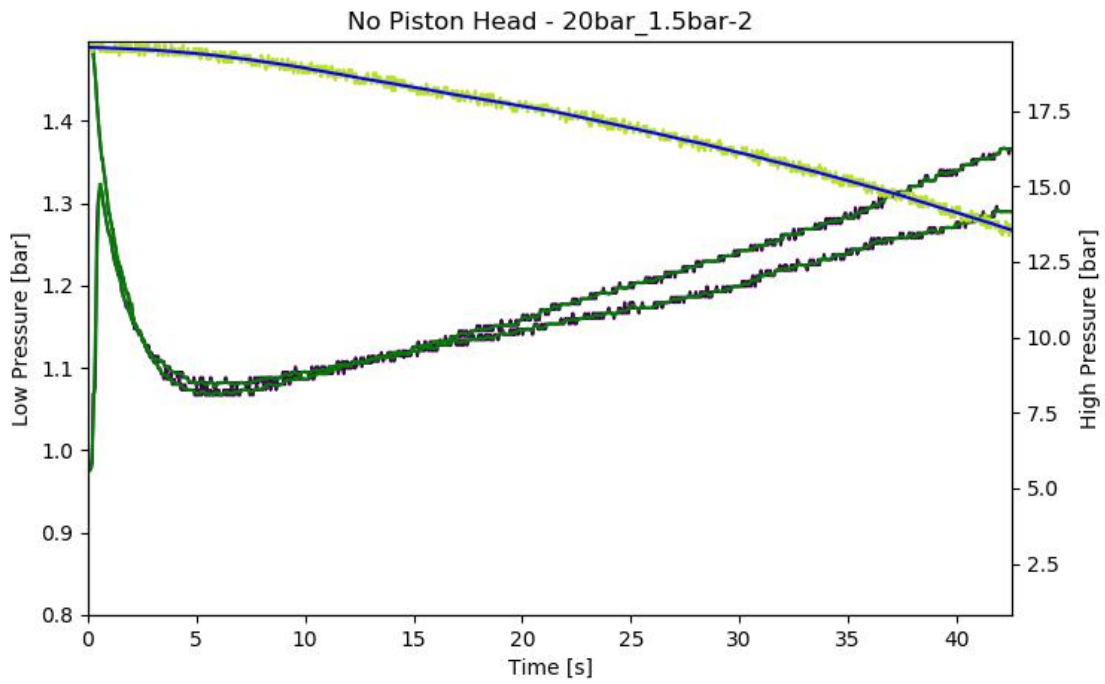


Figure F.8: Pressure data from test - No Piston Head - 20bar_1.5bar-2

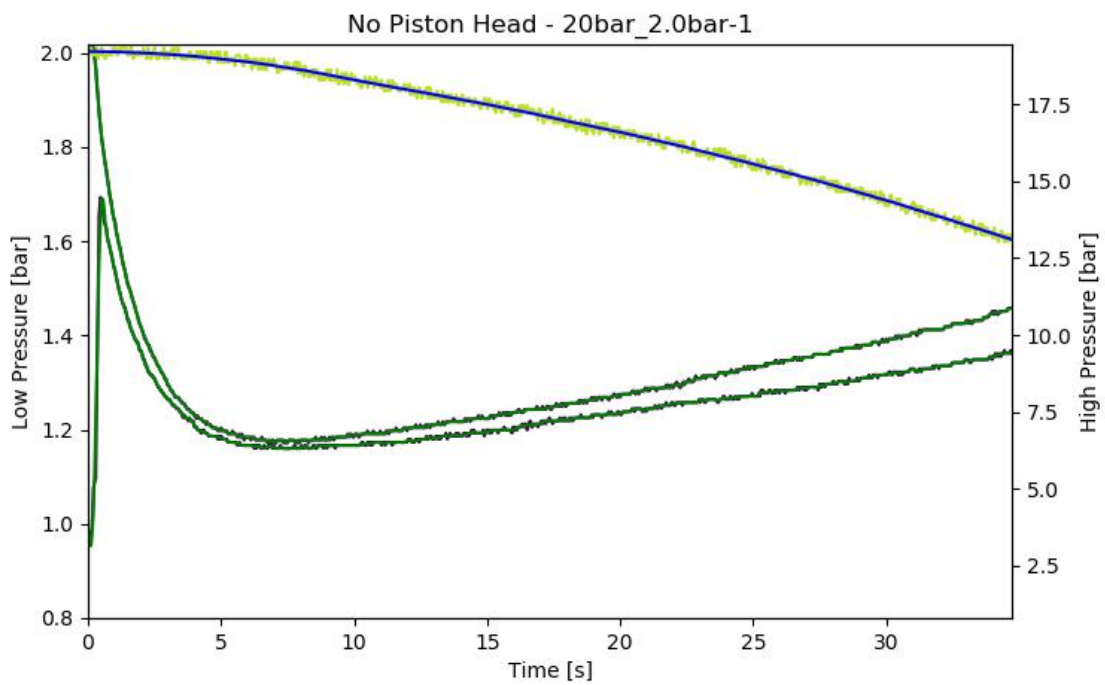


Figure F.9: Pressure data from test - No Piston Head - 20bar_2.0bar-1

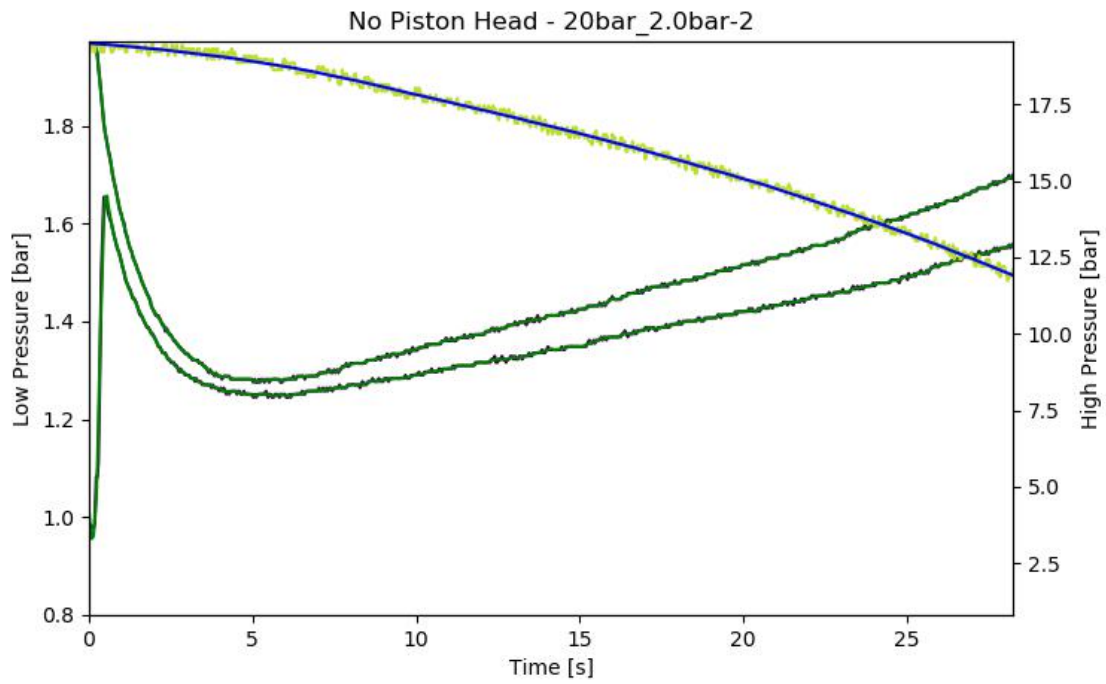


Figure F.10: Pressure data from test - No Piston Head - 20bar_2.0bar-2

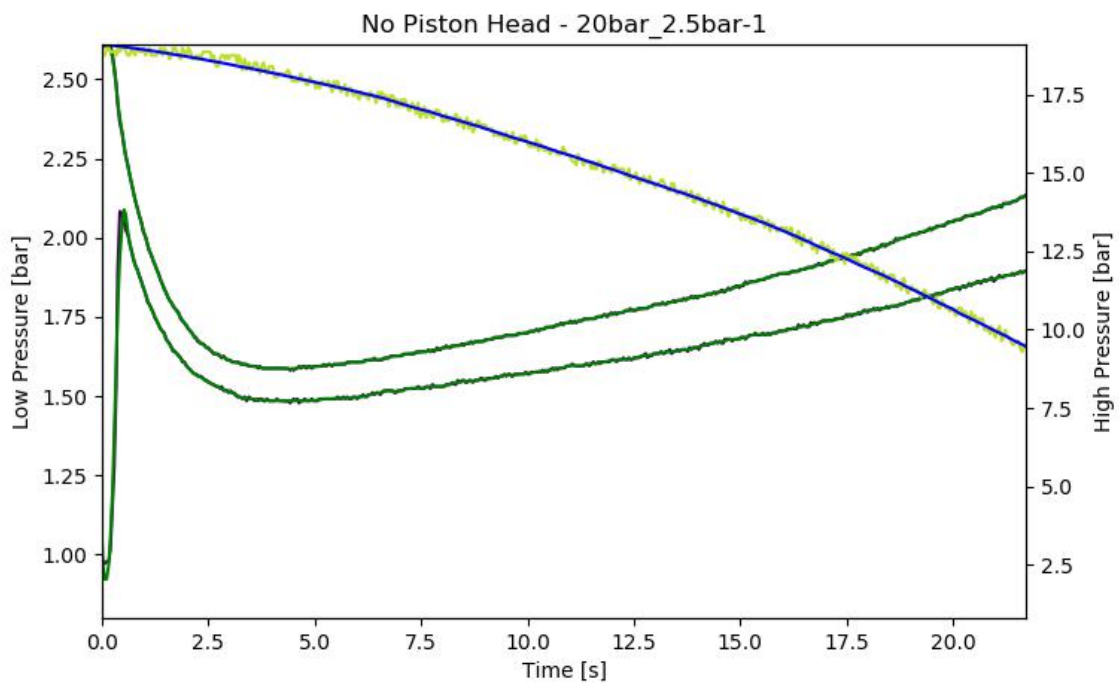


Figure F.11: Pressure data from test - No Piston Head - 20bar_2.5bar-1

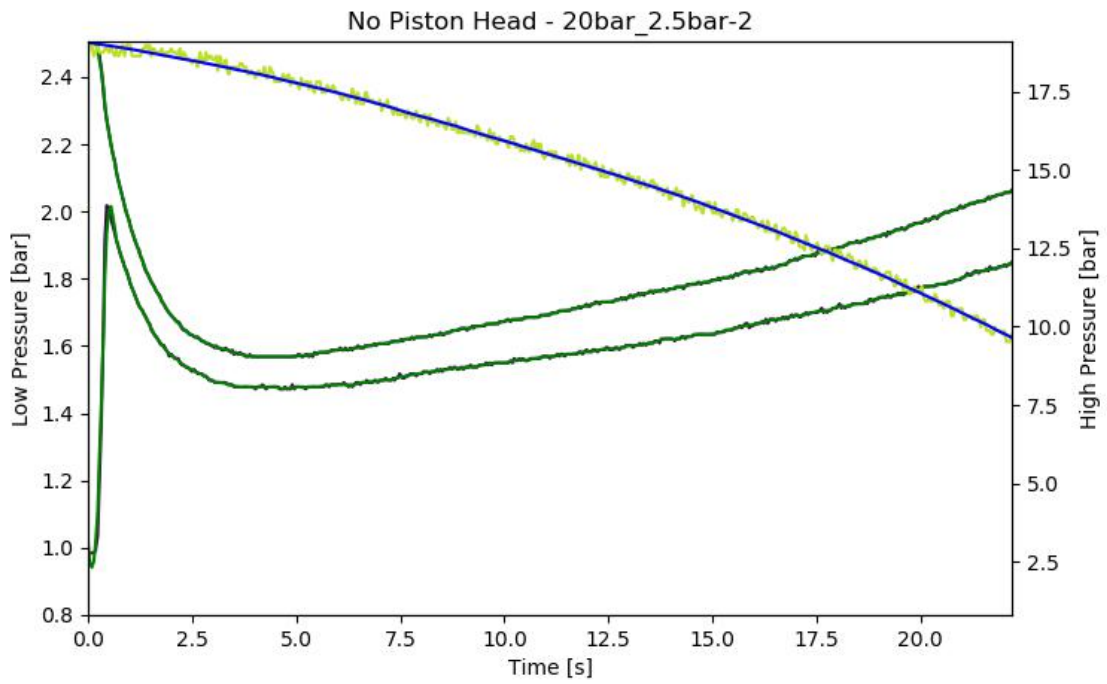


Figure F.12: Pressure data from test - No Piston Head - 20bar_2.5bar-2

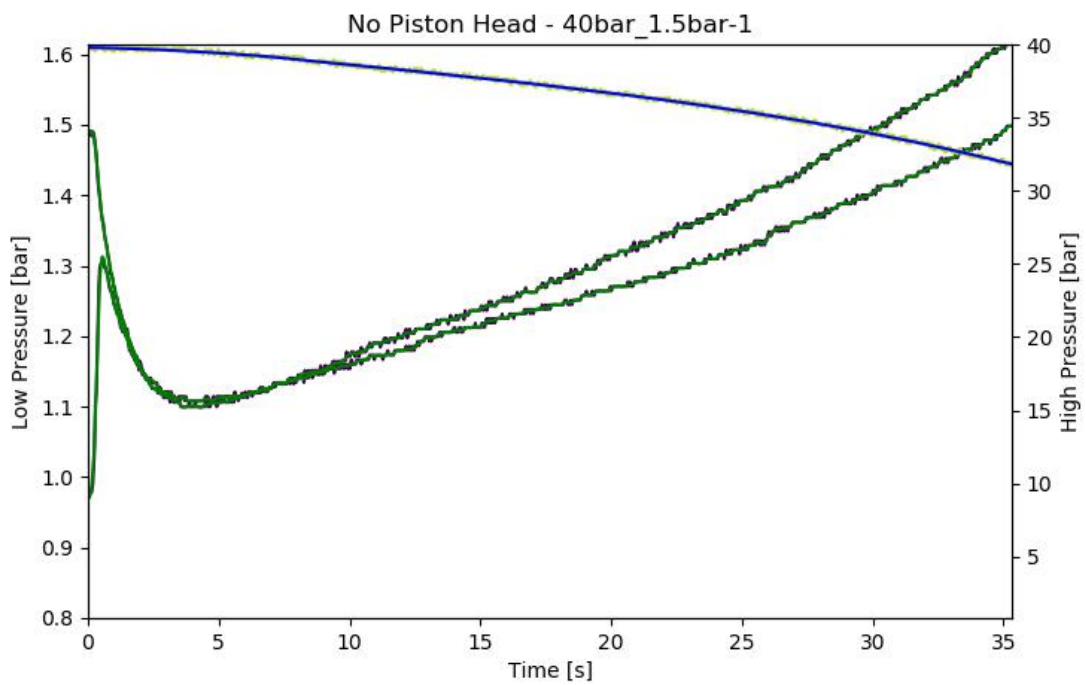


Figure F.13: Pressure data from test - No Piston Head - 40bar_1.5bar-1

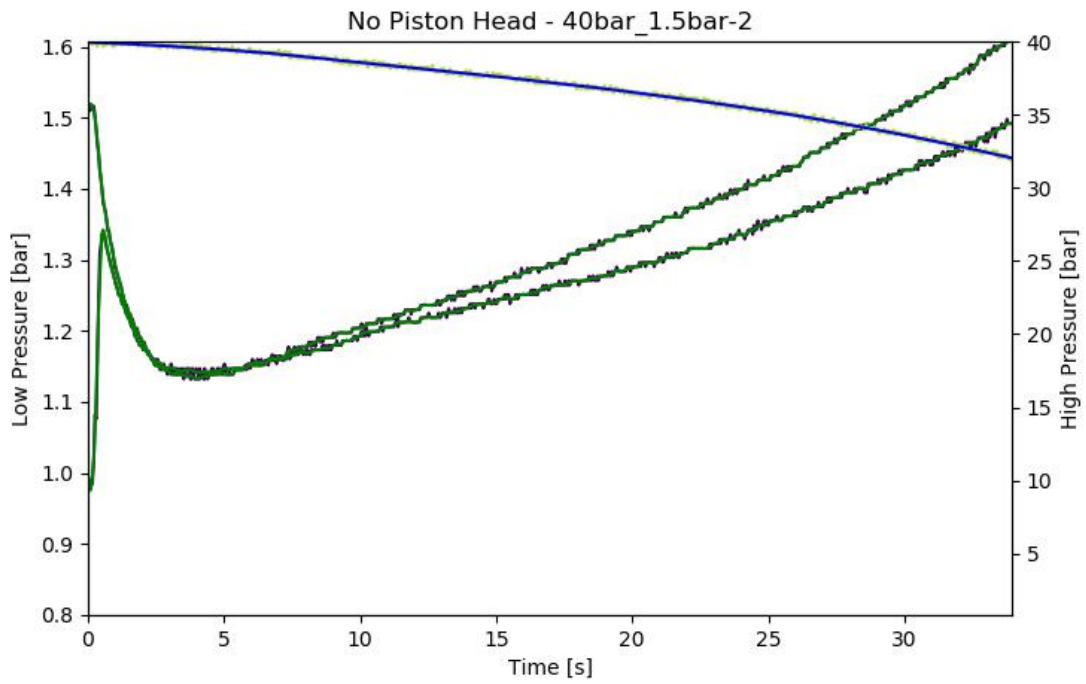


Figure F.14: Pressure data from test - No Piston Head - 40bar_1.5bar-2

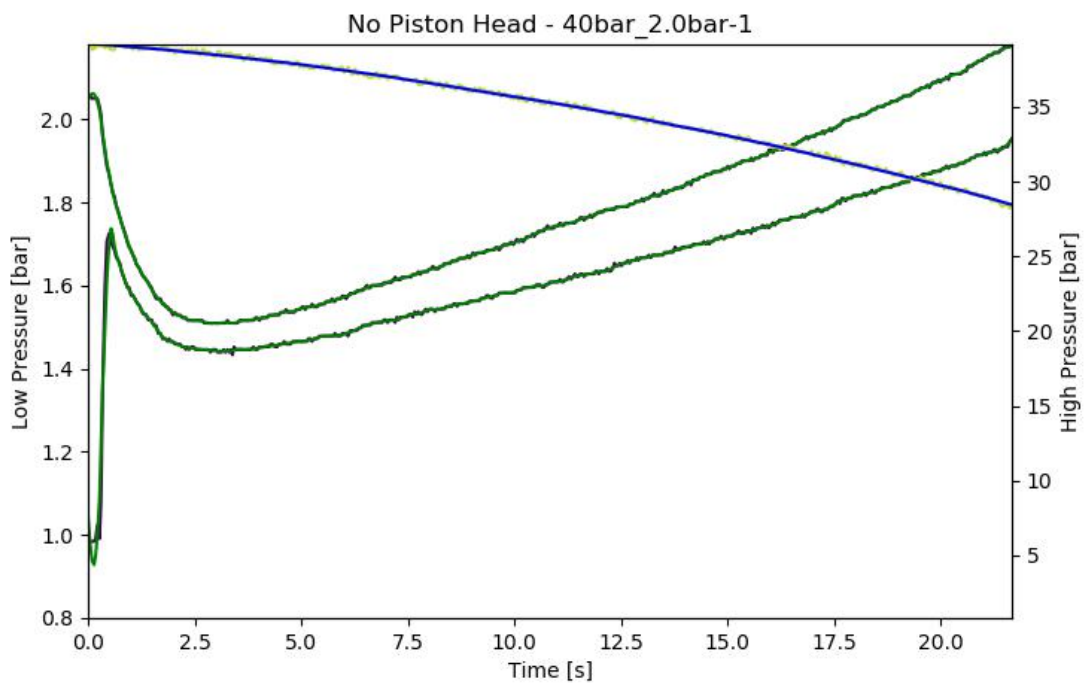


Figure F.15: Pressure data from test - No Piston Head - 40bar_2.0bar-1

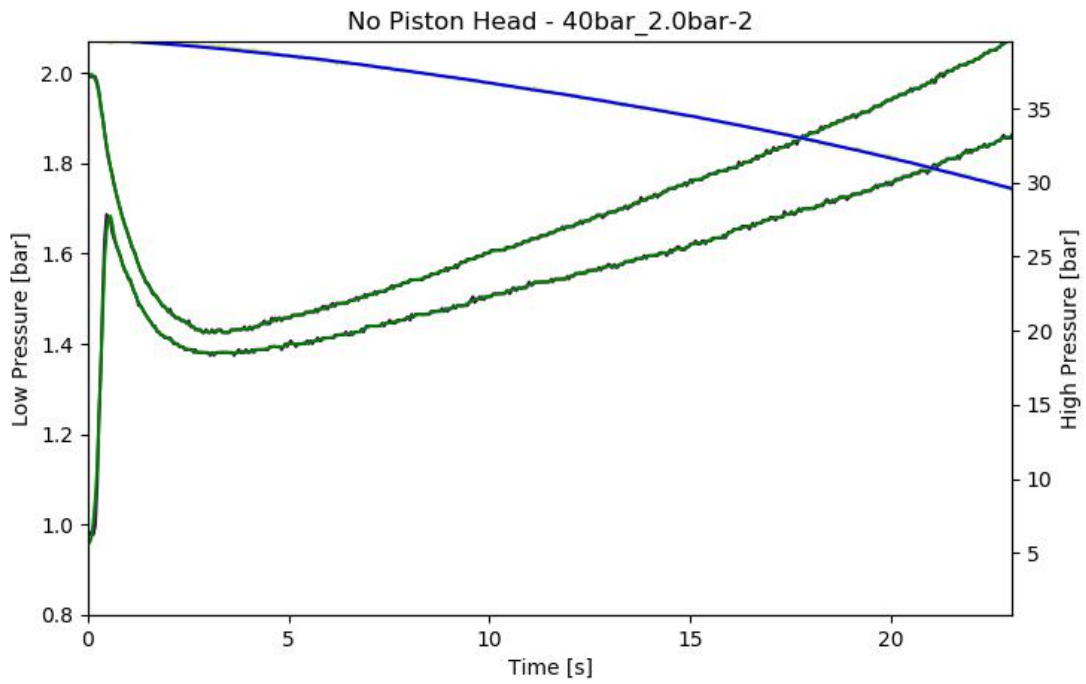


Figure F.16: Pressure data from test - No Piston Head - 40bar_2.0bar-2

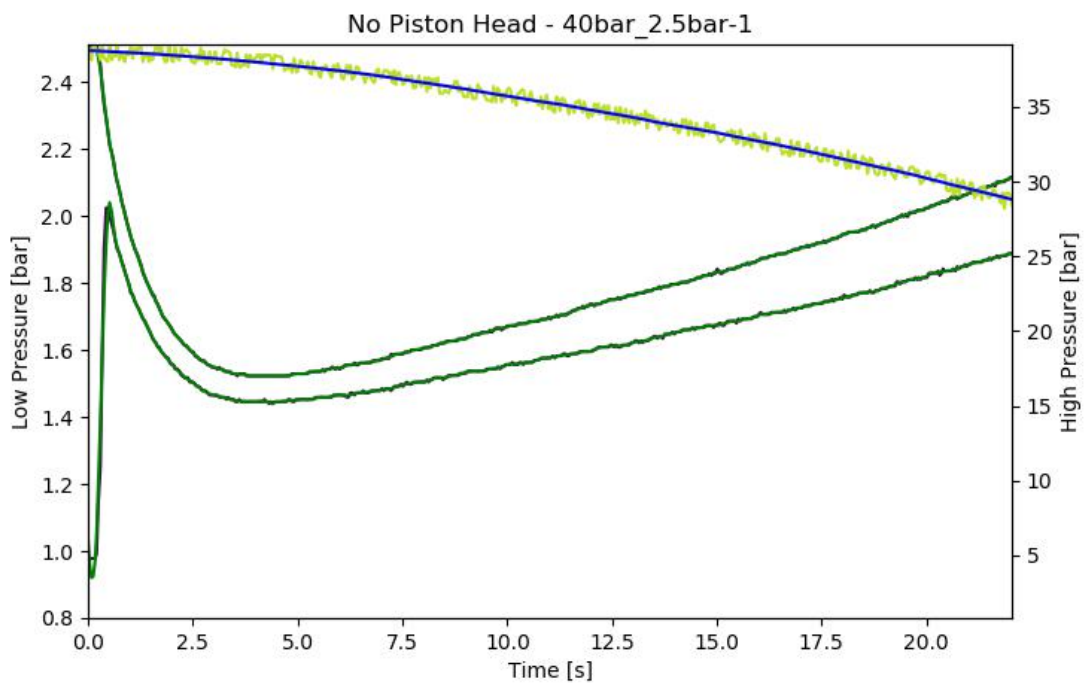


Figure F.17: Pressure data from test - No Piston Head - 40bar_2.5bar-1

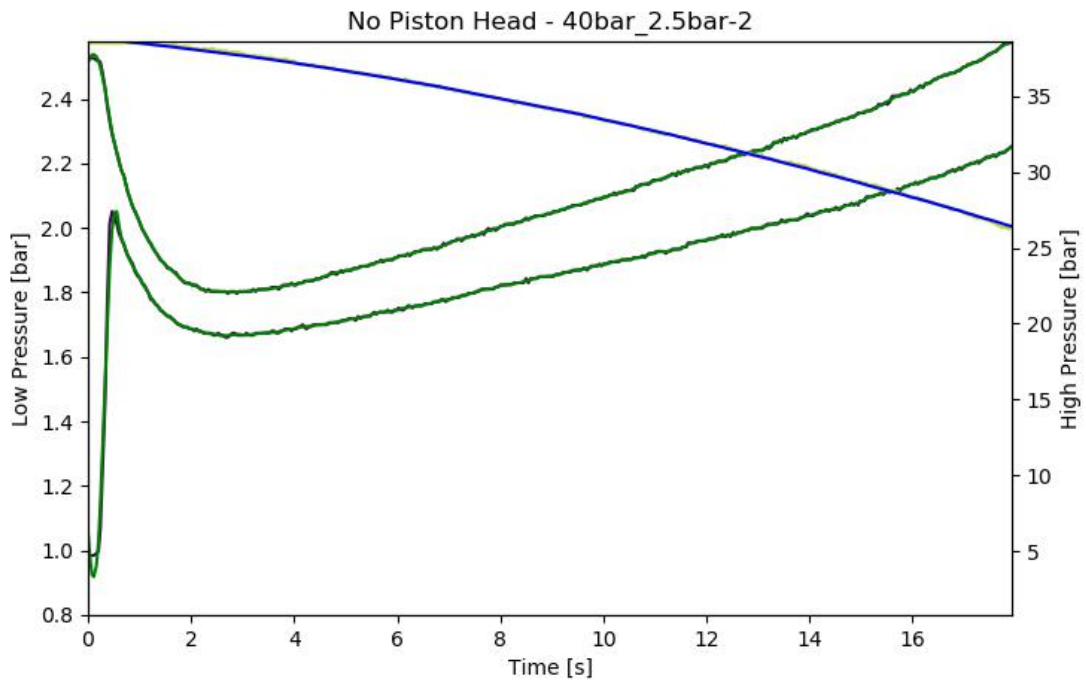


Figure F.18: Pressure data from test - No Piston Head - 40bar_2.5bar-2

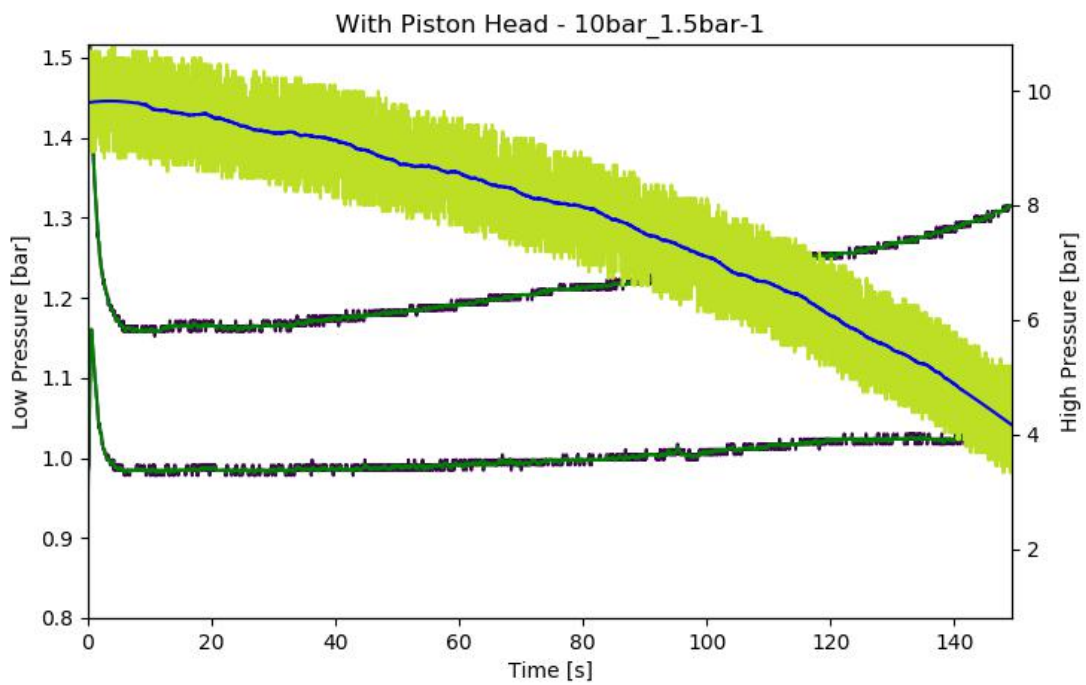


Figure F.19: Pressure data from test - With Piston Head - 10bar_1.5bar-1

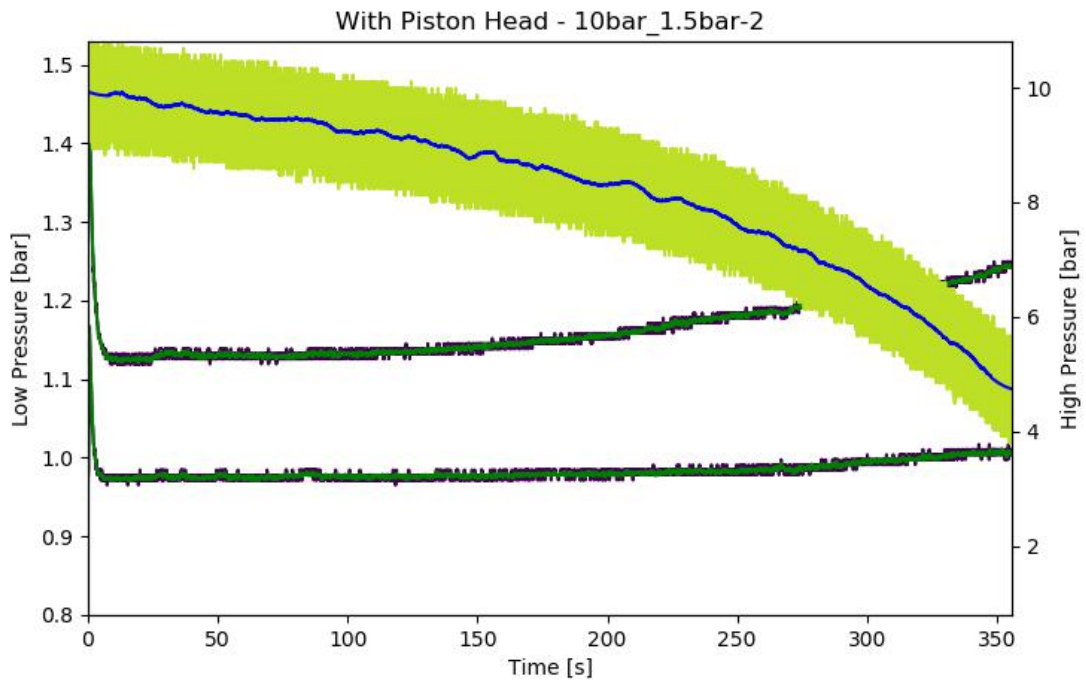


Figure F.20: Pressure data from test - With Piston Head - 10bar_1.5bar-2

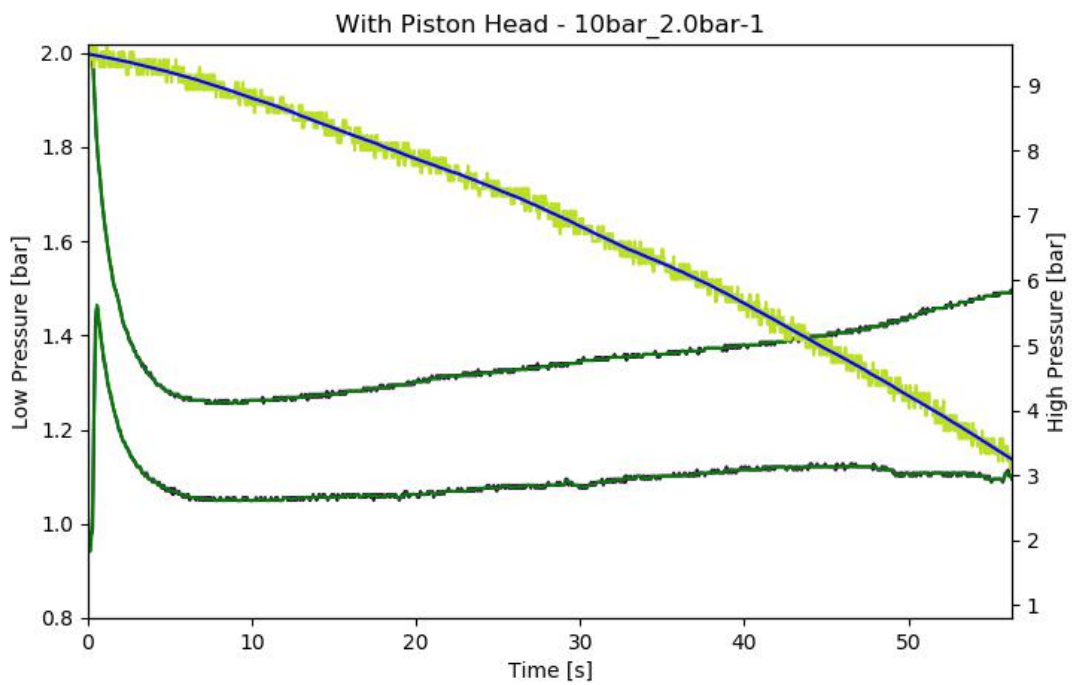


Figure F.21: Pressure data from test - With Piston Head - 10bar_2.0bar-1

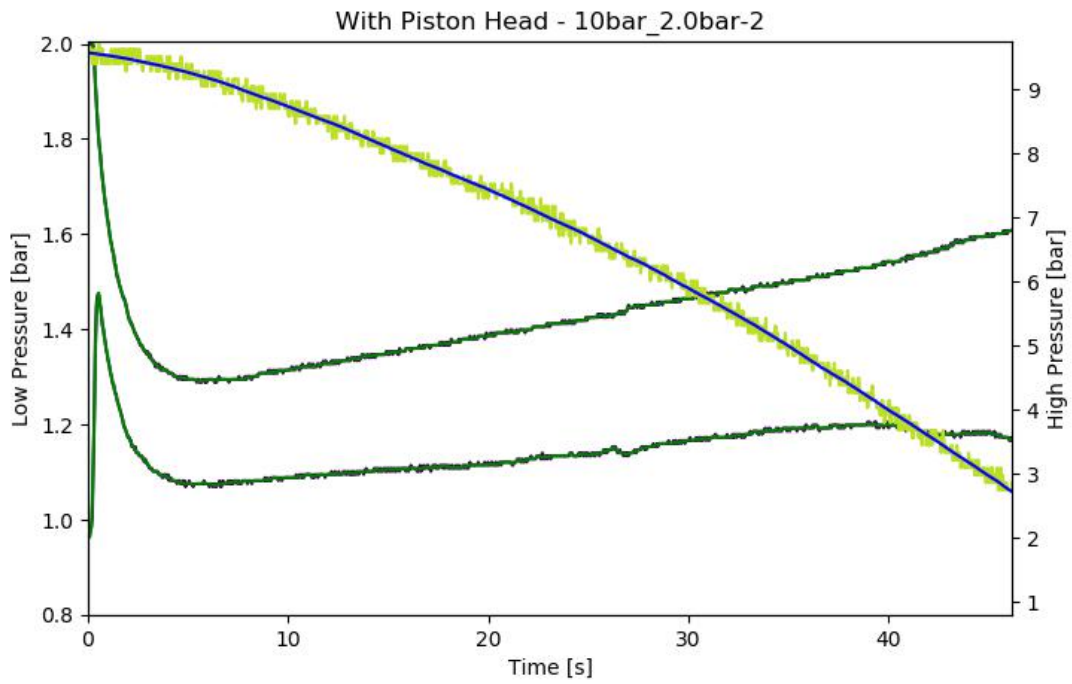


Figure F.22: Pressure data from test - With Piston Head - 10bar_2.0bar-2

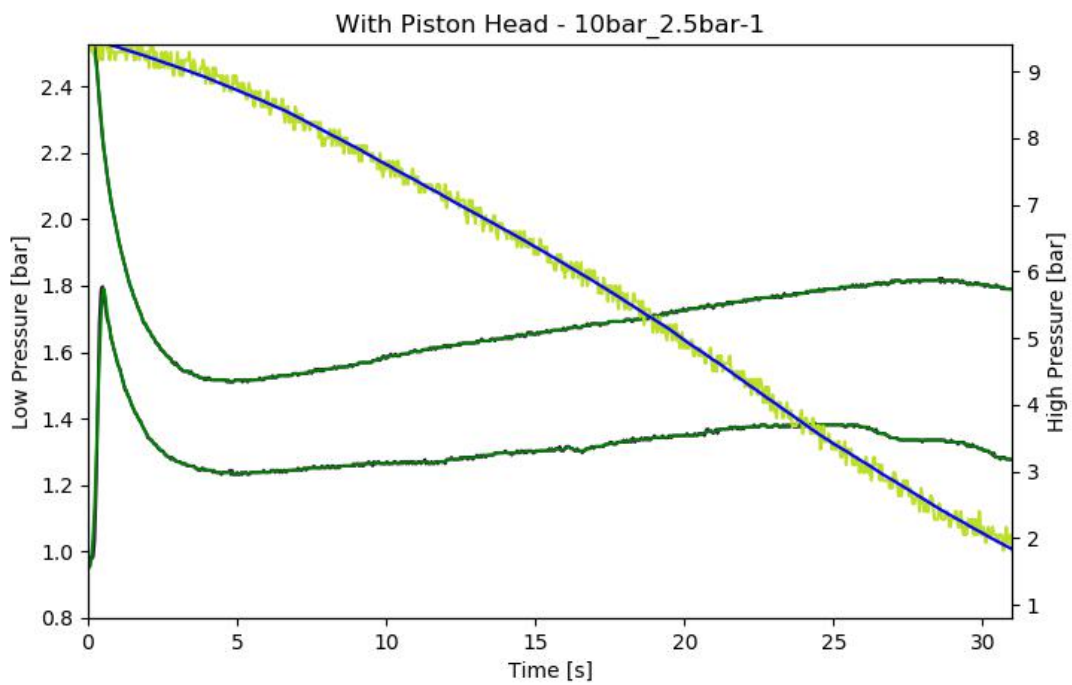


Figure F.23: Pressure data from test - With Piston Head - 10bar_2.5bar-1

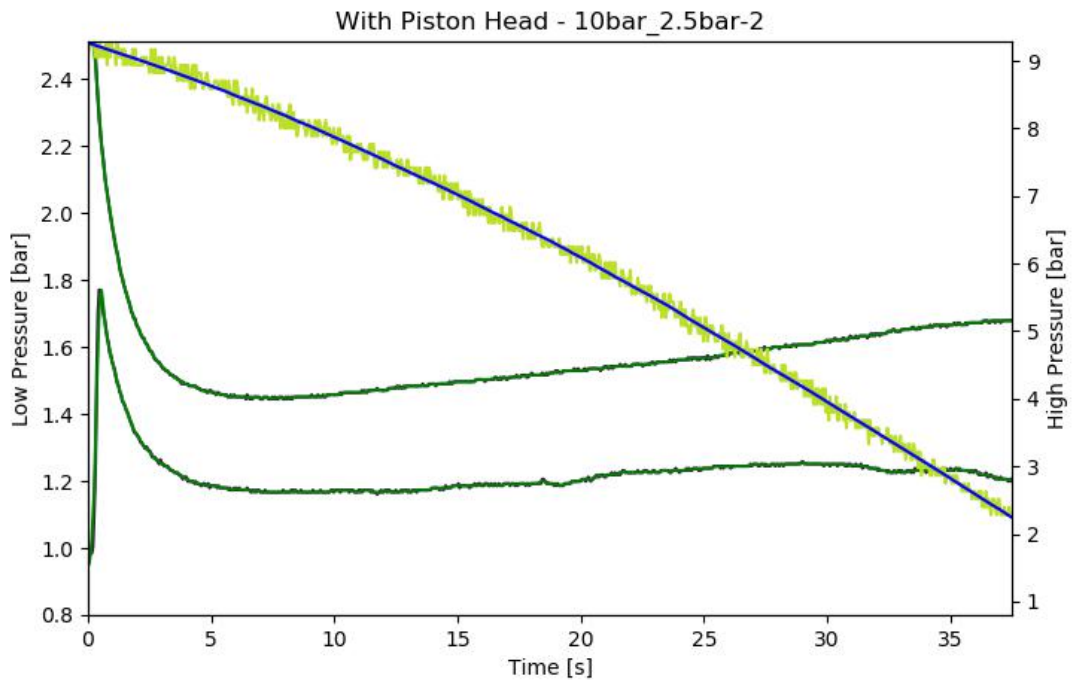


Figure F.24: Pressure data from test - With Piston Head - 10bar_2.5bar-2

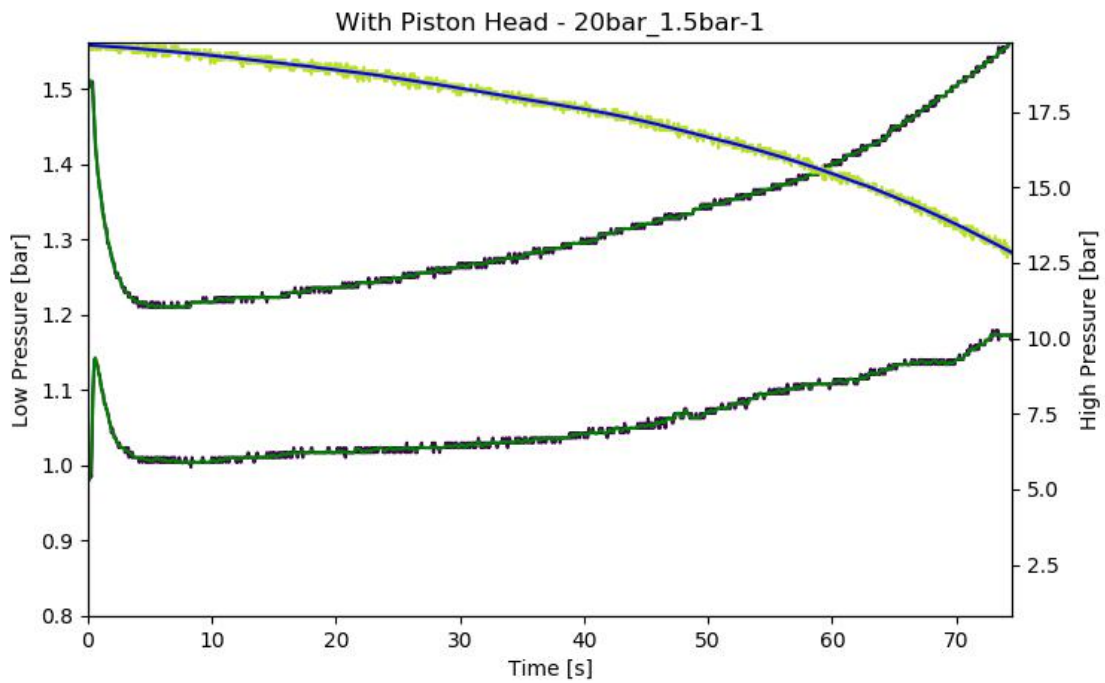


Figure F.25: Pressure data from test - With Piston Head - 20bar_1.5bar-1

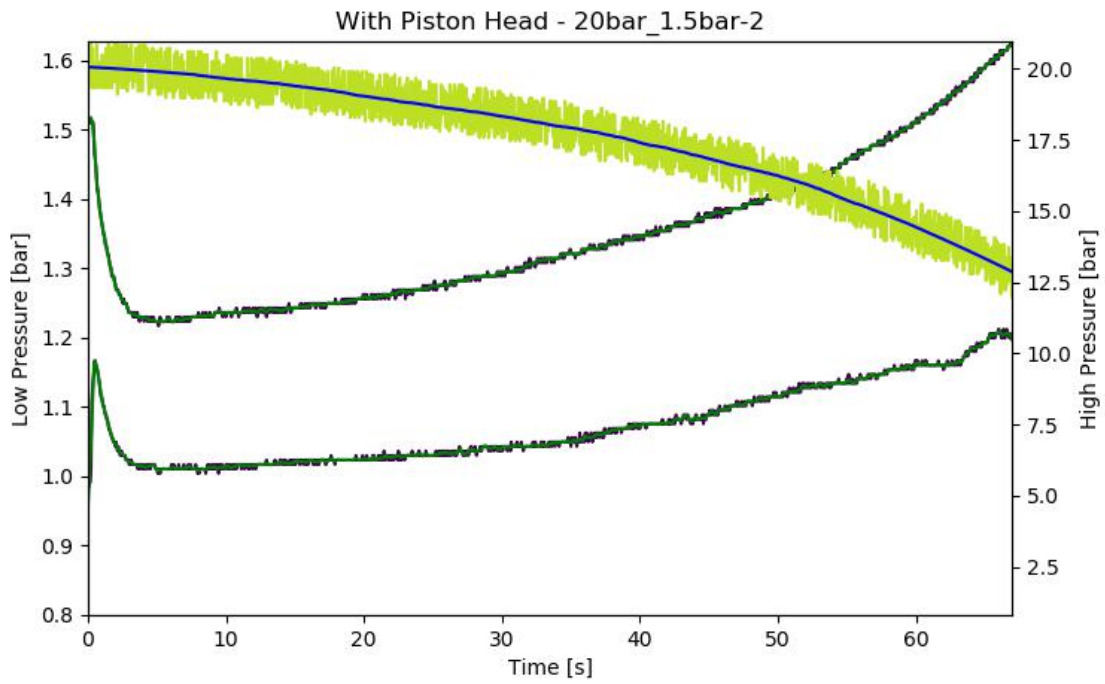


Figure F.26: Pressure data from test - With Piston Head - 20bar_1.5bar-2

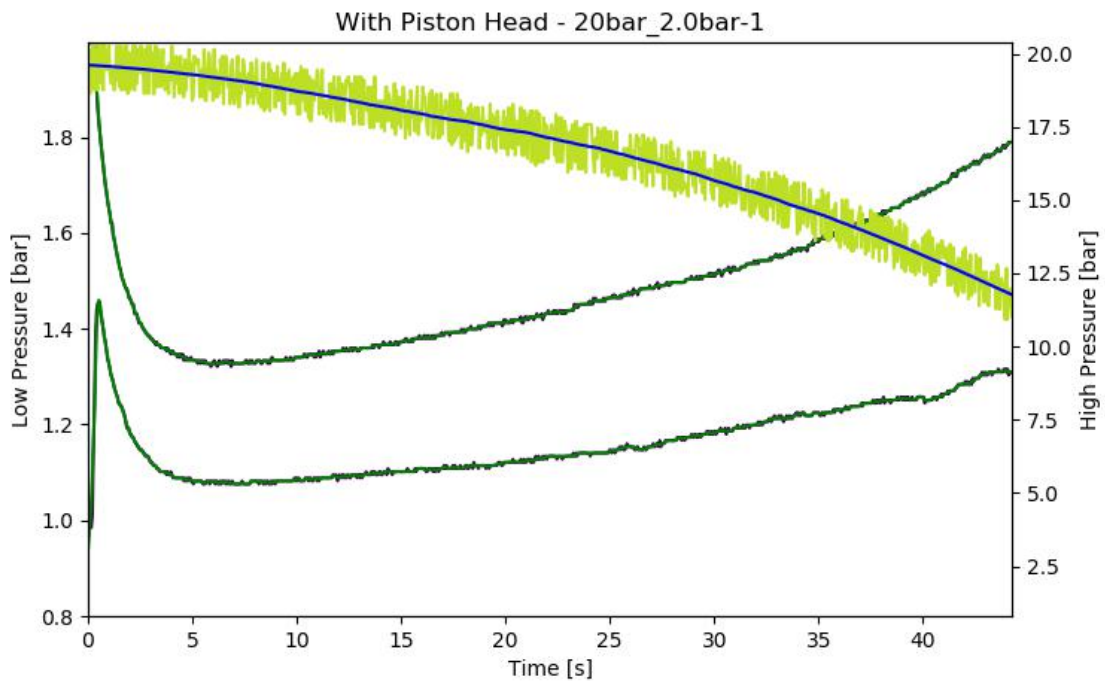


Figure F.27: Pressure data from test - With Piston Head - 20bar_2.0bar-1

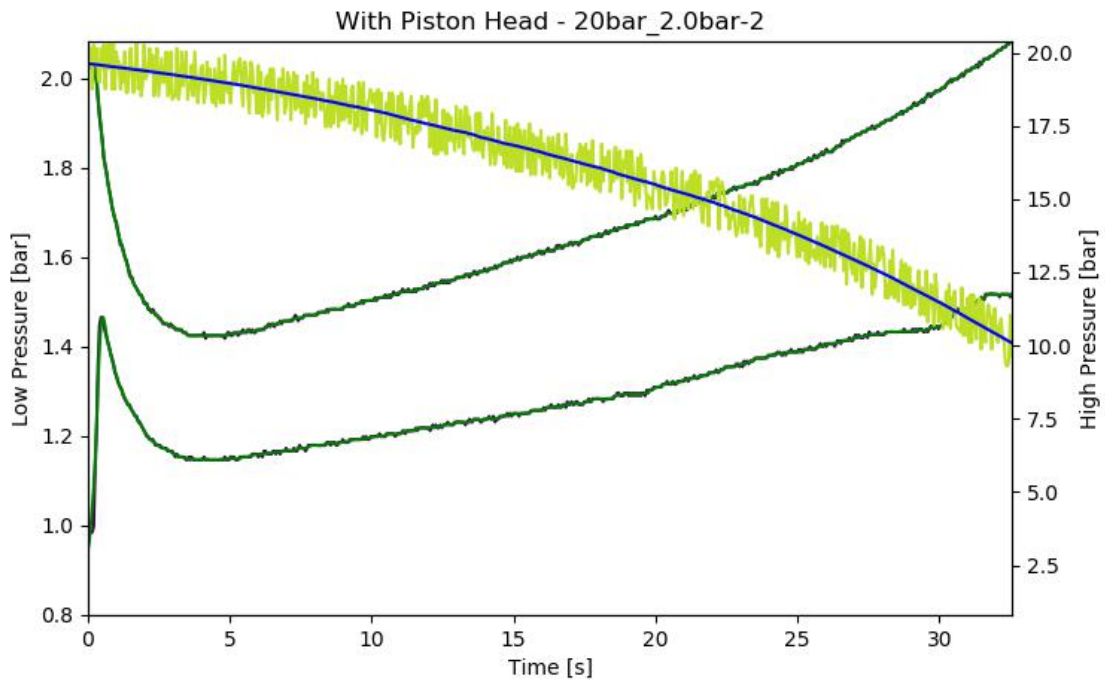


Figure F.28: Pressure data from test - With Piston Head - 20bar_2.0bar-2

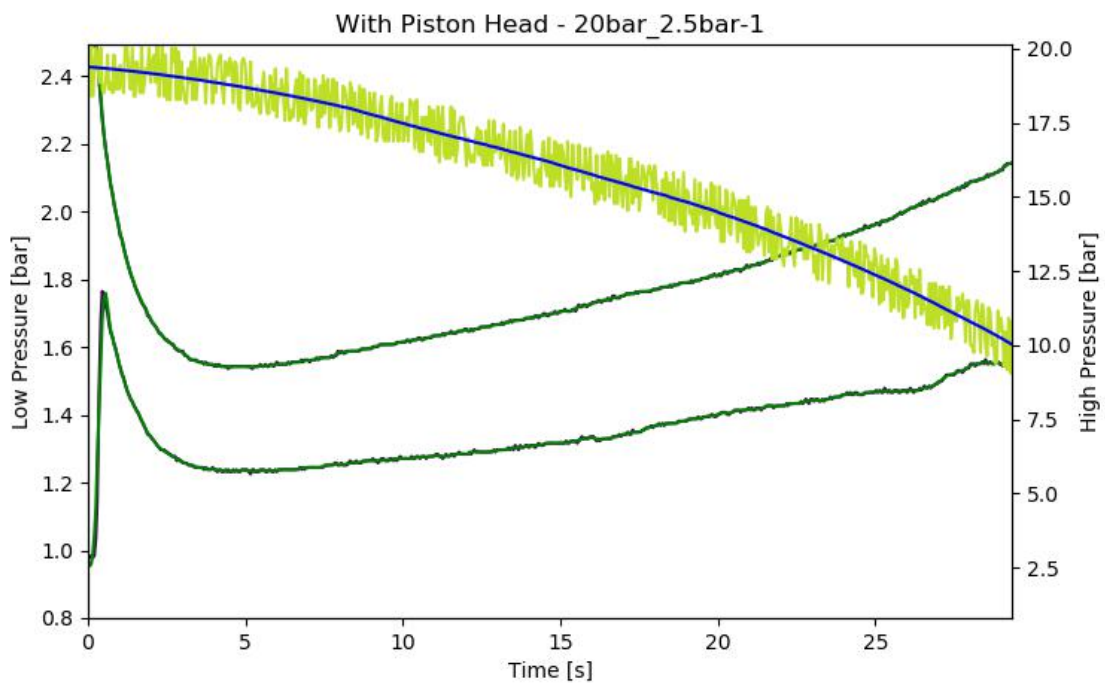


Figure F.29: Pressure data from test - With Piston Head - 20bar_2.5bar-1

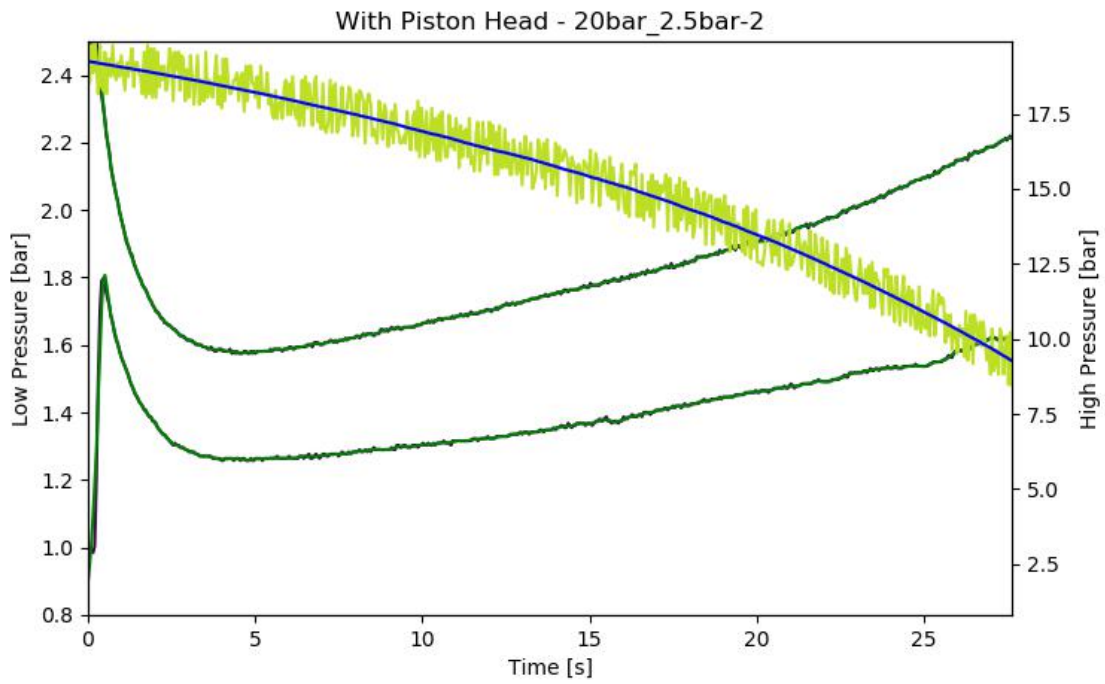


Figure F.30: Pressure data from test - With Piston Head - 20bar_2.5bar-2

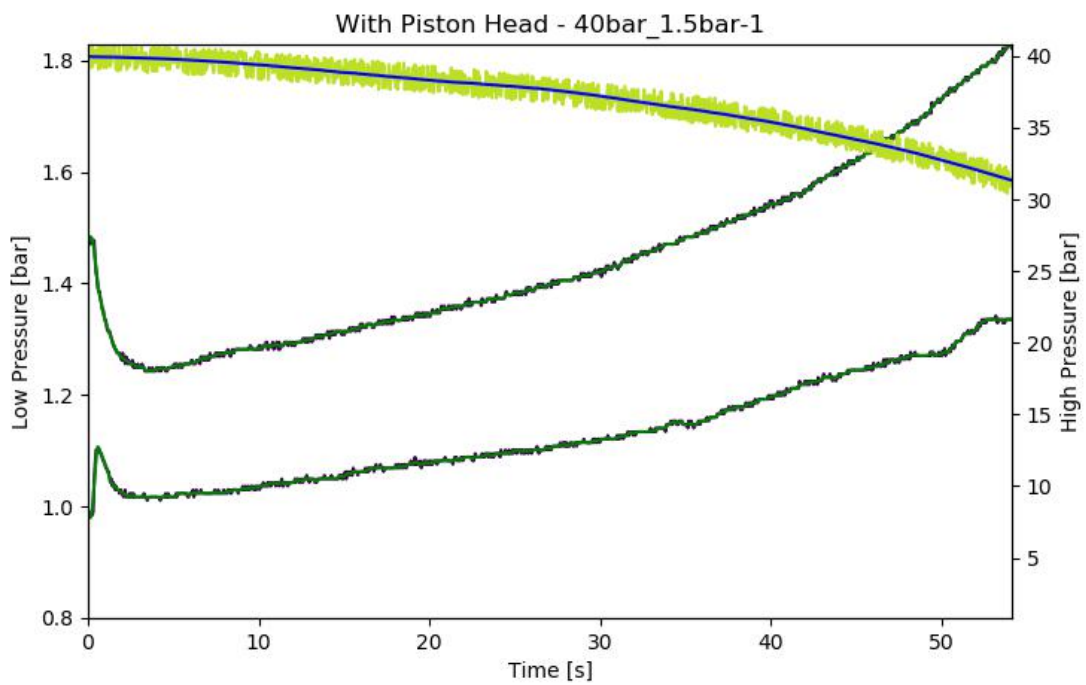


Figure F.31: Pressure data from test - With Piston Head - 40bar_1.5bar-1

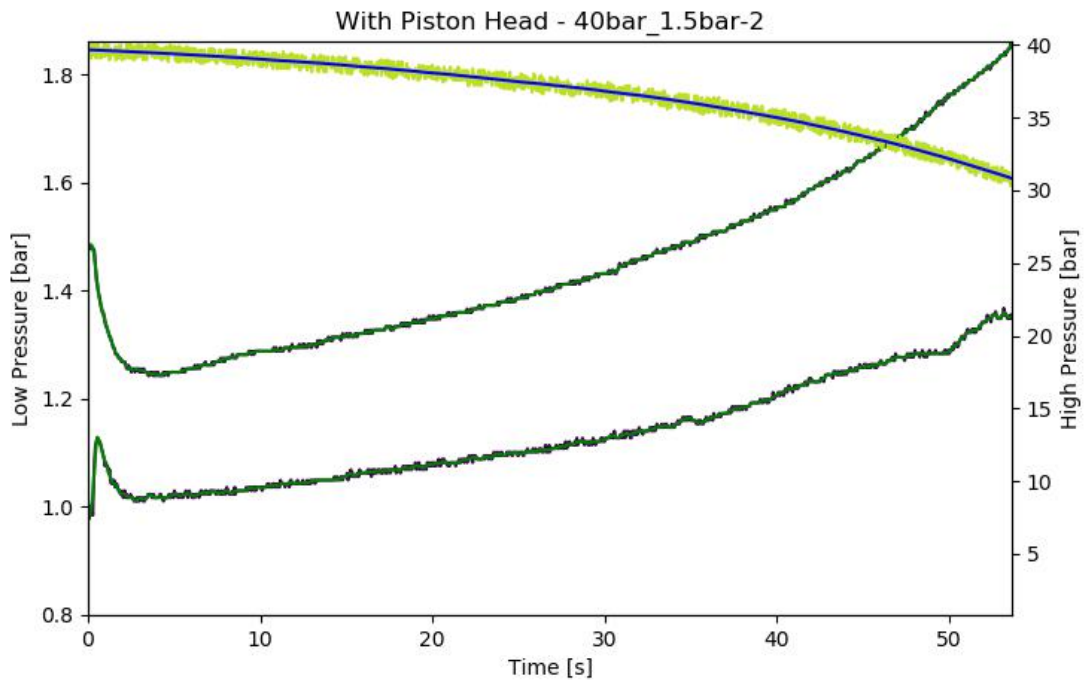


Figure F.32: Pressure data from test - With Piston Head - 40bar_1.5bar-2

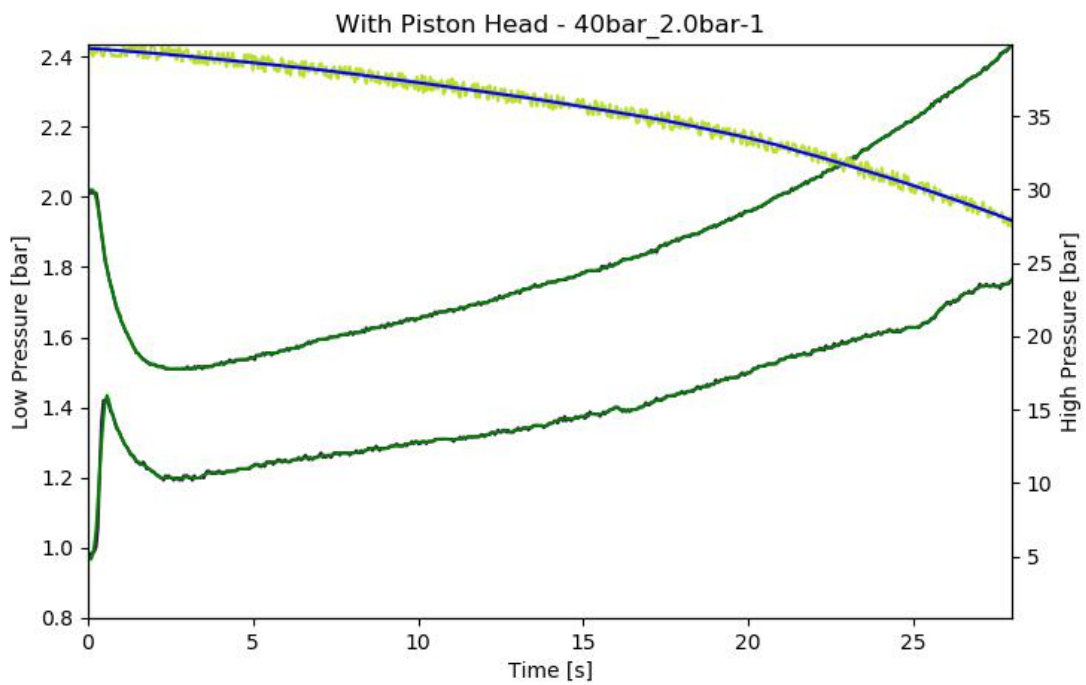


Figure F.33: Pressure data from test - With Piston Head - 40bar_2.0bar-1

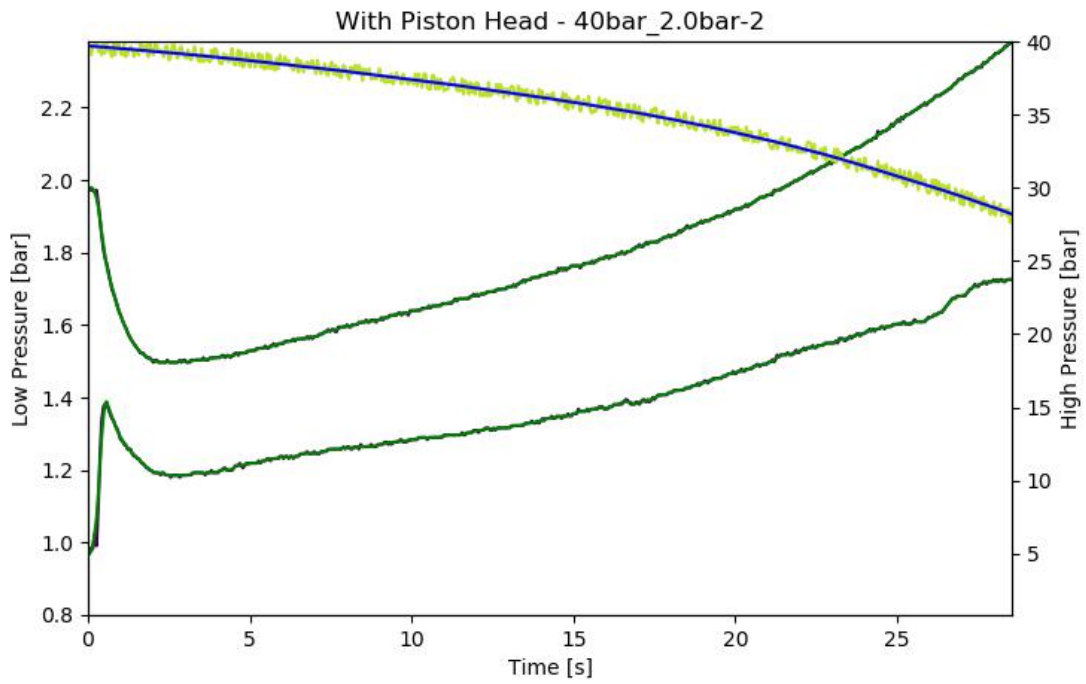


Figure F.34: Pressure data from test - With Piston Head - 40bar_2.0bar-2

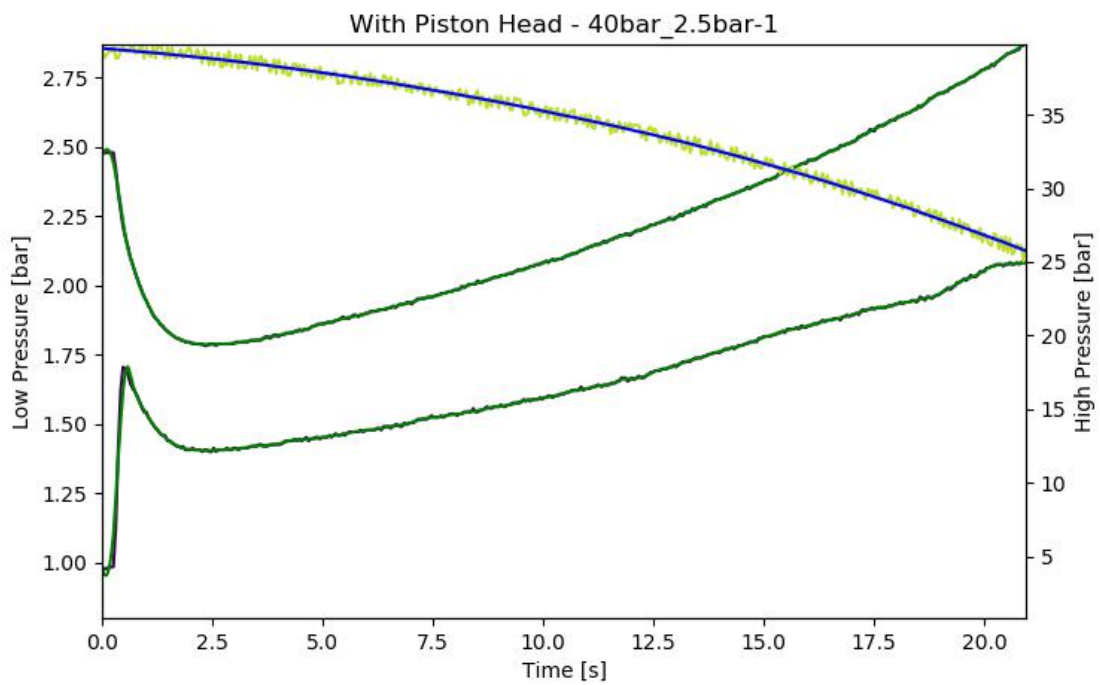


Figure F.35: Pressure data from test - With Piston Head - 40bar_2.5bar-1

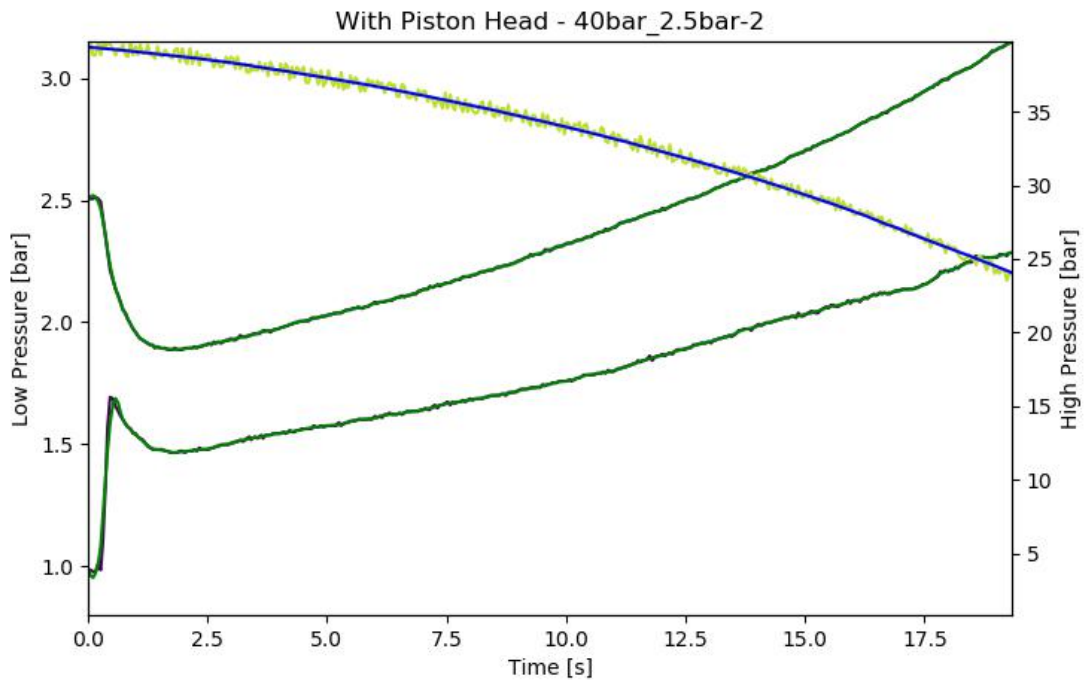


Figure F.36: Pressure data from test - With Piston Head - 40bar_2.5bar-2

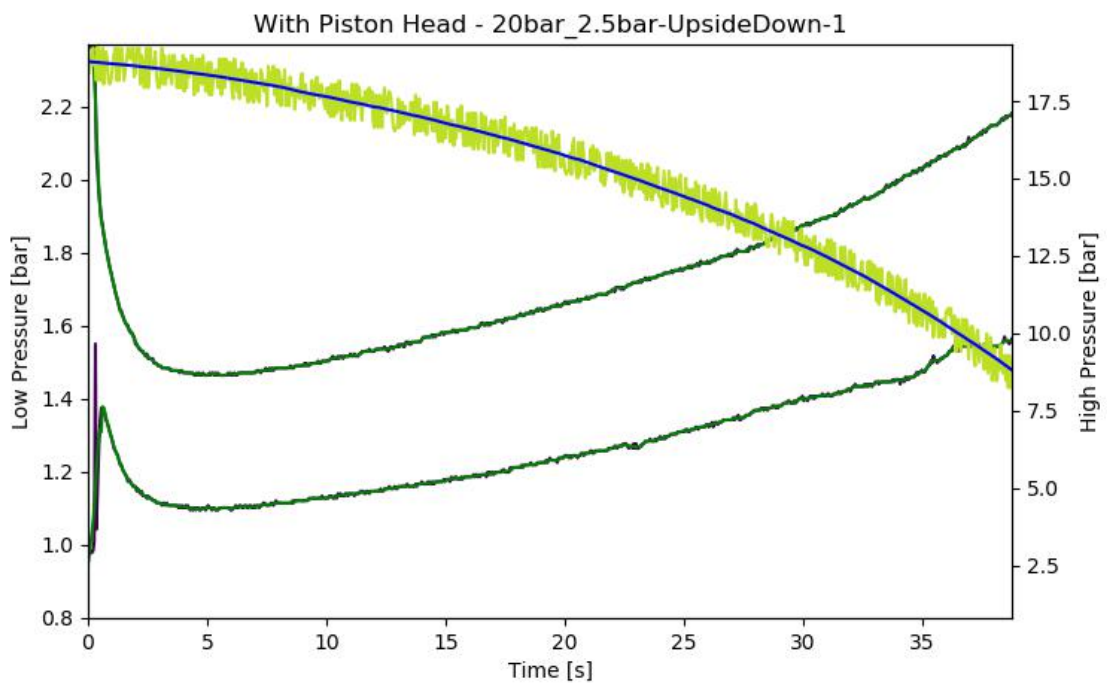


Figure F.37: Pressure data from test - With Piston Head - 20bar_2.5bar-Upside Down-1

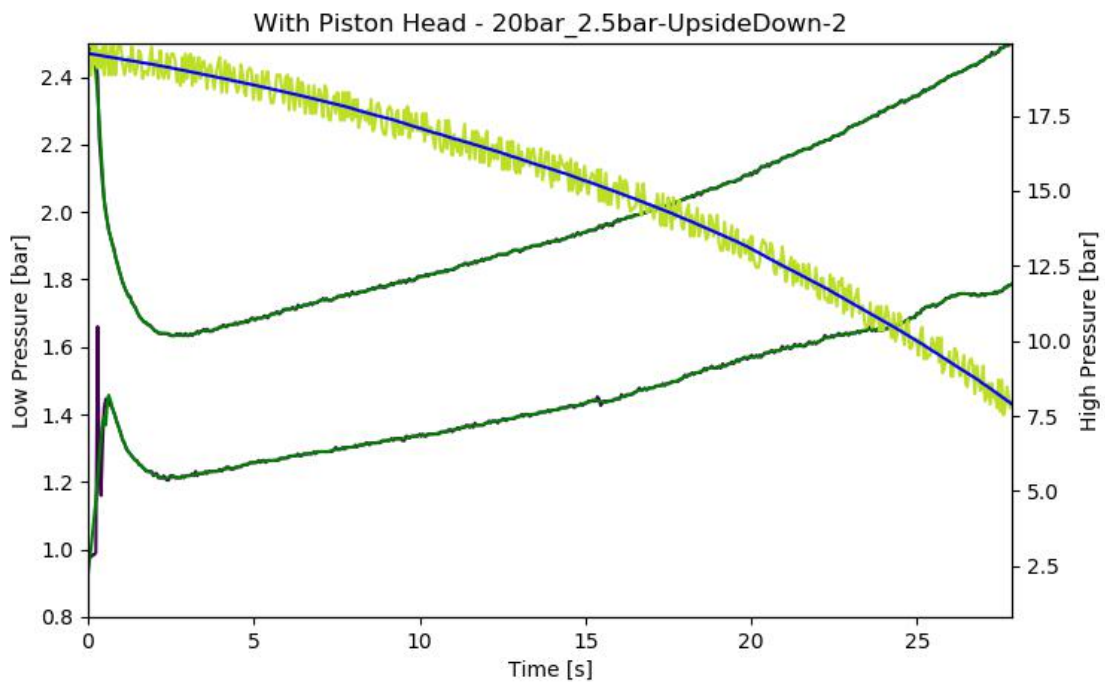


Figure F.38: Pressure data from test - With Piston Head - 20bar_2.5bar-Upside Down-2

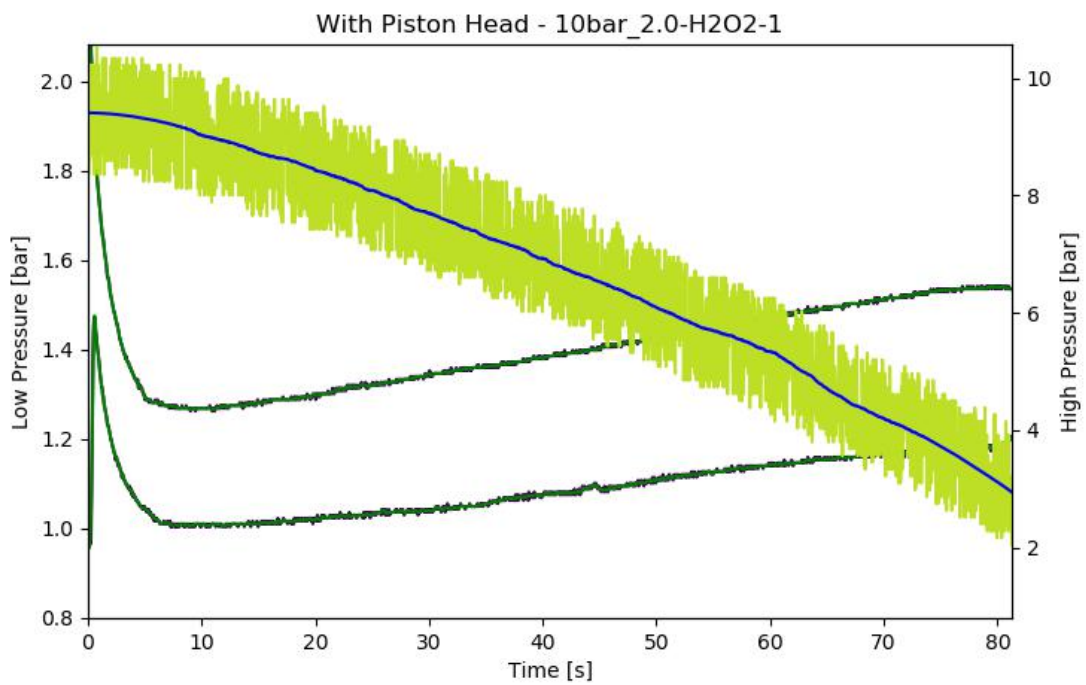


Figure F.39: Pressure data from test - With Piston Head - 10bar_2.0-H2O2-1

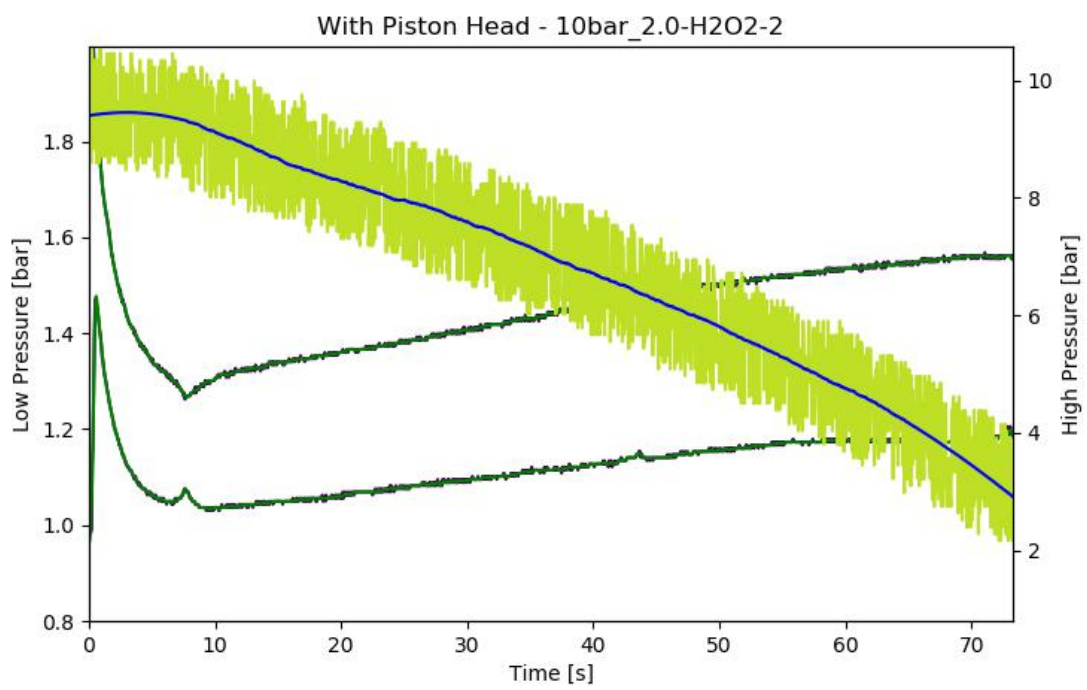


Figure F.40: Pressure data from test - With Piston Head - 10bar_2.0-H2O2-2



Post-processing Python Code

```
# -*- coding: utf-8 -*-
"""
Created on Mon Jul  4 11:16:57 2022
@author: eogha
"""

import numpy as np
from nptdms import TdmsFile
import matplotlib.pyplot as plt
from scipy.signal import butter, filtfilt
import xlrtd
from mpl_toolkits import mplot3d
import itertools

fs = 20.0          # sample rate, Hz
cutoff = 1.0      # 1.2          # desired cutoff frequency of the filter, Hz,
                    # slightly higher than actual 1.2 Hz
nyq = 0.5 * fs    # Nyquist Frequency
order = 3.0
delay = 0 #801 # int(input("P_drop delay"))

highpressures = [10,20,40]
lowpressures = [1.5,2.0,2.5]
tests = [1,2]

TankP0 = []
TankP1 = []
CylP0 = []
CylP1 = []
Duration = []

def find_nearest(array, value):
    array = np.asarray(array)
    idx = (np.abs(array - value)).argmin()
    return idx
```

```

for i in np.arange(len(highpressures)):
    for j in np.arange(len(lowpressures)):
        for k in np.arange(len(tests)):
            # print(highpressures[i], lowpressures[j], tests[k])

            test = "Piston_" + str(highpressures[i]) + "bar_" + str(lowpressures
                [j]) + "bar-" + str(tests[k])
            title = "With□Piston□Head□-" + str(highpressures[i]) + "bar_" + str
                (lowpressures[j]) + "bar-" + str(tests[k])
            filename = "C:/Users/eogha/OneDrive/Desktop/Thesis/Testing/" +
                test + ".tdms"
            print(filename)
            def open_file(path):
                wb = xlrd.open_workbook(path)
                sheet = wb.sheet_by_index(0)

                for row_num in range(sheet.nrows):
                    row_value = sheet.row_values(row_num)
                    # print(row_value)
                    if row_value[5] == test:
                        return(row_value[11])

            path = r"C:\Users\eogha\OneDrive\Desktop\Thesis\System□
                Engineering\Values□for□python□grpahs.xlsx"
            time_end = open_file(path)

with TdmsFile.open(filename) as tdms_file:
    VL = tdms_file["Valve□States"] ["Liquid□Valve"]
    VLarr = VL[:]
    VLarr_open = np.where(VLarr==0)

    Time = tdms_file["Time□in□Seconds"] ["Untitled"]
    Timearr = Time[VLarr_open[0][delay]:VLarr_open[0][-1]]

    Timetest = []
    for l in np.arange(len(Timearr)):
        Timetest.append(((Timearr[l]-Timearr[0]).astype(np.
            int64))/(1*10**6))
    end = find_nearest(Timetest, time_end)

    Timetest = Timetest[0:end]

    LP1 = tdms_file["Pressure□Sensors□Calibrated"] ["PS□1"]
    LP1arr = LP1[VLarr_open[0][delay]:VLarr_open[0][end]]

    LP2 = tdms_file["Pressure□Sensors□Calibrated"] ["PS□2"]
    LP2arr = LP2[VLarr_open[0][delay]:VLarr_open[0][end]]

    REGP = tdms_file["Pressure□Sensors□Calibrated"] ["REG□P"]
    REGParr = REGP[VLarr_open[0][delay]:VLarr_open[0][end]]

    HP = tdms_file["Pressure□Sensors□Calibrated"] ["HP"]
    HParr = HP[VLarr_open[0][delay]:VLarr_open[0][end]]

```

```

# filename = r"C:\Users\eogha\OneDrive\Desktop\Thesis\Testing\
  NoPress_10bar_2.0bar-1.tdms"

# with TdmsFile.open(filename) as tdms_file:
#     VL = tdms_file["Valve States"]["Liquid Valve"]
#     VLarr = VL[:]
#     VLarr_open = np.where(VLarr==0)

#     LP1 = tdms_file["Pressure Sensors Calibrated"]["PS 1"]
#     LP1arrdown = LP1[VLarr_open[0][delay]:VLarr_open[0][-1]]
#     Time = tdms_file["Time in Seconds"]["Untitled"]
#     Timearr = Time[VLarr_open[0][delay]:VLarr_open[0][-1]]

#     Timetest1 = []
#     for i in np.arange(len(Timearr)):
#         Timetest1.append(((Timearr[i]-Timearr[0]).astype(np.
            int64))/(1*10**6))

fig, host = plt.subplots(figsize=(8,5))
par1 = host.twinx()

color1 = plt.cm.viridis(0)
color2 = plt.cm.viridis(0.5)
color3 = plt.cm.viridis(.9)

host.set_xlim(0, Timetest[-1])
host.set_ylim(0.8, max(LP1arr))
par1.set_ylim(0.8, max(HParr))

host.set_xlabel("Time[s]")
host.set_ylabel("Low Pressure[bar]")
par1.set_ylabel("High Pressure[bar]")

p1, = host.plot(Timetest, LP1arr, color=color1, label="
    Density")
# p2, = host.plot(Timetest1, LP1arrdown, color="red", label
    ="Temperature")
p2, = host.plot(Timetest, LP2arr, color=color1, label="
    Temperature")
p3, = par1.plot(Timetest, HParr, color=color3, label="Velocity
    ")

from scipy.signal import lfilter
n = 30 # the larger n is, the smoother curve will be
b = [1.0 / n] * n
a = 1
yy = lfilter(b,a, HParr)
yy = lfilter(b,a,LP1arr)

from scipy.signal import savgol_filter
w = savgol_filter(HParr, 301, 2)

```

```

ww = savgol_filter(LP1arr, 11, 2)
www = savgol_filter(LP2arr, 11, 2)

def butter_lowpass_filter(data, cutoff, fs, order):
    normal_cutoff = cutoff / nyq
    # Get the filter coefficients
    b, a = butter(order, normal_cutoff, btype='low', analog=
        False)
    y = filtfilt(b, a, data, axis=0)
    return y

Butter = butter_lowpass_filter(LP1arr, cutoff, fs, order)
Butter2 = butter_lowpass_filter(LP2arr, cutoff, fs, order)

import statsmodels.api as sm
y_lowess = sm.nonparametric.lowess(HParr, Timetest, frac =
    0.05)
yy_lowess = sm.nonparametric.lowess(LP2arr, Timetest, frac =
    0.007)
yyy_lowess = sm.nonparametric.lowess(LP1arr, Timetest, frac =
    0.007)

p5, = par1.plot(Timetest, w, color="blue", label="High□
    Pressure□Tank")
p7, = host.plot(Timetest, ww, color="green", label="Piston□
    Pressure")
p8, = host.plot(Timetest, www, color="green", label="Outlet□
    Pressure")

# -----
# p4, = par1.plot(Timetest, yy, color="red", label="Velocity")
# p8, = host.plot(Timetest, Butter, color="red", label="
    Velocity")
# p9, = host.plot(Timetest, Butter2, color="red", label="
    Velocity")
# p6, = par1.plot(y_lowess[:,0], y_lowess[:,1], color="green",
    label="Velocity")
# p8, = host.plot(yy_lowess[:,0], yy_lowess[:,1], color="
    orange", label="Velocity")
# p8, = host.plot(yyy_lowess[:,0], yyy_lowess[:,1], color="
    orange", label="Velocity")
# p7, = host.plot(Timetest, yy, color="brown", label="Velocity
    ")
# -----

# Ins = [p7, p8, p5]
# host.legend(handles=Ins, loc='best')

TankP0.append(w[0])
TankP1.append(w[-1])
CylP0.append(ww[0])
CylP1.append(ww[-1])
Duration.append(Timetest[-1])

```

```

plt.title(title)
plt.savefig(title+'.png')
plt.show

# plt.plot(Timetest, LP1arr)
# plt.plot(Timetest, LP2arr)
# plt.plot(Timetest, REGParr)
# plt.plot(Timetest, HParr)
# X, Y, Z = np.meshgrid(TankP0, CylP0, Duration)

T = 293.15 #k
R = 8.314
V = 0.000213032
m = 0.02897

PressMassIdealPist = (np.array(TankP0)-np.array(TankP1))*1E5*V/(T*R)*m
                    *1000

PressMassSuttonPist = 1000*((np.array(CylP0)*10**5)*.001/(R/m*T)
                    *1.0035/(1-np.array(CylP0)/np.array(TankP0)))

fig = plt.figure()
ax = plt.axes(projection='3d')

# ax.plot_wireframe(X, Y, Z, color='black')

ax.scatter3D(TankP0, CylP0, TankP1);

# from skspatial.objects import Plane
# from skspatial.objects import Points
# from skspatial.plotting import plot_3d

array = np.zeros((len(Duration),3))

array[:,0]= TankP0
array[:,1]= CylP0
array[:,2]= PressMassIdealPist

array1 = np.zeros((len(Duration),3))

array1[:,0]= TankP0
array1[:,1]= CylP0
array1[:,2]= Duration

# points = Points(array)

# plane = Plane.best_fit(points)

# plot_3d(
#     points.plotter(c='k', s=50, depthshade=False),
#     plane.plotter(lims_x=(min(TankP0),max(TankP0)), lims_y=(min(CylP0),
#         max(CylP0))),

```

```

# )

PRECISION = 1e-12    # Arbitrary zero for real-world purposes

def plane_from_points(points):
    # The adjusted plane crosses the centroid of the point collection
    centroid = np.mean(points, axis=0)

    # Use SVD to calculate the principal axes of the point collection
    # (eigenvectors) and their relative size (eigenvalues)
    _, values, vectors = np.linalg.svd(points - centroid)

    # Each singular value is paired with its vector and they are sorted
    # from
    # largest to smallest value.
    # The adjusted plane must contain the eigenvectors corresponding
    # to
    # the two largest eigenvalues. If only one eigenvector is different
    # from zero, then points are aligned and they don't define a plane.
    if values[1] < PRECISION:
        raise ValueError("Points are aligned, can't define a plane")

    # So the plane normal is the eigenvector with the smallest eigenvalue
    normal = vectors[2]

    # Calculate the coefficients (a,b,c,d) of the plane's equation ax+by+
    # cz+d=0.
    # The first three coefficients are given by the normal, and the fourth
    # one (d) is the plane's signed distance to the origin of coordinates
    d = -np.dot(centroid, normal)
    plane1 = np.append(normal, d)

    # If the smallest eigenvector is close to zero, the collection of
    # points is perfectly flat. The larger the eigenvector, the less flat.
    # You may wish to know this.
    thickness = values[2]

    return plane1, thickness

plane1, thickness = plane_from_points(array)

a,b,c,d = plane1
print(a,b,c,d)
print(plane1)
X,Y = np.meshgrid(TankP0, CyIP0)
Z = (-d - a*X - b*Y) / c

Z_designpoint = (-d - a*200 - b*3) / c
mass=Z_designpoint*200/1000

print(mass, "[kg]")
tmp_A = []
tmp_b = []
for i in range(len(TankP0)):
    tmp_A.append([TankP0[i], CyIP0[i], 1])

```

```

    tmp_b.append(PressMassIdealPist[i])
b = np.matrix(tmp_b).T
A = np.matrix(tmp_A)
fit = (A.T * A).I * A.T * b
errors = b - A * fit
residual = np.linalg.norm(errors)

E = np.squeeze(np.asarray(errors))
Z1 = np.array(PressMassIdealPist)
r2 = 1 - (E.var() / Z1.var())
r2label = 'R2=□'+str(round(r2, 2))

fig = plt.figure()
ax = fig.gca(projection='3d')
ax.scatter3D(TankP0, CylP0, PressMassIdealPist);
plt.title("With□Piston□Head□-□Pressurant□Mass□Used")
ax.set_xlabel('Tank□P0□[bar]')
ax.set_ylabel('Piston□P0□[bar]')
ax.set_zlabel('Pressurant□Mass□Expelled□[g]')
ax.text2D(0.95, 0.9, r2label, transform=ax.transAxes)
surf = ax.plot_surface(X, Y, Z, alpha=0.2, color='r', shade=False)
plt.savefig('WithPistonPressMass.png')

# -----
# plane2, thickness = plane_from_points(array1)

# a,b,c,d = plane2

# X,Y = np.meshgrid(TankP0, CylP0)
# Z = (-d - a*X - b*Y) / c

# tmp_A = []
# tmp_b = []
# for i in range(len(TankP0)):
#     tmp_A.append([TankP0[i], CylP0[i], 1])
#     tmp_b.append(Duration[i])
# b = np.matrix(tmp_b).T
# A = np.matrix(tmp_A)
# fit = (A.T * A).I * A.T * b
# errors = b - A * fit
# residual = np.linalg.norm(errors)

# E = np.squeeze(np.asarray(errors))
# Z1 = np.array(Duration)
# r2 = 1 - (E.var() / Z1.var())
# r2label = 'R2 = '+str(round(r2, 2))

# fig = plt.figure()
# ax = fig.gca(projection='3d')
# ax.scatter3D(TankP0, CylP0, Duration);
# plt.title("No Piston Head - Transfer Duration")
# ax.set_xlabel('Tank P0 [Bar]')
# ax.set_ylabel('Piston P0 [Bar]')
# ax.set_zlabel('Duration [s]')
# ax.text2D(0.95, 0.80, r2label, transform=ax.transAxes)
# surf = ax.plot_surface(X, Y, Z, alpha=0.3, color='b')

```

```

# plt.savefig('NoPistonDuration1.png')

# from scipy.optimize import curve_fit
# from mpl_toolkits.mplot3d import Axes3D

# def function(data, a, b, c):
#     x = data[0]
#     y = data[1]
#     return a * (x**b) * (y**c)

# parameters, covariance = curve_fit(function, [TankP0, CylP0], Duration)

# # create surface function model
# # setup data points for calculating surface model
# model_x_data = np.linspace(min(TankP0), max(TankP0), 30)
# model_y_data = np.linspace(min(CylP0), max(CylP0), 30)
# # create coordinate arrays for vectorized evaluations
# X, Y = np.meshgrid(model_x_data, model_y_data)
# # calculate Z coordinate array
# Z = function(np.array([X, Y]), *parameters)
# Z1 = function(np.array([TankP0, CylP0]), *parameters)
# tmp_a = []
# tmp_b = []
# for i in range(len(TankP0)):
#     tmp_a.append(Z1[i])
#     tmp_b.append(Duration[i])
# b = np.matrix(tmp_b).T
# a = np.matrix(tmp_a).T
# # A = np.matrix(tmp_A)
# # fit = (A.T * A).I * A.T * b
# errors = b-a
# residual = np.linalg.norm(errors)

# E = np.squeeze(np.asarray(errors))
# Z1 = np.array(Duration)
# r3 = 1 - (E.var() / Z1.var())
# r3label = 'R2 = '+str(round(r3, 2))

# # setup figure object
# fig = plt.figure()
# # setup 3d object
# ax = Axes3D(fig)
# # plot surface
# ax.plot_surface(X, Y, Z)
# # plot input data
# ax.scatter(TankP0, CylP0, Duration, color='red')
# # set plot descriptions
# plt.title("No Piston Head - Transfer Duration")
# ax.set_xlabel('Tank P0 [Bar]')
# ax.set_ylabel('Piston P0 [Bar]')
# ax.set_zlabel('Duration [s]')
# ax.text2D(0.7, 0.95, r3label, transform=ax.transAxes)
# plt.savefig('NoPistonDuration2.png')
# plt.show()

```

```

# TankP0 = np.delete(TankP0, 1)
# CylP0 = np.delete(CylP0, 1)
# Duration = np.delete(Duration, 1)

# # get fit parameters from scipy curve fit
# parameters, covariance = curve_fit(function, [TankP0, CylP0], Duration)

# # create surface function model
# # setup data points for calculating surface model
# model_x_data = np.linspace(min(TankP0), max(TankP0), 30)
# model_y_data = np.linspace(min(CylP0), max(CylP0), 30)
# # create coordinate arrays for vectorized evaluations
# X, Y = np.meshgrid(model_x_data, model_y_data)
# # calculate Z coordinate array
# Z = function(np.array([X, Y]), *parameters)
# Z1 = function(np.array([TankP0, CylP0]), *parameters)
# tmp_a = []
# tmp_b = []
# for i in range(len(TankP0)):
#     tmp_a.append(Z1[i])
#     tmp_b.append(Duration[i])
# b = np.matrix(tmp_b).T
# a = np.matrix(tmp_a).T
# # A = np.matrix(tmp_a)
# # fit = (A.T * A).I * A.T * b
# errors = b-a
# residual = np.linalg.norm(errors)

# E = np.squeeze(np.asarray(errors))
# Z1 = np.array(Duration)
# r3 = 1 - (E.var() / Z1.var())
# r3label = 'R2 = '+str(round(r3, 2))

# # setup figure object
# fig = plt.figure()
# # setup 3d object
# ax = Axes3D(fig)
# # plot surface
# ax.plot_surface(X, Y, Z)
# # plot input data
# ax.scatter(TankP0, CylP0, Duration, color='red')
# # set plot descriptions
# plt.title("No Piston Head - Transfer Duration")
# ax.set_xlabel('Tank P0 [Bar]')
# ax.set_ylabel('Piston P0 [Bar]')
# ax.set_zlabel('Duration [s]')
# ax.text2D(0.7, 0.90, r3label, transform=ax.transAxes)
# plt.show()
# plt.savefig('NoPistonDuration3.png')

```